MIXING ENHANCEMENT AND NOISE REDUCTON IN CIRCULAR AND ELLIPTIC SLOT JETS

A Thesis Submitted in Partial Fulfilment of the Requirements
for the Degree of
DOCTOR OF PHILOSOPHY

by

SHASHI BHUSHAN VERMA

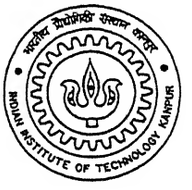

to the
Department of Aerospace Engineering
Indian Institute of Technology Kanpur, India
February, 1998

2/3/98

CERTIFICATE

It is certified that the work contained in the thesis entitled "**Mixing Enhancement and Noise Reduction in Circular and Elliptic Slot Jets** ", by **Shashi Bhushan Verma**, has been carried out under my supervision and that this work has not been submitted elsewhere for a degree.

Prof. E. Rathakrishnan
Department of Aerospace Engineering
Indian Institute of Technology, Kanpur
India

February 27, 1998.

Dedicated
to
my parents

To exist is to be something
as distinguished from the nothing of non-existence

— *Ann Rand*

Acknowledgment

I owe my sincere gratitude to Professor E.Rathakrishnan for his inestimable guidance and incitation. All through the course of this investigation, he patiently followed up my work pointing out the various inconsistencies and errors and invariably providing me with his valuable and erudite suggestions. I am very thankful to him for his benefactions.

I would forever be indebted to my parents for their constant love and confidence in my abilities that brought me this far in my career. My father, Dr. H.K.Verma, has been my idol and the greatest inspiration all through my academic life And I can never repay my mother for her unconditional caring and prayers which has all through been my biggest security. I owe a lot to my sister, Nony too, for always being there for me and understanding and to my brother in-law, Pardeep, for his timely words of encouragement. Their good wishes have helped a great deal to spur me on.

My heartfelt love and gratitude for my wife, Manu. for her co-operation, endurance and patience during the crucial phase of my research programme. She has come so beautifully into my life, adding the love and care I so much needed, and backing me up with her incessant support.

I would also like to put on record the regard I feel for my in-laws for their love, encouragement and good wishes that counted a lot.

I am also obligated to my friend, K Srinivasan, whose co-operation, helpful comments and concurrence made possible the completion of this thesis. My special thanks to Dr. T.J.Ignatius whose efficient packages made data analysis much simpler. My thanks to Pandi Kumar for his useful suggestions. And not the least, my thanks to my friend, Himanshu Agarwal, for his effort in developing the existing computer facility in our lab.

I express my thanks to Dr. Elangovan with whom I had useful and lively discussions and got suggestions that helped me in improving my thesis work.

I am specially appreciative of my 'buddy' Neeraj, who with his light hearting punjabi 'gags' bought a feel of home away from home, and of Kali Prasad for being such a pleasure to talk to. The many thought provoking conversations I had with them helped me in retaining my composture all through the dragging course of my work.

I must acknowledge with lot of gratitude, the spontaneous assistance and co–operation

extended by Mr. S. S. Chauhan, Mr. Bhantu, Mr. Sishupal and Sharad of the High Speed Laboratory, Dept. of Aerospace Engineering. I would like to specially thank our project technician Mr. Suresh Mishra who helped me immensely during the crucial phase of experimentation My special thanks are due to our Scientific Officer Mr. A. K. Rajpal for the zeal with which he tried to sort out the problems regarding instrumentation.

I am also greatful to Mr. Bhattacharya, Technical Officer, Mr. Ganveer, Mr. Tiwari, Mr Johny and other technical staff of the workshop, Aerospace Engineering Department for their kind co–operation during the fabrication of the experimental models.

I express my thanks to Mr.Ahmed, Office Superendentent, and other administrative staff of the Aerospace Engineering Department, particularly, Mr. Sushil, 'Punditji', Mr. Gupta and Mr. Trivedi for their kind and benevolent attitude.

My associations around here have given me everlasting memories. And I would like to thank all my friends around the campus – most specially – Tapo, Vikrant Jain, Alok Srivastava and Manoj for their refreshing company and for being of help whenever there was need. My many thanks to my gym mates. The time spent with them provided the much called for relief in my work schedule.

Above all, I owe my life to '**Vaishnu Mata**' who with her grace, blessings and beneson has guided my every action that has brought me to the place I am today in my life

Shashi Bhushan Verma

Abstract

Experimental investigations were carried out to achieve passive control of the mixing and noise characteristics in slot jets via exit geometry modifications in both circular and elliptic slots. All the slots, i.e., plain and notched/modified, were of equal area which was equal to the area of the circular slot of 10 mm diameter and hence, the equivalent diameter of the non-circular slots was 10 mm. The modifications are in the form of notches with and without sharp corners placed normal to the jet axis. Two notches are symmetrically placed along a diameter for circle and along the minor-axis side of ellipse. Each notch conforms to 5 percent of the equivalent slot area. Further, the effect of three configurations of the notch, namely, triangular, square and semi-circular were investigated. The study relies on mean flow and noise characteristics. Three elliptic slots of aspect-ratio 2:1, 3:1 and 4:1 were studied in the present investigation. Jets from all the modified geometries were experimentally analysed and compared with an equivalent plain slot jet.

The mean flow study was carried out for two conditions: (i) correctly expanded jets, with sonic velocity at nozzle exit and, (ii) underexpanded sonic jets at P_0/P_a of 2.835 and 3.86, corresponding to fully expanded Mach numbers M_j of 1.0 and 1.5. The Reynolds number based on the equivalent diameter and the equivalent exit velocity(based on M_j) for the two conditions ranged from 2.36×10^5 to 3.54×10^5. The noise measurements were carried out for fully expanded Mach number M_j ranging from 1.0 to 2.0. The investigations relied on spectral analysis, radial and azimuthal sound measurements.

The effect of notch presence in a slot geometry with uniform azimuthal curvature variation, i.e., circle, is investigated first. A direct comparison of the results from modified circular slot jets is made with an equivalent plain circular jet. The presence of notch makes the circular slot slightly non-circular(with slight aspect-ratio) thereby inducing axis-switching phenomena in the jet fields from the modified slots. This causes the cut-out jet to spread more in the unmodified plane. As such all the notched/modified circular jets show enhanced mixing characteristics relative to the plain circular slot jet, with higher entrainment(i.e., bulk mixing) and faster centreline decay. At underexpanded conditions, the notched/modified circular slots exhibit slightly weakened cell structure. Screech tones are observed to get reduced by 3-5 dB. Overall

sound pressure levels are observed to get reduced both in radial and azimuthal directions. A comparison of the notch configurations indicates that the triangular notch is the best for screech tone reduction whereas square seems to be the best for the reduction of shock associated noise.

Experiments were carried out to study the changes introduced by the presence of the notch in an exit geometry with non-uniform, smooth azimuthal curvature variation, i.e., ellipse with aspect-ratio 2:1. The study relies, once again, on mean flow and noise characteristics of plain and modified elliptic slot jets. The presence of the notch in the minor-axis plane greatly influences the jet growth in that plane. The pressure relieving effect of notches increases the spread in the notched plane relative to plain ellipse. This cause the notched/modified ellipse to switch axis earlier. As a result, the notched /modified elliptic jets show higher mixing characteristics as shown by higher entrainment(i.e., bulk mixing) and shorter core-lengths and faster jet decay. Triangular notch shows the best mixing characteristics of all the notch configurations. When operated at underexpanded conditions, the modified ellipse with sharp cornered notches indicate significantly weakened shock structure. This plays a vital role in the far field noise reduction of these jets. Square notch shows a drastic reduction in screech tone and shock associated noise. In azimuthal directivity, major-axis side of the plain ellipse is observed to radiate noise significantly lower than that along minor-axis side. Notches drastically bring down the noise radiated along major-axis ends. Square notch seems to be the best configuration for overall shock noise reduction.

An extention of the experiments on 2:1 ellipse were carried out to investigate the effect of aspect-ratio with and without notch presence. The aspect-ratios ranged from 2:1 to 4:1. For plain cases, 3:1 jet shows better jet characteristics than 2:1 and 4:1 jets. The use of sharp cornered notch seems to have a greater influence on 2:1 and 3:1 jets with triangular notch favouring 2:1 ellipse and square notch favouring 3:1 case. However, for higher aspect-ratio, i.e., 4:1, absence of sharp corners in a notch, i.e., semi-circular, seems to be favourable. The presence of the notch significantly weakens the shock structure in all aspect-ratios with 4:1 notched/modified ellipse showing the weakest shocks. Triangular notch brings down the screech tones in all aspect-ratios significantly and seems to be the best for far field noise reduction in 3:1 and 4:1 elliptic jets. The minor-axis side of the 3:1 and 4:1 plain jets shows a reversal in noise trend relative to 2:1 jet. Shock associated noise increases significantly along minor-axis side with aspect-ratio with a simultaneous reduction along major-axis side due to Mach disk

emergence in these aspect-ratio jets. Notches drastically bring down the noise along minor axis ends of 3:1 and 4:1 jets but influences only slightly along major-axis ends. However, for 2:1 jet, notches influence noise levels significantly along major-axis side.

Synopsis

Introduction

Research in the field of jets primarily stemmed from two important considerations, namely, (1) to gain an insight into the jet flow field/structure in order to have an understanding of the physics governing the mixing process and (2) to control these mixing process for the purpose of enhanced mixing and noise reduction. Understanding the physics governing the mixing processes associated with mixing enhancement and noise generation and reduction is crucial to the success of many applications. Control may be defined as the ability to actively or passively modify the development of the mixing processes by directing the available jet energy into selected turbulent scales. Active controls employ external forcing or energy external to the energy of the jet to modify its development and mixing characteristics, e.g., acoustic forcing, suction and blowing etc. Passive controls, on the other hand, use the existing energy to achieve control by special circumstances, e.g., boundary conditions, feedback loops, asymmetry of the jet evolving geometry etc. The most commonly employed passive control is the use of non-circular exit geometries(three dimensional jets)[1, 2, 3, 4, 5, 6], tripping of the boundary layer by using tabs and notches(axial vorticity)[7, 8] and shock shear layer interaction[9].

Mixing is governed primarily by streamwise and cross-stream large-scale vortices[10]. It becomes a matter of primary concern when the jets evolving are in high compressible range where the large-scale structures result in reduced entrainment and hence lower gross mixing[11]. In contrast, streamwise vortices seem to be much less affected by compressibility[12, 13]. In underexpanded jets, streamwise vortices are generated without any external device or force[14, 15]. Further, the interaction of large-scale structures with the periodic shock cell structure results in the generation of broadband shock associated noise. Noise generated by this mechanism can propagate upstream and excite the initial shear layer which in turn can enhance mixing. Screech, which is a pure tone noise, is generated when this feedback loop is created. Overall, the modifications that affect the mixing process of jet will also affect the noise generation and vice-versa[10]. The complexities involved in the shock shear layer interaction make theoretical studies on underexpanded jet flow field very difficult. Hence, for proper understanding of such

flows fields an experimental investigation was carried out on sonic and underexpanded jets in the present study. The studies are primarily aimed at observing the changes introduced in mixing and noise characteristics with notch presence in both circular and elliptic slot jets.

Flows from modified axisymmetric nozzles have been studied by Pannu and Johannesen[8], Norum[16], Wlezien and Kibens[17] and Krothapalli *et al*[18] in supersonic jets and by Longmire *et al*[19] in subsonic jets. The pressure relieving effect of these notches/fingers have been observed to weaken the downstream shock development considerably. All these researchers report enhanced mixing and reduced screech and overall sound pressure levels. A part of the present study focuses on modified circular slot jets. The modifications are in the form of notches placed along a diameter of circle. Slots have been used since the effect of notch geometry is to be investigated. For this, as pointed out by Hussain and Husain[1], the initial flow conditions must remain the same. Since slots have negligible boundary layer growth in them, jets issuing from slots are preferred. Notch presence in an otherwise circular slot induces slight aspect-ratio in the modified slot and hence, are expected to behave like non-circular jets. This may be expected to enhance mixing and noise characteristics in modified circular slots.

Another way of passive control is the use of non-circular exit geometries. These jets bring about axial distortions in the development of the jet. Small aspect-ratio(2:1) elliptic jets have been found to have higher entrainment characteristics than plain axisymmetric jets[20]. Techniques that can accentuate the asymmetry of these vortices are expected to promote entrainment. The second part of the thesis focuses on this aspect. Notches are introduced along the minor-axis sides of 2:1 ellipse to further enhance mixing in that plane. The resulting modified elliptic slot is expected to significantly alter the evolution and deformation of the vortex structures. At underexpanded conditions, this may significantly alter the noise mechanism in modified ellipse and hence help reduce the shock associated noise.

The last part of the thesis deals with investigating the effect of aspect-ratio on the mixing and noise characteristics of elliptic slots. The study is an extension of the study on small aspect-ratio elliptic slots to 3:1 and moderate aspect-ratios 4:1. Further, the effect of notch presence in each aspect-ratio is also studied.

Effect of Notch and Notch Geometry on the Mixing and Noise Characteristics of Free Jets from Circular Slots: The effect of notch presence in a slot geometry with uniform

azimuthal curvature variation, i.e., circle, is investigated first. A direct comparison of the results from modified circular slot jets is made with an equivalent plain circular jet. The presence of notch makes the circular slot slightly non-circular(with slight aspect-ratio) thereby inducing axis-switching phenomena in modified circular slots. This causes the notched/modified jet to spread more in the unmodified plane. As such all the notched/modified circular jets show enhanced mixing characteristics relative to the plain circular slot jet, with higher entrainment(i.e., bulk mixing) and faster centreline decay. At underexpanded conditions, the notched/modified circular slots exhibit slightly weakened cell structure. Screech tones are observed to get reduced by 3-5dB. Overall sound pressure level are observed to get reduced both in radial and azimuthal directions. A comparison of the notch configurations indicate triangular notch the best for screech tone reduction whereas square notch seems to be the best for reduction of shock associated noise.

Effect of Notch and Notch Geometry on the Mixing and Noise Characteristics Free Jets from 2:1 Elliptic Slots: Calculations were carried out to study the changes introduced by notch presence in an exit geometry with non-uniform, smooth azimuthal curvature variation, i.e., ellipse with aspect-ratio 2:1. The study relies, once again, on mean flow and noise characteristics of plain and modified elliptic slots. The notch presence in the minor-axis plane greatly influences the jet growth in that plane. The pressure relieving effect of notches increases the spread in the notched plane relative to plain ellipse. This causes the notched/modified ellipse to switch axis earlier. As a result, the notched /modified elliptic jets show higher mixing characteristics as shown by higher entrainment(i.e., bulk mixing) and shorter core-lengths and faster jet decay. Triangular notch shows the best mixing characteristics of all notch configurations. When operated at underexpanded conditions, the modified ellipse with sharp cornered notches indicate significantly weakened shock structure. This plays a vital role in the far field noise reduction of these jets. Triangular notch shows drastic reduction in screech tone and square notch in broadband shock associated noise. In azimuthal directivity, major-axis side of plain ellipse is observed to radiate noise significantly lower than minor-axis side. Notches drastically bring down the noise radiated along major-axis ends. Square notch seems to be the best for overall shock noise reduction.

Effect of Notch Geometry and Aspect-ratio on the Mixing and Noise Characteristics of Elliptic Slot Jets: An extension of the experiments on 2:1 ellipse were carried out to investigate the effect of aspect-ratio with and without notch presence. The aspect-ratio ranged from 2:1 to 4:1. For plain cases, 2:1 jet shows better jet characteristics than 3:1 and 4:1 jets. The use of sharp cornered notch seems to have a greater influence on 2:1 and 3:1 jets with triangular notch favouring 2:1 ellipse and square notch favouring 3:1 case. However, for higher aspect-ratio, i.e., 4:1, absence of sharp corners in a notch, i.e., semi-circular, seems to be favourable. The notch presence significantly weakened the shock structure in all aspect-ratios with 4:1 notched/modified ellipse showing the weakest shocks. Triangular notch brings down the screech tones in all aspect-ratios significantly and seems to be the best for far field noise reduction in 3:1 and 4:1 elliptic jets. The minor-axis side of the 3:1 and 4:1 plain jets shows a reversal in noise trend relative to 2:1 jet. Shock associated noise increases significantly along minor-axis side with aspect-ratio with a simultaneous reduction along major-axis side due to Mach disk emergence in these aspect-ratio jets. Notches drastically bring down the noise along minor axis ends of 3:1 and 4:1 jets but influence only slightly along major-axis ends. However, for 2:1 jet, notches influence noise levels significantly along major-axis side.

Contents

Nomenclature

D_e	equivalent diameter of plain and notched slots
f	predicted frequency of screech tone
L_a	semi-major axis length of plain elliptic slot
L_{avg}	measured average shock-cell length
m	local mass-flux
m_e	mass-flux at the slot exit
M	local Mach number
M_j	Mach number obtained by correctly expanding an underexpanded jet
OASPL	overall sound pressure level
P_a	atmospheric pressure
P_e	pressure at slot exit
P_0	settling chamber pressure(gauge)
P_t	pitot pressure in subsonic flow conditions
P_{t2}	stagnation pressure behind the standing bow shock in front of the pitot tube
ϕ	azimuthal angular variation
θ	polar angle
St	predicted Strouhal number of screech tone
U	local flow velocity
U_c	local centreline velocity
X	co-ordinate along jet axis
Y	transverse co-ordinate parallel to notched plane(shown in Fig. 3.4)
Z	co-ordinate parallel to the unnotched plane(shown in Fig. 3.4)
$r_{0.5}$	half-width along Y and Z-directions

List of Figures

Chapter 1

Introduction

1.1 Applications of Jets

Research in the field of jets in order to gain insight of the flowfield/structure has been the focus of study to experimentalists since 1940's. Jets find a wide range of applications both in industry and domestic life and its use in the modern world with improved technology, they have become very vital in certain fields.

In industry, jets find widespread applications in high-speed metal cutting procedures, air-conditioning systems,...etc. However, their most significant application, requiring control of mixing, is in the field of Aerospace Technology where they form an important part of the exhaust system of aircraft propulsion units, in powered lift producing devices during the hovering phase of tilt-rotor aircraft, V/STOL or during any high angle of attack operation, etc. In mixing devices such as combustion chambers, chemical reactors etc., they are required to enhance the mixing between reactants at molecular level, a condition necessary for an efficient chemical reaction. At macro levels, however, they are required to sustain combustion processes. In reacting flows, flame stability and heat release are closely related to the interaction between fluid dynamics and combustion[21].

Frequently the jet geometry is dictated by the nature of application. In most cases, the designer wishes to use a configuration that ensures rapid mixing of the jet flow from the nozzle with the surrounding fluid. The various technical applications of supersonic jets can be outlined as:

- **Supersonic Combustion and Noise Suppression**

  With the increasing interest in the oncoming Supersonic Transport(SST) projects and renewed interest in the Supersonic Combustion Research(SCRAMJET development program), the study of the jet characteristics and its related problems have received considerable attention and enthusiasm. These two projects, in which supersonic mixing is important, face two major challenges: firstly, reducing the supersonic jet noise in the SST or HSCT(High Speed Civil Transport) aircraft, and secondly, designing an efficient propulsion system for the hypersonic air breathing engine. In SCRAMJETS, required for the hypersonic aircraft, heat is added to the oncoming airstream by means of either fuel-rich products or direct fuel injection, which results in simultaneous mixing and burning[22]. While supersonic shear flows have inherent low mixing rates, due to increasing compressibility effects[23, 24] requiring a long distance for complete mixing, a drag consideration at high speed makes a shorter combustor length desirable, thereby affecting the performance of the entire vehicle system[22].

- **Ejectors**

  Ejectors find application in thrust augmentation devices and/or noise suppression devices for aircraft applications.

- **Thrust Vector Control**

- **Stealth Capabilities**

  With the air-to-air warfare becoming more complicated with the induction of sophisticated weaponry and radar systems, the aircraft designer, these days is also concerned about the stealth capabilities of modern fighter aircraft. As such they are more inclined towards the use of complex nozzle geometries such as a wide, thin nozzle rather than a circular one[25]. These nozzles generally provide a reduced radar signature as well as a much reduced infrared(IR) signature[26] which is of prime importance since most of the short range air-to-air and ground-to-air missiles rely upon infrared(IR) sensors. The best way, therefore, is to reduce the infrared signature/detectability by cooling the engine

exhaust temperatures through a shortest distance possible[25]. This, in turn, requires rapid mixing of hot gases with the ambient air through improved nozzle design and by employing mixing techniques at nozzle exit[25]. This also helps to reduce far-field noise[26].

- **Metal Deposition**

  To produce fine powders of reactive metals such as Aluminium, Magnesium, and Titanium with uniform size, a supersonic coaxial jet of inert gas can be discharged over a laminar center jet containing molten metal resulting in atomization of metal.

Means should, thus, be explored to achieve fast mixing and as such the underlying process of supersonic mixing must be well understood and carefully controlled. The most challenging task till date remains the suppression of noise of a supersonic/underexpanded jet. However, in addition to noise reduction other characteristics like minimal thrust loss and higher mixing rates should be maintained. Before discussing the various problems of mixing enhancement and jet noise both in subsonic and supersonic regimes , it is essential to have a brief understanding of the structure of jet which plays a dominant role in the mixing and noise mechanism of both subsonic and supersonic/underexpanded jets.

1.2 The Development and Structure of a Free Jet

A free jet may be described[27] as a free shear-layer which on exiting from the nozzle spreads in such a fashion that the ratio X/d at any x-location remains constant, where 'X' is any axial location and 'd' the local diameter of the jet. The free shear-layer is driven by momentum introduced at the nozzle exit[28]. Immediately on exiting the nozzle the outer shear-layer tends to roll-up due to initial instabilities and then breakdown to form vortices. These vortices carry irrotational ambient fluid into the jet and thereby induce mixing at macro-level(bulk-mixing) by wrapping the ambient fluid about themselves. As a result there occurs an exchange of momentum between the jet fluid and the ambient irrotational fluid as the jet propagates downstream. As such, the vortices grow in size as they move downstream and hence, the jet spreads sideways with the thickening of the mixing region. At some distance from the nozzle exit

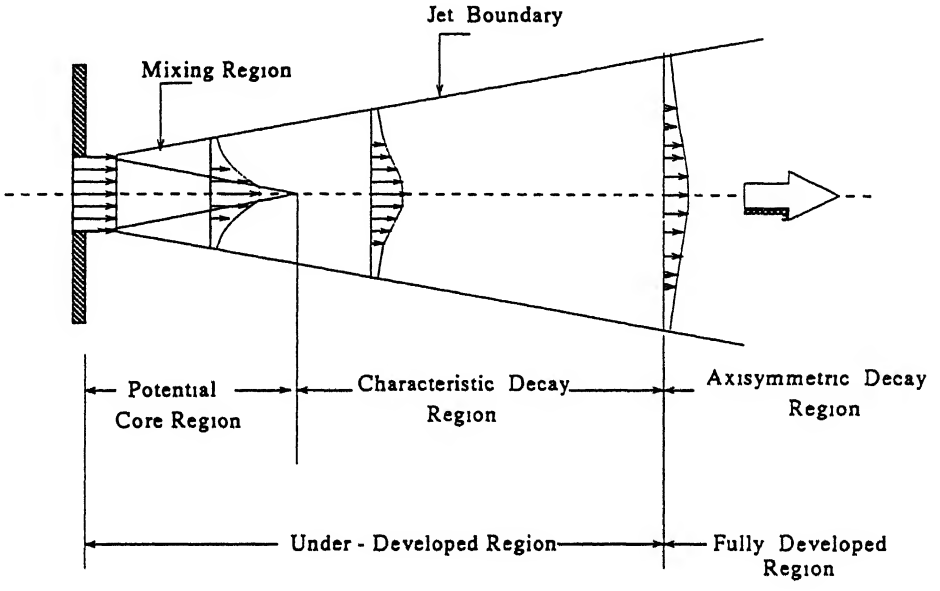

Figure 1.1 Schematic of an incompressible jet regions

plane, the mixing region is wide enough to penetrate the centreline of the jet. Up to this point, the centreline velocity is unaffected by the mixing and remains equal to the jet exit-velocity. Thus, the zone bounded by the two mixing regions where no mean velocity gradients exist is called the *Potential Core*. A more precise definition of the potential core-region has been given by Sforza *et al*[29] as the region in which the mixing initiated at the jet boundaries has not yet penetrated the entire flowfield, thus leaving a region that is characterized by a constant axis velocity close to the jet exit velocity. A schematic diagram of the structure of the free jet as it grows downstream is shown in Figure 1.1.

The length of the potential core has been found[29] to vary with nozzle exit geometry because the formation of this region is influenced by the lateral extent of mixing originating at the boundaries of the nozzle. Immediately downstream of the potential core-region is the *Transition[27]/Characteristic[29] decay region*. In this region the mixing initiated to the centreline velocity is completed so as to result in a smooth velocity-profile with a drastic decay in the centreline velocity. This region is the beginning of the growth of small-scale turbulence in the jet[28]. Thus, the initial growth of the jet(upto 10D, where 'D' is the nozzle exit diameter)

is controlled by the coherent structures formed near the boundaries of the jet[11, 28]. In the axisymmetric decay region the velocity profiles attain similarity and the jet decays oblivious of initial exit geometry[29].

So broadly speaking, the jet structure essentially comprises of two regions; *underdeveloped*(comprising of the potential core region and transition zone) and *fully developed regions*. The developing and the developed regions of the jet are characterized by the presence of large-scale organized motions and fine-scale random motions, respectively. The large-scale motions are known as *Coherent Structures* and are responsible for the transport of mass, momentum and heat without being highly energetic themselves. These large-scale structures play a central role in the growth of the jet. Whereas *incoherent structures*[11](i.e.,fine-scale random motions) are associated with high-levels of kinetic energy and are responsible for mixing at micro-levels ,i.e., in initiating fine-scale turbulence and hence, molecular contact[11]. The underdeveloped region is characterized by a faster moving inner shear-layer and a slower moving outer shear-layer. Further downstream, the faster moving shear-layers fragment. This is in turn an essential attribute to the initiation of a chemical reaction.

A supersonic jet has some basic differences in it's structure relative to its subsonic counterpart. However, the structure of a supersonic jet is determined by the type of the jet nozzle used. When a jet is operating from a convergent nozzle and is desired to operate at supersonic speeds, it is necessarily underexpanded. It is well known[30, 31] that the structure of a choked underexpanded jet has features different from those of subsonic and ideally expanded supersonic jets. These features include discrete tones in the sound spectrum, known as screech tones, and the presence of a repetitive shock-cell system[32, 33]. However, in a convergent-divergent nozzle, the jet can be supersonic and shock-free when it is correctly expanded and when the nozzle is operated at the "design" pressure ratio that corresponds to the nozzle expansion ratio. When the jet is operated at less or more than the design stagnation pressure, the jet is over or underexpanded, respectively. The shock-cell structure is present in both operating ranges, and the shock-associated noise is always emitted in addition to jet mixing noise[33, 34]. Thus, in supersonic over or underexpanded jets, the shock-structure determines the evolution of the jet. As a result of the presence of shock-cell system close to the nozzle exit, the potential core-length in an over or underexpanded jet is taken as the distance from the nozzle exit to the point up to which the shock-cell pattern exists. The remaining regions of the jet are the same

as in the case of incompressible jets.

Thus, the state of the flow as it leaves the nozzle plays a dominant role in the growth of the jet structure and it's characteristics.

1.3 Subsonic and Supersonic Jet Noise

Both the small-scale and the large-scale structures are capable of generating noise. The relative importance of the noise they produce, however, depends to a large extent on the jet Mach number and temperature. For subsonic jets, the turbulence convection Mach number(relative to the speed of sound) is subsonic unless the jet is very hot. As such, the large turbulence structures are ineffective noise generators in these jets. The dominant part of the subsonic jet noise is produced by the fine-scale turbulence.

On the other hand, for supersonic jets, especially high temperature jets, large-scale structures propagate at supersonic Mach number relative to the speed of sound. As a result they produce intense Mach wave radiation. This Mach wave radiation easily predominates over the noise from fine-scale turbulence, making the large-scale structures the dominant noise source of supersonic jets. Since most of the supersonic jets are imperfectly expanded, a quasi-periodic shock-cell structure is formed in the jet plume. This causes the radiation of additional noise from the jet. As such, shock-associated noise consists of two components:(i) One with discrete frequency,*screech*,and (ii) the other, *broadband shock-associated noise*. These two components make supersonic jet noise distinctly different from that of subsonic jets. The details of the noise from both subsonic and supersonic jet will be dealt with in detail in the later sections.

1.4 Mixing Enhancement Techniques

The existence of large-scale structures in the shear layer and their relation to flow instability make it possible to control the development of shear layer and hence, affect it's mixing characteristics. The various mixing control methods usually employed are broadly classified into two types:

- **Active Control**

  Such controls use external forcing or energy external to the energy of the jet to modify

its development and mixing characteristics. The flow in this case can be excited by mechanical means such as fluctuating flaps, vibrating ribbons, acoustical perturbation, suction and blowing etc.

- **Passive Control**

  Such controls use geometrical modifications of the element from which flow separation occurs to change the shear layer stability characteristics. These controls can be further classified into three types:

  (i) *Three-Dimensional Jets:*

  In such jets, the fluid properties vary along both Y and Z-directions in the plane of the jet, e.g, slot jets; rectangular, elliptic, triangular, square; multistep jets and others like crown shaped, beveled and fingered nozzles. As such, these jets bring about axial distortions in the development of jet giving rise to enhanced mixing characteristics. Also the highly curved flow at the corners helps augment strong vortex bending in addition to the small-scale turbulence initiated by the axial vortices formed in the corners inside the nozzle[2, 3]. This vortex bending and self-induction process increases the spreading rate of the jet at the flat sides. This combination of large-scale structures providing bulk mixing and fine-scale mixing contributing to the reaction rate and better flame holding characteristics makes these non-circular jets advantageous for combustion systems as well[4].

  (ii) *Axial Vorticity:*

  This concept involves the introduction of discontinuities in the exit plane of the jet so as to produce an array of streamwise vortices thereby distorting the cross-sectional shape of the jet as it grows. Such an arrangement results in improved mixing. For example, tabs, notches, tapered slot nozzle, lobed nozzle, ramp nozzle and swirl etc.

  (iii) *Shock-Shear Layer Interaction:*

  Shock waves generated in a plane perpendicular to the mixing layer can interact with the flow separating at the splitter plate tip to produce a streamwise vortex that enhances the mixing rate of shear layer[9].

;ing Mixing Enhancement

:rs effecting mixing enhancement in jet fields:

:ic fluctuations, and pressure matching at the nozzle exit.

for particular techniques may depend on the convective
echanisms that augment the mixing are also affected by

ıt

oundary layer characteristics thereby reducing the core
ssure gradient can create baroclinic torque which induces
gross distortions[36].

Chapter 2

State of the Art of Free Jet Studies

2.1 Introduction

The first monograph on turbulent jets written by Abramovich[27] came out in 1936 and dealt solely with free submerged jets, i.e., jets spreading into a medium at rest. Since that time, the theory of the turbulent jets have been enriched with a large amount of experimental material and has been applied in different branches of engineering.

Turbulent jets have been the subject of experimental research since 1940's. Early investigations reported distributions of mean properties such as velocity and pressure. Later, the availability of hot-wire anemometry led to the time resolved measurements performed by many researchers. These measurements provided in depth information about the structure of plane jets[37, 38]. More recent studies performed using Laser Doppler Anemometer revealed the existence of flow reversals and provided further information about the mechanics of the jet boundaries[39].

2.1.1 Subsonic Shear Layers

Experiments carried out by Roshko[11] in incompressible range have revealed the presence of large-scale structures which have the appearance of breaking waves or vortices. An early flow visualization study by Brown and Roshko[40] revealed that this breakdown process and vortex formation occurred alternatively on the two sides of the jet and that these large-scale structures control the dynamics of all free shear flows including plane mixing layers, jets of

different geometries and wakes. The formation of coherent structures in the shear layer is initiated by Kelvin-Helmholtz instability, governed by Rayleigh's equation for inviscid flows. The exponential growth of velocity and vorticity perturbations leads to a non-linear process that eventually causes the roll-up of the shear layer into vortices. The initial vortex shedding frequency is determined by various characteristics of exit velocity profile, such as shape, turbulence structure, initial shear layer momentum thickness and jet exit velocity. This vortex shedding property was found to be a function of Reynolds number based on nozzle exit diameter, Re_D, and the axial distance. The shedding process is also found to play a dominant role in the acoustics of the jet as the exit velocity ranges into the supersonic regime. At low Reynolds numbers, small-scale turbulence is largely absent[11]. However, at larger Reynolds number values, small-scale eddies have been observed to be superimposed on the large-scale, two-dimensional motion. The mean flow is controlled by the large, organized structures and remains unaffected by the appearance of small-scale turbulence at higher Reynolds numbers. This large-scale external mixing is known as the entrainment process. A fundamental property of turbulent shear-flow, related to its growth, is the phenomena of entrainment which has been defined[11] as the incorporation of non-turbulent, usually irrotational fluid into the turbulent region or, conversely, the diffusion of turbulent region into the ambient flow. The initial vortices grow in the shear layer and coalesce as they are convected downstream in a "pairing" process [41, 42]. Figure 2.1 shows the process of growth of shear layer by vortex pairing as observed by Roshko[11].

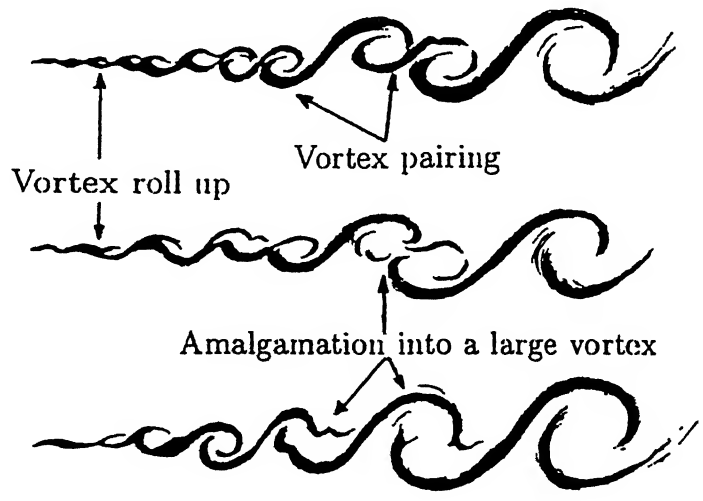

Figure 2.1: Process of growth of shear layer by vortex pairing

In pairing, the neighbouring pair of vortices rotate around each other and amalgamate into a larger one. Due to merging and entrainment, the shear layer spreads and the frequency associated with large-scale vortices decreases. The entrainment of irrotational mass by the large-scale structures leaves the entrained fluids essentially unmixed during the lifetime of vortices[43, 44]. However, intense mixing occurs during pairing or other amalgamation processes. The further breakdown of these large-scale eddies into smaller eddies (resulting in turbulence) is merely a stage in the dissipation of energy[11] that has been extracted from the mean flow. Once the large-scale coherent structures are completely broken into small-scale eddies(incoherent structures), the jet is said to be fully-developed[28]. It has been found[28] that in the initial region the local entrainment depends upon the axial distance but is constant for the fully-developed region.

The growth of the jet, therefore, is closely related to the entrainment process. The rate of growth and hence a qualitative measurement of the entrainment can be made by the jet half-width[45] which may be defined as the transverse distance from the jet axis up to which the local velocity reduces to half the centreline velocity.

While the coherent structures are beneficial in enhancing large- scale mixing, they, however, prevent fine-scale(molecular) mixing, particularly during the initial vortex development process[46]. In the final stages of vortex roll-up process, fine-scale mixing is increased by vortex break-up initiating the reaction and leading to sudden heat release. An earlier increase of small-scale mixing is, therefore, important to prevent the periodic heat release that follows the vortex roll-up process and to obtain higher initial temperatures, before the air, entrained into the reaction, cools down the reaction products[46].

2.1.2 Supersonic Shear layers

Supersonic shear layers spread or mix at a slower rate than their subsonic counterparts due to compressibility effects introduced at high Mach numbers[47, 10, 24]. The compressibility level is best described by a parameter called the *"Convective Mach Number(M_c)"*[48, 23]. This parameter is defined as the relative convective speed of the large-scale structures in the shear layer to one of the free stream, normalized by speed of sound of that stream[4, 22]. Therefore, if U_1 and U_2 are the mean velocities of the two streams, than the respective convective Mach numbers are given by $M_{c_1} = (U_1 - U_c)/a_1$ and $M_{c_2} = (U_2 - U_c)/a_2$, where U_c is the convective

velocity of the structures and 'a' is the speed of sound. These convective Mach numbers are equal to each other in shear layers with equal static pressures and specific heat ratios in the two streams. Under such conditions,

$$M_c = \frac{(U_1 - U_2)}{a_1 + a_2}$$

For $M_c < 0.5$, supersonic shear layers exhibit characteristics of an incompressible shear layer with two-dimensional organized structures[9] with a braided structure between the vortices However, vortex pairing typical of incompressible shear layers was reported[49] at M_c=0 51 and not at M_c=0.86. As the convective Mach number increases, the mixing layer becomes highly three-dimensional with nearly indiscernibly organized two-dimensional structure[49] due to a non-linear interaction of axisymmetric and helical modes. One potential mechanism for the stabilization of the compressible shear layer relative to incompressible flow is the suppression of upstream and cross-flow communication paths within the shear layer due to high Mach numbers[49]. Also the density gradients in compressible shear layers, coupled with large pressure gradients across shocks, produce vorticity due to baroclinic torque, uncommon to incompressible shear layers. Schlieren study has revealed[23] that the structures get elongated and tilted with high speed flow, without evidence of vortex pairing.

2.1.3 Supersonic Jets

When a supersonic jet operates at off-design conditions, the interaction between the expansion/compression waves and the jet shear layer can result in increased jet spread[50]. Increasing the level of pressure mismatch causes large variations of the jet spreading rate and internal structure. This behaviour is attributed to an acoustic feedback formed by sound waves that originate at the downstream section of the jet during shock/shear layer-vortex interactions. Chuech *et al*[51] reported that compressibility effects at M_c >0.5 reduce the mixing rate of an underexpanded jet, thus, increasing the length of the shock-wave containing region. Increasing the turbulence level at the jet exit has an opposite effect.

As such, means have to be explored to enhance mixing in both subsonic and supersonic jets for the efficient functioning of the system in which they are installed as per the need of

application. Various of mixing enhancement techniques have been tested by experimentalists. The following sections give a brief outline of the efforts focused on this topic in literature.

2.2 Mixing Enhancement

The technological challenge of mixing enhancement in compressible flows stems from the inherently low growth rates of supersonic shear layers. The study of compressible shear layers have built on the knowledge accumulated in the subsonic flow research. The discovery of large-scale coherent structures in subsonic shear layers and in underexpanded supersonic jets[52, 14, 15]and their importance to mixing process led to the development of numerous mixing control techniques.

Each of these techniques will be discussed separately starting with early research in subsonic regimes to recent supersonic mixing control. Emphasis has been given to passive control techniques since it is directly related to the present topic of research work.

Various methods have been devised to alter the mixing characteristics of the jet as it leaves the exit plane as per the mode of application of jet. On these basis, the mixing enhancement methods are broadly classified into two categories, namely, the *Active* and the *Passive* methods.

2.2.1 Active Control

Active controls use external forcing or energy external to the energy of the jet to modify its development and mixing characteristics. The most popular active method is the use of acoustic energy (i.e., sound waves). To maximize the effect, the external perturbation should match the flow instability band to take advantage of the natural amplification of the flow as shown by Crow and Champagne[53]. Sound waves at particular frequencies have been reported in literature to greatly alter the growth of the jet. Hussain and Hussain[1, 54] used a loud-speaker arrangement in the settling chamber to alter the characteristics of incompressible elliptic slot jets. He observed that at a particular frequency, the sound waves profoundly affected the axis-switching location and spread of the jet. Such observations have also been made in the supersonic regime by Pimshtein[55] where the sound waves were made to break the acoustic feedback loop outside the nozzle and alter the jet characteristics. Tam[56] used external excitation in the form of sound and found that a narrow beam aimed at an angle of 50^o to 80^o to the flow direction was most

effective in exciting instability waves. Some similar observations were made by Lepicovsky *et al*[57] where an internal acoustic excitation in both subsonic and low supersonic jets resulted in faster velocity decay along the jet axis.

However, such active controls of jets for the purpose of enhanced mixing characteristics in both subsonic and supersonic regimes require extensive external excitation mechanisms which are, therefore, not feasible in applications involving hot gases, e.g., in exhausts systems of aircrafts and combustion chambers etc. Also, for hot flows existing inside combustors it is preferable to use passive means[58] since such control techniques generally use geometrical modifications of the jet exit surfaces for mixing enhancement.

2.2.2 Passive Control

Such controls use geometrical modifications of the element from which flow separation occurs to change the shear layer stability characteristics or in other words such controls use the energy of the jet itself to alter its mixing characteristics. Various methods of passively improving the jet characteristics have been reported in literature. The first and the foremost method makes use of non-circular geometries at the nozzle exit plane. Since jet characteristics are most receptive to changes in initial conditions, exit geometry variation plays a dominant role in the development of both low and high-speed jets. Thus, to study the effect of initial geometry alone on the development of the jet, jets issuing from slots or orifices are preferred[59, 1]. Other means include the use of intrusive mechanical devices and non-intrusive(e.g, cavities, notches etc.) means in the form of notches in the periphery of the nozzle exit plane.

Since the present study focuses on passive control of elliptic jet for enhanced characteristics through the introduction of discontinuities in the exit plane the present literature survey is focused mainly on this particular aspect of mixing control.

Non-Circular or Three-Dimensional Jets

Various passive means have been investigated to increase the entrainment rates to achieve better mixing and to augment thrust. Past studies using different nozzle shapes and attachments have revealed that mixing enhancement is possible via axial vortices or three-dimensionality in the flow. Non-circular jets being inherently three-dimensional, in addition to the highly curved flow at the corners which augments strong vortex bending[2], caught the attention

of researchers. These non-circular geometries have been reported in literature [29, 60, 61, 62, 59, 1, 3, 46] to result in enhanced mixing, a characteristic making them far superior to the conventional circular jet. This is attributed primarily to the axis-switching phenomenon associated with the distortion of the large-scale vortical structures caused by the non-uniform azimuthal curvature variation resulting in a non-uniform self-induction process[63, 1]. This phenomenon is responsible for higher amounts of ambient fluid engulfed by these jets thereby, ensuring higher rates of mixing than the conventional circular jets.

An early investigation carried out by Sforza *et al*[29] on various jet orifices(circle, ellipse, square, rectangle and triangle) revealed a great dependence of the initial geometry on the jet characteristics up to the end of the characteristic decay(CD)/transition[27] region beyond which the jet tends to axisymmetry oblivious of the slot geometry. The presence of sharp corners in the form of vertices of triangular slot and aspect-ratio variation were observed to affect the potential core length. The effect is primarily due to the secondary motions(small-scale eddies) initiated at the sharp corners. Thereafter, to gain insight of the effects brought about by sharp corners in exit geometries, considerable attention was focused to understand the growth and mixing of large aspect-ratio rectangular jets. Experiments conducted by Marsters[61, 62] revealed intense turbulence activity at the corners of the jet which was observed to be responsible for enhanced mixing. Velocity peaks near the ends were observed resulting in the saddle-back profiles typical to rectangular jets. These peaks merge inwards as the distance from the exit plane increased. The peaks in turbulence observed near the velocity peaks, according to Marsters[61, 62], is probably due to the end shear-layer growing inward and interacting with the shear-layer along the long sides of the jet. Saddle-back profiles were also observed by Krothapalli[5] which, according to him, are indicative of the end of the potential core-region, and thus marks the merging of shear layers of the jet. However, the mechanism responsible for their emergence(velocity peaks) is not clearly understood[61].

Quinn[59] carried out a very detailed study of the flowfield to gain insight of the mechanisms responsible for the growth and mixing of a large aspect-ratio(20:1) rectangular jet. As carried out by Marsters, grid study at various X-locations proved beneficial to him. He confirmed that the near-field of the jet was dominated by counter-rotating pairs of streamwise vortices which facilitate enhanced mixing of the jet by acting as vehicles of transfer of high-momentum fluid to areas of low-momentum fluid and vice-versa. The off-centre peaks(i.e, saddle-back

profiles) were suggested to be due to the self-induction of the counter-rotating streamwise vortices initiated by the presence of sharp edges of the rectangular orifice. This was observed to result in change of shape from rectangular to elliptic in the far-field and hence enhanced mixing. Thus, the major effort of investigators had relied on the regular breakdown of the large-scale coherent structures to fine-scale eddies through vortex dynamics introduced by azimuthal instabilities in the exit plane.

Since sharp corners were observed in large aspect-ratio rectangular jets[61, 62, 5, 59] to enhance mixing at micro-levels, efforts were made to introduce acute angled corners in the exit geometry. Improvement in the flowfield were observed by Gutmark[3] in triangular jets wherein the small-scale eddies shed from the sharp corners induce turbulence near the exit plane thereby interacting strongly with the large-scale vortices shed from the plain sides. The jet orifice geometries that were studied included an isosceles triangle with an apex angle of 30 degrees, an equilateral triangle and a square.

The special features of these nozzles were tested in reactive flow of square and triangular flames[46]. The flow behaviour observed in cold flows was observed to affect the results in reacting tests. The investigations revealed that the highly turbulent flow at the corners helps initiate the reaction close to the nozzle exit, which increases the local temperature of combustion products(due to reduced entrainment by fine-scale eddies). On the other hand, the large-scale mixing at the flat sections provides the necessary amounts of air to sustain combustion. The difference between the two flame sections was observed by Gutmark *et al*[46], to be more pronounced for smaller corner angles. Later, they extended their study to sonic and supersonic underexpanded jets[4]. They observed that the structure of the sonic non-circular jets with corners is similar to the subsonic one. In supersonic underexpanded jets, the shock structure determines the evolution of the jet due to asymmetry of expansion waves originating from the flat and vertex sides of jet geometry. Combustion characteristics were observed to increase with decreasing corner angle with the isosceles triangle showing highest combustion intensity. However, the square jet was similar in characteristics to circular one.

As such passive means are preferred wherever efficient mixing is crucial e.g, combustion chambers, exhaust nozzles of propulsion units, chemical reactors etc. In hot flows existing inside combustors, e.g, it is preferable to use passive controls[46]. In combustion processes, efficient mixing is beneficial not only in initiating molecular contact but also in attaining the necessary

temperature over a required distance. On the other hand in combat aircrafts, enhanced mixing of high temperature exhaust with the ambience is very crucial to elude the infrared detection system so common in air-to-air warfare[25].

Due to its smooth azimuthal curvature variation,elliptic jets caught the attention of researchers. The flow here is less complex due to absence of sharp corners and as such leads to a better understanding of the development of non-circular jets[1]. Recent investigations on elliptic jets for non-reacting flows in the incompressible range[1, 58] has shed light on the details involved in its evolution. Hussain and Hussain[1] confirmed that an elliptic jet undergoes a 3-D deformation process associated with the bending of the elliptic vortex. The differential pressure along the two axis of the jet starts a pumping action wherein ambient mass is brought in towards the jet-centreline along the major-axis side and jet mass is thrown out along the minor-axis side. This self-induction process results in enhanced mixing between the jet and ambient irrotational mass[1, 20, 59, 58]. As a result the jet switches axis, entrains more fluid and spreads faster in the minor plane as was also observed for rectangular jets[59, 5]. Similar observations were made by Ho and Gutmark[20] where they concluded that the enhanced entrainment in the portion near the the minor-axis were due to the azimuthal distortion of the elliptic vortex ring. These distortions were responsible for the faster spread of the shear layer in elliptic jets.

Axis-switching has also been observed in supersonic/underexpanded elliptic jets by Gutmark and Schadow[46], a characteristic favorable from mixing and noise suppression problems in high-speed jets. The presence of large-scale structures in supersonic flows[64] have opened up possibilities of controlling the jet characteristics by regular breakdown through vortex dynamics.

Aspect-ratio is another parameter found in literature to have a profound influence on the development of jet. Hussain and Husain[1, 65] made a comparative study of the effect of aspect-ratio and observed that for a given equivalent diameter, D_e, aspect-ratio is an important parameter controlling the deformation and topological changes,i.e., bifurcation, of large-scale vortical structures in elliptic jets and that the dynamics of low aspect-ratio jets are basically different from jets of moderate to high aspect-ratios. For a low aspect-ratio elliptic jet, the deformation as well as the self-induced inward and outward displacement of parts of elliptic structures are small. Whereas they are higher for large aspect-ratios because the structures

along the minor-axis side are closer to the jet centerline[1]. As a result, in a low aspect-ratio jet, the azimuthal deformations are fast enough due to dominance of large-scale activity[5]. However, in high aspect-ratio jet, when the distortion becomes appreciable, the vorticity has already diffused. And since, entrainment of mass-flow is due to large-scale activity, a low aspect-ratio jet shows higher bulk mixing[20]. Axis-switching location is found to be a linear function of aspect-ratio in elliptic and rectangular jets[1, 5].

Axial Vorticity

Tapered Slot Jets

Though non-circular configuration itself is found to be a very efficient passive device efforts have been made to further enhance the jet characteristics through additional passive means. For reacting flows, Gutmark *et al*[58] was able to enhance small-scale mixing in the near-field by introducing a contraction before an elliptic slot of aspect-ratio 3:1. The arrangement generated a three-dimensional vorticity component when changing shape from conical to slot geometry. This additional vorticity component was observed to interact with the initial circumferential vortices to distort their coherence and hence, increase small-scale activity both in the core-region and jet circumference. Unlike the usual elliptic jet, the jet is found to spread more in the major-axis plane with no axis-switching.

Intrusive Methods

In addition to the use of non-circular exit plane geometry, means were also developed to interfere with the growth of the shear-layer by the use of intrusive means in the nozzle periphery to enhance fine-scale mixing in conventional geometries. The streamwise vortices thus generated provide the necessary secondary instabilities and alter the flow field significantly. Gross distortions in the jet structure have been observed using intrusive means in circular jets e.g, tabs both in subsonic[7] and supersonic regimes[66, 16, 67, 68]. Bradbury[7] observed that the introduction of rectangular tabs in the nozzle perimeter that protrude into the flow(with area blockage of 1-2 percent per tab)introduce circumferential variations in the jet flow angle and produce profound effect on the jet development by splitting the jet into two high velocity regions on either side of the diameter joining the two tabs. The gross distortions brought about increase in entrainment into the jet. They observed that the most effective configuration consisted of

two tabs. Later, enhanced mixing and reduced noise were observed using tabs in supersonic flows[49]. The tabs were observed to improve mixing in the shear layer surrounding a sonic and supersonic underexpanded jet potential core[12, 13, 69, 70]. For a tab to produce an effective streamwise vorticity, a favourable pressure differential must exist across the tab as is the case in underexpanded cases. However, the adverse pressure jump at the nozzle exit(as in the case of overexpansion) dilutes the pressure differential created by tab making it less effective for this case[12]. Tabs were also observed to drastically weaken the shock structure accompanied by noise reduction[71]. The tabs in this case were placed inside the diverging section of a Mach 2 converging-diverging nozzle. It was observed that the shock produced by the tabs interacted with the jet flow resulting in a baroclinic torque(i.e., when density and pressure gradients are not aligned). Reduced noise levels were also observed by Tanna[66], Norum[16], and Norum and Seiner[68]. Introduction of tabs in supersonic jets help weaken the shock-structure considerably and hence eliminate screech as seen by Norum[16] and Krothapalli[67]. However, the use of tabs does effect the overall thrust. As such non-intrusive means are preferable.

Non-Intrusive Methods

According to Powell[30], the best way to weaken the shock-structure in the near-field and hence enhance mixing close to the exit is by relieving the excess pressure at the nozzle exit by means of notches or fingers. This concept was later used by some researchers[8, 17, 19] to enhance mixing in underexpanded jets. A study of an underexpanded notched circular(fish-tail configuration) jet[8] revealed a much higher spread in the notched plane with the shedding of vortices from the swept edges of the notches. This vortical structure is found to act as a shielding device to the shock-structure/noise sources resulting in noise reduction. Norum[16] and Krothapalli[18] used fingers/slots in the nozzle parallel to the jet axis. The pressure relieving effect of the slots greatly weakens the shock-structure and hence suppresses screech. However, the pressure relieving effect of fingers/slots, once again results in thrust loss.

Effect of Nozzle Geometry

Modification of the nozzle geometry by introduction of azimuthal asymmetry is another technique for controlling development of high speed jets[72, 17, 73]. The various configurations tested included sliced, single and multi-tab which revealed jet vectoring, mixing enhancement

and noise reduction. Yu *et al*[22] tested a Mach 2 convergent-divergent nozzle with 5 swept ramps on its diverging sections. The shear layers of the ramp jets had significantly higher growth rates compared to those of circular jet. Flow visualization revealed well-defined, large-scale organized structures, possibly axial vortices, within the shear layer thereby increasing shear layer growth for the ramped case. Supersonic combustion test of ramped injectors revealed increased combustion rate/heat release in the near field of the jet.

The concept of baroclinic torque effect has also been used to enhance mixing in supersonic flows. It has been reported by Yu *et al*[22] that a fuel injection system in hypersonic applications used ramps to create oblique shocks that crossed cylindrical fuel jets, thereby creating the baroclinic torque in the streamwise direction resulting in increased molecular mixing. The baroclinic torque exists when pressure and density gradients are not aligned. When a shock wave interacts with a jet of different density relative to the ambient flow, e.g, a hydrogen fuel jet etc., the pressure gradient across the shock interacts with the density gradient between hydrogen and air to generate vorticity. This vorticity increases strain rates and enhances molecular mixing by diffusion[49].

2.2.3 Other Passive Control Techniques

(i) *Acoustic feedback enhancement* : Enhancement of the acoustic feedback loop responsible for the generation of screech tones in an underexpanded choked supersonic jet has been achieved by impinging the jet on a circular cylinder[74] which resulted in increased spreading rate. Elongated paddles parallel to its long dimension and near the jet edges were used by Rice and Raman[75] for enhancing the mixing rate by increasing screech level due to feedback from paddles. They also observed that blocking the feedback acoustic loop using baffles, thus suppressing screech, also affected the mixing rates.

(ii) *Interaction with flow instabilities* : Ponton and Seiner[76] studied the effect of lip thickness surrounding a nozzle on the spreading rate and sound emission characteristics of a choked underexpanded jet. Though spreading rates were altered only marginally, screech characteristics were significantly altered due to reflection of sound from thick lips stimulating the initial shear layer.

(iii) *Multiple shear layer* : Interaction between multiple supersonic jets can lead to resonant conditions resulting in increase in growth rates of jets[77]. It has been observed by Wlezien

that resonant conditions depend on the jet separation, mixing layer thickness and Strouhal number.

2.3 Jet Noise/Aeroacoustics

Since the late 1970's, steady progress has been made in understanding the noise mechanism of supersonic jets and in the predictions on their radiated noise. From practical point of view, noise reduction is probably the most important challenge of all. Improved mixing reduces turbulence and hence noise. This experience has led to the channeling of most of the current noise reduction effort into the development of enhanced mixing devices.

2.3.1 Noise from Subsonic Jets

Realization of the presence of large-scale structures in turbulent shear flows[78, 53] generated a growing interest in advancing the understanding of their role in the production of jet noise. The state of the flow as it leaves the exit plane of the nozzle plays a dominant role on the jet noise. In subsonic regime the major contributor to noise as observed by Sarohia[79] is the mixing process brought about by the growth of the large-scale vortices. Hussain and Zaman[80] argue that the subsonic jet noise is primarily the result of a breakdown of the toroidal vortical structures. They point out that the breakdown occurs at the end of the potential core, which is thought to be the region of maximum sound generation[81]. Sorohia[79] identified the role of large-scale structures in the production of noise in excited jets. The large-scale vortices were observed to approximately double in spacing which was preceded by a merging process similar to one shown for incompressible flows by Brown and Roshko[40]. The process of formation and merging was slowed down by introducing organized structures of controllable frequency and amplitude artificially. Near-field pressure measurements indicate that a single convecting organized vortex is a very weak source of jet noise. This was seen as a small change in pressure signal. However, when this organized structure interacted with another vortex nearby, a relatively rapid rising strong pressure signal was observed. The experiments thus indicated that a significant part of the near-field pressure signal was contributed by the merging of the large-scale organized structures in the jet flow. This observation is also confirmed by Ho and Gutmark[20] for subsonic elliptic(2:1) jets. Thus, if the merging process among organized

structures are subdued, jet noise reduction can be achieved. This in turn is related to the breakdown of these structures into small-scale structures.

So the state of the flow as it leaves the orifice is important in determining jet noise[82, 83], because of its influence on the turbulent mixing process. In subsonic jets, the bulk of the noise arises from the turbulent mixing of the jet. The power spectrum of a subsonic jet is characterized by a broad single maximum with no discrete frequencies showing noise purely due to turbulent mixing[30]. It has been found[30] that the frequency of the maximum does not vary with velocity and that the wavelength of the most intense noise may be of the order of 4 to 5 exit diameters. The jet issuing from an engine is more turbulent and hence, more noisy owing to the history of gases and noise from combustion, in all which adds to the aerodynamic noise of the jet. The major difference between the model jet and the engine jet is its temperature. A low density jet(i.e., a heated jet) has a much higher spread[30] and is, therefore, expected to have differences in the noise produced.

2.3.2 Structure of an Underexpanded Jet

Past investigations have revealed that the noise energy radiated from the jet may increase at a much greater rate once the pressure-ratio exceeds the critical value. The critical pressure-ratio may be defined as that at which the local speed of sound is first reached in the nozzle, i.e., the jet/nozzle is choked. Some major physical changes in the jet flow occur at underexpansion(see Fig. 2.2). The most dominating feature is the emergence of the cellular wave pattern[84, 34] in

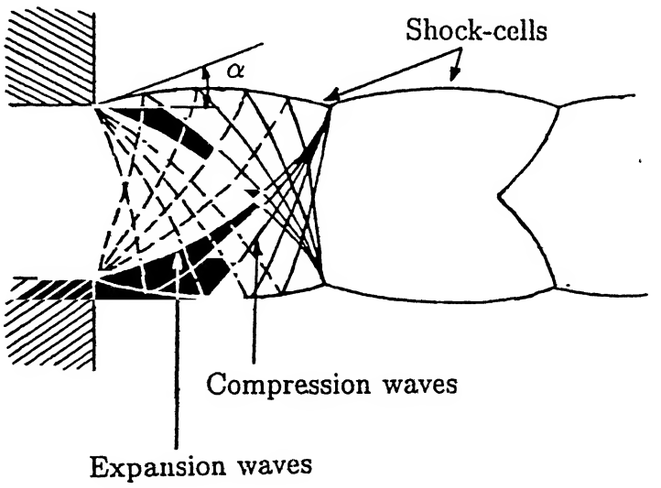

Figure 2.2: Structure of a sonic underexpanded jet

the potential core which greatly alters the jet growth and adds to the jet noise as shock-cell noise.

Under choked conditions($P_e/P_a > 1$), the flow at first expands around the corners of the nozzle(the angle of expansion being determined by the value of underexpansion level, P_e/P_a), but the reflection of the expansion waves at the constant pressure boundaries(originating at the edge of the exit) as compression waves causes the free boundary to curve inwards so that at some downstream distance the flow approaches conditions very similar to those existing at the orifice. The jet flow along the centerline undergoes maximum expansion from both sides resulting in a much less pressure than outside air. In a bid to equalize the pressure a normal shock may form replacing the tip of the conical shock. The whole process than starts afresh and would repeat indefinitely if it not for turbulence setting in from the edges/boundaries of the jet. Turbulent mixing appears to take place less rapidly than in subsonic jets so that sonic conditions at the centerline may prevail up to considerable distance from the exit. This is the main reason of reduced mixing levels and hence, low spread rates in supersonic/underexpanded jets. As such efforts need to be concentrated in breaking the process of shock-cell formation as close to the exit as possible. Passive means of achieving the same is through the introduction of discontinuities in the exit geometry, e.g, fingers for pressure relief, notches, tabs etc., so that the shear layer spreads/creeps faster towards the jet centreline.

Supersonic Jet Noise

The emergence of shock-cell structure for imperfectly expanded jets is the major source of jet noise. This noise produced as a result of jet operating at off-design Mach numbers/supercritical conditions is physically different from that produced by nozzles operating under subcritical or fully expanded conditions. In the latter case, the noise is of broadband nature[66] with a broad and a smooth acoustic spectrum consisting of purely turbulent mixing noise(and is due to small-scale eddies in the early mixing region giving rise to weak waves). The acoustic spectrum of the former contains an extra noise contribution, due to the presence of shocks in the jet flow. Thus, the shock-related noise can be divided into two distinct types, each having its own characteristic properties. The first component is discrete in nature, usually with several harmonics, and is often referred to as "screech" component. The second component is broadband in nature with a well-defined peak frequency. Figure 2.3 shows a typical narrow-band noise spectrum of an

imperfectly expanded jet[33].

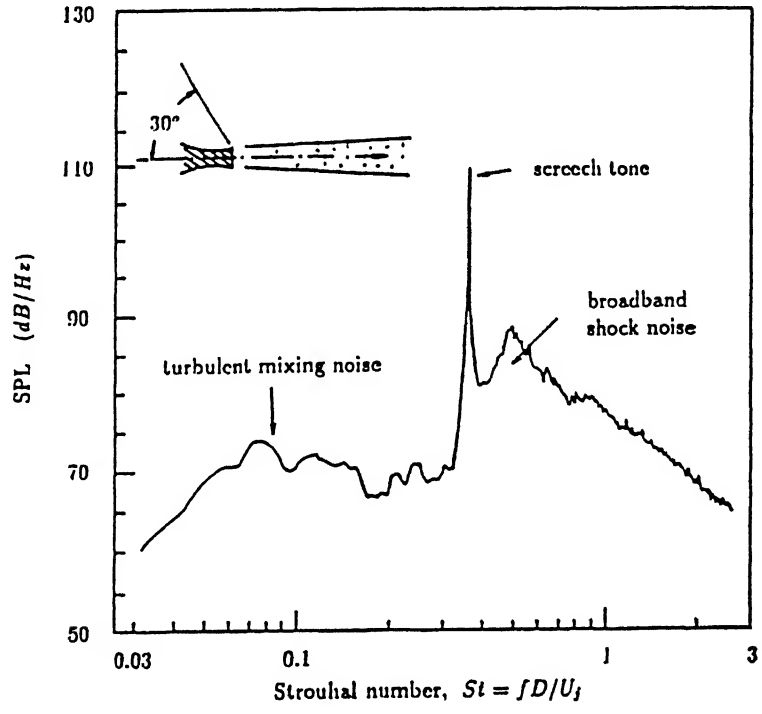

Figure 2.3: Typical far-field narrow-band supersonic jet noise spectrum

The noise from shock-containing supersonic jets consists of three principal components: turbulent mixing noise, broadband shock associated noise and screech tones. The last two sources of noise exist, of course, only when a shock cell structure is present inside the jet flow. The relative intensity of the three noise components is a strong function of the direction of observation. In the downstream direction of the jet, turbulent mixing noise is the most dominant noise component. In the upstream direction, the broadband shock-associated noise is more intense and the screech tones radiate primarily in the upstream direction.

Characteristics of Turbulent Mixing Noise

It has been suggested by number of investigators that the dominant part of turbulent mixing noise of supersonic jets is generated directly by the large turbulent structures or instability waves of jet[81, 85, 86]. McLaughlin *et al*[64, 87] showed experimentally that instability waves were the primary noise generators for perfectly expanded low Reynolds number supersonic jets. Later, Tam and Burton[88] developed a mathematical theory suggesting that the instability

waves or the large turbulent structures are the dominant noise generators in supersonic shock free jets and their theory agreed well with experiments..

Role of Instability Waves to Jet Noise

The major obstacle to a complete theory in jet noise analysis has been the identification of the fluctuations in the jet which generate the radiated sound. Lighthill's classical formulation[89, 90, 91] provided the groundwork for relating the acoustic radiation to the disturbances in the jet. The study was further extended to supersonic regime by Ffowcs *et al*[92] and Ribner[93]. Although there are many similarities between the subsonic and supersonic noise phenomenon, there are differences in the generation mechanisms which tend to be of fundamental nature. First of all, in any supersonic jet there exists a cell structure which has a controlling influence on the behaviour of disturbances within the jet. Second, the acoustic radiation emitted from the supersonic part of the jet.

The orderly structures inevitably interact with its shock cell system as they propagate downstream giving rise to disturbances which are coherent over many jet diameters and have space-time characteristics similar to those of large-scale structures, i.e., these disturbances are wave like. These disturbances may have components that are subsonic or supersonic phase velocities relative to the speed of sound. By wavy wall analogy far field signatures of subsonic components decay very rapidly as the transverse distance from jet axis increases. However, for supersonic phase components, far field signatures consist of Mach wave radiation that constitutes what is called the shock associated noise[94].

In short, the shock-associated noise is generated by weak interaction between downstream propagating large-structures and the shock-cell structure. The noise is a form of Mach wave radiation caused by the supersonic phase components of disturbances associated with the weak interaction[33].

Broadband Shock-Associated Noise

Thus, it turns out that the instability waves or large turbulence structures are also responsible for producing broadband shock associated noise as well as screech tones when the jet is operated at off-design condition[95]. Tam and Tanna[94] proposed that the broadband component is generated by the weak interaction between the downstream propagating large turbulence

structures and quasi-periodic shock cell structure of the jet. They used simple analytical models to represent large scale structures and shock cells to derive a noise intensity scaling formula and peak frequency formula which agreed well with experiments.

The spectrum of broadband shock-associated noise is dominated by a single spectral peak. This peak frequency is found to be a function of the direction of noise radiation, θ, measured from the jet flow direction. At small angles to the jet axis, the spectral peak of broadband noise is quite wide. As the observation angle is increased the width decreases and becomes increasingly narrower as the jet exit direction is approached. Thus, the peak frequency exhibits a Doppler shift phenomenon. The large turbulence structures/shock-cell interaction model by Tam[94] gives the following formula for the frequency of the n^{th} spectral peak of broadband shock-associated noise:

$$f_n = U_c \, k_n/[2\pi(1 - M_c \cos \theta)]$$

where $(1 - \cos\theta)$ is the Doppler factor

In the above equation, U_c is the phase velocity of the instability wave of frequency f_n which makes up the large turbulence structures and k_n is the wave number of the n^{th} Fourier component of the shock-cell structure. Within the framework of this model, the dominant part of the source of broadband noise is located in the region of the jet where the instability wave attains maximum amplitude.

Since both these noises are generated by the same mechanisms, Tam, Seiner and Yu[95] suggested that this noise and tones are closely related. They concluded that the screech tones could be treated as a very special case of broadband shock-associated noise. One careful observation made by them from the narrowband shock-associated noise spectrum as is seen in Figure 2.4 produced from their paper, is that fundamental screech tone frequency is always smaller than the frequency of broadband shock-associated noise. As θ(the angle which the microphone makes with the flow direction) increases towards the nozzle exit plane the shock-associated noise frequency decreases. At $\theta = 150^o$, the lowest part of the spectrum approaches that of screech tones. Thus, screech tones are limiting case of broadband shock-associated noise when θ approaches the limiting value of 180^o.

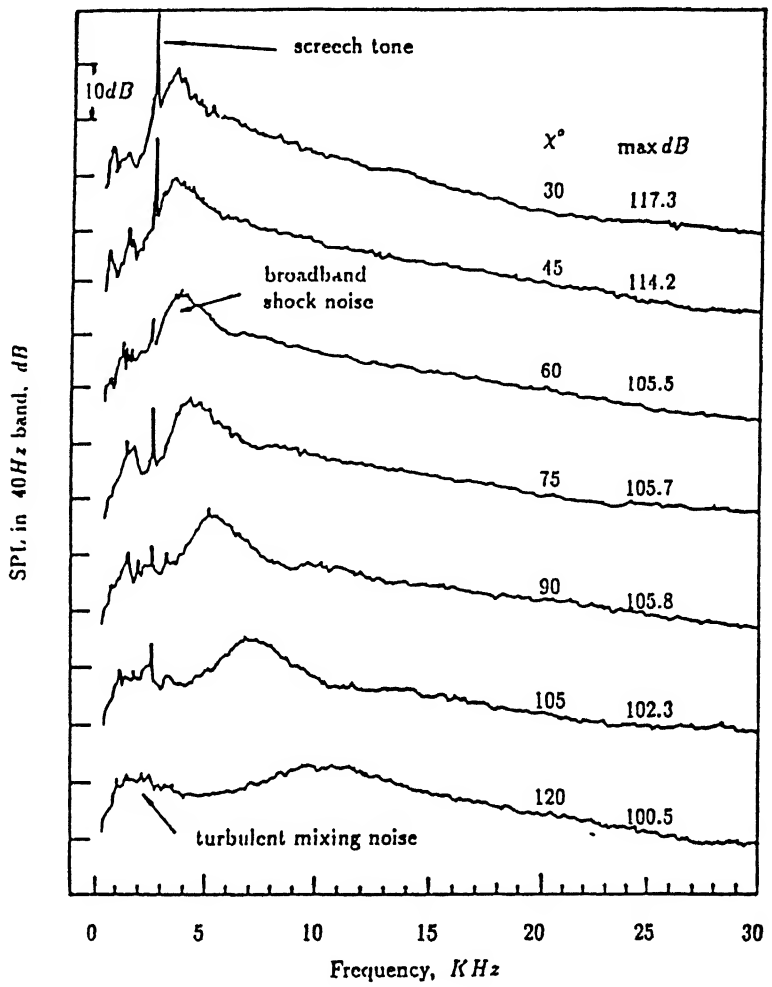

Figure 2.4: Narrowband shock associated noise spectrum[16]

It has been found by Norum[16] that the fundamental screech tone radiates primarily in the upstream direction whereas the principal direction of radiation of first harmonic is at 90^o to the jet flow direction. When the jet emits strong screech tones, the jet flow undergoes two types of strong oscillations, namely Toroidal mode oscillations and Helical/Flapping mode oscillations. With the toroidal mode oscillations, both the jet flow and acoustic field exhibit axisymmetry. With the flapping mode, the jet oscillates up and down across a flapping plane. The screech tone mode changes with jet Mach number. At low Mach number, screech tones are associated with toroidal mode. As M increases there is a switch over to flapping/helical mode. The intensities of screech tones are affected by jet Mach number M_j, temperature of jet T_j, nozzle lip thickness and the presence of sound reflecting surfaces in the immediate vicinity of the jet.

In a series of papers, Tam[96, 97] developed a semi-empirical stochastic model theory for the prediction of broadband shock-associated noise which was found to agree well with experiments for both hot or cold and under or overexpanded jets. The model is based on the observation that the spreading rate of high-speed jets is very small, i.e., the flow variables as well as turbulence statistics change only very slowly in downstream direction. However, the theory is only capable of predicting noise of axisymmetric jets for which the shock-cell structure can be calculated relatively easily. For non-axisymmetric jets there is no simple way of determining the shock-cell structure[97, 98, 99, 100] and as such the theory does not apply to this class of jets.

Screech Tones

The intensity of screech tones have been found in the near-field to be as high as 160 dB[32]. At such high sound pressure level(SPL), the tones can cause structural fatigue of the aircraft components in the vicinity of the nozzle and cause other undesirable vibratory problems. Hubbard and Lassiter[101] have reported failures of secondary structures of wings and fuselages in some configurations from accelerated fatigue due to intense fluctuating pressure field near the jet orifice. Such fatigue failures have also been reported by Hay and Rose[102] from their flight experiments. Thus, it is believed that an understanding of the nature and sources of noise is necessary before any progress is made in controlling it. The nature and sources of sound can be understood from the mechanism by which noise is generated which will be helpful in understanding its characteristics. As such, there is currently a renewed interest to gain insight of the flow phenomena and thus have a better understanding of the screech phenomenon.

Tone Generation Mechanism

In the past, Powell[84, 34] did a pioneering work on imperfectly expanded/screeching jets and their related acoustic field optically. He concluded from his investigations that screech tones were generated by a feedback loop existing in the jet flow field. The instability of the shear-layer at the nozzle exit results in an alternate eddy formation crudely resembling a Karman vortex street. Lighthill[89, 90, 91] has shown how turbulence gives rise to acoustic energy as it traverses a shock wave. On this basis, Powell[84] formulated a theory concerning this noise. According to him, as the stream disturbances(caused by fluctuating pressures at the orifice result in the boundary taking up slightly different directions on leaving the orifice since

pressure-ratios across it will be fluctuating) cross each shock, it will generate a sound wave. Physically, this is because the changes in pressure upstream of shock produce corresponding changes downstream which in part may be relieved by radiation in the form of sound waves[96]. These upstream moving waves were found to strongly govern the stability of the mixing layer at the nozzle exit where it is thin and most receptive to excitations, thus giving rise to "embryo" disturbances. These "embryo" disturbances get amplified as they move downstream at a certain velocity by extracting energy from the mean flow of the jet[32]. Having acquired large enough amplitude(to about 4 to 5 shock-cells), the disturbances strongly interact with the shock-cell structure inside the jet plume. This unsteady interaction results in the emission of intense acoustic waves, some of which propagate upstream outside the jet plume. On reaching the nozzle lip, these acoustic waves further trigger the generation of downstream propagating flow disturbances or the instability waves, closing the feedback loop.

Powell's explanation led the acoustic model of spatially stationary sources located at the ends of the shock-cells, with phasing between them determining the convection velocity, U_c, of disturbances[16]. Since end of each shock-cell is a source of acoustic radiation(due to interaction), the arrangement is equivalent to a line array of variable strength monopole sources whose phase is dependent upon the source spacing[103] (shock-cell length) and disturbance convection velocity. In the far field($X/D_e > 15D_e$), the observer sees the total integrated effect of the array, since he observes all sources at a similar angle. The far field observer can, therefore, detect a Doppler factor with an angle that is solely a function of the phase between sources. In the near field of the sources, by virtue of his proximity, an observer integrates much less of the total phased array properties and has a wide angle of view to the individual sources. However, Doppler factor is also observed in the near field suggesting that in the far field the shift may be due to source convection effects rather than from the effect of phased array. Thus, shock positions cannot be considered stationary when propagating into regions with time-dependent disturbances. As such the shock-cells are set into oscillation at the screech frequency[16].

It has been observed by Powell[30] and Hammitt[104] that the sound waves cause the pressure ratio at the nozzle exit to fluctuate as well and so making angle α of the jet boundary to fluctuate as well. According to Roshko[11], the alternate shedding of vortices/disturbances on each side of the jet causes the sound waves on each side to be out of phase with each other. As a result, both sides of the jet are deflected in like directions giving the stream a sinuosity.

Intense violent oscillations of the jet have been observed by Hammitt[104] after the third cell upto which the jet is found to be relatively stable.

Powell[84] found that the upstream traveling waves are uniquely dependent upon the pressure ratio(R) and closely related to the cell spacing(s). According to him,

$$s = 1.89\ (R - R_c)^{\frac{1}{2}} \times \text{jet depth}$$

$$\lambda = 0.63\ (R - R_c)^{\frac{1}{2}}$$

Where, jet depth is the smaller dimension of the orifice and R_c the critical pressure ratio

Since the wavelength(λ) is roughly proportional to the cell spacing, it seems therefore, that the mechanism responsible for sound may be stabilized at a certain frequency. This is the basis of the phenomena of "sensitive jets", when a distinct vortex pattern may be produced in the flow. Glass[50] was successful in breaking the feedback loop suggested by Powell[84] by reflection of the upstream traveling sound waves from a reflector plate placed at 45^o to the jet axis at nozzle exit. These reflected (acoustic feedback) were observed to significantly increase the rate of jet spread and decay. As much as 50% reduction in centerline velocity(at $15D_e$) were observed. An insulation applied at the exit intercepted the acoustic feedback causing a decrease in jet spread and screech elimination. He, therefore, concluded that the reflected sound waves were the main culprit in inducing the phenomenon of screech. Thus, disturbing the shock-cell structure or making the shocks weak is another way of reducing the effects of acoustic feedback.

Lassiter and Hubbard[101], with the aid of high speed motion photography, were able to show that the shock-cell structure to be unstable during screech and the shocks to oscillate at the frequency of the fundamental screech tone. Hammitt[104] explored the possibility of stabilizing the jet by shielding its base from sound waves. Jet oscillations were found to be sensitive to these external sound waves. Placing a sound absorbing material at the jet base was observed to stabilize the jet oscillations in the entire field and almost complete elimination of screech frequency. They thus concluded that the oscillations of the jet and the associated sound field are directly related to the size of the shock-cells.

Thus, in short, as outlined by Tam *et al*[32] the feedback loop consists of three basic components, namely, the feedback acoustic waves, the instability wave, and the shock-cell

structure. A schematic sketch of the feedback loop is shown in Fig. 2.5.

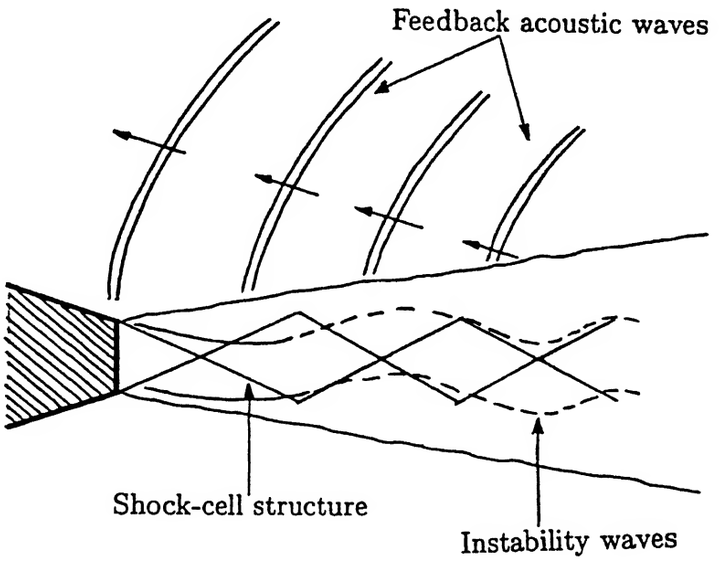

Figure 2.5: Schematic diagram of the screech tone feedback loop.

Each of these components plays a different but an essential role in the maintainence of the feedback loop. The acoustic waves have been found to form the weakest link of the loop. A lot of work has been reported in literature to stabilize the jet and reduce jet noise by shielding these acoustic waves.

A reexamination of the different links of the complete feedback cycle made Tam[95] to suggest that the inner loop of the feedback cycle is formed by large scale instability waves of the jet flow. The screech tones are generated by weak interaction of these instability waves and shock cell structures. The above explanations clearly suggest that the two noises are closely related, both being generated by interaction between downstream propagating large turbulent structures and the quasi-periodic shock cells of the supersonic jets.

An important aspect of the study of shock-associated noise, both discrete tone and broadband, is the accurate evaluation of the shock-cell length in the cellular jet plume. Prandtl was the first to analyze the shock-cell of supersonic jet. He modeled the jet as a column of gas bounded by a vortex sheet. Later, Pack[99] gave a complete solution of the linear vortex sheet jet model of Prandtl for slightly imperfectly expanded jets. He proposed a hypothetical shock-cell length L_j that corresponds to the fully expanded jet diameter D_j using a vortex-sheet

shock-cell model solution.

To a good approximation,

$$L_j = \frac{2\pi}{\lambda_1}$$

$$= \frac{\pi(M_j - 1)^{1/2} D_j}{\nu_1}$$

where $\nu_1 = 2.40483$ and D_j= fully expanded jet diameter

However, the vortex-sheet model is not valid except near the nozzle exit where the mixing layer of jet is thin. Better agreement especially in terms of gross features such as shock-cell spacing and amplitude was achieved by a model developed by Tam *et al*[96] through use of multiple scales method by extending the linear shock-cell solution to jets with realistic mean flow profile[97].

It is generally agreed, as has been found experimentally by several investigators, that the effective source is located at or downstream of the end of third shock-cell[84, 34, 104, 50, 103]. The shock-cell length decreases with distance downstream of nozzle due to viscous and mixing effects, and its accurate measurement at downstream location is sometimes very difficult. This is because that at these locations the jet is often very unstable; The shock-cells are obscured by turbulence in the jet, and the shocks in the shear layer are too dispersed to form a clear image especially at their extremities[105]. Usually an average value of shock cell length, L, is obtained by dividing the length of the potential core of jet by the number of shock-cells. Powell[84] suggested L = 80% of L_1, Norum used a value of 90% of L_3, and Tam *et al*[95] 80% of L_j. A value of $U_c/V_j = 0.70 \pm 0.05$ was used by number of investigators[84, 16, 95, 94].

2.4 Reduction of Choked Jet Noise

Since the noise, characteristic to choked jets, is a resonance mechanism, it is clear that several factors might affect the noise. Clearly the most direct method to reduce jet noise is to weaken the shock waves[30]. This may be done either by using a divergent exit of appropriate expansion

ratio, or adding a gauze cylinder as an extension to the nozzle so as to permit the excess static pressure at the exit to leak away.

Alternatively, it is known[30], that stream disturbances become less unstable if the free boundary layers are increased in thickness. Hence, a noise reduction ensues if the turbulent mixing can be brought forward to nearer the orifice. One way of doing this is to place a series of notches in the exit edge of the orifice and the other is by using small radial vanes in the exit or teeth[30]. These alter the structure of jet as well, tending to diffuse the shock wave patterns. According to Powell, notches are the most practical and would not be expected to have much influence on engine or rocket performance.

2.5 Motivation Behind the Present Investigation

An elliptic geometry is intermediate between the two limiting shapes, i.e., the often-studied circular and planer jets. Elliptic jets are quite different from the above two shapes – owing mainly to the fact that the azimuthal curvature variation of the vortical structure causes non-uniform self-induction and hence, complex three-dimensional deformations[1]. These deformations in elliptic structures make them as effective pumping devices to mix ambient and core fluids resulting in higher mixing than in circular jets. This process of axis-switching which improves the entrainment process and hence, the jet spread is also prevalent in jet flows of triangular and square geometries. However, the coherent structures in these jets are complicated, owing particularly to the intense self-induction at sharp corners. Among irregular geometries, an elliptic jet is less complex and better defined because of the smooth variation of azimuthal curvature. Thus, an elliptic jet leads the way to a better understanding of other irregular jets[1].

Earlier studies on jets emerging from non-circular geometries with corners, e.g., triangle, square or rectangle, showed that the introduction of sharp corners at the nozzle outlet can significantly increase the small-scale turbulence intensity at the corners[29, 60, 106, 5]. This small-scale turbulence was generated by axial vortices formed in the corners inside the nozzle[4] and augmented by strong vortex bending induced by the highly curved flow at the corners[2].

The present work is aimed at taking advantage of both the higher entrainment/mixing characteristics of elliptic jets plus the presence of discontinuity in the form of notches with sharp corners, e.g., triangle and square. The combined exit geometry, i.e., ellipse with notch, is expected to have a coexistence of both large and small-scale structures in the flowfield. Such

flowfield have been observed to be advantageous for combustion processes in case of triangular and square nozzle jets[4].

Since sonic and underexpanded elliptic jets exhibit slightly higher spreading rates relative to rectangular jets with same aspect-ratio[21], the present arrangement of notched ellipse is investigated in the range of M_j=1.0 to 1.52(underexpanded). This has been done, in particular, to achieve enhanced mixing and reduced noise.

On the basis of the past studies, the present problem is outlined in the following manner:

- Effect of notch:
  (i) In an exit geometry with uniform curvature variation(i.e. circle).
  (ii) In an exit geometry with non-uniform curvature variation(i.e. ellipse).
- Effect of sharp corners in notch geometry for both circular and elliptic jets.
- Effect of aspect-ratio on plain and notched elliptic jets.

The above problems are dealt with for both mean flow and noise characteristics. Further, since it is aimed here to investigate the effect of these notches on mixing and noise characteristics, in order to avoid the effect of boundary layers as an initial condition, jets issuing from slots are chosen for investigation.

Chapter 3

Experimental Setup and Procedure

3.1 Introduction

This chapter describes the experimental setup, the instrumentation, and the experimental procedure. In addition to this, the precautions observed during the experimentation and the accuracy of measurements are also discussed.

3.2 Experimental Details

3.2.1 Air Supply System

The compressed air supply system consists of a two-stage reciprocating compressor, capable of delivering 360 cfm air at 500 psig. It is driven by a 3 phase 150hp induction motor. The compressed air is cooled by passing through an inter-cooler and then fed to a pre-filter to remove solid contaminants and oil-droplets. The filtering action is performed by porous stone candles. After passing through an activated carbon filter the compressed air is dried in a dual tower semi-automatic air dryer using silica gel as desiccant. A portion of dried air is heated and is used for alternate reactivation of each tower. The air dryer is followed by a diaphragm type back pressure valve operated by a pressure relief pilot, which permits the air dryer to operate at 500psig as the pressure in the receivers builds up from atmospheric to storage pressure. A non-return valve prevents the back flow at the air dryer. Air is stored in three tanks with total capacity of 3000 ft^3 at a pressure of 300 psig. The tunnel control section includes a gate valve followed by a pressure regulating valve. The pressure regulating valve is connected to a mixing

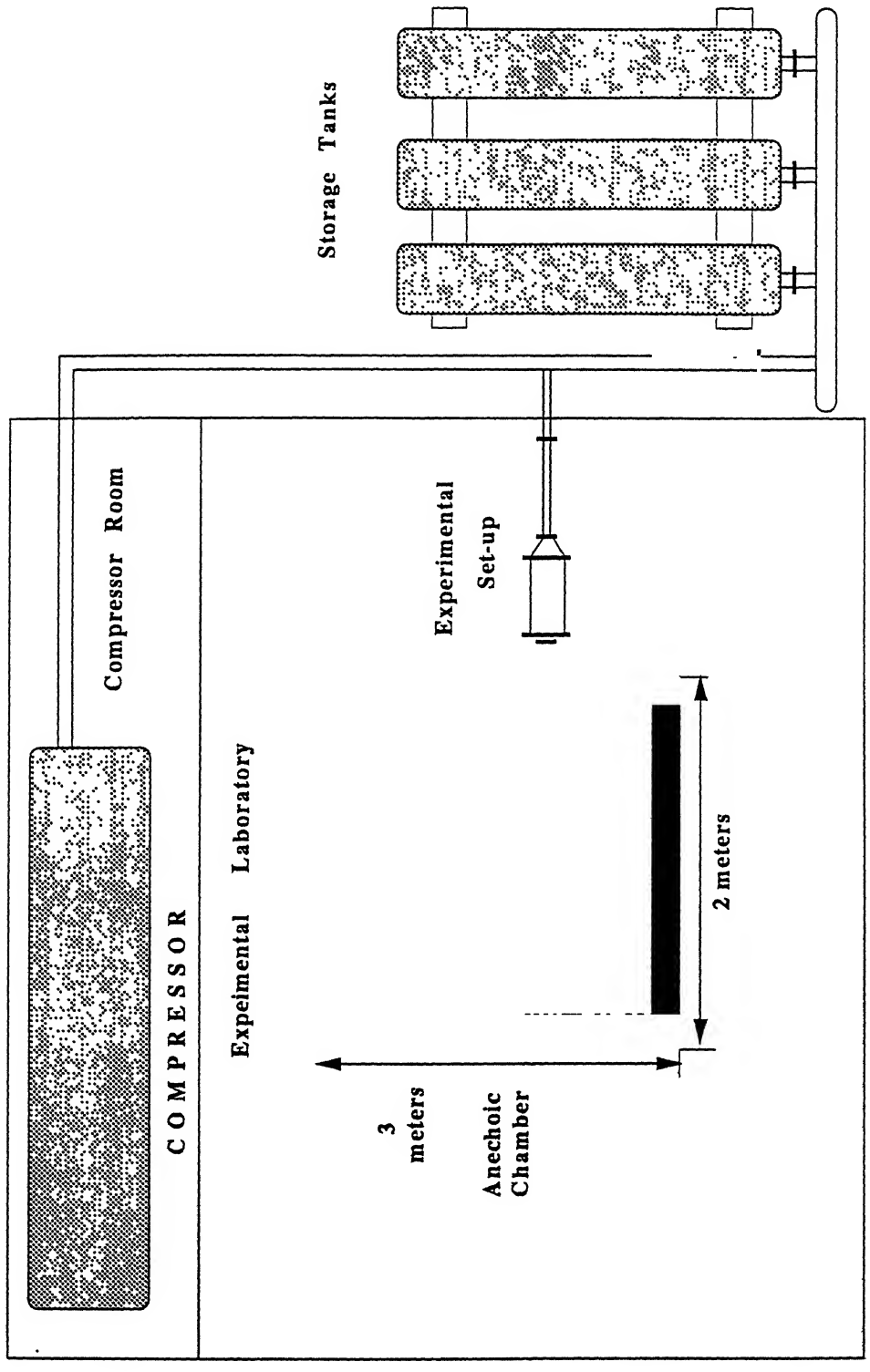

Figure 3.1: Layout of the Laboratory

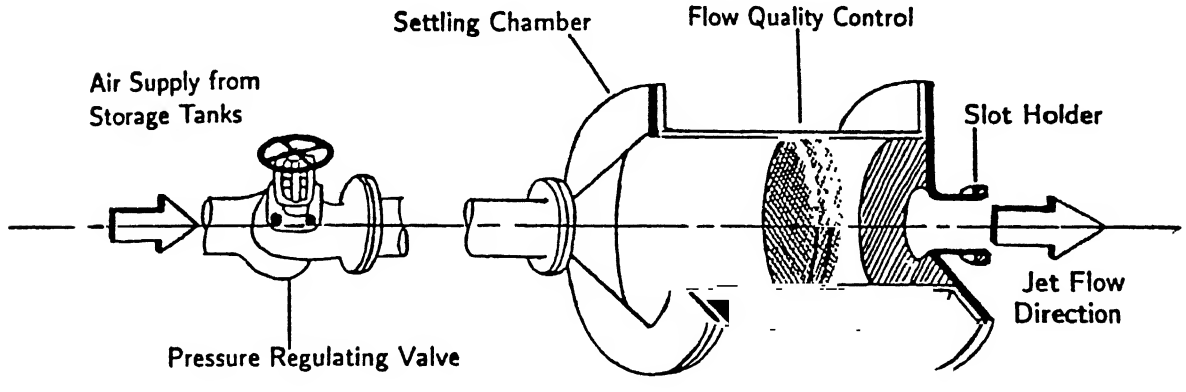

Figure 3.2: Schematic representation of the jet test facility

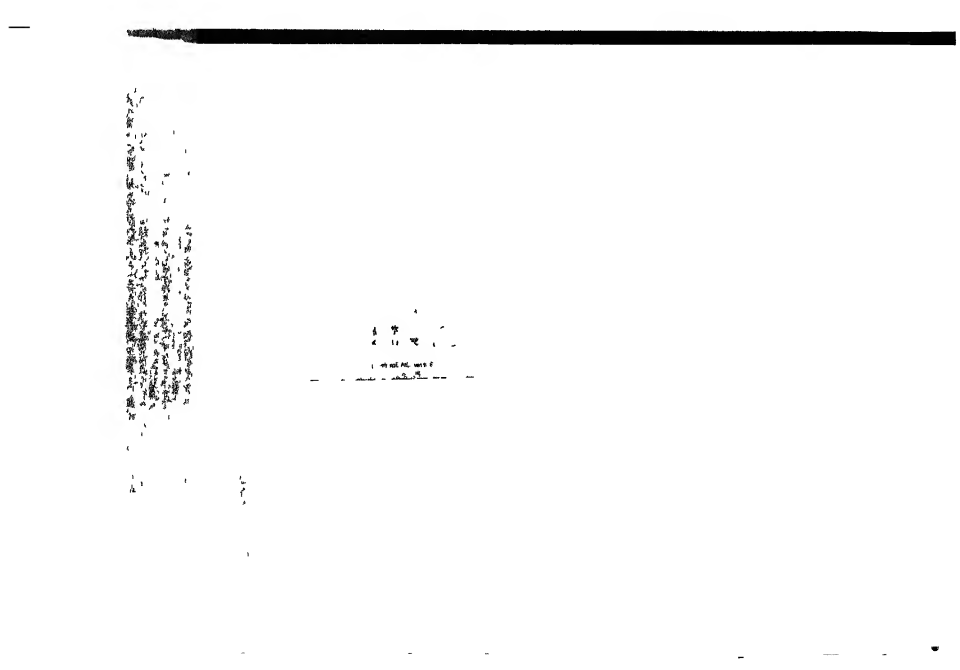

Figure 3.3: Photograph showing the experimental set up

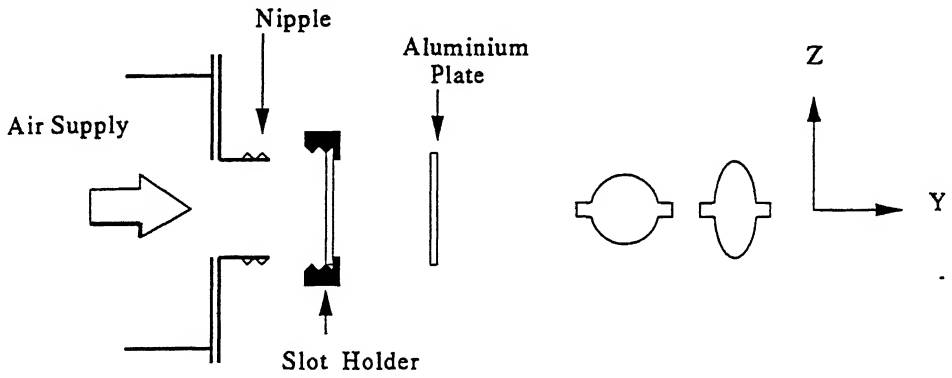

Figure 3.4: Schematic diagram of nipple and mounting attachments for slot jets

length of 3 inch diameter and then to a settling chamber. The layout of the experimental high speed test laboratory is as shown in Fig. 3.1.

3.2.2 Jet Test Facility

The experiments were conducted using a high-speed jet facility which consists of a cylindrical settling chamber connected to high pressure storage tanks. A schematic representation of the high-speed jet facility is shown in Figure 3.2. As shown, the settling chamber is connected to the mixing length by a wide angle diffuser followed by three screens or closely meshed grids set 3 cms apart for minimizing turbulence at the slot inlet. These screens are inserted in the constant area circular section of 300 mm diameter and 600 mm in length. The settling chamber has tapings for stagnation temperature and pressure measurements. The temperature in the settling chamber was measured by a mercury thermometer. The stagnation pressure in the settling chamber were made using a long U-tube mercury manometer. A photograph of the experimental set up along with the instrumentation is as shown in Fig. 3.3.

The compressed air is regulated via pressure regulating valve and is supplied through one end of the settling chamber through the mixing length. The flow exits through a 100 mm diameter "nipple" on the opposite end of the settling chamber to which test models with desired geometries could be attached. The area ratio between the settling chamber end plate and slot

is 100. Figure 3.4 shows the schematic representation of the nipple and the model mounting attachments for the case of slot jets. Circular Aluminium plates of 1.3 mm thickness and diameter 100 mm were fitted perfectly to the end of the settling chamber using an O-ring so as to ensure no leakage even at very high operating pressures. The slot holder could be screwed to the end of the nipple to secure the test model plates firmly.

The settling chamber pressure P_0, which was the controlling parameter in our investigation, was regulated using a pressure regulating valve.

3.2.3 Experimental Models

The prime objective in our present investigation is to study the effect the exit geometry variation on the development of jet. Since jet development is significantly influenced or is most receptive to changes in initial conditions[17], jets issuing from slots were preferred. For this purpose, circular Aluminium sheets of 1.3 mm thickness were chosen over which slots of desired geometry were made. The sheet thickness was considered to be sufficient to ensure negligible boundary layer growth. This caution has been exercised because it has been reported by Hussain and Husain[1] that boundary layer growth within the nozzle strongly influences the initial development and hence, mixing characteristics of jets. According to them, the deformation and evolution of large-scale vortical structures and jet characteristics are very sensitive not only to state of exit boundary layer but also to its thickness and spanwise uniformity.

To study the effect of exit geometry alone, the initial condition(i.e., jet exit plane details) for all the nozzles must be kept the same while discontinues in the form of sharp corners are introduced along the periphery. Since it is practically impossible to achieve this condition using contoured nozzles of various shapes[1], the problem is, therefore, addressed by using slots which are characterized by initial shear layers of practically zero boundary layer thicknesses. However, the effect of *vena-contracta* typical to sharp edged slots was taken care of by smoothening the outer edges of the slot resulting in square-edged slots so that the jet expands smoothly as it does from a contoured nozzle. This configuration was suggested by Ramjee and Hussain[107] and was found by them to be absent from the effects of *vena-contracta*. The slots thus formed were named as "Disk Nozzles".

Turbulent jets issuing from slots are useful in number of areas of interest to engineers, such as augmentation of thrust in V/STOL[59, 108] and combustion in propulsion units[59,

58]. In some of these applications requiring rapid mixing, expeditious manufacturing and ease of installation may necessitate the use of sharp edged slots in preference to nozzles with contoured upstream shaping. Another reason was that non-circular ducts with non-conventional geometries would complicate and increase the cost of production[58]. It was shown by Gutmark and Schadow[58] that orifice slot jet has large and small-scale mixing characteristics similar to jets with gradual contraction. This feature is important for engineering applications where the simplicity of slot design, especially from non-circular geometries, is advantageous. As such the overall characteristics of slot jets can be related to jets issuing from nozzles. Thus, it is quite safe to carry out investigations with jets issuing from slots.

So keeping into consideration all these facts concluded by previous investigators, we have carried out a study on the mean flow characteristics of jets issuing from circular and elliptic slots. All the slots, i.e., plain and notched, were of equal area, which is equal to the area of a circular slot of 10 mm diameter and thus, the equivalent diameter, D_e of the non-circular slots was 10 mm. Also for a given equivalent diameter D_e, the aspect ratio is an important parameter controlling the deformation of large-scale vortical structures in elliptic jets[1]. As such the study was extended from small aspect ratio(2:1) ellipse to moderate aspect ratios(4:1).

Earlier studies on slot jets were carried out for rectangular[59, 29, 60, 61, 62] and elliptic[1] exit geometries in incompressible range and revealed that these non-circular geometries enhance mixing characteristics relative to conventional circular jet. Further, sharp corners have been observed by Quinn[108, 59] and Marsters[61, 62] in square and rectangular slot jets and by Schadow *et al*[3, 46, 4] in square and triangular nozzle jets to shed small scale eddies which induce turbulence in the region of the corner, and thereby influence the overall jet mixing characteristics. No work seems to report improving the flow from circular and elliptic slots by the introduction of sharp corners. Our present effort is to enhance the mixing characteristics of circular and elliptic slot jets by introducing notches in the periphery. Three types of notch configurations were tested, they are:

- Square
- Triangular(vertex angle 60^o)
- Semi-circular(absence of sharp corner)

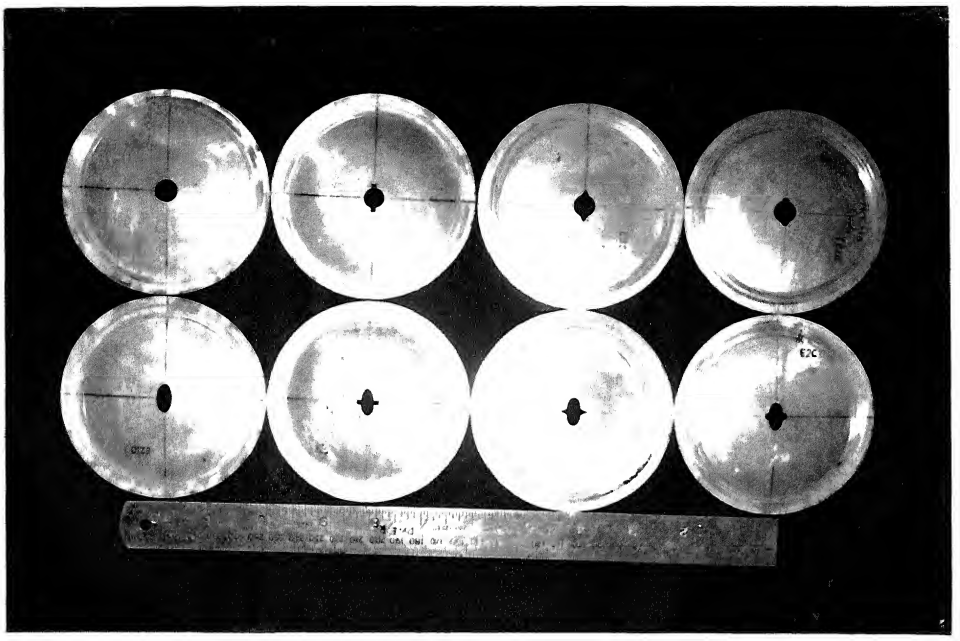

Figure 3.5(a): Photograph showing the experimental models: plain and modified circular geometries(top row); 2:1 plain and modified elliptic geometries(bottom row)

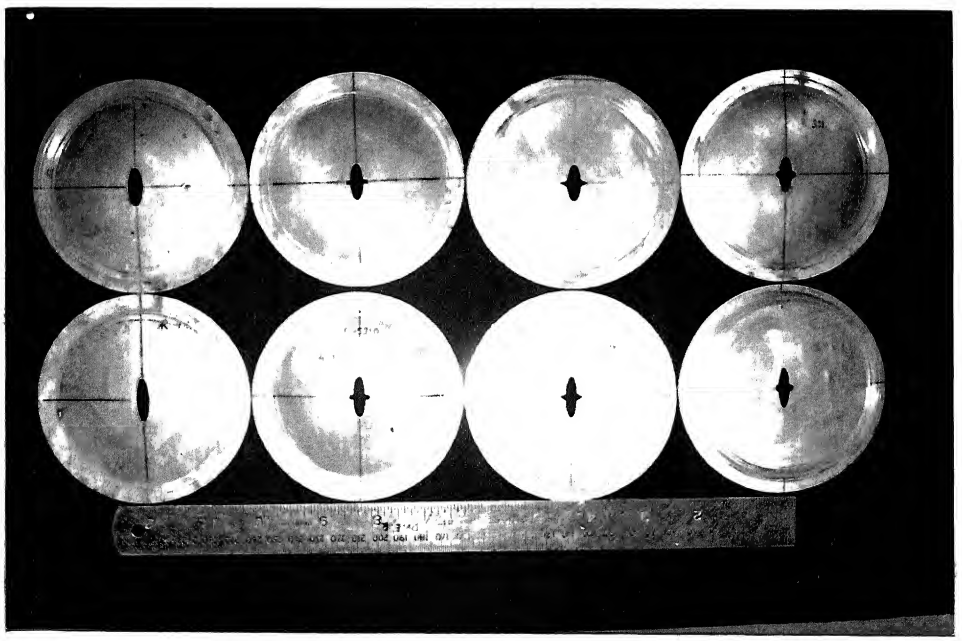

Figure 3.5(b): Photograph showing the experimental models: 3:1 plain and modified elliptic geometries(top row); 4:1 plain and modified elliptic geometries(bottom row)

Each notch configuration comprises of 5 percent of the total slot area (circle or ellipse), i.e., 10 percent of the plain geometry for notches plus 90 percent of the plain geometry for the basic shape. Two such notches were placed symmetrically at the minor-axis ends of the ellipse and at a diameter of circle as shown in Fig. 3.4. The placement of the notches on the minor-axis ends was done to to further enhance mixing in that plane and hence, effect the overall mixing in elliptic jets as will be discussed in subsequent chapters.

The experimental models studied in the present investigation are:

- Plain and notched circle
- Plain ellipse with aspect ratio varying from 2 to 4
- Notched ellipse with aspect ratio varying from 2 to 4

The photographs of the experimental models used in the present investigation are as shown in Figure 3.5(a)-(b). A direct comparisons of the notched jet characteristics are made with plain cases for both circular and elliptic slot jets and for each aspect-ratio to study the changes in the flow characteristics brought about in the jet flowfield by presence of notch and by a change in notch geometry.

3.3 Instrumentation

3.3.1 Pressure Sensing Probe

The sensing probe used for the present study for mean flow measurements was the conventional Pitot tube. This was done keeping in mind the fluctuating nature of the flowfield in such flows and also due to the fact that the core region of the underexpanded jets is shock-dominated. Pitot tube has been used for measuring pressure in the jet field by many researchers[8, 18, 12, 109, 110, 13].

Rice and Raman[75] have reported that as the flow exiting from their rectangular nozzle was supersonic, it presented considerable measurement problems in using hot-wire or hot-film anemometry. They avoided these difficulties by just measuring the total pressure referenced to the room pressure(P_a) using a simple total pressure tube. They presented the data derived from this raw total pressure, which would be the total pressure downstream of the bow-shock formed ahead of the pressure probe in supersonic flows.

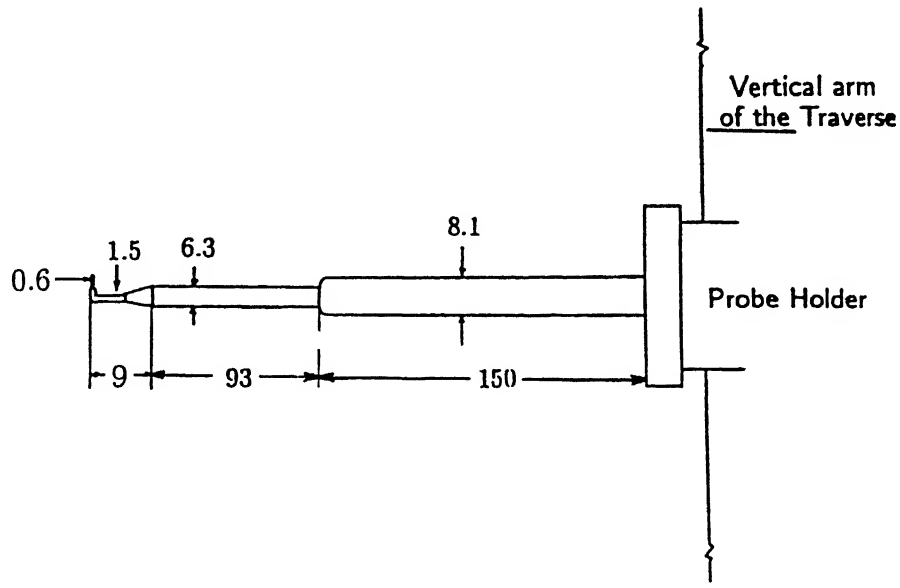

Figure 3.6: Pressure measuring probe with dimensions in mm

The Pitot tube used in the present investigation for sonic and underexpanded jets had an inner diameter of 0.4 mm and an outer diameter of 0.6 mm as shown in Fig. 3.6. This probe size has been arrived at after surveying the available literature in this area where this size is found to give satisfactory results[18, 12, 109, 110]. Krothapalli *et al*[67] had used a Pitot probe of external diameter 0.46 mm for studying the jet flow field issuing from a rectangular nozzle of smaller dimension 3 mm. The ratio of the probe outer diameter to the smaller dimension of the nozzle in their case was 0.6522. In the present study, non-circular slots were used and it was found that the elliptic-slot of aspect-ratio 4:1 had a smaller dimension(which is the smallest among all the non-circular slots) of 5.0 mm and the corresponding ratio turns out to be 8.33. Thus, a reasonable spatial resolution was ensured. In addition to this, it was observed that close to the exit, i.e., for X/D_e=0.1, the pressure is nearly constant for 80 percent of the orifice width for all the cases tested. Also, the pressure obtained at the centre was within 2 percent of the total stagnation pressure. It can thus be considered that the magnitudes of the pressures obtained with this probe size relative to the orifice width, were quite accurate.

The flow at the farthest downstream location for all models can be expected to be uniform

and parallel to the X-direction. The use of Pitot tube close to the exit plane was considered acceptable because the flow divergence may not be significant enough. The probe was initially aligned along the jet axis to face the jet. Therefore, measurements along the jet axis was with proper orientation of the probe. However, the probe orientation was not changed while making measurements at other locations in the jet . Thus, the probe was not facing the flow, in fact the probe was at an angle to the flow. This will introduce some error in measurement of pressure. But since Pitot probe pressure measurements will be in negligible amount of error for flow angularities of $\pm 20^o$ the error by the flow angularties will not be significant and are in the order of $\pm 2\%$[111].

Another point to be noted in Pitot pressure measurements is that in the supersonic core, what the probe measures is the total pressure behind the bow shock that stands ahead of the probe. Thus, it is not the actual total pressure. If the actual total pressure is required one has to correct for the pressure loss across the shock. But the core is wave dominated, the Mach number at the core is varying from point to point and also the shocks in different cells are of varying strength. Therefore, no attempt is made to correct the measured total pressure for shock loss. In fact it is a practice to use the measured pressure as such to analyze the supersonic jet field assuming static pressure inside the jet equal to ambient pressure[110, 75, 109, 13]. It has to be emphasized that in supersonic regions there is some measurement error due to probe interference with shock-structure and so the results in supersonic regions should be considered only qualitative and good enough for comparative purposes[12, 109, 110]. In all the pressure measurements the sensing probe stem was oriented parallel to Y-axis with the sensing probe facing the jet axis.

Since we are dealing with high stagnation pressures, a long column U-tube mercury manometer was connected to the pitot tube. The controlling parameter in our experiments is the stagnation pressure P_0 in the settling chamber and was regulated by means of a pressure regulating valve. During the experimental runs, the settling chamber pressure was measured by another long column U-tube mercury manometer. The accuracy of the measured pressures is $\pm$ 3 percent. The room temperature was measured during the experimental runs by a thermometer. The day to day changes in ambient pressure, P_a, were measured by a mercury barometer placed in the laboratory and averaged over the duration of experiment.

The movement of the sensing probe(i.e, Pitot tube) was facilitated by a three-dimensional

traversing system having 6 degrees of freedom that was driven manually and having a least count of 0.1 mm in linear motion and of 0.5 degrees in angular motion. A cartesian co-ordinate system(X,Y,Z), defined in Fig. 3.2, was employed with its origin located on the centreline of the slot. The accuracy of traverse movement in X, Y and Z directions was ± 0.1mm.

3.3.2 Sound Measuring Instruments

In addition to the study on mean flow characteristics of plain and notched jets, a detailed noise study was carried out. For this purpose, a $\frac{1}{8}$ inch Larsen and Davis microphone and 800B Model sound level meter is used to obtain the jet noise measurements. The accuracy, according to the manufacturers specifications, is within ±0.3 dB in the range of 20 Hz to 20 kHz. The sound level meter was calibrated using a Larsen and Davis CA250 precision acoustic calibrator with corrections for day to day changes in atmospheric pressure.

While carrying out the noise measurements, 800B sound level meter can be stopped and started any number of times. It incorporates parallel integration mode(rms) and peak mode detectors which can be read alternately without data interruption, during or at the conclusion of an integration sequence. It has five selectable settings with a large overlap area between ranges 30-90, 50-110 and 80-140 dB. The sound level meter has provisions of frequency weighting filters, i.e., A, C-weight, flat and high pass, and detectors, i.e., fast, slow, impulse, peak with a rise time of 20μsec, integrate. The instrument is capable of operation in the temperature range of -10 to +50 °C and humidity of 0 to 90 percent.

3.3.3 Anechoic Chamber

The jet noise measurements were carried out in a ($2 \times 2 \times 3$ m)anechoic chamber developed in the lab details of which are available in [112]. The chamber was mounted on wheels so that it could be moved to house the jet facility during noise measurements. The chamber had a door to enclose the open jet portion of the test facility and a window to allow the jet air to exit the chamber as shown in Fig. 3.7. A 3 inch thick polyurethene foam(PUF) formed the inner layer of the chamber. The outermost layer of the inner walls was covered by wedges made of $\frac{1}{4}$ inch PUF and housed in foam boxes as shown in Fig. 3.8. These boxes were mounted on a wire mesh fixed ahead of the inner PUF layer. An air gap was thus provided between the two layers of foam used. Several such boxes containing the wedges were also used on the floor

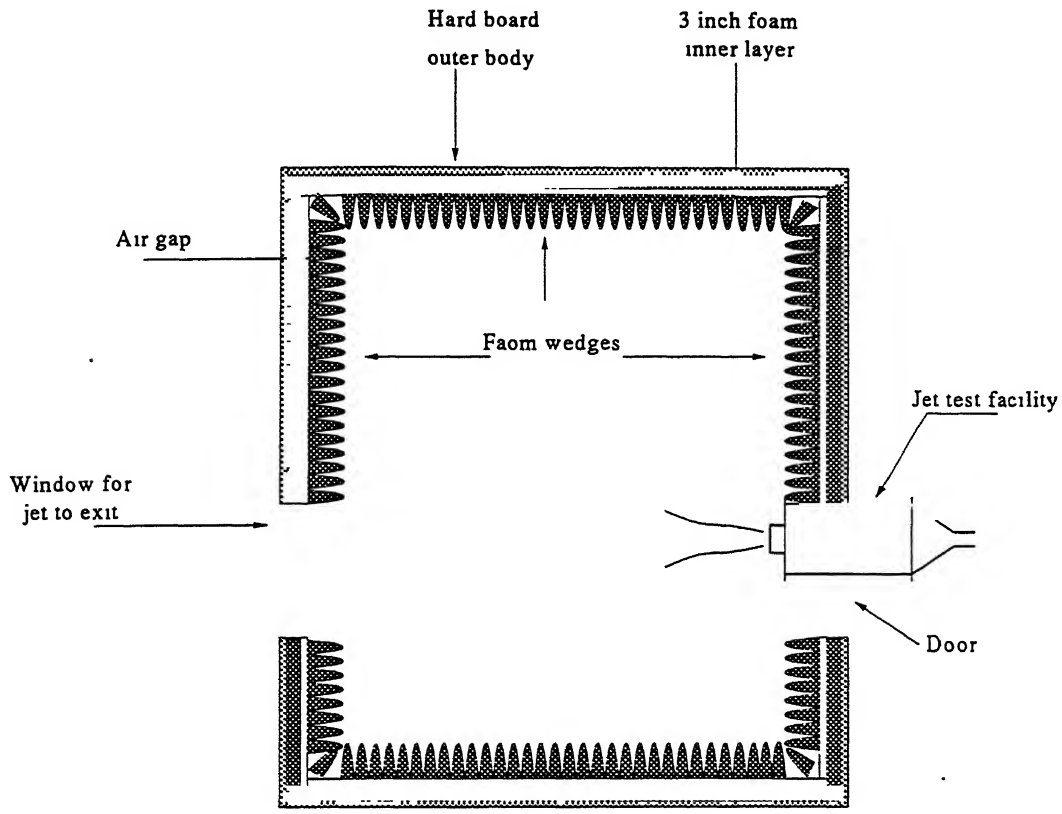

Figure 3.7 : Schematic diagram showing the cross-sectional view of the anechoic chamber

Figure 3.8 : Photograph showing the inside view of wedges in the anechoic facility

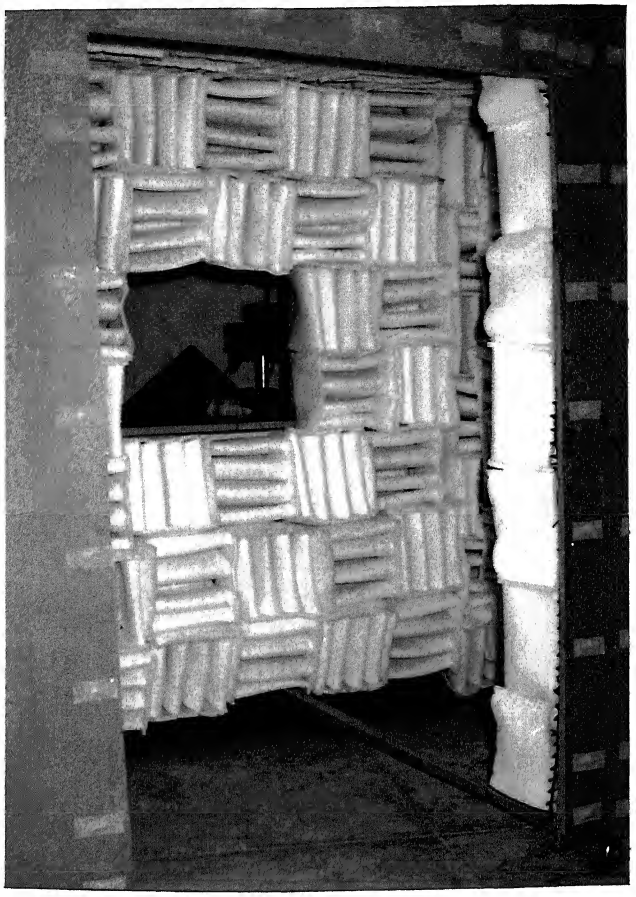

Figure 3.9 : Photograph showing the anechoic facility

of the chamber during the experimental runs so as to prevent sound reflection from the floor. The chamber satisfied anechoic conditions in the range of $16D_e$ to 80_e and at frequencies of 630 Hz and above. Therefore, the experiments were conducted in this range to ensure free field conditions. Figure 3.9 shows the photograph of the anechoic chamber.

The traverse used for radial directivity was also covered by thin sheets of foam and boxes.

3.3.4 Spectrum Analyser

A dual channel AD3525 fast fourier transform (FFT) spectrum analyser was used for obtaining the spectral characteristics of jet noise. The spectrum analyser had a frequency range up to 50 kHz. Output from the sound level meter is fed into the FFT analyser. Instantaneous spectra could be obtained with the analyser during the test runs.

The analyser is capable of operation in the temperature range of 0°C to 40°C and relative humidity of less than 85 percent.

3.3.5 Pressure Transducer

A Pressure Systems pressure transducer, model number 9010, was used for the sound analysis part of the investigation. This was done because study was to be carried out for higher pressures at which U-tube Mercury manometers become unmanageable. The transducer had an averaging rate of 250 samples per second and capable of operation up to 300 psi. The transducer had 16 channel pressure measuring devices with true differential(reference per channel) or common reference pneumatic manifolds and could be operated in temperatures ranging from -20°C to +60°C and 95 percent humidity.

The transducer is provided with a 9000 Start-up software that can be executed on any IBM-PC compatible computer. The software has an option of measuring pressures in different units, e.g., inches of water, inches of mercury, kPa, Mbar, bar and Atmosphere. Before a test run is carried out, a rezero function is activated to null the transducer offset drift errors. The transducer had a measurement resolution of ±0.003 and the readings were accurate up to ±1 percent.

3.3.6 Shadowgraph System/Flow Visualization

A conventional shadowgraph system is used to capture the overall features of jet shock-structure, i.e., average shock-cell length, L_{avg}, its shape, as it exits from geometries with varying shapes and notch configurations. The system uses one 250 mm diameter concave mirror in conjunction with air-cooled mercury spark light source. The image is captured on a screen that allows continuous observation of the shock flow in the open test-section during the run. Later photographs of shadowgraph images of the shock structures were taken using a camera.

3.4 Experimental Procedure

3.4.1 Test Conditions

The investigation was carried out for two conditions: (1) Correctly expanded jets, with sonic velocity at nozzle exit (2) Underexpanded sonic jets at P_0/P_a of 2.835 and 3.86 corresponding to level of underexpansion of 1.5 and 2.0, respectively. The Reynolds number based on the equivalent diameter and the equivalent exit velocity (based on M_j) for the two conditions ranged

from 2.36×10^5 to 3.54×10^5. All the tests were carried out at a room temperature of 30 °C and 730 mmHg of pressure averaged over the time taken for the completion of experiments. The variation in temperature was less than 0.1 percent and that for pressure about 2 percent. The pressure(P_t) was measured with an accuracy of ± 3 percent.

3.4.2 Shock-Structure and Centreline Pressure Decay

For the purpose of measuring the centreline pressure decay for both sonic and sonic underexpanded jets, the Pitot tube is moved from the exit of the slot in the downstream direction and the pressures at various axial locations were recorded. For the fully-expanded jet, the measured Pitot pressure corresponds to the stagnation pressure P_t of the jet flow field at the point of measurement. For underexpanded conditions, however, in the supersonic regions of the jet, the measured stagnation pressure P_{t2} corresponds to the stagnation pressure behind the standing bow shock in front of the pitot tube. Nonetheless, the data are accurate enough to capture the overall features[12], e.g, the number of shocks and their spacings. However, in the subsonic regions of the jet, there is no shock/probe interference and the data represents the actual stagnation pressure[12, 109, 110, 13]. The results in the supersonic regions should, therefore, be considered only qualitative and good enough for comparison purposes[12, 13].

For underexpanded conditions, the measurements were not made at predetermined axial locations but at locations where maxima and minima in P_{t2} were observed. The data is obtained upto $30D_e$ in order to have an idea of the decay and hence, the mixing characteristics of the jet once the end of the core is encountered. Any decline in P_{t2} is indicative of the presence of shock termination and an increment in P_{t2}, the cell itself showing expansion[71].

Further, it is worth pointing out that the present work on slot jets has the absence of *vena contracta* effect as is generally the case with orifice flows. Hussain and Husain[1] observed in their experiments on elliptic orifice jets that the issuing jet formed a *vena contracta* downstream of the exit plane. The formation of *vena contracta*, in their case, increased the jet centreline velocity U_c downstream of the jet exit plane by about 50%, thereby delaying the decay. It may be noted that Hussain and Husain[1] used sharp-edged orifice, whereas in the present investigation, square-edged orifices of **disk nozzles** have been used. Earlier studies by Hussain and Ramjee have shown that *vena contracta* effect is absent in the case of **disk nozzles**. This supports the absence of *vena contracta* effect in the present orifice jet results as will be seen in

subsequent chapters.

3.4.3 Iso-velocity Contours and Entrainment

To obtain a picture of the jet structure as it grows in the YZ-plane at various axial locations, iso-velocity contours have been obtained from the grid study as proposed by Marsters[61] and Quinn[59]. Pitot pressures are noted at various grid points in a quadrant of the flowfield because of the symmetric placement of the notches. The data is reduced to velocities in both supersonic and subsonic parts of the jet by using the well known isentropic relation

$$P_t/P_s = (1 + \frac{\gamma - 1}{2} M^2)^{\frac{\gamma}{\gamma - 1}}$$

Here, γ is equal to 1.4 and P_t is the measured pitot pressure and P_s is the local static pressure. This relation is used with the assumption that the local static pressure inside the jet is the ambient pressure so as to provide comparative values of iso-velocity contours. The approximation improves as we move downstream into the subsonic regions[75]. The following procedure is followed while taking pressure measurements:

- Firstly, we take the centreline pressure decay data(up to 30De).
- And secondly, from the plots of shock-structure variation and centreline pressure decay, axial locations are determined at which grid study is to be carried out for the purpose of obtaining iso-velocity contours and hence, entrainment plots, e.g., near exit of nozzle, in between shock-cells at two locations, end of potential core and some other locations up to 30De.

In the case of sonic underexpanded jets, for the first axial three locations at which the grid study is carried out, the total pressure probe passes through a complex shock-cell system and therefore, the data should be viewed as being qualitative[75, 109, 13]. Further downstream, once the flow becomes subsonic everywhere, the measurements are more reliable. The results presented in this study are mostly of comparative nature(comparison of notch geometry effect) and hence, the inferences made out of the results may be considered reasonably relevant to realistic and practical situations.

From the above data the entrainment calculations were carried out. The mass-flux ratio which is used here as an indicator of jet mixing enhancement is obtained using the Pitot tube data and is calculated as follows:

$$\frac{m}{m_e} = \int\int \frac{(\rho U)dydz}{\rho_e U_e A_e}$$

where,

$$\frac{\rho U}{\rho_e U_e} = \frac{P_s}{P_e}\frac{M}{M_e}\left(\frac{1+0.2M^2}{1+0.2M_e^2}\right)^{0.5}$$

The mass-flux values have been obtained by integrating the velocities across the whole jet cross-section with the assumption of static pressure inside the jet field equal to the atmospheric pressure. The assumption improves as we move downstream where the flow becomes subsonic. This calculation method described above was used previously by Zaman et al[Zaman94] and more recently by Taghavi and Raman[109] and Raman and Rice[110]. Here too it may be emphasized that for $X/D_e \leq 5$, the data is good enough to provide comparative values[Taghavi94, Raman94]. The uncertainties in the mass-flux calculation is ± 7 percent. The uncertainty in centreline pressure measurement is ± 6.16 percent(considering measurement up to $15D_e$).

The Y and Z-axis of the slot geometry were carefully aligned parallel to the Y and Z-axis of the traverse. The experimental data for mass flow calculation was acquired in one quarter plane of the jet flowfield starting from the centreline. The measurements were made in the form of a grid in the Y-Z plane with a uniform step of 1 mm. These grid measurements were made at various axial locations starting from close to nozzle exit up to $30D_e$. The symmetry of the flowfield for all the cases of slots was ensured and found to be valid within ± 5 percent by measurements on both sides. Therefore, to avoid repetition of measurements, the grid data was taken on one side, i.e., a quadrant, and extended to the whole flowfield assuming symmetry of flowfield about Y and Z-axis. It is emphasized that sufficient number of data points were taken to define the jet cross-section, i.e., approximately 40 points in the exit plane($X = 0.5D_e$) to 400 points at $15D_e$.

3.4.4 Shock-Cell Length Measurements

A simple non-intrusive technique for measurement of shock-cell lengths has been carried out. A sharp tipped pointer was attached to the traversing system and positioned in such a way that it was exactly at the slot exit plane, but sufficiently away from the flowfield so as not to be of any disturbance to flow. The shadowgraph images of the underexpanded jets were captured on a screen along with the pointer. The angle made by the light source with the parallel beam reflected from the mirror was kept less than 5 degrees ensuring proper accuracy of the quantitative measurement of shock-cell length using shadowgraph images in conjunction with the pointer and the traverse arrangement. Thereafter, the pointer was moved parallel to the jet axis from the beginning of each shock-cell to its end with the movement of the pointer being constantly monitored on the screen. The distance traveled by the pointer for each cell was measured by the movement of the traverse. Knowing the total length of the repetitive shock-cells, up to four shock-cells, the average shock-cell length was calculated for calculating the predicted values of Strouhal number.

3.4.5 Strouhal Number and Screech Tone Frequency

The screech tone frequency, f_s, of the underexpanded jets can be approximately predicted from the measured average shock cell length, L_{avg}. The expression for f_s given by Tam[113] is as follows:

$$f_s = \frac{U_{cv} k_1}{2\pi(1 + U_{cv}/a_\infty)}$$

where k_1 is the fundamental(the smallest) wavelength of the shock cell system, U_{cv} is the convection phase velocity of the large-scale instability waves of the flow and a_{inf} is the ambient speed of sound. U_{cv} is assumed, as in literature[105, 113], to be equal to $0.7U_j$. The smallest wave number k_1 may be obtained from the measured shock cell spacing, using the relation

$$L_{avg} = 2\pi/k_1$$

Thus, knowing the value of k_1 from the above equation(with the value of L_s substituted as the measured average shock cell length, L_{avg}), the screech tone frequency can be predicted. Further, the Strouhal number for the corresponding screech frequency can be calculated as

$$St = \frac{f_s D_e}{U_j}$$

3.4.6 Jet Noise Measurements

Jet noise directivity measurements of the sound pressure level(SPL)(R,θ) with the ambient fluid at rest are usually made with the microphone placed on a circle with radial distance R from the center of the nozzle/slot exit plane as a function of the polar angle θ to the jet axis[114]. The noise measurements by Lush[115] of an unheated subsonic jet were performed at R/D_e=120. Ahuja[116] also measured the noise of unheated jets at subsonic Mach numbers at three distances,i.e., R/D_e=25, 30, 47. Though these distances were considerably closer than those of Lush, he ruled out any spurious near field effects in the low frequency regime by comparing the results at R/D_e=25 and 47. The measurements with heated and unheated supersonic jets reported by Tanna[66] were made at an intermediate distance, R/D_e=72. Many other investigators carried out far field jet noise measurements at distances ranging between 25 to 100[10, 117, 79, 103, 17, 118, 119]. Taking into consideration the above measurement conditions, the following schedule was adopted in the present investigation for far field measurement of jet noise:

- It is known that the second harmonic of screech peaks at 90^o, while the first harmonic peaks at an angle of 150^o from the jet axis[16, 10, 76]. As such spectrum analysis is made at an angle of 150^o to the upstream jet axis with the microphone placed on a circular arc of radius R/D_e=50 from the center of the jet exit plane. Instantaneous spectral plots were obtained at two exit Mach numbers, M_j=1.0 and 1.5 only in the notched plane.

- The overall sound pressure level(OASPL) data is obtained with the microphone positioned at two polar angles, θ=90^o and 150^o to the upstream jet axis and at $R/D_e = 50$ as shown in Fig 3.10. Figure 3.11 shows a photograph of the arrangement. This was done since it is seen from literature that mixing noise is radiated at polar angle of 90^o whereas

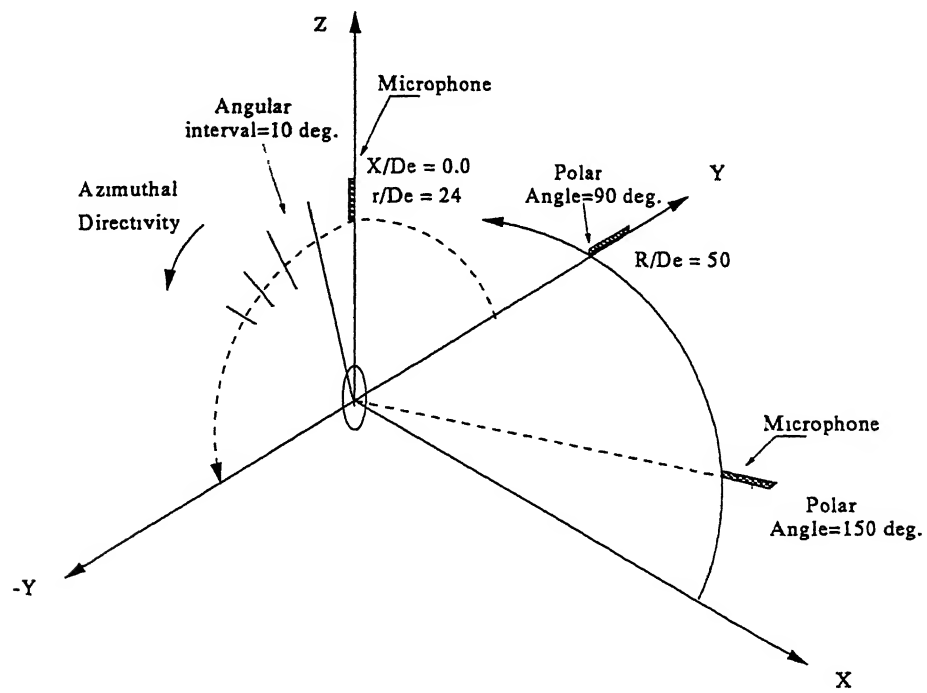

Figure 3.10: Orientation sketch for sound measurements. Microphone position for azimuthal directivity measurements, r/D_e=24, θ=90°; Broadband shock noise measurements, R/D_e=50, ϕ=0°, θ=150°

Figure 3.11: Photograph showing the microphone position during OASPL measurements

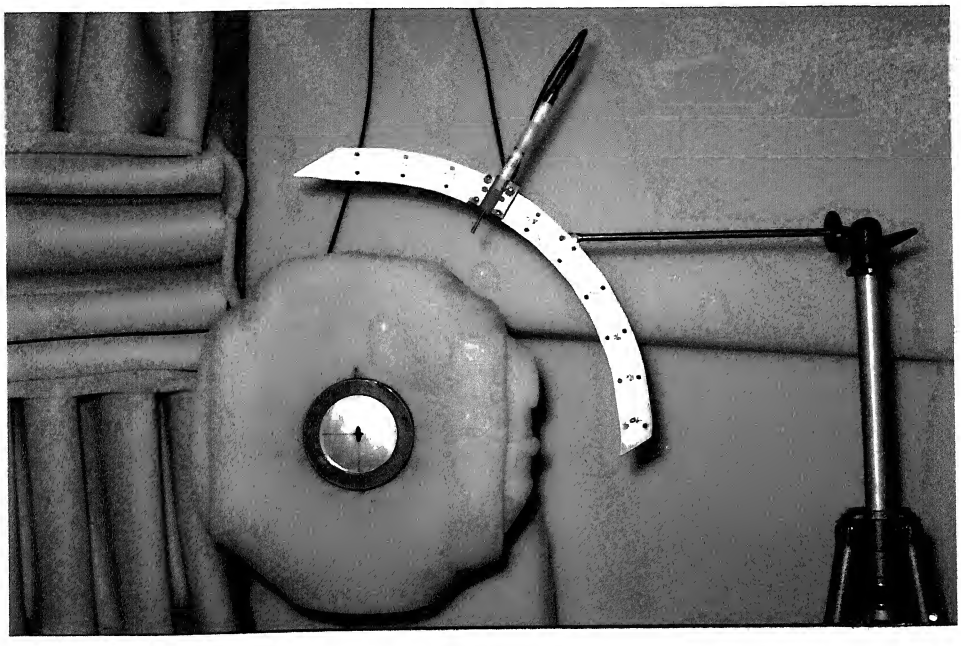

Figure 3.12: Photograph showing the microphone position during azimuthal sound measurements

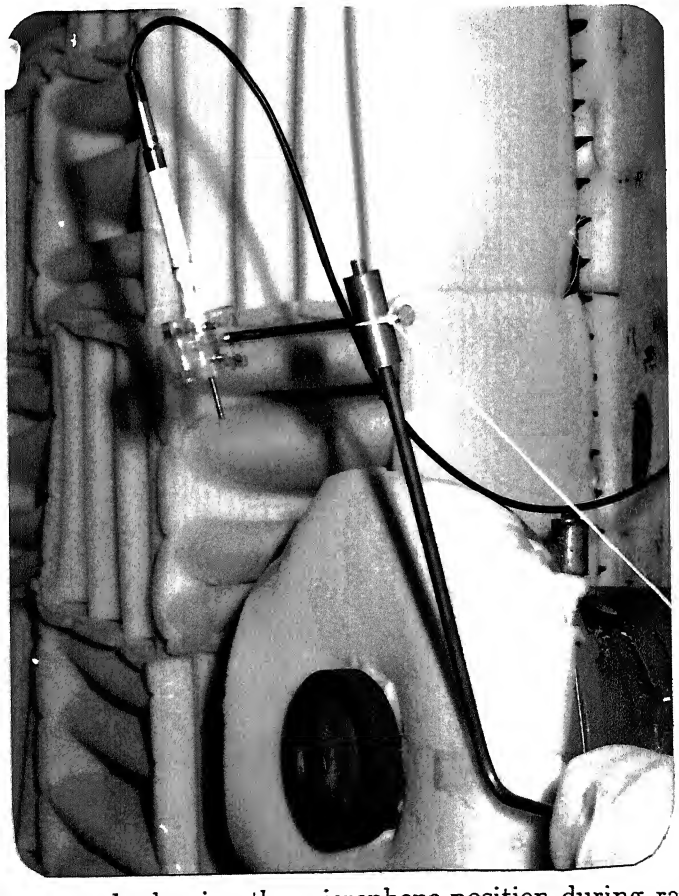

Figure 3.13: Photograph showing the microphone position during radial sound measurements

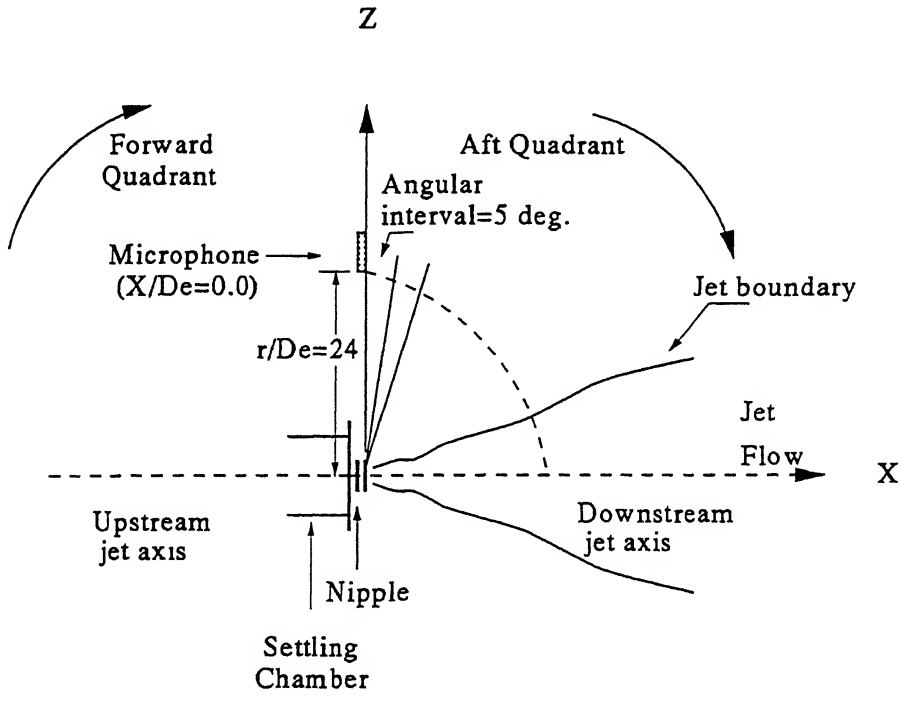

Figure 3.14: Orientation sketch for radial sound measurements

the broadband shock associated noise at 150°[66, 76, 33]. Further, for a fixed value of θ, the jet Mach number is varied for different levels of underexpansion starting from $M_j = 1.15$ to 2.0 by varying the stagnation pressure inside the settling chamber. The measurements were carried out in both notched and unnotched planes.

- For azimuthal directivity measurements, the microphone was mounted on a Aluminium quadrant of radius $24D_e$ and held in the exit plane with a rod mounted on a tripod stand. The Aluminium quadrant was fabricated in such a way that the microphone could be moved at an angular interval of 10 degrees, Fig. 3.10. After measurements were carried out in half quadrant of the exit slot geometry, the slot geometry was adjusted for the other quadrant so as to span one half of the slot geometry. Measurements are once again made for $M_j = 1.0$ and 1.5. Figure 3.12 shows a photograph of the arrangement during azimuthal noise measurements.

- Jet noise is a strong function of the observer angle and therefore, exhibits directivity characteristics. As such, measurements are carried out to study the radial directivity characteristics in the aft quadrant, as defined in Fig. 3.14, for $\theta > 90^o$ up to 160^o in both notched and unnotched planes of the cases investigated. The microphone is mounted on angled brass rod which in turn is fixed to the traverse as shown in Fig 3 13 so that the microphone moves in a circular arc of radius $24D_e$. The movement of the microphone is controlled by a rotating knob in the traverse which helps to move the microphone in an arc in the aft quadrant, Fig.3.13. Measurements are carried out at an angular interval of 5 degrees and at two exit Mach numbers, $M_j = 1.0$ and 1.5. Figure 3.14 shows an orientation sketch for radial sound measurements.

3.5 Experimental Precautions

The following precautions were taken into consideration while carrying out the experimental investigation:

- The settling chamber was carefully aligned in the horizontal direction so as to ensure a horizontally aligned flow.
- Wire mesh screens were placed inside the settling chamber to reduce the disturbances at the nozzle exit and to a settled equilibrium.
- The probe was carefully aligned with the flow direction parallel to the Y-axis of the slot geometry, facing the nozzle exit.
- The apparatus was placed in a large room with constant ambient temperature.
- The distance from the apparatus to the nearest wall was about 250 cm. Therefore, the wall effect during the experimental measurements was negligible.
- Before the experimental runs, leakage test was performed so that the experimental set up was leak free even at the maximum working pressure.
- The stagnation pressure and the air flow rate in the settling chamber were kept constant during the experiments by adjusting the pressure regulating valve.

- All the jet noise measurements were made inside an anechoic chamber, ensuring that the external noise is not influencing the measurements. Further, all the noise measurements were made during night time so that the environment was quiet.

3.6 Data Accuracy

The uncertainty analysis[120] was carried out to find the accuracy of the data in the present investigations. The procedure adopted for the uncertainty analysis is described in the Appendix.

The possible sources of error in the present investigation are due to linear movement of traverse along X, Y and Z directions, the settling chamber stagnation pressure measuring manometer, in measurement of pitot pressure in the jet field, noise measurements using sound level meter, and shock-cell length analysis using the traverse. The traverse is provided with a vernier scale with a resolution of 0.1 mm. Hence, the accuracy of traverse movement along X, Y and Z directions was ± 0.1 mm. The pressure measuring manometers were provided with graduations with a resolution of 1 mm. All the pressure measurements were accurate up to ± 1 mm of mercury column and all the measurements were found to be repeatable within ± 3 percent. For noise measurements, the accuracy of sound level meter readings, according to manufacturers specifications was within ± 0.3 dB in the range of 20 Hz to 20 kHz. The shock-cell lengths measured were accurate up to $\pm 2\%$. The measured OASPL were accurate up to ± 0.3 dB. To ensure this the sound level meter was calibrated everyday with th CA250 precision acoustic calibrator.

Finally, although great care was taken in Pitot pressure measurements, the possibility of some inaccuracy in these measurements, in a highly turbulent and three dimensional flow field as in the present case cannot be ruled out. But it may be assumed justifiably that this slight inaccuracy may not effect the results significantly as the results are primarily of comparative nature.

Chapter 4

Circular Slot Jets

Effect of Notch and Notch Geometry on the Mixing and Noise Characteristics of Free Jets from Circular Slots

4.1 Introduction

Supersonic jets show low spread rates than their subsonic counterparts. This becomes a serious disadvantage in applications like supersonic combustion where efficient mixing over a specified axial distance is crucial. When a jet is operating at off-design conditions, this effect is further aggravated due the presence of the repetitive shock-cell structure in the core region. With the increasing interest in the oncoming Supersonic Transport(SST) projects, the study of jet characteristics and its related problems has received considerable attention and enthusiasm. The most challenging task till date remains the suppression of noise of a supersonic/underexpanded jet. However, in addition to noise reduction other characteristics like minimal thrust loss and higher mixing rates should be maintained. The presence of large-scale vortical structures in supersonic flows[64, 98] have opened up avenues of possible shear-flow control in this regime. In addition to the large-scale structures, which are primarily responsible for entrainment(bulk-mixing), mixing at fine-scale level is necessary in processes like combustion. Thus, enhancement in the jet characteristics can be achieved by the careful breakdown of the large-scale structures into small-scale eddies through longitudinal and azimuthal instabilities at the nozzle exit plane[3].

Various methods of passively improving the jet characteristics have been reported in literature. Since jet characteristics are most receptive to changes in initial conditions, exit geo-

metry variation plays a dominant role in the development of both low[3, 61, 62, 59] and high-speed[Wlezien88] jets. From literature it is seen that jets from non-circular geometries[3, 29, 60, 61, 62, 59, 1] result in enhanced mixing, a characteristic making them far superior to the conventional circular jet. This is attributed primarily to the axis-switching phenomenon associated with the distortion of the large-scale vortical structures caused by the non-uniform azimuthal curvature variation resulting in a non-uniform self-induction process[1, 63]. Improvement in fine-scale mixing have been observed by Schadow *et al*[3] in triangular nozzle jets wherein the small-scale eddies shed from the sharp corners induce turbulence near the exit plane, thereby interacting strongly with the large-scale vortices shed from the plain sides. Some similar observations have been made for square and rectangular slot jets[121, 59]. Thus, the regular breakdown of the coherent structures by the process of vortex dynamics[3] can be used to modify the flowfield as per need of application. As such they are preferred wherever efficient mixing is crucial e.g., combustion chambers, exhaust nozzles of propulsion units, chemical reactors etc.

Flows from modified circular/axisymmetric nozzles have been studied by a number of investigators. Gross distortions in the jet structure have been observed using intrusive means in circular jets e.g., tabs both in subsonic[7] and supersonic regimes[66, 16, 68, 71]. Bradbury[7] observed that the introduction of rectangular tabs in the nozzle perimeter introduces circumferential variations in the jet flow angle and produces profound effect on the jet development by splitting the jet field into two high velocity regions on either side of the diameter joining the two tabs. The gross distortions bring about increase in entrainment into the jet. Introduction of tabs in supersonic jets help to weaken the shock-structure considerably and hence, eliminates screech as seen by Norum[16] and Krothapalli *et al*[67]. However, the use of tabs to some extent adversely effects the overall thrust. As such non-intrusive means are preferred. A study of notched circular(fish-tail configuration) jet[8] revealed a much higher spread in the notched plane with the shedding of vortices from the edges of the notches. This vortical structure is found to act as a shielding device to the shock-structure resulting in noise reduction. Norum[16] and Krothapalli *et al*[18] used fingers/slots in the nozzle parallel to the jet axis. The pressure relieving effect of the fingers/slots greatly weakens the shock-structure and hence, reduces shock associated noise. However, the pressure relieving effect of fingers/slots, again results in thrust loss.

The present chapter aims at understanding the changes introduced by the presence of a discontinuity in the form of a notch in circular slot jets for the purpose of enhanced mixing and noise reduction. Two such notches are symmetrically introduced along a diameter of the circle. A direct comparison of the jet characteristics are made with a plain circle of same equivalent area to study the changes brought about in the jet flowfield by notches when introduced in a geometry with a uniform azimuthal curvature variation. Although a plethora of study on circular jets have been carried out, no work seems to report the effect introduced by notch geometry variation on the mixing and noise characteristics of sonic underexpanded circular slot jets. Such sharp corners have been observed[3, 121, 59] to improve the flowfield considerably near the exit plane, and so these initial instabilities are also expected to enhance mixing in circular slot jets as well. The effect of notches on far field shock associated noise is also investigated. Since the source of noise has been reported by Hammitt[104], Glass[50] and Krothapalli[18] to be located approximately at the end of third shock-cell, weakening the shock-structure with variation in notch geometry may help to reduce the shock noise of sonic underexpanded circular slot jet.

4.2 Results and Discussions

4.2.1 Iso-velocity Contours

Figures 4.1(a)-(d) show the iso-velocity contours for a plain circular slot jet as it develops in the downstream direction. The figures show smooth contours indicating the absence of any discontinuity in either X-Y or X-Z planes. However, the shape gets distorted from the expected circular shape as the jet propagates downstream. This may be due to the asymmetric shear activity, along the periphery of the jet core where active entrainment is taking place, which need not be symmetric even though the slot geometry is symmetric. However, this is not very important since the prime importance here is to have a comparative study for cases when notch is introduced. Let us now observe the effect of notch introduction in the circular slot periphery.

Figures 4.2(a)-(d) show the iso-velocity contours for the square notched/modified circle at P_e/P_a=1.0, i.e., M_j=1.0. In these plots the local velocity U is normalized by the exit centreline velocity U_c. The presence of the notch in circular geometry makes it slightly non-circular with

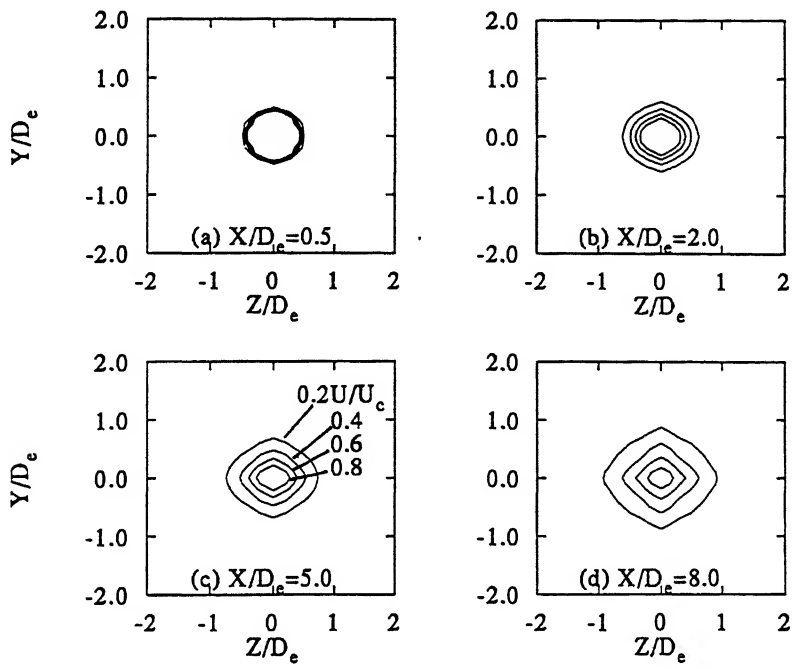

Figure 4.1: Iso-velocity contours for plain circular jet, M_j=1.0

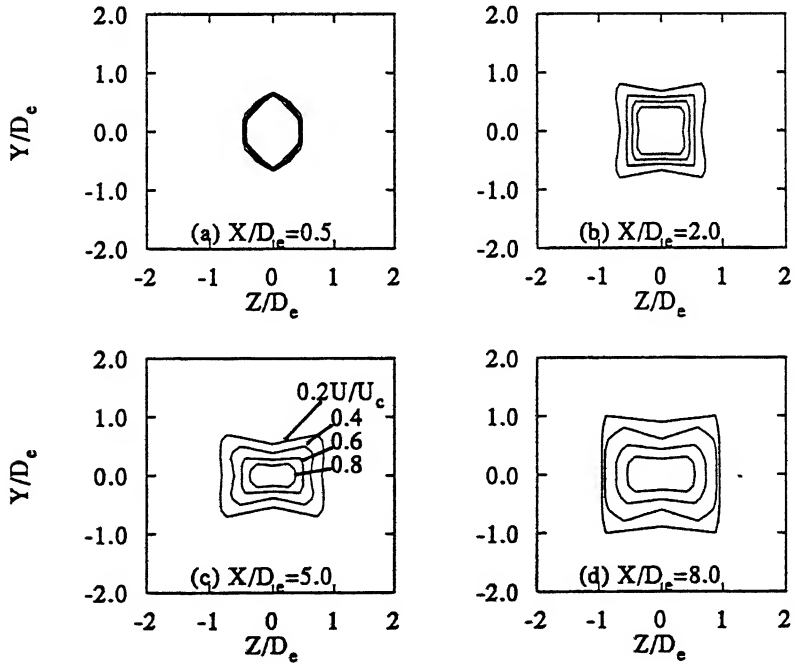

Figure 4.2(a)-(d): Iso-velocity contours for square notched circular jet, M_j=1.0

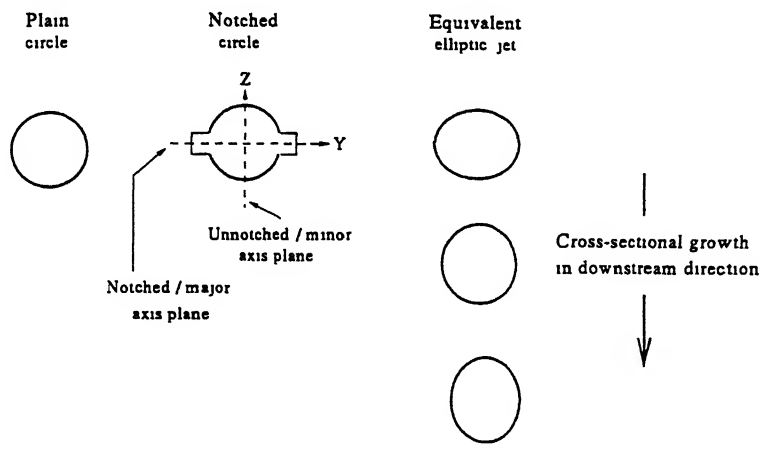

Figure 4.2(e): Cartoon showing the cross-sectional growth of a notched circular jet

its major-axis along the notched plane, as shown in Fig. 4.2(e), resulting in an equivalent elliptic jet. In other words, a slight aspect-ratio in introduced in the modified circular slot geometry by notch presence. Designating the notched/modified(X-Y) plane as the major-axis plane and the unmodified(X-Z) plane as the minor-axis plane of the modified circular geometry, as shown in Fig. 4.2(e), it is observed from Fig. 4.2(a)-(b) that at X/D_e=5.0, the two axis interchange/switch, i.e., the initial(designated) major-axis becomes the new minor-axis and vice-versa. In other words, an axis switching is observed as is typical to jets issuing from non-circular exit geometries. This feature is totally absent in plain circular jets owing to symmetry of geometry about the jet axis(Fig. 4.1). The sharper curvature at the location of the notch relative to the remaining portions of the slot results in the local bending of the vortex and hence, causes self-induced azimuthal deformations which is responsible for axis-switching and enhanced mixing in non-circular jets[1].

Due to the uniform azimuthal curvature of circle the jet grows uniformly outward in the unnotched plane. However, the slight aspect-ratio introduced by the notches causes the jet to grow slowly along the notched plane(i.e., the designated major-axis for this case) with a simultaneous bulging/spreading along the unmodified(X-Z) plane. The above process is

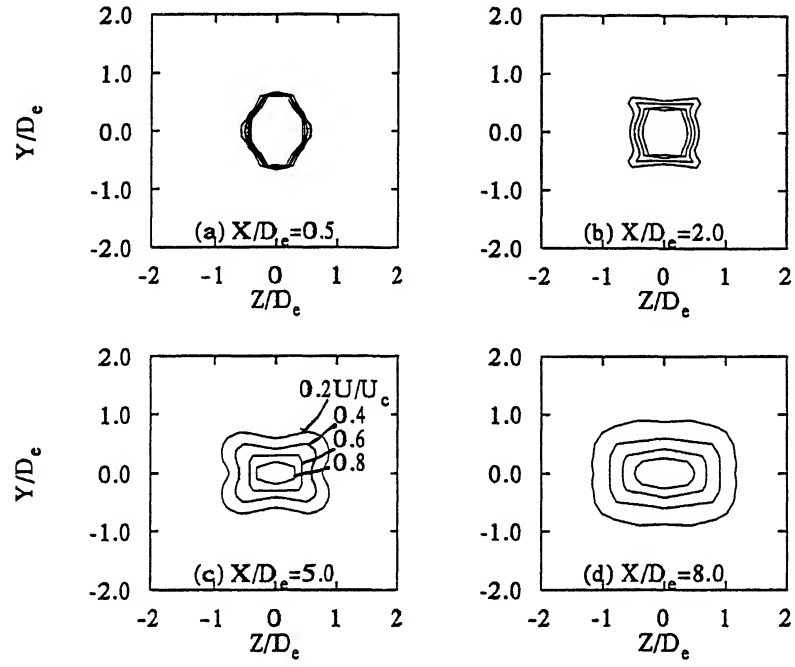

Figure 4.3: Iso-velocity contours for triangular notched circular slot jet, M_j=1.0

illustrated through Fig. 4.2(e) showing the cartoon of the cross-sectional growth of the modified circular or equivalent elliptic jet. As seen, the first switch in axis occurs in the unnotched/minor-axis plane of the modified circular geometry. This is the major difference that is brought about by the presence of notch in a geometry with uniform azimuthal curvature variation, compared to notches in a geometry with non-uniform curvature variation(i.e., ellipse), as will be seen later in chapter 5. This axis-switching phenomena in the non-circular jets is responsible for higher bulk mixing[20, 1] and hence, higher entrainment.

Let us now observe the change introduced by the triangular notch in circular exit geometry. Figures 4.3(a)-(d) show the iso-velocity contours for a jet from a circular slot with triangular notches. It is discernible from the plots that at X/D_e=0.5 and 2.0, with the introduction of a sharp corner in the form of the vertex of an equilateral triangle, the growth along the major-axis side(notched plane) is delayed because of the restricted growth at the vertex of the triangular notch. As a result only the pressure relief along the flat sides of the triangular notch effects the growth resulting in a squeezing of the jet along these sides as is seen in figure 4.3(b). The

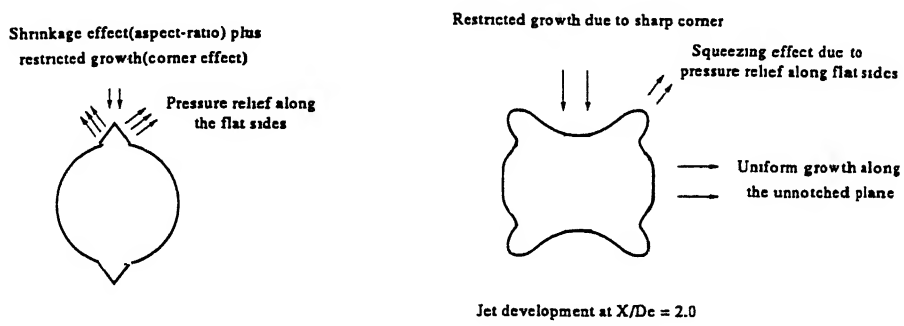

Figure 4.3(e): Cartoon showing the jet development from triangular notched jet

process is elucidated in the cartoon developed from these contour plots in Figure 4.3(e). This squeezing seen at X/D_e=2.0 is distinguishable relative to the jet growth along the unnotched plane. Since the restricted growth at the corners may be due to the generation of small-scale structures[58, 121, 59], and entrainment is primarily due to large-scale structures or bulk-mixing therefore, this particular notched jet is expected to show lesser entrainment relative to square notched jet.

Semi-circular notch on the other hand due to absence of any sharp corner in it shows the absence of restricted growth in the notched plane and as such grows like a typical non-circular jet, Figs. 4.4(a)-(d). The major-axis side(notched plane) grows uniformly as is seen by flat contours along X-Y plane at X/D_e=2.0. Moreover, the squeezing effect observed in triangular notched jet is not seen here. Beyond X/D_e=2.0, the jet grows in a fashion similar to other notched jets. However, the absence of sharp corners in this notch geometry expedites axis-switching relative to triangular notched jet where the restricted growth at the vertex of notches(major-axis ends) delays this phenomena.

Thus, square notch which has a better pressure relieving effect in the three directions along with generation of secondary motions initiated at the corners[29, 61, 5, 59, 3, 46, 4] and is expected to entrain more than the semi-circular notch which has an absence of sharp corners in its geometry. Whereas triangular notched case with a vertex angle of 60^o is not expected to be beneficial from the view point of bulk-mixing for reasons stated above.

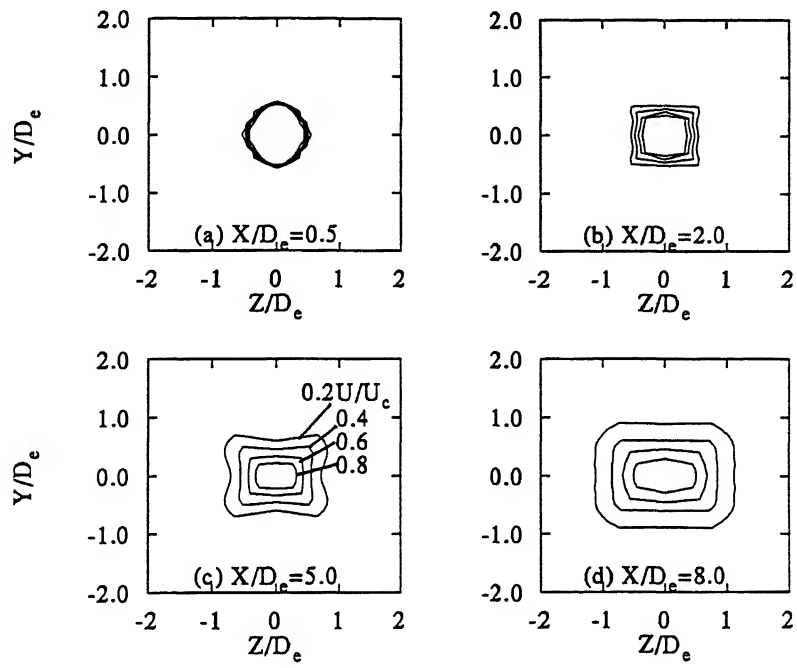

Figure 4.4: Iso-velocity contours for semi-circular notched circular slot jet, M_j=1.0

Figure 4.5(a) shows the entrainment plot at correct-expansion for the above cases. In these plots the local mass-flux is subtracted from the mass-flux at the slot exit and then normalized by the mass-flux at the slot exit. For comparison Samimy *et al*[12] data for two tabs in circular nozzle jet at M_j=0.5 is included, i.e., to observe the difference between the entrainment nature of the nozzle and slot jets along the jet axis. Relative to the plain circular-slot jet, considerable increase in entrainment is observed when notches are introduced. It is discernible from the plot that square notched jet shows a higher value of entrainment followed by the semi-circular notched jet. Relative to the plain circular jet at X/D_e=5.0, square notched jet shows an increase in entrainment value by 500% followed by semi-circular notched jet with 400% increase. At 15.0D_e, the increase is 67% and 25% for square and semi-circular notched cases, respectively. Thus, in the initial region of the jet where there is a dominance of large-scale structures[11], the local entrainment shows an increase

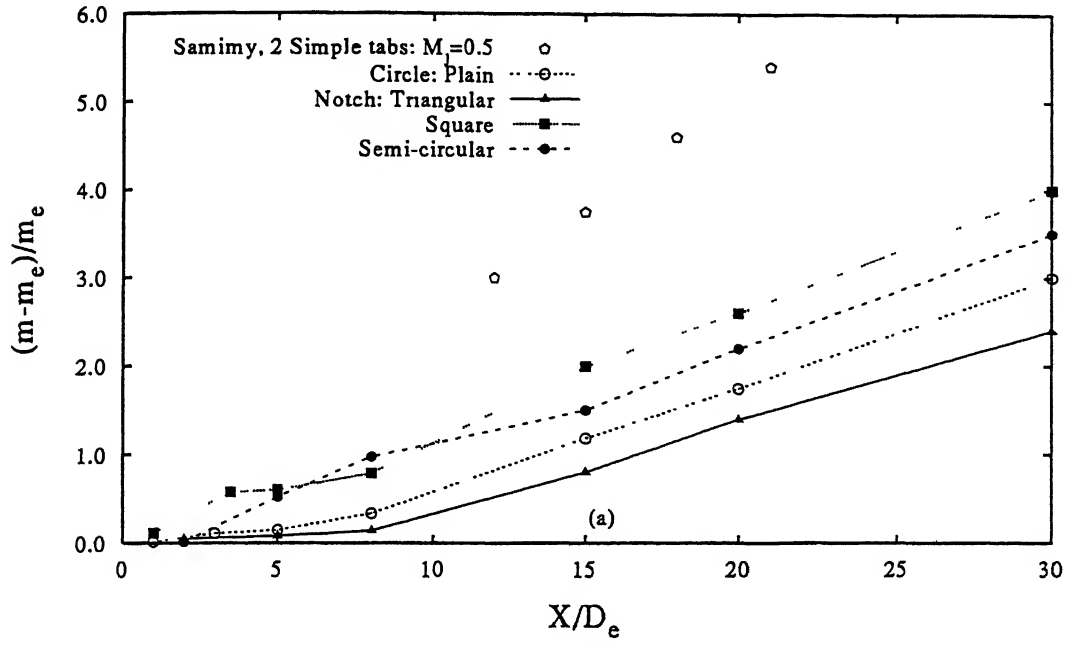

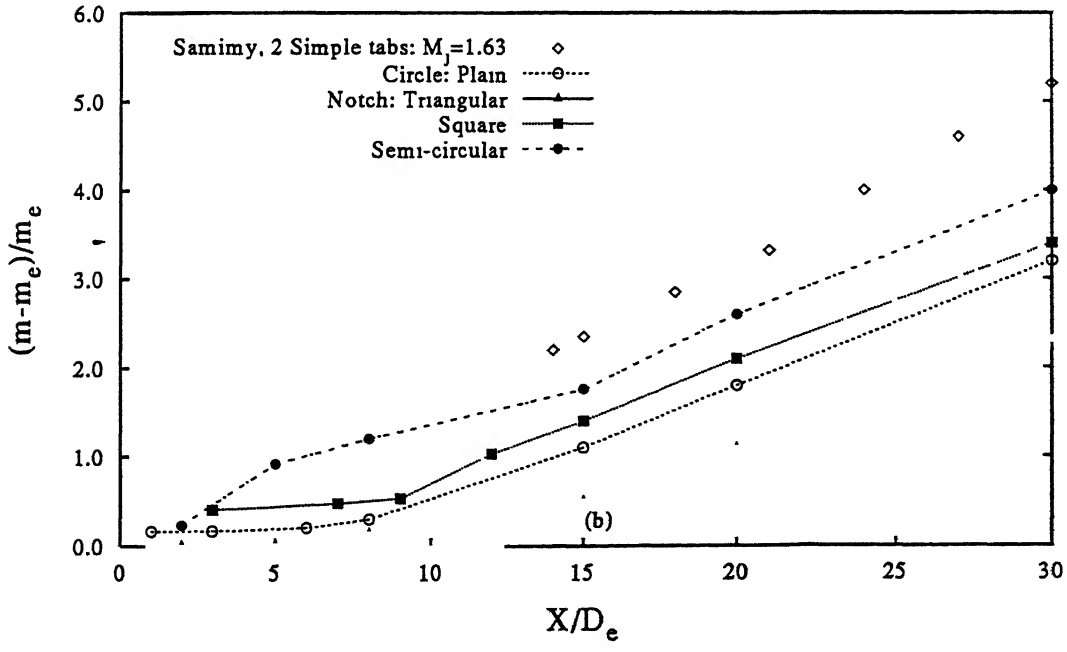

Figure 4.5: Entrainment comparison for plain and notched circular slot jets at (a) M_j=1.0, (b) M_j=1.5

in value relatively whereas its value comes down at a downstream location, e.g. at X/D_e=15.0. Thus, square and semi-circular notched jets seem to have a dominance of bulk-mixing in the near region of the jet relative to plain and triangular notched jets. The triangular notched jet however, shows a lesser value of entrainment relative to plain circle. This may be due to the fact that though a slight aspect-ratio is introduced by the notches, the presence of a sharp cornered notch(triangle with vertex angle of 60^0) restricts the growth of the jet and hence, prevent the roll of uniform vortices in that plane. This is in confirmation to Schadow *et al*[3] and Gutmark *et al*[46, 4] study that decreasing the vertex angle of triangular jet increases fine-scale mixing at that corner region, thereby greatly restricting bulk mixing in that region. However, increasing the corner angle in the notch to 90^0 and above(semi-circular notch) reduces the restricted growth in the notched plane and hence, results in higher bulk mixing. Thus, notches seem to be effective in circular-slot jet at correct expansion.

Figure 4.5(b) shows the entrainment comparison for the cases at M_j=1.52. The effect of notch geometry at underexpansion is clearly seen. For comparison Samimy *et al*[12] case of two tabs at M_j=1.63 is also included. It is observed that in the underexpanded condition the semi-circular notched jet shows a higher value of entrainment followed by square notch. Relative to the plain circle, at $5D_e$, semi-circular notch case shows an average of 350 % increase and square notch case approximately 125 %. At $15D_e$ this value comes down to 80% and 40% for the two cases, respectively. Triangular notched jet once again, however, shows lesser entrainment relative to the plain case. Thus, it is clear that the geometry of the notch has a strong influence on the mixing characteristics of circular slot jets. The sharper is the corner in the notch, less favourable is the jet bulk mixing[3, 4]. The above process is clearly illustrated in Fig.4.5(a)-(b) where the semi-circular and square notched jets show higher large-scale mixing and hence, higher values of mass-flux ratios. Further, in underexpanded cases a lesser restricted growth at the slot exit is beneficial since it increases the pressure relieving effect. As such, the semi-circular notch shows a higher entrainment than square notched jet at M_j=1.52.

Since a sharp corner initiates the generation of small-scale discontinuities thereby restricting the growth of uniform vortices in that plane[3, 4], the sharper is the notch angle, the more will be the restricted growth of uniform vortices in that plane and hence, lesser the entrainment of that jet[46, 4]. However, a larger angle of the corner in the notch causes a lesser restricted growth of large-scale vortices in that jet near the exit plane thereby resulting in higher entrainment

for square and semi-circular notched jets. This explains the observations in entrainment plots. However, for noise reduction the presence of small-scale structures near the slot-exit is necessary for a weaker shock-cell system[30, 84]. This aspect is discernible later in the noise investigation of these cases.

Let us now observe the effect of Mach number on entrainment. Figure 4.6(a) shows such a plot. For Samimy[12] case of two tabs, a considerable decrease in entrainment is seen as the jet Mach number is increased from 0.5 to 1.63. This is primarily due to compressibility effects creeping in at high Mach numbers[49] plus the presence of shock-structure in the jet core which further delays mixing. For the present modified circular geometries, square notched jets show a slight reduction in entrainment values as M_j is increased from 1.0 to 1.52. However, semi-circular notched jet shows a reverse trend showing an increase in entrainment with increase in M_j indicating the dominance of bulk-mixing and better pressure relieving effect of this notch geometry. This is a favourable characteristics from the viewpoint of underexpanded jets.

Figure 4.6(b) shows a cross-plot of entrainment versus M_j. It is seen that as M_j is increased, the local entrainment shows a decreasing trend at all the downstream locations under consideration. However, for semi-circular notched case, an increase in entrainment is seen with increasing M_j.

Thus, the geometry of the notch introduced in the periphery of a circular-slot jet has a strong influence on the entrainment characteristics and that the angle of the corner in a notch is a strong parameter controlling mixing in these jets.

4.2.2 Pressure Profiles and Jet Spread

The changes introduced by the presence of notch on the spread characteristics of circular-slot jets is investigated. Here, the pitot pressure P_t is divided by the stagnation pressure P_0 and plotted against the non-dimensionalized lateral distance, Y/D_e or Z/D_e. The effect of notch geometry on the jet spread and growth can be seen clearly in the pressure profiles at various axial locations(X/D_e) in both notched and unnotched planes. Figure 4.7 shows the comparison of semi-circular notch and triangular notched circle at M_j=1.0 as the jet grows in the downstream direction. It is clearly seen from the plots that beyond $1D_e$ the shear layer for the semi-circular notched jet penetrates faster towards the jet centreline as is indicated by a steeper pressure profile at $3.0D_e$. This indicates an earlier switching of axis for this case

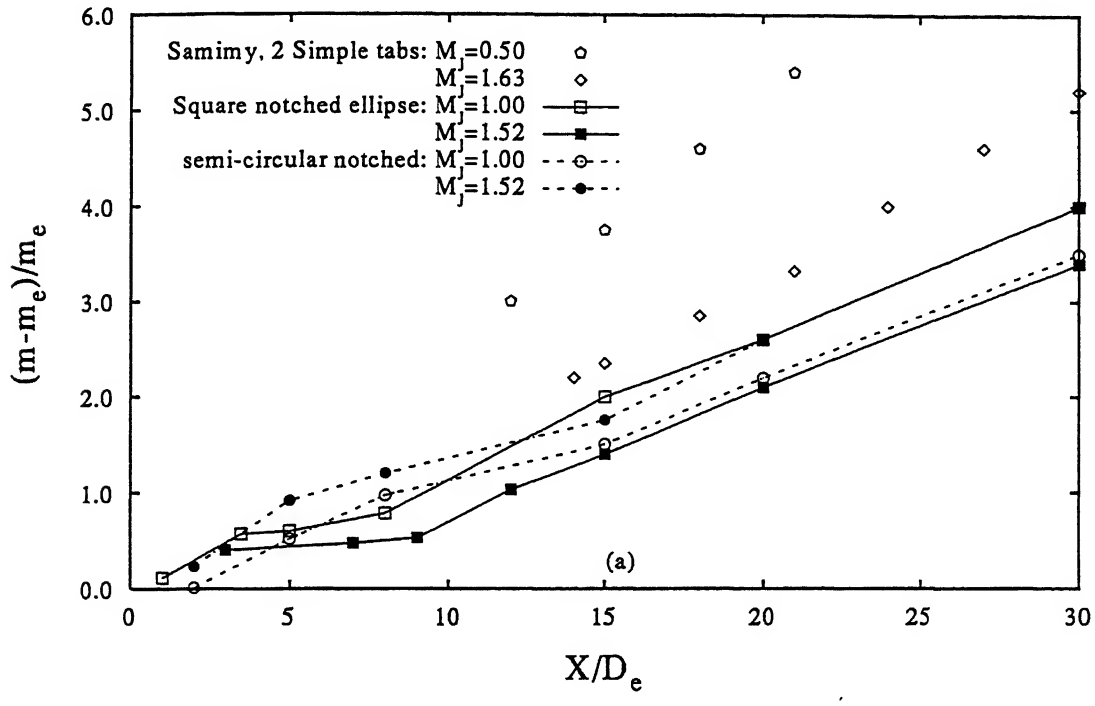

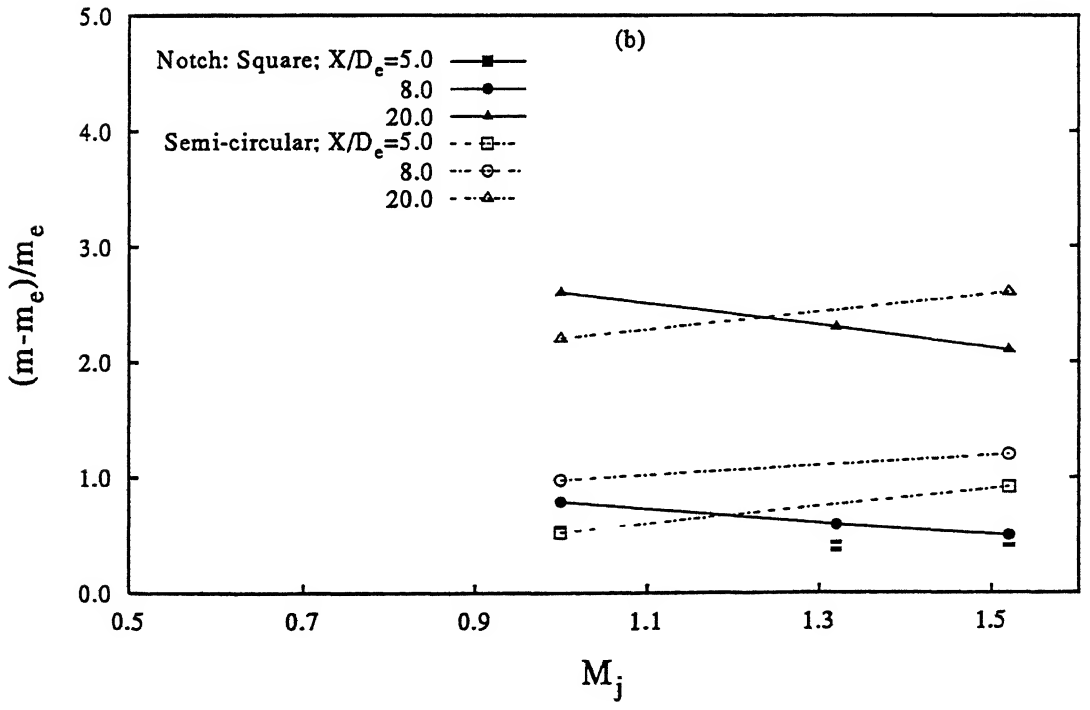

Figure 4.6: Plots showing (a) the effect of Mach number on entrainment, (b) cross-plot of entrainment versus M_j

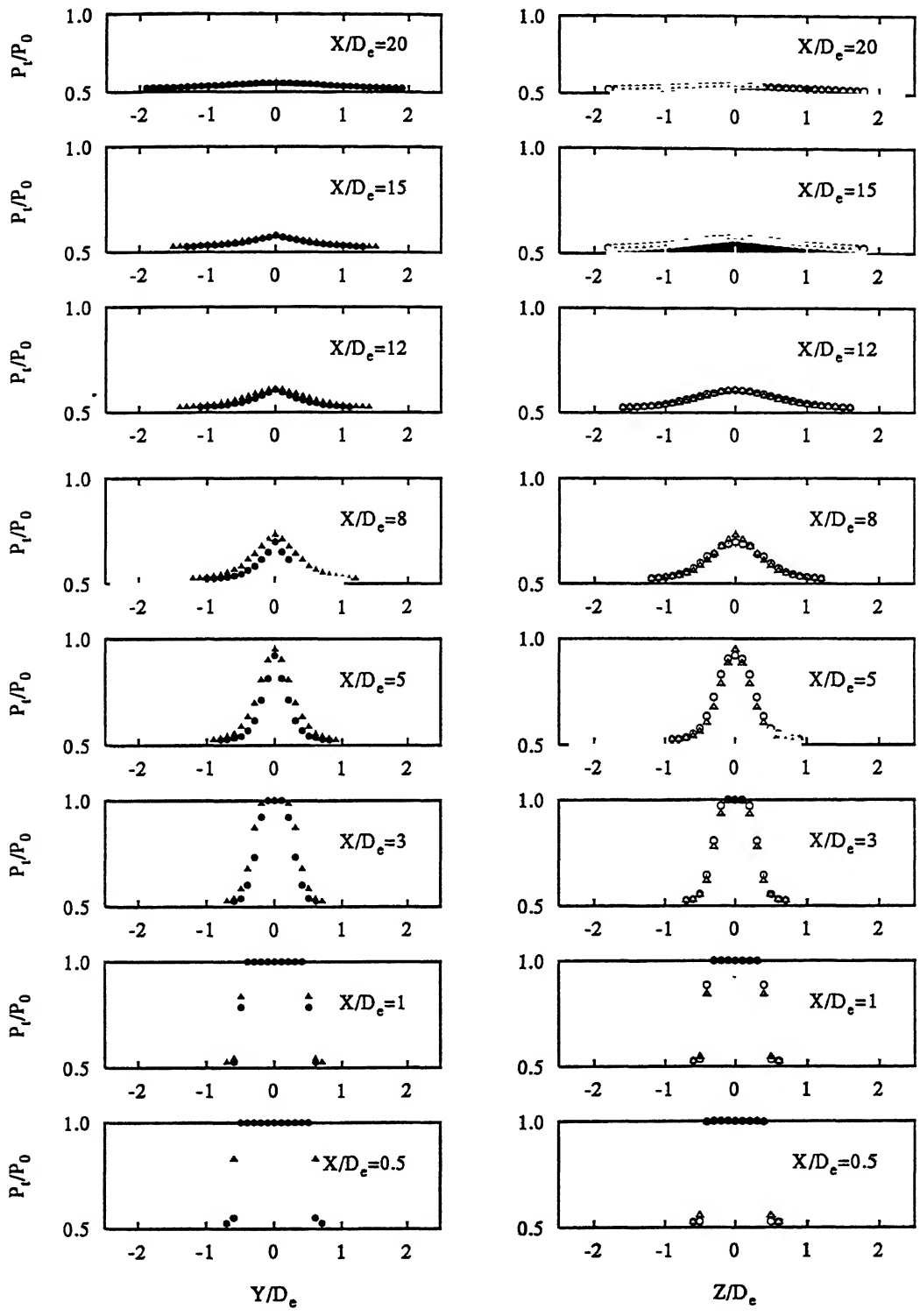

Figure 4.7: Comparison of the pressure profiles of semi-circular and triangular notched circular jets, M_j=1.0; Semi-circular notch: X-Y/notched plane •, X-Z plane ○; Triangular notch: X-Y/notched plane ▲, X-Z plane △.

which is responsible for enhanced mixing[1] as is also indicated by increased entrainment in Figure 4.5(a)-(b). For triangular notch on the other hand, the penetration effect due to notch is almost absent because of the restricted growth at the vertex of triangle reducing the advantage of aspect-ratio introduced by the presence of notch. Upto $3.0D_e$, the shear layer spreads faster towards the jet centreline but almost insignificantly towards the surroundings. Beyond $3.0D_e$ the jet starts spreading faster into the surroundings. At $5.0D_e$, a slight reduction in the magnitude of centreline pressure is seen for semi-circular case relative to the triangular notched jet indicating that the semi-circular notched jet begins to decay faster. The effect is clearly elucidated in the plots upto $12.0D_e$ where the two centreline pressures meet showing similar decay thereafter. However, the spread is higher for triangular notched jet upto $15.0D_e$ after which the two jets spread equally. In the unnotched plane, however, the spread is same throughout for the two cases with the spread in the unnotched plane being more than that in the notched plane from $8.0D_e$ onwards. This validates the explanation of slight aspect-ratio introduced by the notches in circular geometry as discussed earlier.

The sharp corners in the triangular notched circle restricts the growth of the jet in the notched plane and the pressure drops to the ambient earlier and faster thereby delaying shear layer penetration of notched plane and hence, an effective axis-switching is seen in the pressure profiles for both planes from X/D_e=1 to 5. This may be due to the fact that the sharp corners introduce discontinuities in the initial region of the shear layer and prevent the roll up of uniform vortices in this region[3, 46, 4]. This fact is confirmed in the unnotched plane for the two jets at same axial locations.

Now consider the effect introduced by two sharp corners in the form of a square notch. The result of this case is plotted in Fig. 4.8 and compared with the semi-circular notch case. Close to the exit, the square notch shows a restricted growth in the notched plane upto $1.0D_e$ where the jet is seen not spreading appreciably into the surroundings. The extent upto which the restricted growth prevails in the downstream direction is governed by the angle of the sharp corner in the notch. In the triangular notch case, it was observed that the jet shows only marginal spread into the surroundings upto $3.0D_e$ whereas this effect is well pronounced for square notch only upto $1.0D_e$. Further, the spread of the square notched jet in the X-Z plane is more than that for semi-circular case. Thus, it seems that the presence of two sharp corners

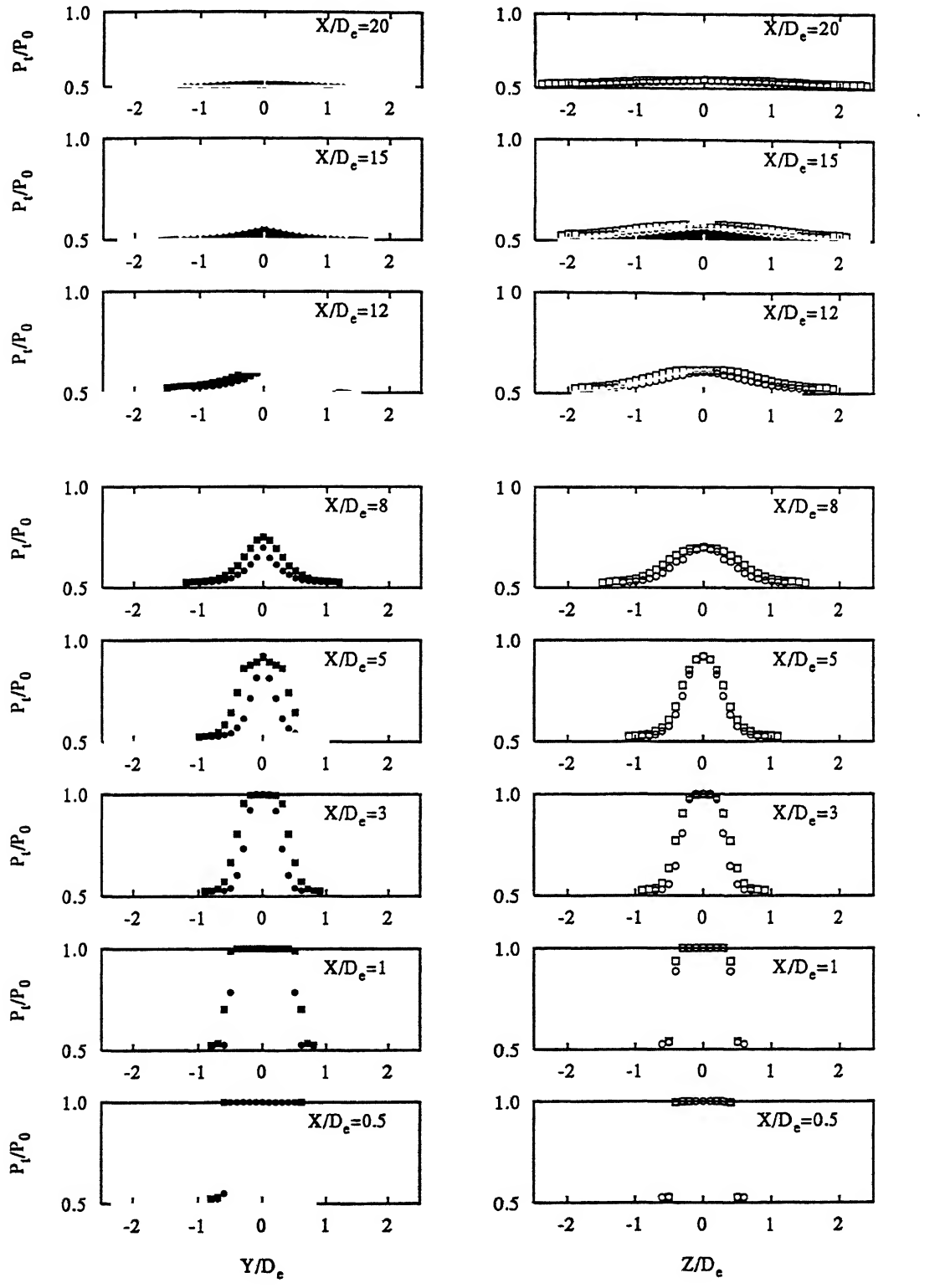

Figure 4.8: Comparison of the pressure profiles of semi-circular and square notched circular jets, M_j=1.0; Semi-circular notch: X-Y/notched plane •, X-Z plane ○; Square notch: X-Y/notched plane ■, X-Z plane □.

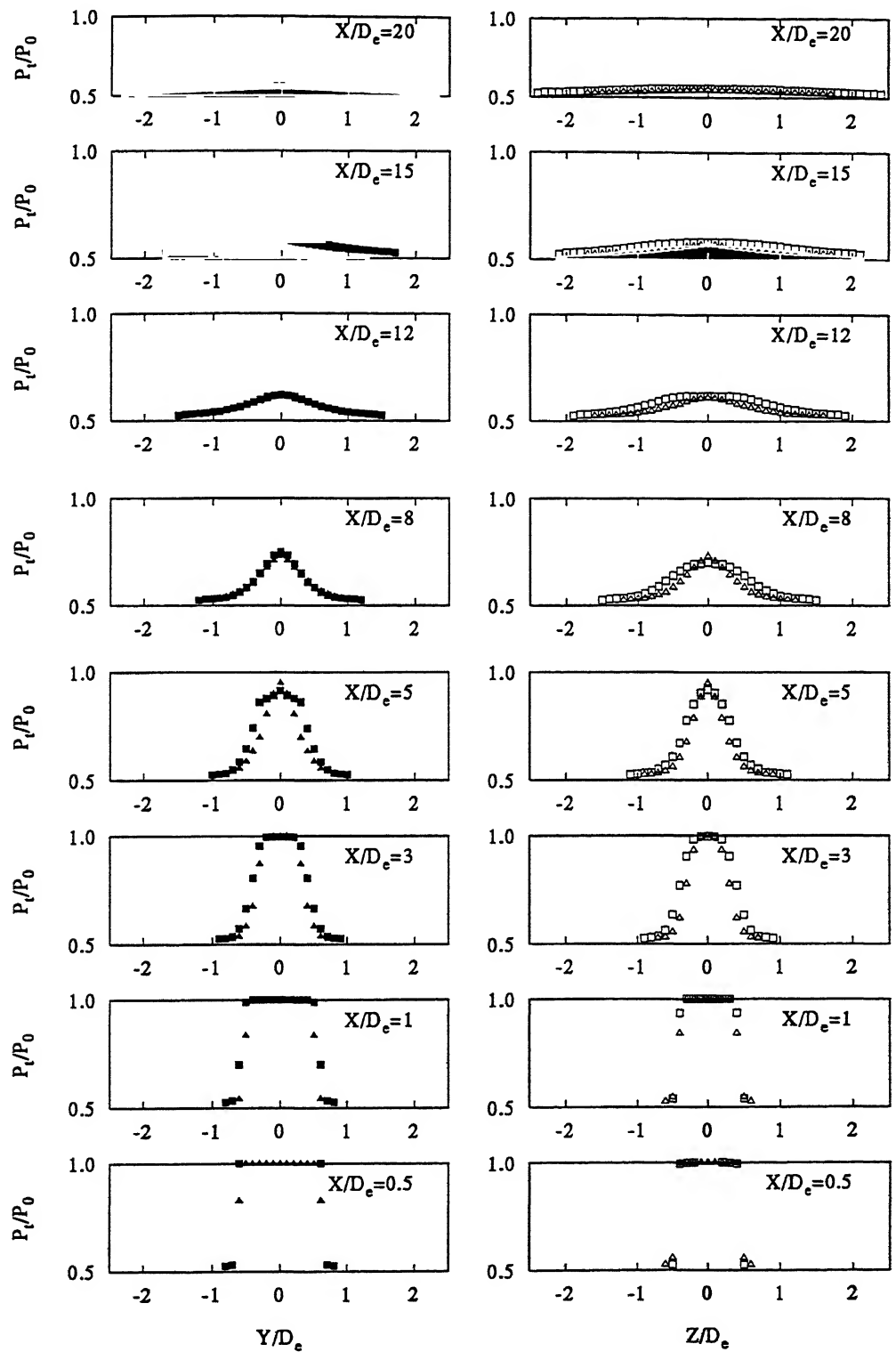

Figure 4.9: Comparison of the pressure profiles of triangular and square notched circular jets, M_j=1.0; triangular notch: X-Y/notched plane ▲, X-Z plane △; Square notch: X-Y/notched plane ■, X-Z plane □.

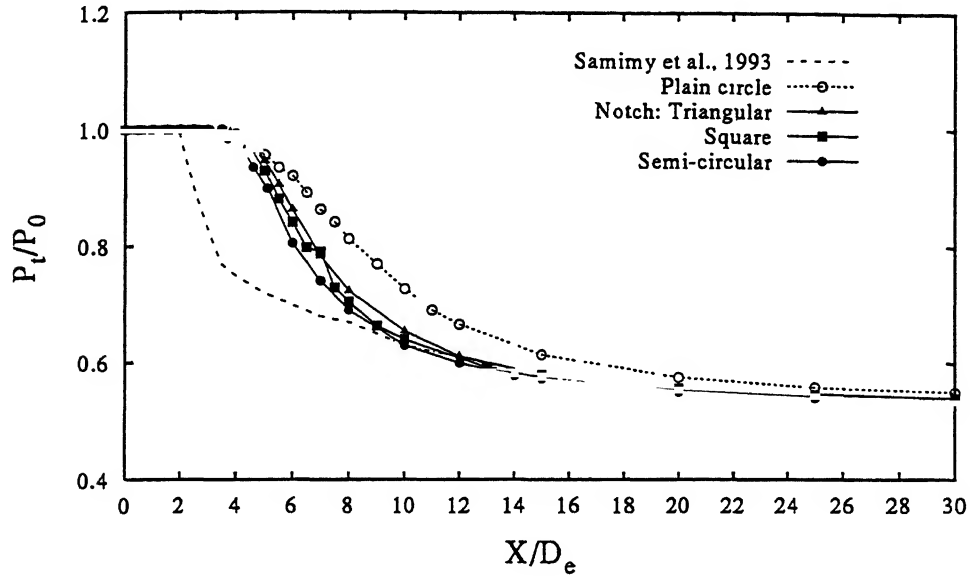

Figure 4.10: Centreline pressure decay comparison for the cases investigated at M_j=1.0

has a better effect on the spread and growth of circular-slot jet in both notched and unnotched planes.

Figure 4.9 showing the pressure profiles of square and triangular notched jets elucidates this fact. It is seen, once again, that the square notched jet spreads faster in both the planes relative to the triangular notched case. Also, the square notched jet decays faster as seen from X/D_e=5.0 onwards upto $8.0D_e$ after which the two jets decay equally upto $20.0D_e$.

4.2.3 Centreline Pressure Decay

When a jet spreads faster, its centreline pressure decreases faster. Thus, different jets with different spread rates result in different centreline decay. Figure 4.10 shows the decay of centreline pressure with axial distance for the four cases investigated at M_j=1.0. The pitot pressure P_t is divided by the stagnation pressure P_0 and plotted against the non-dimensionalized downstream distance X/D_e. A faster centreline pressure decay is usually a reasonable measure of faster jet spread[7, 12]. Also, it has been observed by Roshko[11] that the breakdown of the large-scale structures into fine-scale structures begins at the end of the potential core and this is seen as a drastic decay in the centreline pressure[29]. Thus, a shorter potential core-length

coupled with a faster centreline decay thereafter are indicative of enhanced small-scale mixing characteristics.

The plot clearly indicates that under the action of the notch, the jet decays faster than the plain cases with the plain circle having the least decay followed by triangular, square and finally by semi-circular notched jet which has the maximum. The potential core-length is observed to be affected, but slightly, by the presence of the notch with the semi-circular notched jet showing a minimum core length followed by square and finally, by triangular notched jet which has the maximum. However, the decay, once the end of the core is encountered, is greatly influenced. This is due to the slight aspect-ratio introduced by the presence of notches that initiate high rates of mixing, though it takes some axial distance to do so. At $20.0D_e$, the centreline decay of all the jets slows down and attains an approximately constant value beyond $30.0D_e$. This indicates the beginning of axisymmetric or the fully developed region where the breakdown of large-scale structures initiated at the end of the potential core is completed[11]. Also, beyond $30.0D_e$ all the jets decay almost similarly and oblivious of the initial geometry. The two tab case in a circular nozzle of Samimy *et al*[12] is included in the plot for the purpose of qualitative comparison with the present work. It is clearly seen that the core-length for Samimy *et al*[12] is the minimum. However, after $4.0D_e$, all the jets decay similarly.

4.2.4 Flow Visualization and Shock Structure

As the stagnation pressure inside the settling chamber is increased, the jet becomes underexpanded with the jet core dominated by a repetitive shock-cell structure. This shock structure gradually gets diffused in the downstream direction by turbulence arising from the shear layer spreading towards the jet centreline and the surroundings. How fast these mixing layers spread and diffuse and hence weaken the shock structure depends primarily on the generation of turbulence as close to the jet exit as possible[30]. This strongly depends on the the slot exit geometry and discontinuities introduced in the exit periphery[30, 16, 17].

Figures 4.11(a)-(c) shows the shock-cell structure as captured by shadowgraph photography for the underexpansion level of 2.0, M_j=1.52. The plain circular-slot jet is seen to exhibit strong shocks in the core of the jet, Fig. 4.11(a). A comparison of the Figs. 4.11(a) and 4.11(b)-(c)

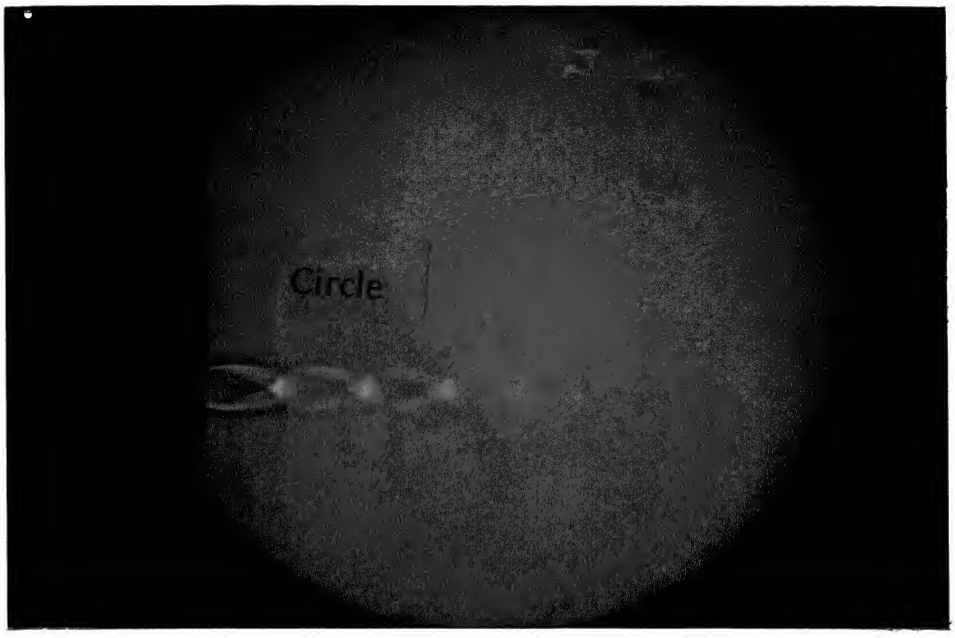

Figure 4.11(a): Shadowgraph picture of plain circular slot jet

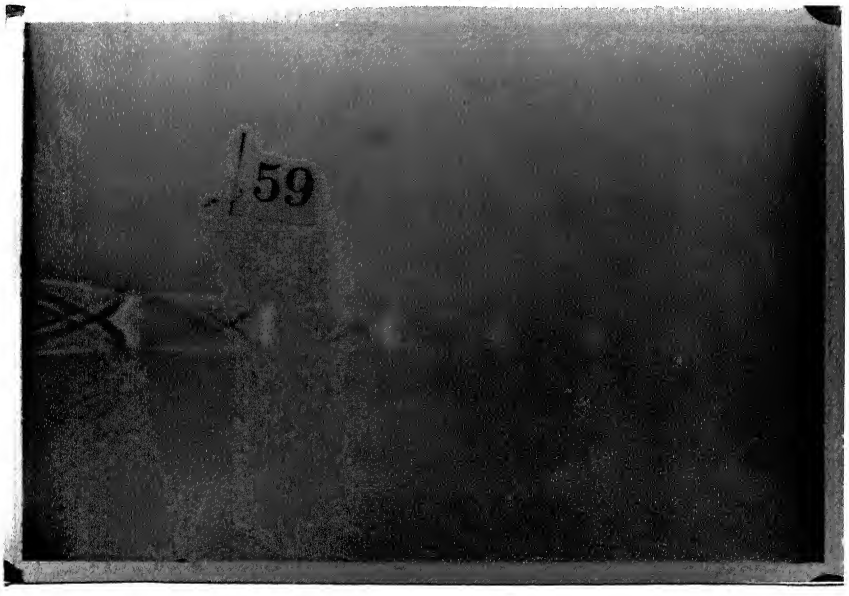

Figure 4.11(b): Shadowgraph picture of notched circular slot jet in notched/modified plane

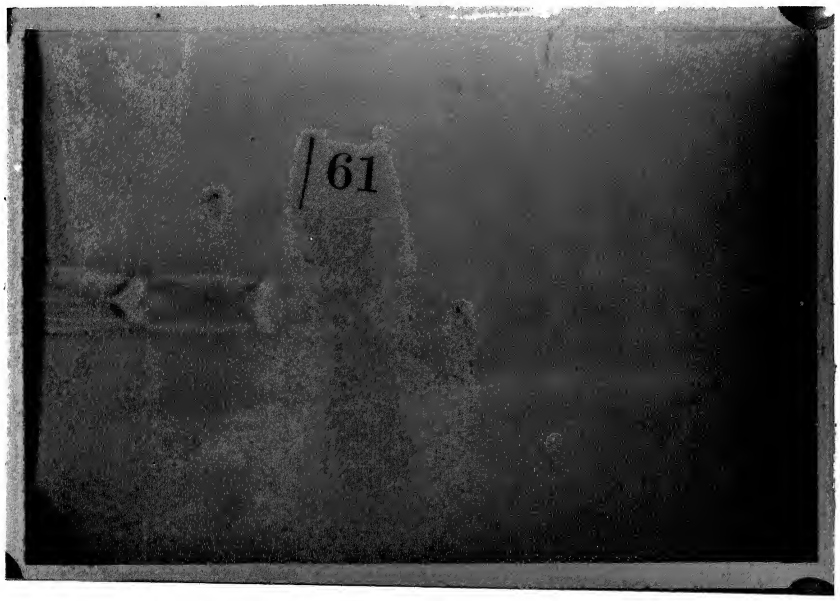

Figure 4.11(c): Shadowgraph picture of notched circular slot jet in unnotched/unmodified plane

clearly illustrates the effect of notch introduction on the downstream development of shock-cell structure. The notches, see Figs. 4.11(b)-(c), are seen to modify the initial shock-cell development(first two cells). Additional expansion and compression waves are seen to emanate from the notches. The interaction of these additional waves with the evolving shear layers leads to appreciable changes in the shock development. In addition to this, the small-scale structures generated at the corners[21, 4] help diffuse the shock structure faster resulting in weaker downstream shocks[4]. Further worth observing is that the lateral dimension of the shocks in the notched/modified plane(Pic. 59), Fig. 4.11(b), decreases in the downstream direction whereas it remains approximately constant in the unnotched/unmodified plane(Pic. 61), Fig. 4.11(c), indicating that the notched jet behaves like a non-circular jet(due to slight aspect-ratio introduced by notch presence in an otherwise circular exit geometry).

Further details of shock strength and jet decay is illustrated by Pitot tube traverses along the jet centreline. Figure 4.11(d) shows the centreline pressure decay plot for the cases investigated at M_j=1.52. The pressure oscillations in the upstream regions are due to the stationary shock structure in the jet. In the supersonic regions of the flow, the measured stagnation pressure P_{t2} corresponds to the stagnation pressure behind the standing bow shock in front of the pitot probe.

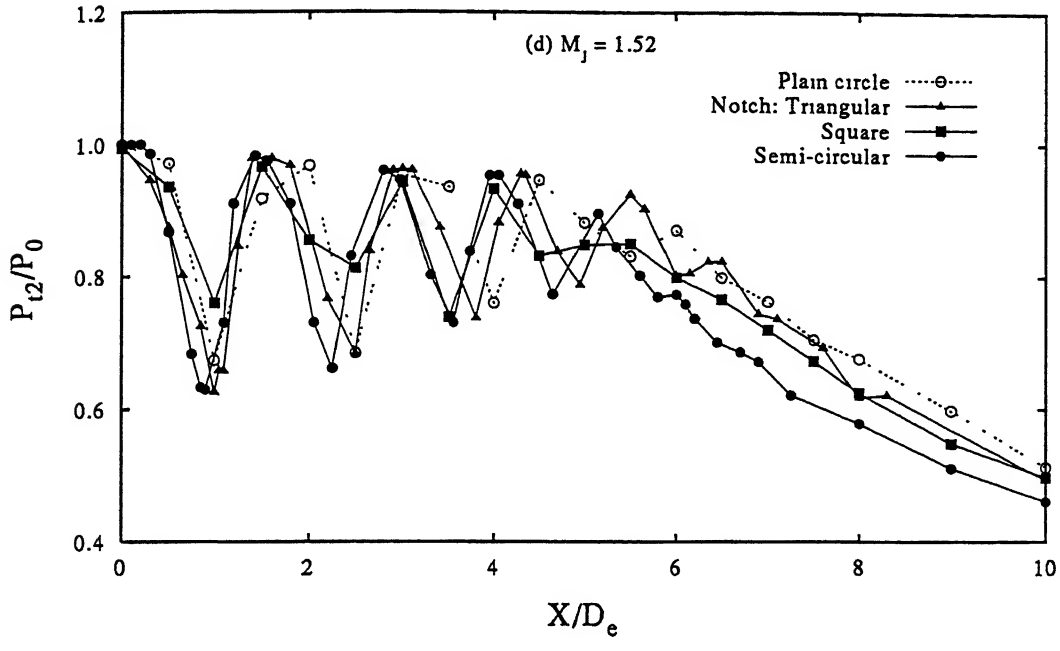

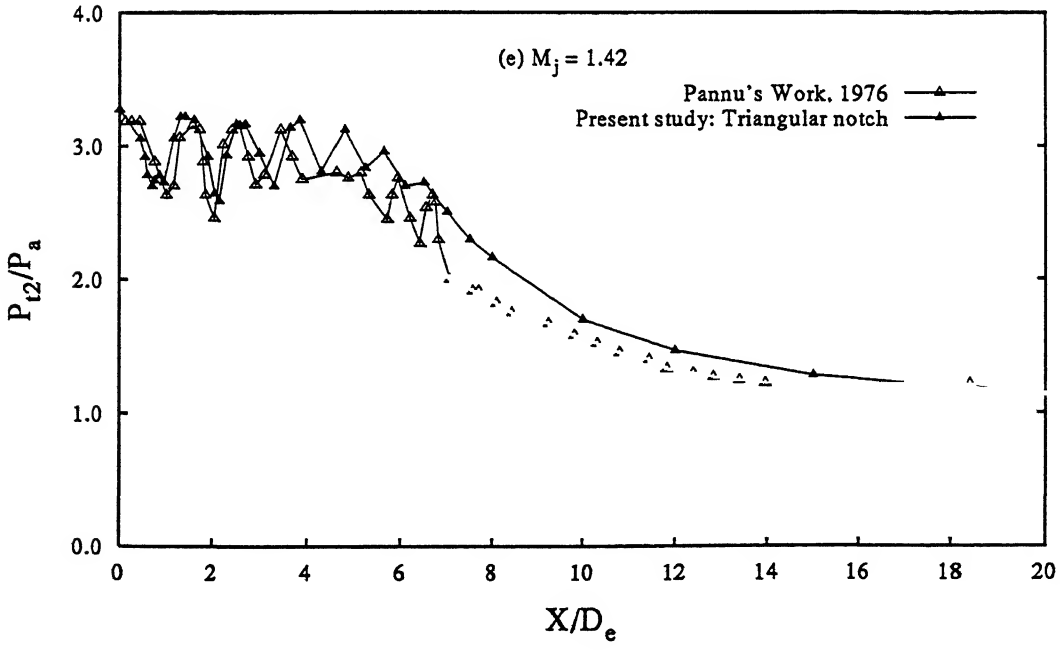

Figure 4.11(d)-(e): Plots showing the comparison of shock strength for the cases investigated at (d) M_j=1.5 and (e) M_j=1.42

In a steady supersonic flow with a single normal shock ahead of the pitot tube, a sharp drop in P_{t2} followed by a rise signifies the presence of a stronger shock wave[18]. The data presented is, therefore, accurate enough to capture the overall features ; e.g, the number of shocks and their spacing etc.[12]. As is seen from Figure 4.11(d), the shock-cell structure is weakened by the presence of the notch with a slight reduction in the shock-cell spacing. The semi-circular notch jet shows stronger shocks resulting in shorter cells relatively. Triangular notch, on the other hand shows relatively weaker shocks which may be due to mixing initiated at the vertex of this notch. Square notch case shows the weakest of all shocks in the core region. Thus, the sharp cornered notches show reductions in shock strengths as well as shock spacings which becomes more prominent in the third and the fourth shock-cells and are, therefore, expected to result in noise attenuation of these jets.

Figure 4.11(e) shows qualitative comparison of an underexpanded circular jet with triangular notch of vertex angle 60^o with Pannu and Johanneson[8] fish-tail(vertex angle of 45^o) triangular notch in a conical nozzle. Here, the measured stagnation pressure P_{t2} is non-dimensionalized by the atmospheric pressure P_a for comparison with Pannu's study[8]. The decay, once the core is over, is faster for Pannu's nozzle but follows the present case after $15.0D_e$.

4.2.5 Shock-cell Length and Screech Tone

The choked jet-noise and hence the screech frequency are primarily dependent on the length of the shock-cells and hence, on the strength of the shocks in the shock-cell system[16]. Therefore, the effect of notch on the average length of shock cell, averaged up to four shock cells, was investigated. Figures 4.12(a) shows the variation of L_{avg}/D_e Vs M_j. Here, L_{avg} is the measured average shock-cell length and D_e the equivalent diameter of notched/modified circular jets. For comparison, Tam's theory[113] for circular jets is included. It can be seen clearly that the shock-cell length for plain circle is close to Tam's theory though the curve for the present case lies a little below it. For notched cases, a decrease in the length of third shock-cell is seen with the curves following the trend of Tam's theory[113] but lying well below the plain case. The reduction in shock-cell length/spacing in the case of plain circular jets relative to the curve of Tam's theory may be due to the fact that in the case of slot jets, the extremely thin initial boundary layer produces slender vortical structures with very thin cores(thus high

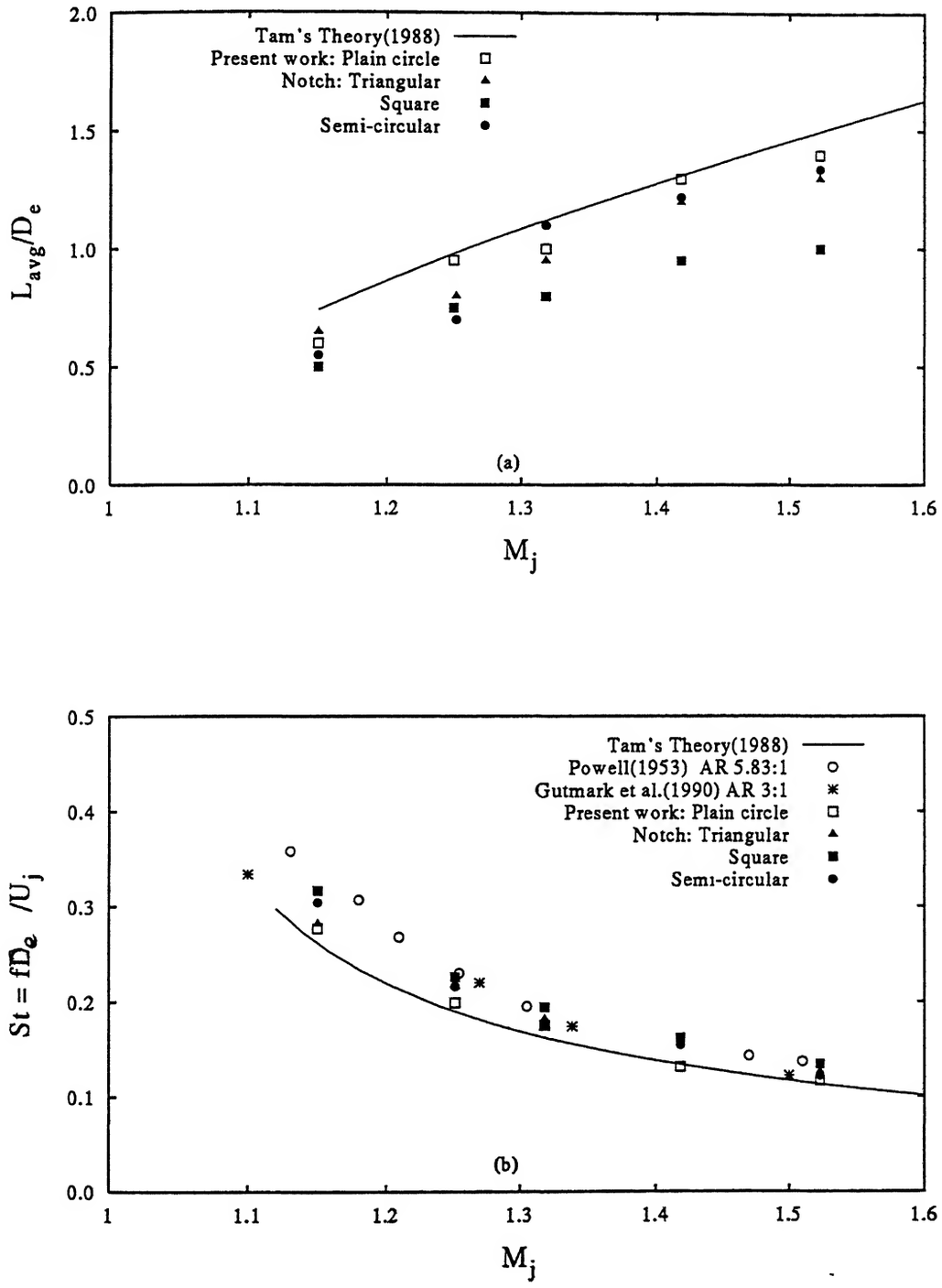

Figure 4.12: Plots showing the comparison for the effect of notch on (a) average shock cell length and (b) Strouhal number

vorticity) and with strong azimuthal variations in induced velocity. Hence, the deformation of the vortex structure is speeded up. This, perhaps, leads to faster diffusion of shock-cells[88] leading to shorter shock-cell length. The addition of notches brings in secondary instabilities in the form of streamwise vortices shed from the corners[3, 46, 4], speeding up the deformation process further.

Figure 4.12(b) shows a plot of predicted Strouhal number(fD_e/U_j) of the screech tone versus the fully expanded Mach number M_j. As the Mach number increases, the Strouhal number of screech decreases. This decrease is due to the increase in shock-cell spacing with Mach number, which causes an increase in the screech wavelength and consequently a decrease in screech frequency[110]. In the calculation of predicted Strouhal number, the average shock-cell length, L_{avg}, was considered up to four shock cells at different underexpanded levels. This value of L_{avg} was used in the screech tone frequency formula obtained by Tam *et al*[95] in conjunction with Tam's formula[113] for shock-cell length of elliptic jets with aspect-ratio less than four. In Fig. 4.12(c), Tam's analytic solution[113] of the screech Strouhal number versus M_j for circular/round jets, is also shown for comparison of our present work with Tam's theory. The present work shows good agreement with Tam's analytic solution with the points following the same trend though they lie a little above it. This is once again due to jets issuing from slots as stated earlier. Since with increasing M_j, an increase in Strouhal number relative to other cases indicates decrease in shock-cell spacing[110], the plot clearly shows that square notch is expected to have better noise characteristics followed by triangular notch relative to its plain counterpart. This is because the presence of corners greatly alters the shock-cell structure, which, affects the evolution of the shear layer and hence shock development[4, 21].

Experimental work for rectangular jets is also included to show the Strouhal number trends in literature and for comparison with rectangular and elliptic jets. These points lie well below Tam's theory for 2:1 elliptic jets. However, these are measured Strouhal number values instead of predicted values.

4.2.6 Aeroacoustic Characteristics

The experimentally observed characteristics of sound radiation from fully expanded(shock-free) and underexpanded(shock-containing) circular slot jets with and without the notches are described in the present section. In particular, the characteristics of *broadband* shock-associated

and *turbulent* mixing noise from underexpanded jets are examined over an extensive envelope of supercritical jet operating conditions and observer angle.

Acoustic Spectrum Analysis

Here it is worth mentioning that in the following discussions, notched plane will be referred to as the major-axis plane and the other as the minor-axis plane Figure 4.13(a)-(b) shows the power spectrum of a plain circular jet at full expansion, M_j=1.0, and at underexpanded condition with equivalent Mach number of M_j=1.5. The measurements were made with the microphone placed at a polar angle, θ, of 150^o to the jet upstream direction where the fundamental harmonic of screech frequency is prevelant[76, 33, 32]. Further, the spectrum analysis was carried out only in the notch or major-axis plane. The power spectrum of the fully expanded jet, Fig. 4.13(a) is broad and smooth and consists of purely turbulent mixing noise. A peak in the jet mixing noise at 6 kHz is observed. On the other hand, when the jet is operated at underexpanded condition, the acoustic spectrum contains an extra noise contribution due to the presence of shock structure in the jet flow, in addition to the turbulent mixing noise, as seen by the higher noise intensity in the spectrum, see Fig. 5.13(b). The broadband peak occurring at approximately 3-5 kHz, Fig. 5.13(b), is associated with *jet mixing* noise, while the broadband spectrum for frequency > 15 kHz is the *broadband* shock-associated noise of an underexpanded jet as per the findings of Ponton and Seiner[76] and Tam[33]. Very prominent in the acoustic spectrum are some discrete peaks in the 13 kHz range indicating the *screech* component of jet noise.

A direct comparison of the acoustic spectrum of the jet with notches is made relative to datum jet. Figures 4.14(a)-(b) show such a spectrum for a square notch circular-slot jet. At full expansion, Fig. 4.14(a), the peak noise due to turbulent mixing decreases in the low frequency range(2-9 kHz) by 5 dB, relative to the datum jet while the high frequency jet noise remains approximately the same. If a comparison is now made for the underexpanded case, Fig. 4.13(b) and 4.14(b), the square notch jet shows a reduction in the peak component(approx. 6 dB). The broadband shock-associated noise to the right of this peak shows a slight decrease in the high frequency jet noise, indicating a weaker shock-cell system[76, 26]. Further, to the left of the peak component(low frequency range), the jet mixing noise is observed to remain more or less the same. Some similar trends in the acoustic spectrum of triangular and semi-circular

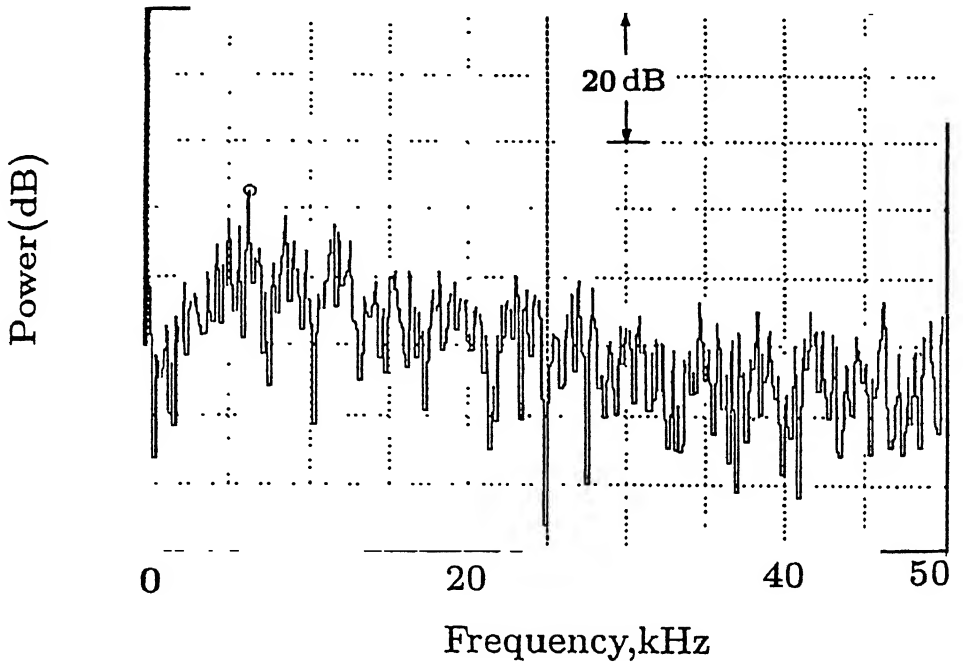

Figure 4.13(a): Far field spectral characteristics for the plain circular slot jet at M_j =1.0, $\theta = 150^o$

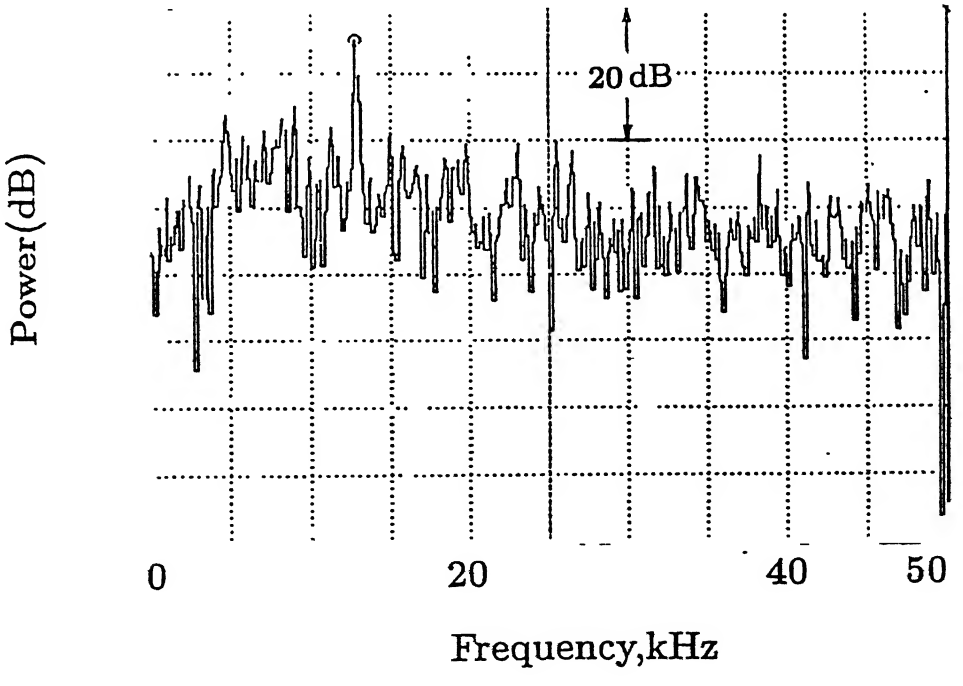

Figure 4.13(b): Far field spectral characteristics for the plain circular slot jet at at underexpanded condition with equivalent Mach number, M_j =1.5, θ=150^o

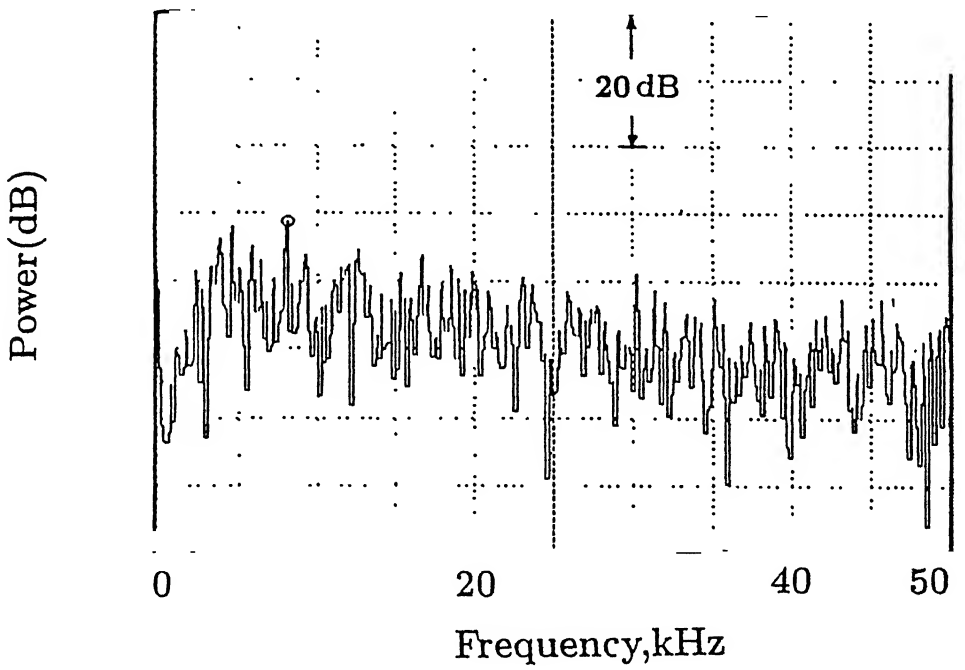

Figure 4.14(a): Far field spectral characteristics for the square notched circular slot jet at M_j =1.0, θ=150°

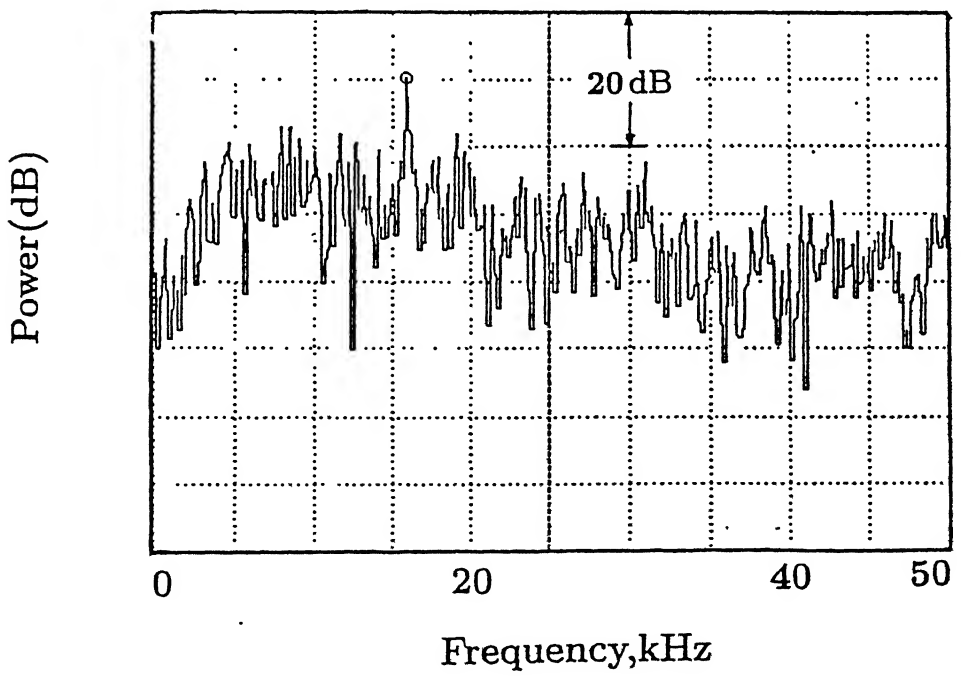

Figure 4.14(b): Far field spectral characteristics for the square notched circular slot jet at at underexpanded condition with equivalent Mach number, M_j =1.5, $\theta = 150°$

notch jets were observed. However, the peak component in triangular case shows a reduction of 8 dB whereas the semi-circular case shows the same magnitude of screech component as the plain circular jet. The acoustic spectrum of these notch configurations are not shown since the overall characteristics are approximately are the same as that for square notch slot jet shown.

The acoustic spectrum results indicate that the differences in the slot perimeter, provided by variation in notch configuration, may alter the acoustic emission characteristics of these jets not only in the screech component but also in the turbulent jet-mixing and broadband shock noise. These differences point out the aerodynamic changes[76] brought in by notch introduction. Further, the relative intensity of these three noise components is a strong function of the direction of observation as well as the operating pressure ratio[76, 33, 118, 66] as will be seen in the following sections.

Overall Sound Pressure Results

The noise characteristics of underexpanded circular-slot jets with and without notches are presented in Figs. 4.15(a)-(d). The noise intensity is examined at two observer angles, i.e., θ=90°, 150°, R/D_e=50, as the level of underexpansion is increased. These values of θ and R/D_e were selected after a detailed survey of literature[66, 118, 26, 76, 119].

The measurements were made from the fully expanded condition to high level of underexpansion with an equivalent Mach number of M_j=2.0. It is clearly discernible from the plots, Figs. 4.15(a)-(d), that the noise intensity jumps as soon as shocks begin to appear in the jet flow. Further, all the jets show a significant increase in OASPL with increasing pressure ratio.

At θ=150° to the upstream jet axis, i.e., 30° to the jet downstream flow direction, the contribution from shock-associated noise seems to be significant relative to that at θ=90° as is apparent from Figs. 4.15(a)-(d) in both the major and minor planes. As the observer moves from θ=90° to 150°(i.e., in the aft quadrant as defined in Chapter3) the significance of shock-associated noise increases progressively, and at θ=150° the levels at supercritical pressure ratios are dominated by the contribution from shock noise[66, 76]. At θ=90°, in the major plane, Fig. 4.15(a), the jets show a steady increase in OASPL with approximately same value for all cases up to M_j=1.4. Beyond M_j=1.4, significant difference in OASPL values can be seen for different slot jets. Plain circular jet shows a minimum sound intensity with higher jet mixing

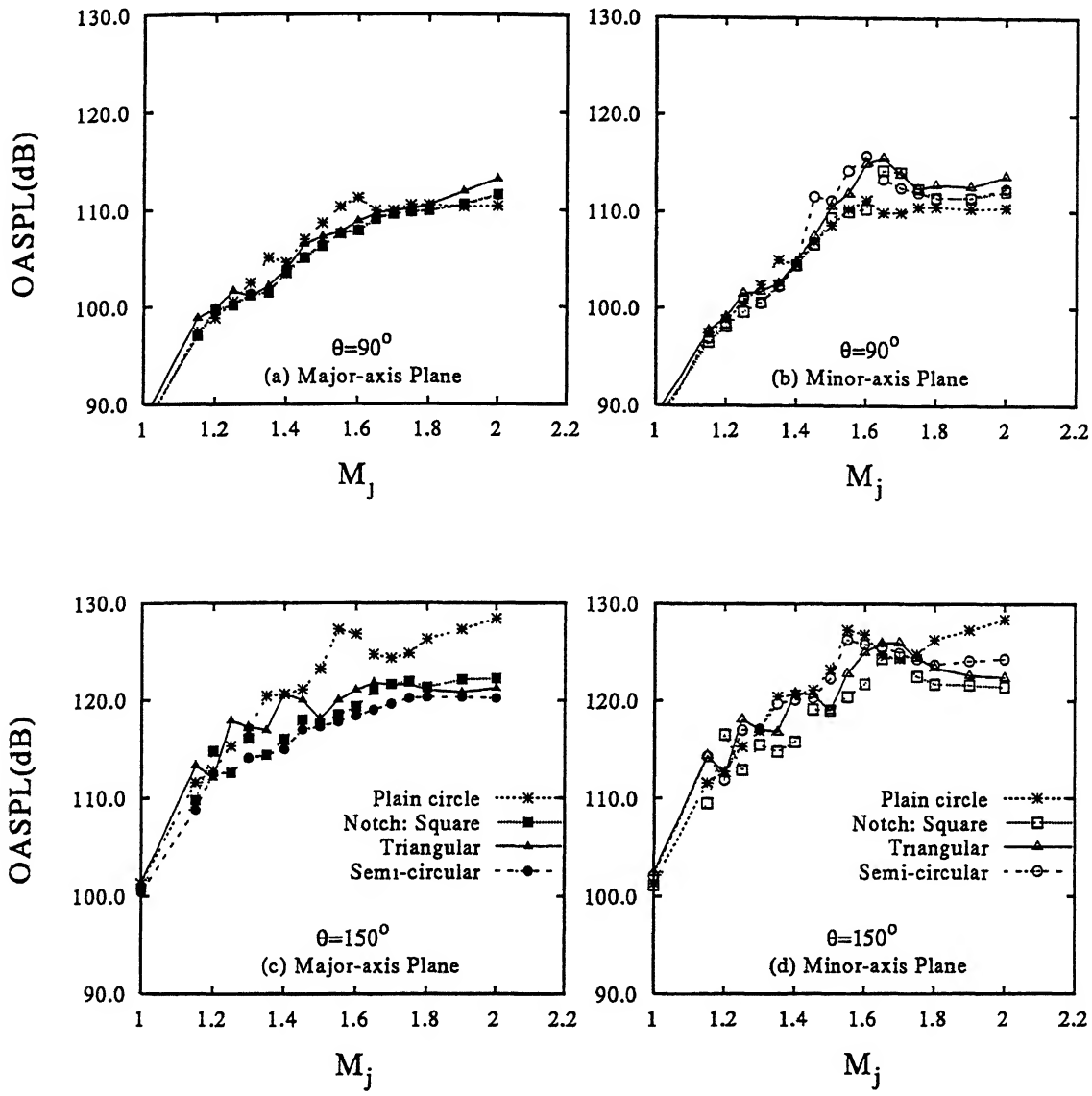

Figure 4.15: Far field overall sound pressure results for notched circular slot jets for various levels of underexpansion tested, R/D_e=50

noise from notch jets. This seems to indicate higher turbulence levels[66, 33, 118] in notch jets. At M_j=2.0, relative to the plain case, triangular notch jet shows a 4 dB increase in sound intensity followed by square and semi-circular notches with 2.5 dB increase. Thus, the turbulent mixing noise from notch jets is higher than the plain case which seems to indicate higher turbulence levels in these jets.

For observer angle of θ=150°, however, a different trend in OASPL is observed as was also observed by Powell[119]. Since this is the direction in which the shock-associated noise is radiated[66, 76, 33, 118, 32], plain circular-slot jet is seen to radiate higher noise levels relative to

notch jets, Figs. 4.15(c)-(d). Fluctuation in OASPL values is seen between M_j=1.2 to 1.7 after which the values show a definite trend. These fluctuation in OASPL values may be due to the jet oscillations setting in for 1.1< M_j < 1.7[104, 6] as observed by Hammitt[104], Sarohia[79]. These jet oscillations according to Hammitt[104] do not grow uniformly stronger with increasing pressure ratio but reach a peak, fall off, and then rise to a new peak. Since these jet oscillations are directly related to the acoustic emission of broadband shock-associated noise at 30^o to the downstream jet direction[32, 33, 76, 66] as such the radiated noise will have a fluctuating value in this range of M_j, as seen in Figs. 4.15(c)-(d). As observed from Figs. 4.15(a)-(d), the fluctuations in OASPL are more prominent at θ=150^o, than at θ=90^o. This is because the noise radiated by the jet oscillations are radiated along this direction[104, 84, 76, 118, 66]. Above M_j=1.7, the jet seems to stablise and it can be seen, Fig. 4.15(c), that square notch jets show minimum OASPL followed by triangular and semi-circular notch jets. At M_j=2.0, relative to plain jet, square cut-out jet shows a 8 dB reduction followed by triangular and semi-circular cases with 7 dB and 5 dB reduction, respectively.

In the minor-axis plane of notch jets, however, a reversal in trend relative to major-axis plane is observed. The semi-circular notch jet shows a minimum noise intensity, at M_j=2.0, followed by triangular and square cases. This difference in acoustic characteristics between major and minor-axis planes is typical of non-circular jets(especially ellipse) where minor-axis sides show lesser noise intensity due to higher spread in this plane relative to major plane[26, 122, 123, 124, 21, 125]. Thus, the concept of notch jet being considered as an equivalent elliptic jet, as discussed in the preceding sections of mean flow measurements, seems to agree well with the acoustic characteristics of elliptic jets studied in literature.

The above observations help to conclude that the notched jets seem to have a higher level of turbulence levels and a weaker shock-cell system in the jet flow.

Pannu and Johanneson[8] observed that a triangular notch in a conical nozzle generates small-structures that shielded the shock-structure of the jet and hence, acted as silencers to jet noise. Further, this fine-scale mixing from sharp corners of triangular nozzle jets causes a faster spread of shear-layer towards the jet centreline[21] and hence, seems to weaken the shocks in underexpanded jets. It may, therefore, be suggested that the reduction in the magnitude of

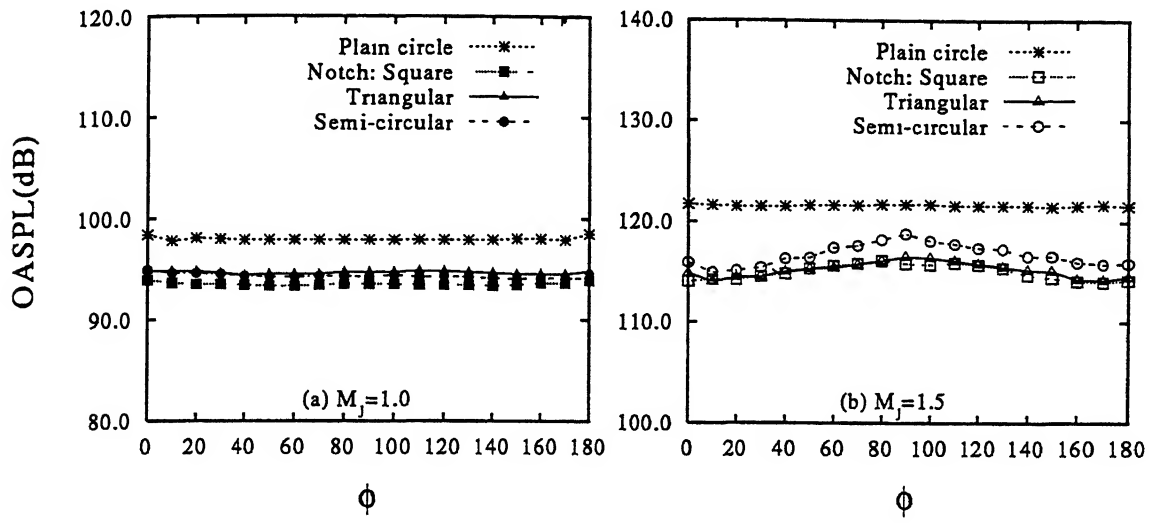

Figure 4.16: Azimuthal directivity plots for plain and notched circular slot jets at R/D_e=24 and (a) M_j=1.0 (b) M_j=1.5

OASPL is due primarily to the weak shock-cell structure in notch jets and hence, significantly reduced shock-associated noise. Further, the square notch configuration seems to be the best for far-field noise reduction of circular slot jets.

Azimuthal Directivity

It is well known that non-circular jets spread differently in different planes and as such radiate different noise intensities in different planes[26, 21, 125, 124, 123]. The present section discusses the results of azimuthal directivity for jets with and without notches for two values of Mach number, M_j=1.0 and 1.5. The measurements were made starting from minor-axis side, passing through the major-axis side(having the notch) and ending up at the other end of minor-axis side. The microphone was positioned and moved in a circular arc on a fixed aluminium quadrant, mounted on a tripod stand, at fixed intervals of 10°, R/D_e=24. Figures 4.16(a)-(b) shows such a plot. At full expansion, Fig. 4.16(a), plain circle shows the minimum noise intensity without any preferred direction as is expected due to symmetry of slot geometry. Notched jets show significant increase in jet mixing noise with square notch jet showing maximum value(2 dB increase) followed by semi-circular and triangular notch jet(3.0 dB). Further, a slight increase

in noise levels is apparent in the region of the notches(ϕ=80^o to 100^o).

At underexpanded condition, Fig. 4.16(b), the difference in noise radiated from plain and notch jets widens. The plain circular jet shows the maximum shock noise with no preferred direction. However, the notched jets show a dependence on the azimuthal angular variation of shock noise. As much as 6-8 dB reduction is seen in the minor-axis/unmodified plane(absence of notch) relative to plain case. As the notch region is approached, a significant increase in OASPL is observed. This may be due to the additional expansion and compression waves originating from the notch geometries as seen in the shadowgraph photographs(Pics. 59, 61), Figs. 4.11(b)-(c). These waves modify the downstream shock-structure development and hence, alter the acoustic emission of these jets. Also, as will be observed in the subsequent chapters on elliptic jet studies, major-axis ends emit higher noise levels relative to minor axis ends due to different spreading rates along the two planes. Here the results are in conformity to these studies[125, 124, 123, 21]. The minor-axis(absence of notch) sides radiate lesser noise intensity relative to major-axis(having the notch) sides which shows higher noise levels.

Radial Directivity in the Aft-Quadrant

In the preceding sections we have discussed about the spectral and overall sound intensity characteristics with the microphone positioned at two polar angles, θ=90^o*and*150^o. In the present and concluding part of our acoustic study on circular slot jets, we will discuss the angular directivity of jet noise in the aft quadrant. Here, the region defined by θ=0-90 degrees is referred to as the forward quadrant and by θ=90-180 degrees as the aft quadrant in accordance with the norms followed by Alvi *et al*[26].

Figures 4.17(a)-(b) show the cases investigated at full expansion in both planes. The jets show a clear and distinct noise intensity pattern. It is discernible that the dominant part of the noise is confined in the aft quadrant at angles greater than 100 degrees. Whereas for angles less than 100 degrees, the jet noise is low and relatively independent of direction. It is believed[126, 33, 66, 118] that this low level noise is generated by fine scale turbulence of the jet flow whereas the dominant part is generated directly by large-scale structures in the jet flow. Relative to plain circular jet, notch jets show higher noise intensity in both planes for all angles in the aft quadrant. This may be due to the dominance of turbulence structures in notch jets in accord with the present understanding of turbulent mixing noise of jets[33]. Further, for

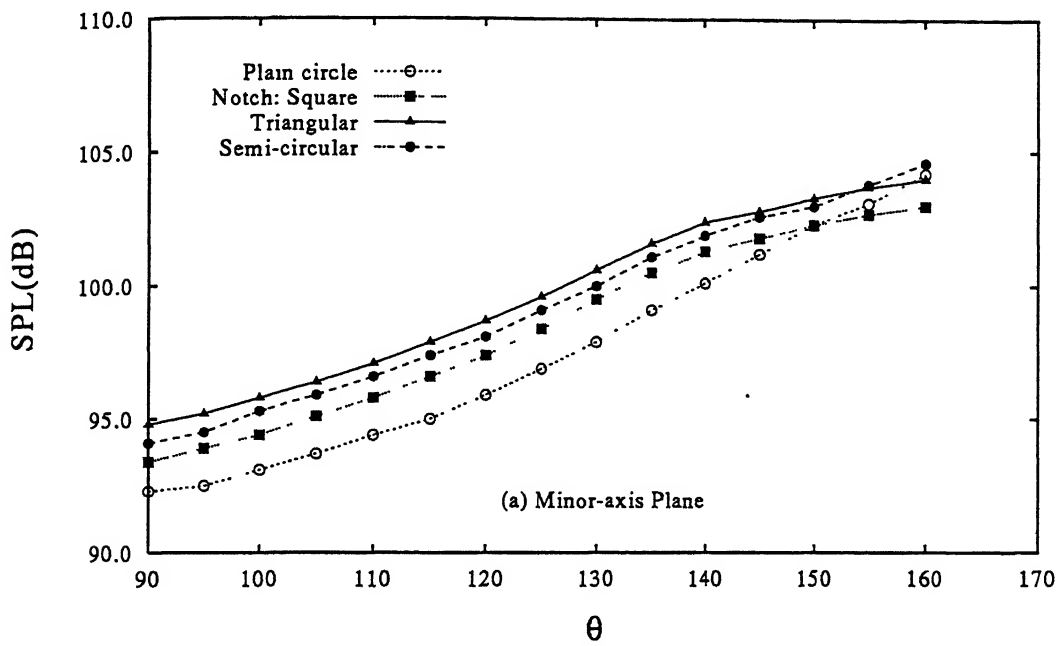

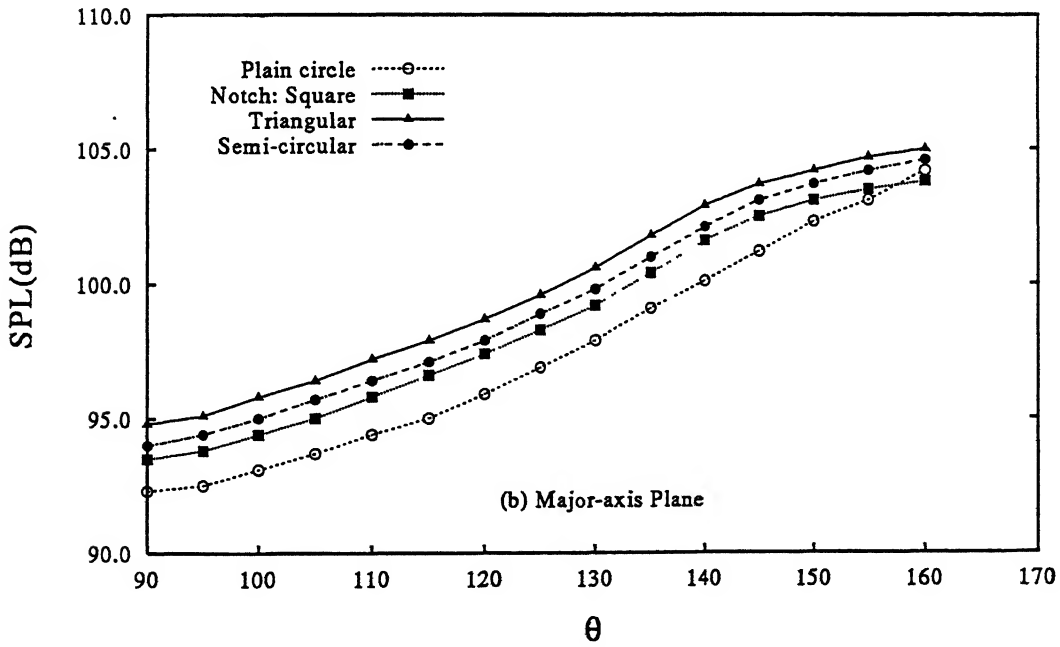

Figure 4.17: Radial directivity for circular slot jets at M_j=1.0

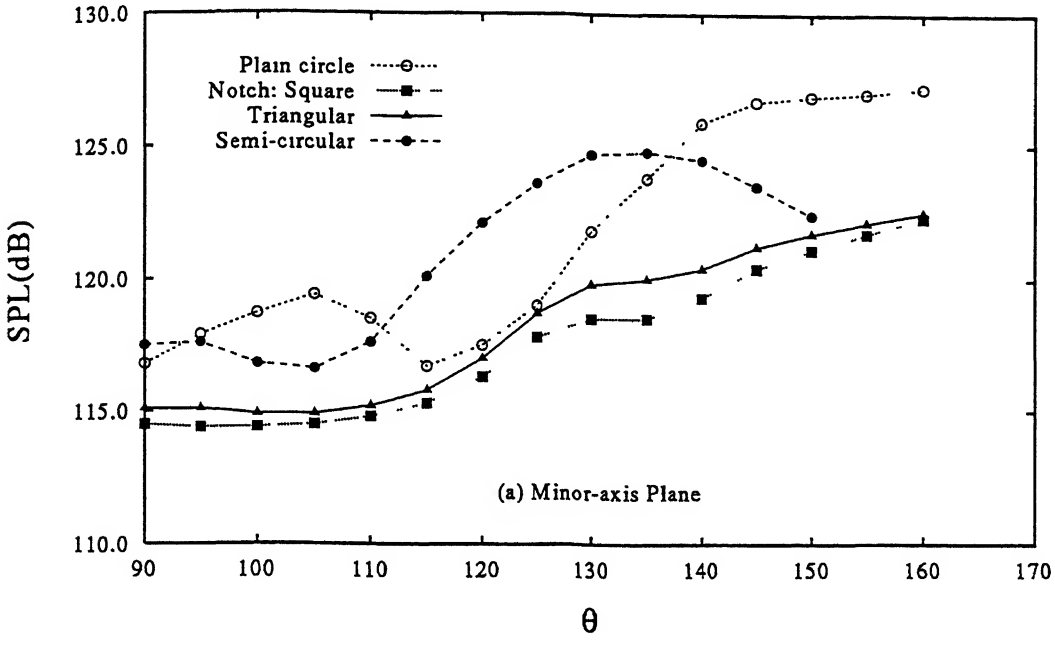

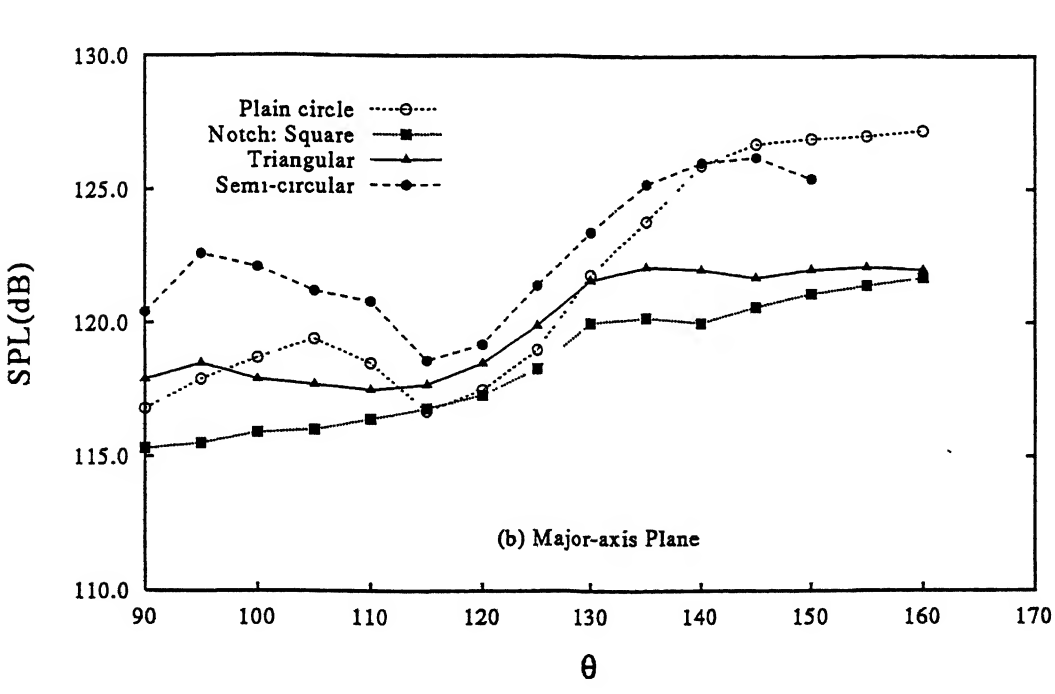

Figure 4.18: Radial directivity for circular slot jets at M_j=1.5

notch jets, for $\theta > 140^o$, the jet noise intensity ceases to increase and attains an approximately constant value. Cut-out geometry, further, has influence on noise intensity. Triangular notch jet shows a dominance, as was also observed in azimuthal directivity plots, of jet noise followed by semi-circular and finally, by square case which shows minimum value.

Figures 4.18(a)-(b) depicts the case of underexpanded(shock-containing) jets at an equivalent Mach number, M_j=1.5. It is discernible from Figs. 4.17 and 4.18, that shock-associated noise dominates over the turbulent mixing noise levels at all angles. All jets, excepting square and triangular notched jets, show a fluctuating noise intensity pattern between observer angle of 110^o and 130^o. This may be due to the jet oscillations which as explained by Hammitt[104] result in fluctuating frequencies and hence noise levels[123] as the shock-cells are set into oscillations by this jet motion. Triangular and square notch jets seem to stablise these jet oscillations to some extent as is seen by a near absence of fluctuating OASPL values with observer angle. Triangular and square notch jets show no preferred direction of noise radiated by presence of shocks up to θ=120^o. In the minor-axis plane, Fig. 4.18(a), the noise levels are slightly lesser than that along major-axis side, Figs. 4.18(a)-(b). Triangular and square notched jets show a steady increase in OASPL at all angles whereas the semi-circular case shows a significant increase in shock noise for $\theta > 110^o$ up to 130^o after which it tends to stablise. The plain circle, however, shows a dominance of shock noise for $\theta = 105^o$ and at $\theta = 150^o$, where its value reaches a maximum at 127.5 dB. At this angle, the triangular and square notch jets show an approximate reduction of 10 dB.

In major-axis plane, for $\theta > 130^o$, noise intensity tends to become uniform, Fig. 4.18(b). At θ=150^o, the notch jets show a marked reduction in shock-associated noise relative to plain circular jet. Square notch jet, which shows minimum noise levels at all angles, indicates an 11 dB reduction followed by triangular with 10.5 dB and semi-circular with 6 dB reduction.

In summary, therefore, it appears that the sound intensity of both turbulent mixing and shock-associated noise is relatively dependent upon the notch geometry and hence, the initial jet conditions and shear layer development. Further, major-axis sides radiate higher noise levels relative to minor-axis sides and, finally the noise intensity is principally a function of jet pressure ratio. In other words, the sound field from jets is characterised by three basic parameters (i) Pressure ratio P_e/P_0 or level of underexpansion P_e/P_a (ii) the observer angle θ, and (iii) the slot perimeter variation(notch geometry) with same area as datum slot. From

the trends discussed above, it becomes evident that the contribution of shock-associated noise to the total noise is significant at (i) supercritical pressure ratios and (ii) large angles to the downstream jet axis.

4.3 Conclusions

A passive control of achieving near-field mixing enhancement in circular slot jets is demonstrated. Mixing is initiated by introducing instabilities at the exit in the form of notches. This instability results in the faster decay for notched jet both for P_e/P_a=1.0 and P_e/P_a=2.0.

The results of the experimental investigation are summarized as follows:

- The presence of a notch in circular geometry makes it slightly non-circular with its major-axis along the notched plane. This induces a slight aspect-ratio in the otherwise circular geometry causing the modified circular jet to switch axis like any other non-circular geometry. This results in higher spread in the unnotched plane and the process induces higher mixing.

- The notch geometry seems to have a powerful influence on jet growth. The angle of the notch corner governs the mixing characteristics. Sharper notch corner causes lesser relative bulk-mixing. Thus, from viewpoint of bulk-mixing, semi-circular and square notch seem favourable in both fully-expanded and underexpanded circular slot jets.

- For underexpanded condition, additional expansion and compression waves emanate from the corners and flat sides of notch. This greatly alters the shock-cell structure, which, affects the initial shear layer development and hence results in weaker downstream shocks relative to the plain circular jet.

- The variation of average shock cell-length of both plain and notched jets with fully expanded jet Mach number, M_j, follows the trend predicted by Tam. But the shorter cell lengths for notched cases may be due to the relatively faster diffusion of cells due to thicker shear layers emanating from the corners. The fact that the square notched jet shows the least shock-cell length followed by triangular and semi-circular cases indicates that the notch geometry greatly influences the shock-cell development for underexpanded conditions.

- The predicted screech tone frequency of plain and notched slot jets closely follow Tam's theory. The deviation observed is due to complicated shock-shear layer interaction and secondary instabilities shed from the corners of notch.

- The acoustic spectrum results indicate that the differences in the slot perimeter, provided by variation in notch configuration, may alter the acoustic emission characteristics of these jets not only in the screech component but also in the turbulent jet-mixing and broadband shock noise. These differences point out the aerodynamic changes[76] brought in by notch introduction.

- The fine-scale mixing from sharp corners of triangular nozzle jets causes a faster spread of shear-layer towards the jet centreline[21] and hence, seems to weaken the shocks in underexpanded jets. For the present slot jets also it may, therefore, be suggested that the reduction in the magnitude of OASPL is due primarily to the weak shock-cell structure in notch jets and hence, significantly reduced shock-associated noise.

- The azimuthal directivity results indicate some interesting results. The notch presence increases the noise in the notched/modified plane. This may be due to the additional expansion and compression waves originating from the notch geometry thereby modifying the downstream shock development.

- The modified circular slot jet radiates noise like a typical non-circular jet with higher noise intensity along major-axis/modified plane and lesser along minor-axis/unmodified plane.

- Shock associated noise dominates over the turbulent mixing noise.

- Dominant part of the noise is confined in the aft quadrant for $\theta > 100^o$

- The square notch configuration seems to be the best for far-field noise reduction of circular slot jets.

- The sound intensity of both turbulent mixing and shock-associated noise is relatively dependent upon the notch geometry and hence on the initial jet conditions and shear layer development.

- The noise intensity is principally a function of jet pressure ratio. In other words, the sound field from jets is characterised by three basic parameters (i) pressure ratio P_e/P_0 or level of underexpansion P_e/P_a (ii) the observer angle θ, and (iii) the slot perimeter variation(notch geometry) with same area as datum slot. From the trends discussed above, it becomes evident that the contribution of shock-associated noise to the total noise is significant at (i) supercritical pressure ratios and (ii) large angles to the downstream jet axis.

Chapter 5

2:1 Elliptic Slot Jet

Effect of Notch and Notch Geometry on the Mixing and Noise Characteristics of Elliptic-Slot Free Jet

5.1 Introduction

In the previous chapter we discussed the effect of notch and notch geometry on the mixing and noise characteristics of circular jets, i.e., longitudinal instabilities in an exit geometry with uniform azimuthal curvature variation. The present chapter discusses the results of introducing the same instabilities in an exit geometry with non-uniform, smooth azimuthal curvature variation, i.e., ellipse. Since jet characteristics are most receptive to changes in initial conditions, exit geometry variation plays a dominant role in the development of both low and high-speed jets. From literature it is seen that jets from non-circular geometries[1, 3, 29, 60, 61, 62, 121] result in enhanced mixing, a characteristic making them far superior to the conventional circular jet.

Non-circular jets, due to their non-uniform azimuthal curvature variation spread differently in different planes[21, 1, 5, 20]. As such, these jets change shape as they grow in the downstream direction[20]. One important feature of non-circular jets is the process of axis-switching which is responsible for higher mixing rates[20, 1, 5]. Earlier studies of jets emerging from non-circular geometries with corners, e.g., triangular and square nozzle jets, rectangular and square slot jets, show that the introduction of sharp corner in the periphery of the geometry can significantly increase small-scale turbulence intensity at the corner, and hence, enhance overall mixing[29, 106, 60, 5, 3, 108]. Further studies revealed that the small-scale turbulence was

generated by axial vortices formed in the corners and augmented by vortex bending induced by the highly curved flow at the corners[127, 2]. In addition to vortex bending and self-induction process, the non-linear interaction of turbulence generated at the corners with the mean flow resulted in an increase in jet spread at other sections of the exit periphery[4]. It was observed by Gutmark *et al*[4, 46] that the fine-scale structures generated from the sharp corners of triangular and square nozzle jets are advantageous for combustion systems. The enhanced fine-scale mixing at the corners makes this section the best location to initiate combustion[4].

Small aspect-ratio(2:1) elliptic jets have been observed to result in higher mixing rates relative to the axisymmetric jets[20, 1]. Hussain and Husain[1] confirmed that an elliptic jet undergoes a three-dimensional deformation process associated with the bending of the elliptic vortex. This three-dimensional deformation is primarily responsible for the flow self-induction process resulting in axis-switching phenomenon. This phenomenon plays a vital role in the enhanced mixing and larger spread rates observed. Axis-switching has also been observed in supersonic/underexpanded elliptic jets by Gutmark and Schadow[46], a characteristic favorable from mixing and noise suppression points of view in high-speed jets.

Enhancement in small-scale mixing was achieved by Gutmark *et al*[58] by providing a conical contraction before an elliptic slot wherein the axial vorticity component arising as a result of the contraction strongly interacts with the roll up of the circumferential vortex thereby inducing turbulence in the near-field. Powell[31] pointed out that relieving the excess pressure at the nozzle exit in the form of slots or fingers[16, 18, 17, 8] greatly weakens the shock-structure and introduces turbulence in the near-field, thus drastically reducing the screech component.

The present study combines the characteristics of small aspect-ratio(2:1) elliptic jets and sharp corners for the purpose of enhanced mixing. Since an elliptic jet spreads more along the minor-axis side, two notches are symmetrically introduced along the minor-axis side of the ellipse so as to further enhance the mixing process in that plane. A direct comparison of the jet characteristics are made with a plain ellipse(aspect-ratio 2:1) and a plain circle of same equivalent area to study the changes brought about in the jet flowfield by notches when introduced in a geometry with non-uniform azimuthal curvature variation(ellipse). Although elliptic jets have received extensive attention, no work seems to report improving the flow from elliptic slots by introduction of sharp corners in the form of notches in the slot periphery. Since such sharp corners have been observed[3, 46, 4, 29, 60, 5, 108, 59] in both nozzle and slot

jets to improve the flowfield considerably near the exit plane, these initial instabilities are also expected to further enhance the mixing of elliptic jets.

5.2 Results and Discussions

5.2.1 Iso-velocity Contours

Figures 5.1(a)-(d) show the iso-velocity contours for plain ellipse at M_J=1.0. A smaller spacing between the contour levels indicate less ambient fluid entrained by the jet and vice-versa[121]. As observed by Hussain and Hussain[1, 20], the plain elliptic jet initially has lesser growth along its major-axis side before it starts to grow in that direction with a simultaneous outward movement of the jet along the minor-axis side. Hussain and Husain[1] attribute the comparatively reduced growth of the jet along the major-axis plane to the deformation of non-circular vortical structures. The explanation given is that, the extremely thin initial boundary layer in slot jets produces slender vortical structures with very thin cores(thus high vorticity) and with strong azimuthal variations in induced velocity. The self-induced velocity of a curved vortex filament[1] is,

$$u = b_n \frac{\kappa}{4\pi\rho} ln \frac{\rho}{\sigma}$$

where κ is the vortex strength(i.e., circulation), ρ is the radius of curvature, σ is the core radius and b_n is the local unit vector in the direction of the binormal. This azimuthal variation of induced velocity results in the deformation of the convecting vortex structures and consequent axis switching. Thus, a pumping action[1] starts bringing in ambient fluid towards the jet-centreline along major-axis side and vice-versa along the minor-axis side, and hence initiating the axis-switching phenomena typical to non-circular jets. This axis-switching phenomena is responsible for higher mixing rates observed in elliptic jets.

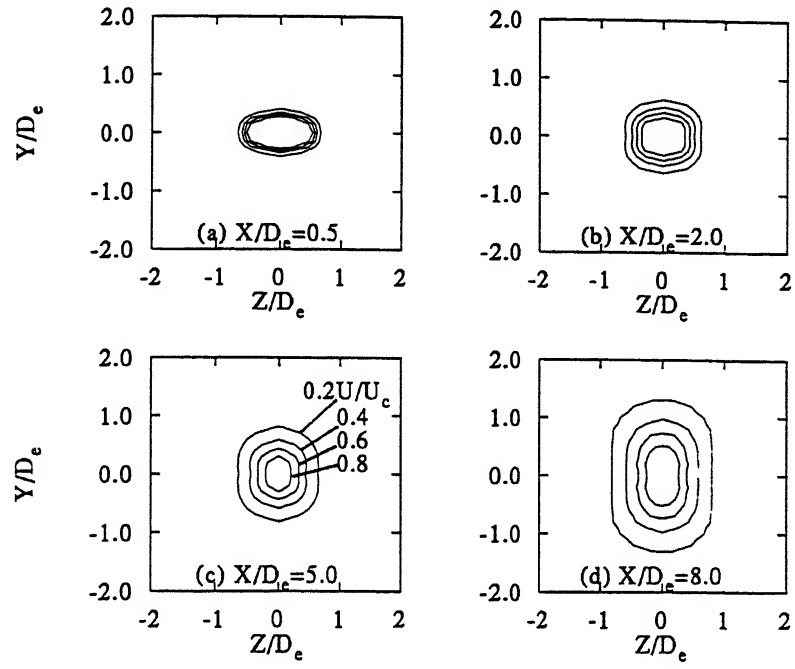

Figure 5.1: Iso-velocity contours for plain elliptic slot jet. M_j=1.0

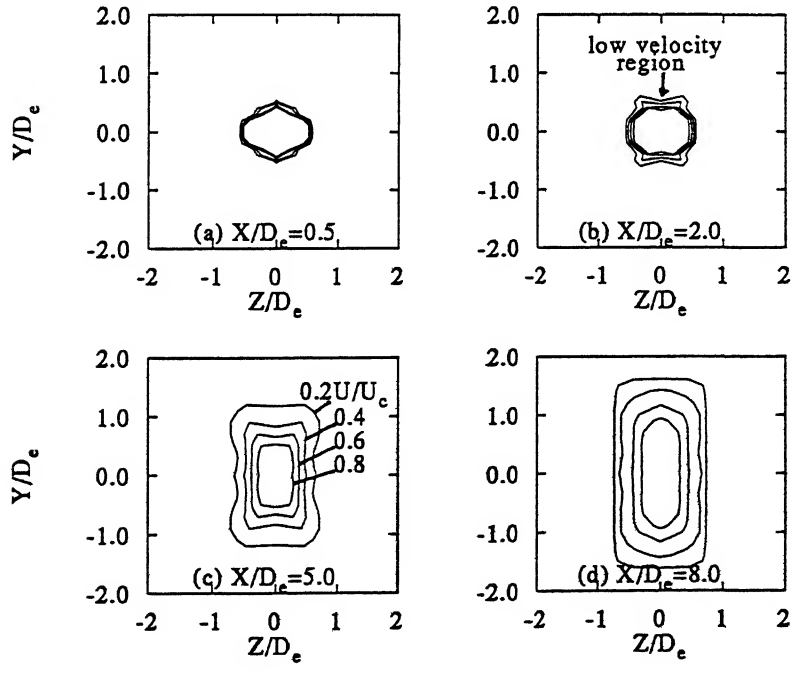

Figure 5.2: Iso-velocity contours for square notched elliptic slot jet, M_j=1.0

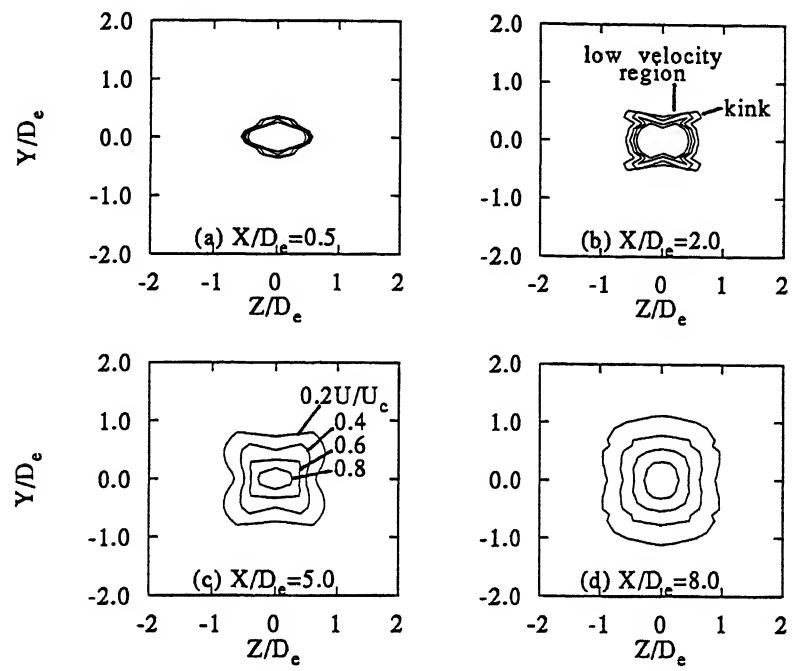

Figure 5.3: Iso-velocity contours for triangular notched elliptic slot jet, M_j=1.0

A comparison of the iso-velocity contours at the same axial stations for plain and notched cases very clearly indicates the effect introduced in the flowfield by the presence of notches, Figs. 5.1(a)-(d) for plain case and Figs. 5.2(a)-(d) for square notch. First we will discuss the results of notch introduction alone on jet development after which we will deal with the effect of notch geometry variation. The physics for this peculiar flowfield, with notch introduction on the basic shape, lies with the presence of longitudinal instability in the form of sharp corner notches. This greatly influences the uniform growth of the jet structure along the minor-axis sides as seen by a low velocity region in Fig. 5.2(b) for $X/D_e = 2.0$. This may be due to the fact that the sharp corners introduce discontinuities in the initial region of the shear layer and prevent the roll up of uniform vortices in this region[3]. Now due to the non-uniform curvature variation, a non-uniform self-induction process begins with the initial retarded growth of the major-axis side as is typical to non-circular geometries. The interaction of the low velocity regions provided by the notches with the mean flow results in an increase in jet growth. This enhanced mixing process at the minor-axis region makes the jet grow faster in that plane compared to the growth along major-axis plane thereby causing an upstream shift in the axis switchover location(refer Figs. 5.1 and 5.2). As such the jet brings more of the ambient fluid

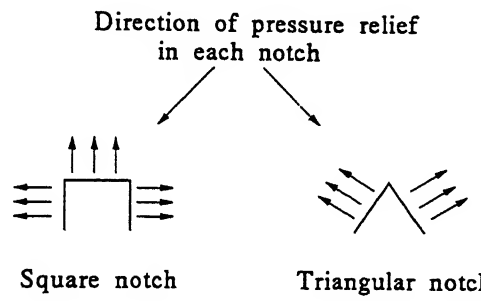

Figure 5.4: Cartoon showing the pressure relieving effect in square and triangular notches

towards the jet-centreline causing the notched jet to entrain more and hence, induce higher mixing relative to plain case.

Let us now discreetly observe the effect of notch geometry on the development of elliptic jet near the exit plane. Powell[30] in his pioneering work on choked jet noise pointed out that notches help relieve jet pressure near the nozzle exit. This effect is clearly indicated by the iso-velocity contours of Figs. 5.1(a), 5.2(a), and 5.3(a). A comparison of Figs. 5.2(a) and 5.3(a) shows that the pressure relieving affect is more pronounced for square notch relative to triangular notch as seen by a higher growth of iso-velocity contours for square notch in the notched plane at X/D_e=2.0. This is dictated by the geometry of the square notch which has a higher area of influence to the jet flowfield away from main jet relative to triangular notch. However, higher area of triangular notch close to the main jet relieves pressure more in the direction of the major plane as seen by the outward kink, Fig. 5.3(b), than in the minor plane. These flow developments near and away from the main jet greatly influence the entrainment of the jets in which these notches are introduced. Further downstream, this effect on the iso-velocity contours along the major and minor axis sides is clearly seen where the square notch shows higher growth in the notched plane, Fig. 5.2(c), while triangular notch shows, relatively, higher jet growth in the unnotched plane, Fig. 5.3(c). The pressure relieving effects of each notch are elucidated in cartoons developed from the iso-velocity contours, Fig. 5.4.

Let us now observe the change in shape of iso-velocity contours at a underexpansion level of 2.0, M_j=1.5, for square and triangular notched cases, Figs. 5.5(a)-(d) and Figs. 5.6(a)-(d). Figure 5.6 clearly shows a higher growth of iso-velocity contours along the notched plane indicating a higher pressure relieving effect at underexpanded conditions. In other words, the square notch provides a low velocity region in the plane of the notch close to the exit even at

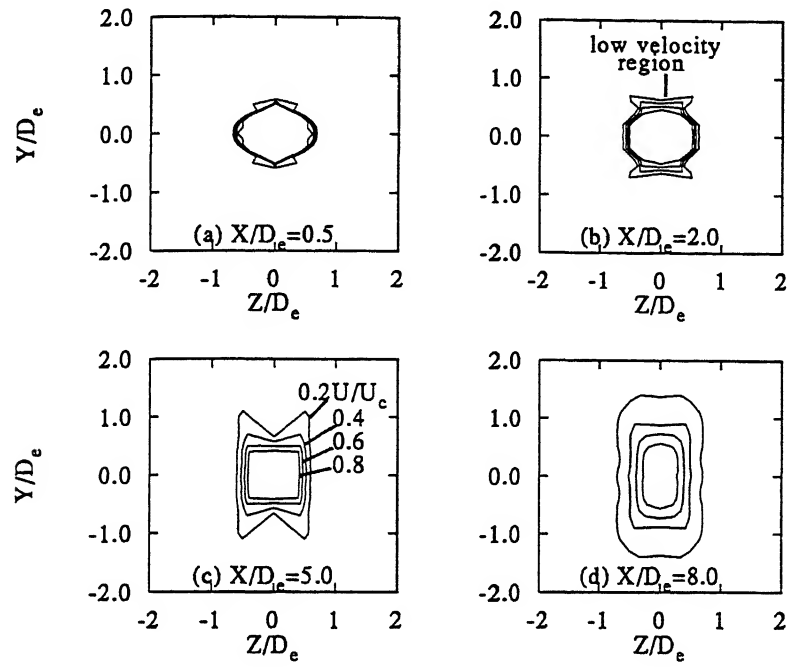

Figure 5.5: Iso-velocity contours for square notched elliptic slot jet, M_j=1.5

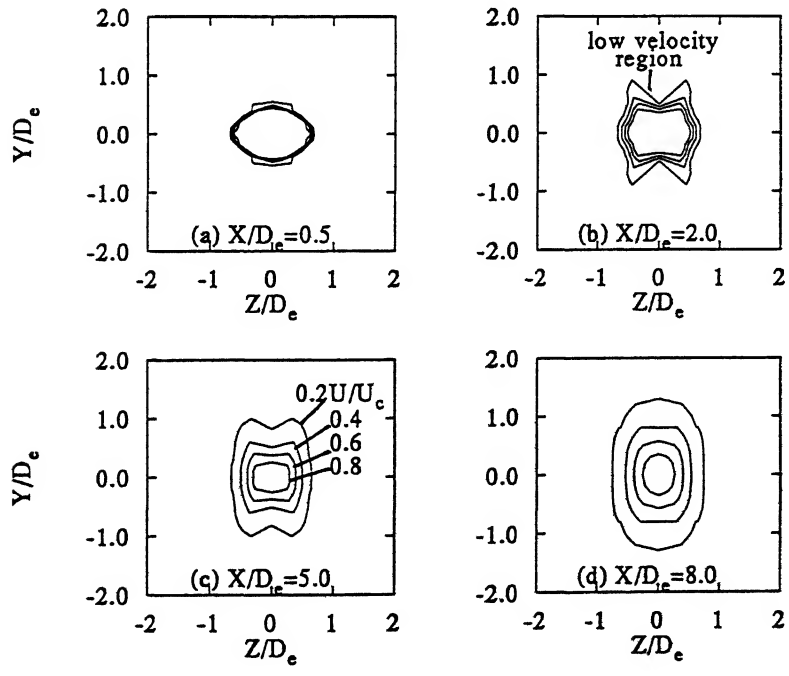

Figure 5.6: Iso-velocity contours for triangular notched elliptic slot jet, M_j=1.5

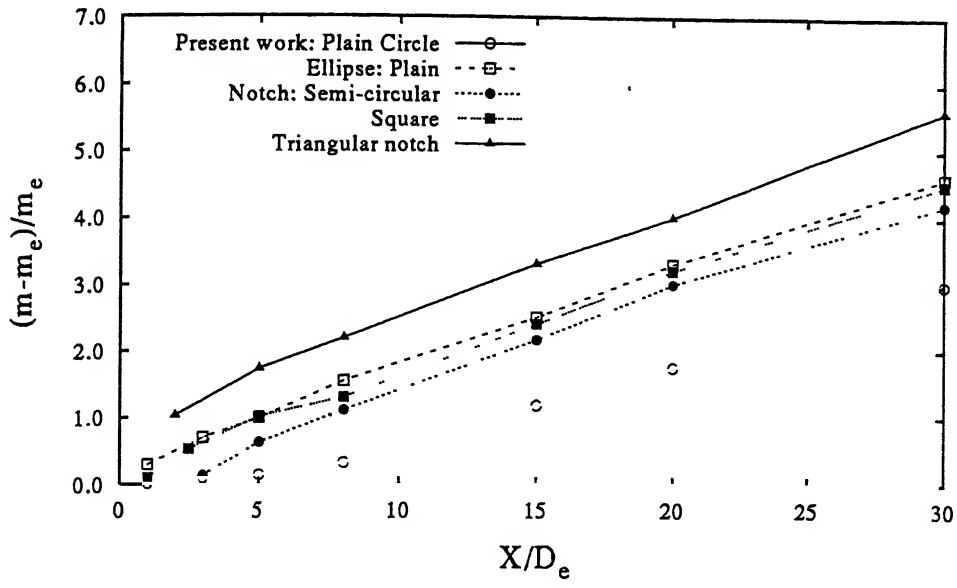

Figure 5.7(a): Entrainment comparison for the cases investigated at M_j=1.0

underexpansion.

The triangular notch on the other hand is observed to induce low velocity regions about the notched/modified plane and not in the notched plane as dictated by its geometry. Further, a stretching of the velocity contours in notched plane is observed relative to the contours at M_j=1.0 for both square and triangular notched cases at X/D_e=2.0. This may be primarily due to the increasing pressure relief required over the same slot area at underexpansion. This higher pressure relieving effect in the notched plane of square notched elliptic slot jet seems to enhance the mixing characteristics in underexpanded conditions as will be seen later in entrainment plots. However, the lesser pressure relieving effect dictated by triangular notch geometry puts a check to this jet growth and hence, delays mixing at underexpanded conditions.

After having an idea of the mechanism of jet development for different notch geometries, let us now study the entrainment characteristics of these jets. Figure 5.7(a) shows the entrainment plots for the cases investigated at M_j=1.0. The effect introduced by the sharp corners in notch geometry is discernible from the plots. Relative to the plain ellipse, triangular notched case shows considerably higher entrainment at each x-location. In these plots 'm' is the local mass-flux and 'm_e' the mass-flux at nozzle exit. Square notch case, however, shows approximately the same value of entrainment as the plain case. Further, if a comparison is made relative to plain circle, we can easily see the advantage of using an elliptic jet with and without notch.

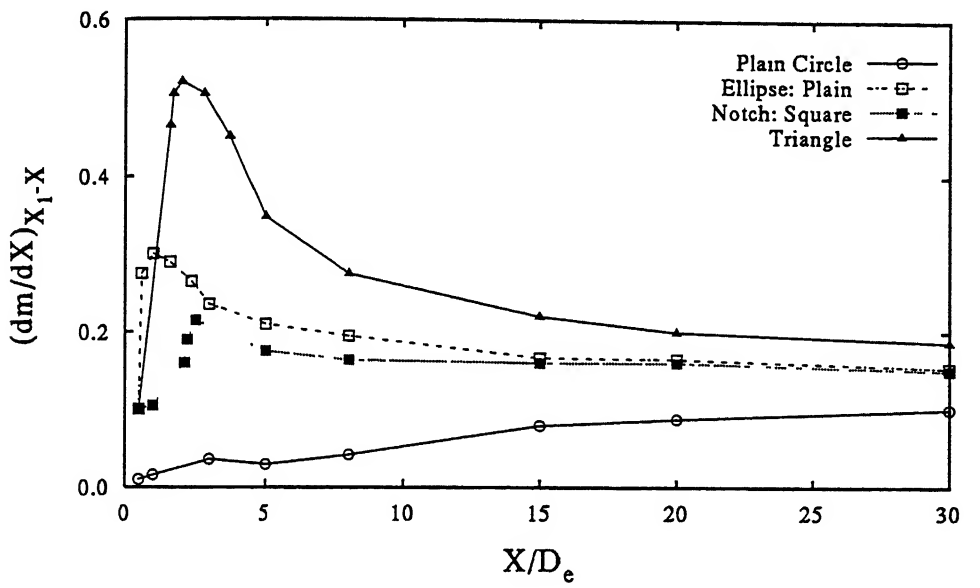

Figure 5.7(b): Plot showing the entrained mass at each X-location, M_j=1.0

At X/D_e=2.0, triangular notched jet shows 900 percent increase in entrainment relative to plain circular case whereas plain and square notched ellipse show 300 percent increase. At X/D_e=5.0, triangular notched jet shows 750 percent increase while plain and square notched jets show 400 percent increase. Further downstream, the entrainment curve shows a decreasing trend relative to its value at X/D_e=2.0. At X/D_e=15.0, this increase drops to 166 percent and 83 percent for triangular and square notched cases, respectively. Thus, it is clear from the above quantifications that, close to the slot exit the increase in entrainment relative to plain circle is the maximum and that this increase starts to drop as we move downstream beyond X/D_e=5.0.

Taking into consideration the above discussion, we now present the entrainment values for each jet in a different form of plot.

$$\begin{aligned} \text{If } (dm/dt)_e &= \text{mass flux at the slot exit} \\ \text{and, } (dm/dt)_X &= \text{total mass flux at a given X-location} \\ \text{then } (dm/dt) &= \text{total entrained mass flux up to that X-location} \\ &= (dm/dt)_X - (dm/dt)_e \end{aligned}$$

Thus at another X-location, say X_1, the total entrained mass between X and X_1 is

$$(dm/dt)_{X_1-X} = (dm/dt)_{X_1} - (dm/dt)_X$$

Figure 5.7(b) shows such a representation of entrainment. Here, the total entrained mass between the two X-locations 'dm' is non-dimensionalised by the axial distance between the corresponding X-locations 'dX = X_1-X'. It is discernible from the plot that (dm/dX) increases all the way. However, the slope initially increases, just downstream of slot exit, peaks and then starts decreasing and reaches an asymptotic value as X increases. This trend is seen for all the cases investigated except circular jet which shows a steady increase in the values. But after $20D_e$, its values also reach an asymptotic value. However, the asymptotic value for triangular notched jet is much higher than square notched and plain ellipse which show approximately same values. Plain circle shows a very low asymptotic value, relatively The above trends indicate that the jet entrains most of the ambient fluid close to the exit where there is a dominance of large-scale structures.

The above plots, Figs. 5.7(a) and (b), clearly indicate that the angle of the sharp corner in a notch has strong influence in controlling the mixing in an elliptic slot jet. This is in confirmation to Gutmark *et al*[4] study where they observed that the vertex angle of the triangular nozzle jet increased mixing. In elliptic slot jets, such notch geometries greatly influence the jet growth in the region of the notch thereby introducing enhanced mixing.

Some different trends in entrainment ratio are evident at M_j=1.52 from Fig. 5.8(a) for the notched ellipse. The effect of delayed mixing with underexpansion is clearly seen in this plot. Once the shock-structure gets weakened at some downstream location, increase in entrainment ratio is observed. It is observed that the square notched elliptic jet shows a marked increase in entrainment relative to the plain case at M_j=1.52. Also, the triangular notched ellipse shows higher entrainment than the plain case but the value is much less than the square notch case. Figure 5.8(b) shows the variation of (dm/dX) relative to each X-location for the underexpanded condition. Here too the trends are similar to that observed at fully expanded condition with the mass flux showing an increase in value, reaching a peak and then decreasing. However, after decreasing the (dm/dX) value jumps and then attains an asymptotic value. At this

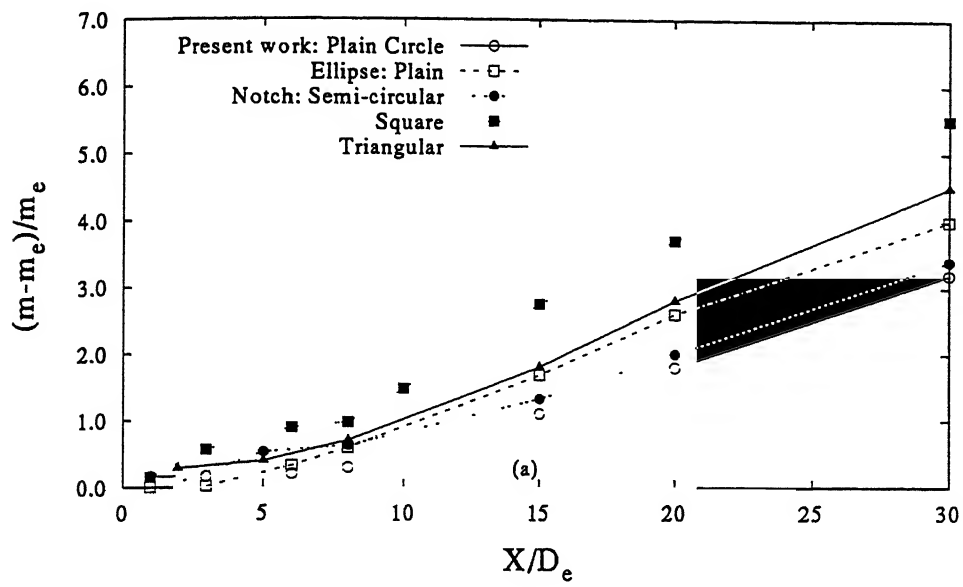

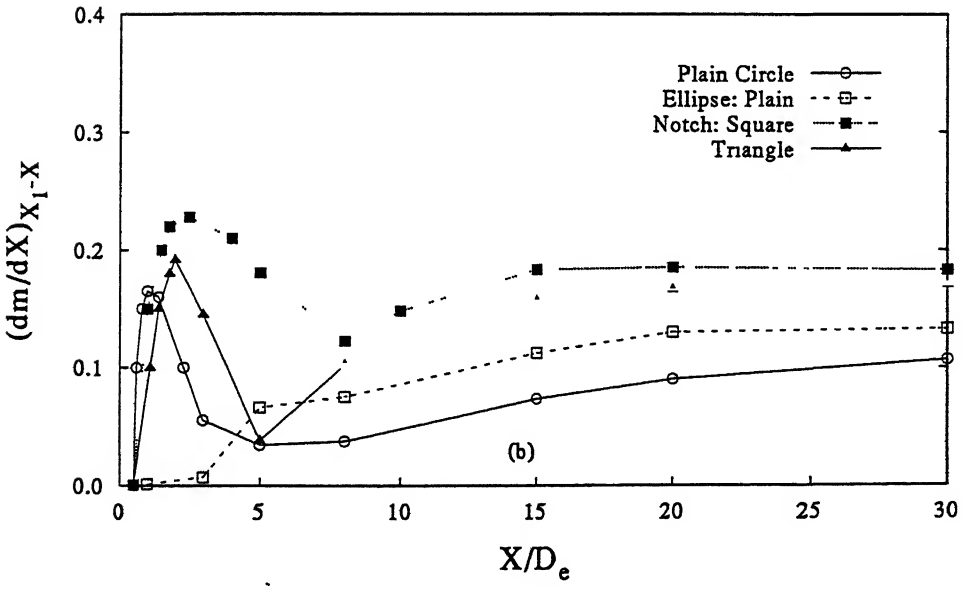

Figure 5.8: (a) Entrainment comparison for the cases investigated at M_j=1.52 (b) Plot showing the entrained mass at each X-location, M_j=1.52

underexpansion, square notched jet shows the highest peak followed by triangular notched jet and plain circle.

Thus, from Figs. 5.8(a) and (b), it is observed that square notch configuration, with two sharp corners, seems to be more beneficial from the view point of enhanced mixing at high levels of underexpansion. This is primarily due to the higher pressure relieving effect of square notch away from the main jet that improves mixing at underexpanded conditions. However, at full expansion, a sharper vertex angle of notch(i.e., in a triangle) is more beneficial due to the higher pressure relieving effect close to the main jet as governed by its geometry. Also the sharp corner triggers the generation of discontinuities which have earlier been found to enhance fine-scale mixing[21, 4].

Let us now observe the effect of Mach number on the entrainment characteristics of these jets, Figure 5.9(a). It is discernible from the plot that as Mach number increases, the mixing characteristics show a decline. This is primarily due to the compressibility effects coupled with a strong shock-cell system in the core-region which impede the jet growth. Samimy *et al*[12] case of two tabs is also included for qualitative comparison. Here it is interesting to observe that the Samimy's result and the triangular notched elliptic jet shows considerable decrease in entrainment with underexpansion. The present case of square notched jet initially shows a decrease upto $12.0D_e$ beyond which it shows a higher entrainment relative to that at M_j=1.0 and goes on increasing in the downstream direction.

Figure 5.9(b) shows a cross-plot of entrainment with Mach number M_j for three different axial locations, i.e., X/D_e=5, 8, 20. Since only sharp cornered notched jets show increase in entrainment relative to plain elliptic jet, therefore, only the case of square and triangular notches is discussed. At X/D_e=5 and 8, for triangular notch, entrainment shows a considerable decrease as M_j is increased. At X/D_e=20.0, entrainment decreases as M_j is increased from 1.0 to 1.32. However, at M_j=1.52, triangular notched jet shows an increasing trend in entrainment value. Square notched jet, on the other hand, shows some very impressive results. At X/D_e=5.0, the entrainment values show approximately constant trend for the three M_j considered. However, at X/D_e=8.0, M_j=1.32 shows an increase in trend entrainment value relative to that at M_j=1.0 but at M_j=1.52 it's value falls even below that at M_j=1.0. At X/D_e=20.0, this effect becomes more pronounced at M_j=1.32 showing considerable increase in value relative to that at M_j=1.0 and the entrainment value decreases again at M_j=1.52

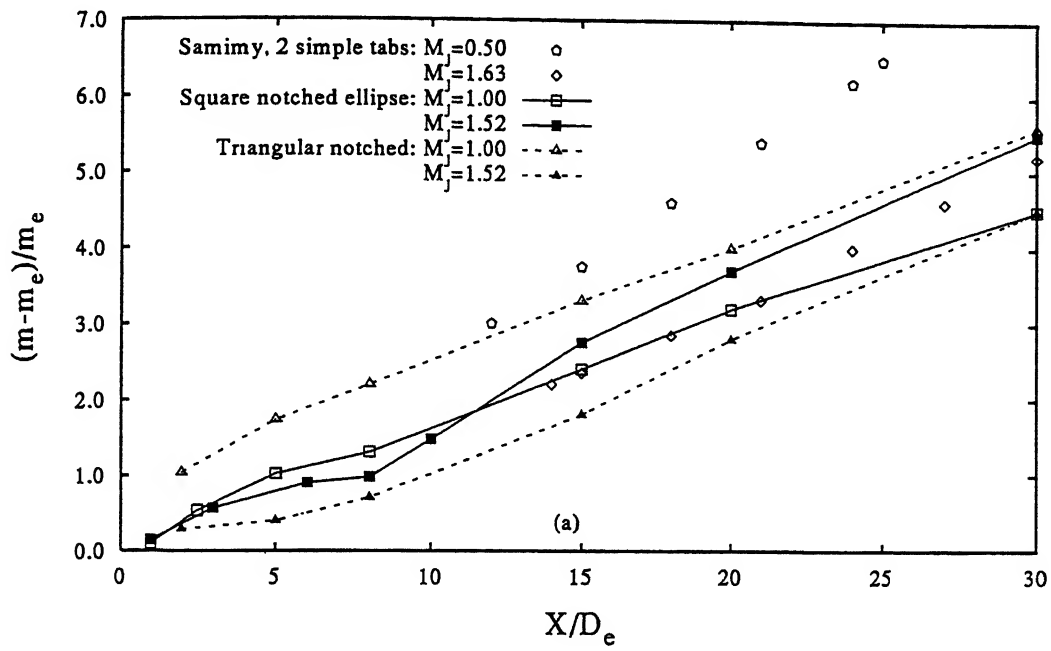

Figure 5.9: (a) Plot showing the effect of Mach number on entrainment (b) Cross-plot showing the entrainment variation with M_j

but is not less than that at M_j=1.0 as observed at X/D_e=8.0. Moreover, square notched jet shows higher entrainment values at M_j=1.32 and 1.52 relative to triangular notched elliptic jet.

5.2.2 Pressure Profiles and Jet Spread

Effect of notch in an Ellipse

The effect of a notch introduced in the elliptic geometry can also be seen in the pressure profiles taken at various X-locations in the X-Y and X-Z planes. Figures 5.10 show the pressure profiles for the plain and the notched ellipse in X-Y and X-Z planes for P_e/P_a=1.0, superimposed for a better comparison of jet spread. Here, the pitot pressure, P_t, is divided by the stagnation pressure P_0 and plotted against the non-dimensionalized lateral distance, Y/D_e or Z/D_e. The spread in the two planes is noticeably different. Along the major-axis side(i.e, X-Z plane, Fig. 5.10), for both jets the shear layer is seen to spread faster towards the core indicating comparatively lesser growth along the major-axis side as we move axially downstream from $0.5D_e$ onwards to $8.0D_e$. Whereas along the minor-axis side(i.e, X-Y plane, Fig. 5.11), the shear layer spreads widely into the surroundings indicating a higher spread throughout and even at $15.0D_e$ showing that the jet has not become axisymmetric.

Relative to the plain case, the notched elliptic jet shows a much higher spread in the notched plane as is evident in the pressure profiles, beyond $3.0D_e$ and this spread increases with increasing X/D_e. On the other hand, in the unnotched plane at X/D_e=3.0, notched jet shows a slightly lesser growth initially. Beyond $3.0D_e$, both plain and notched jets spread approximately similarly. This results in the faster spread of shear layer towards the jet centreline relative to plain case as is seen by an earlier reduction in the magnitude of centreline pressure for notched case in both planes. Some similar trends have been observed at levels of underexpansion 1.5 and 2.0.

Effect of notch geometry

The effect of the notch geometry on the jet spread and growth can be seen clearly in the pressure profiles at various axial locations in both the notched and unnotched planes. For better comparison, all the three cases are superimposed, for each plane, on a single plot. Figure 5.11 shows such a plot at M_j=1.0 as the jet grows in the downstream direction. Near

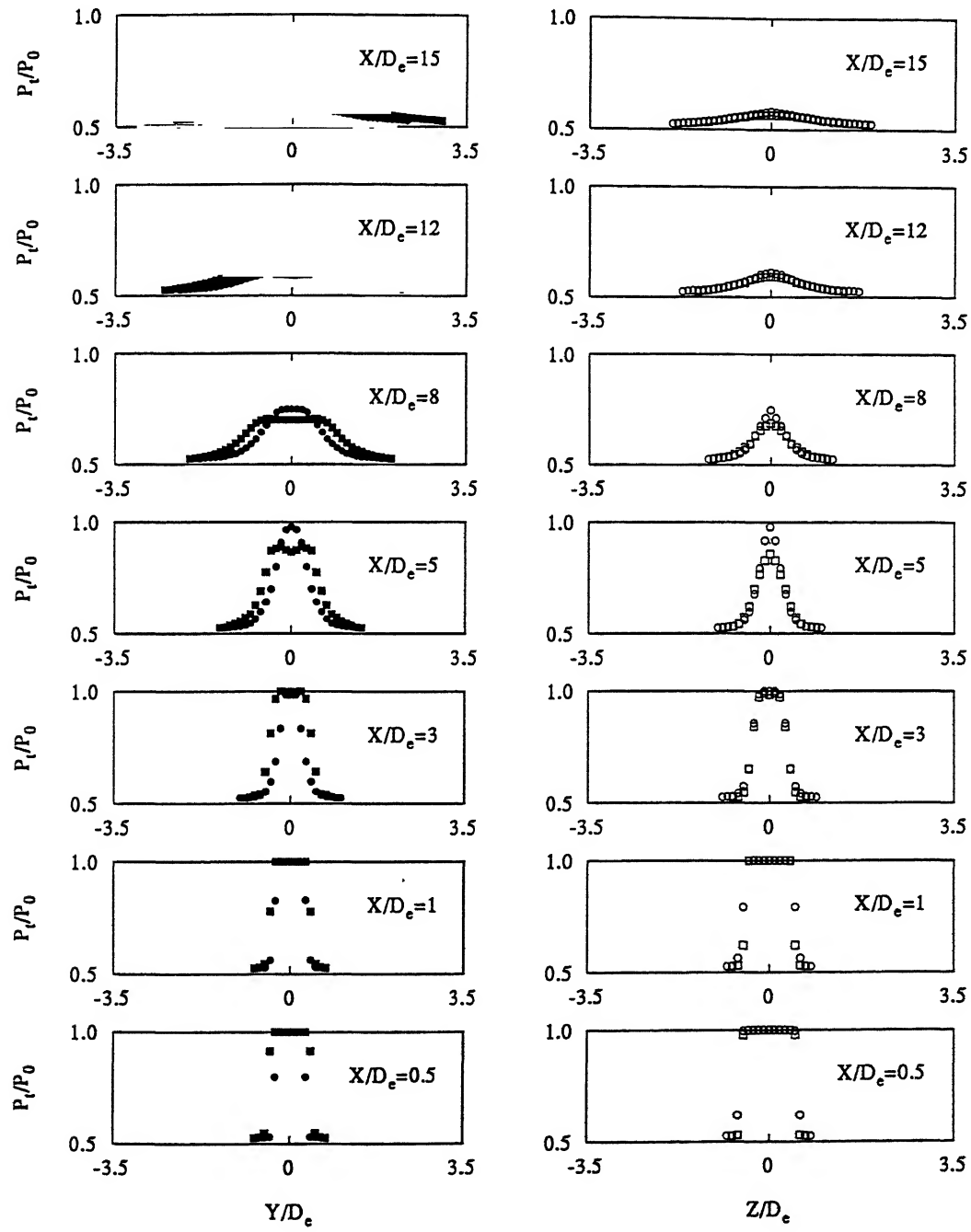

Figure 5.10: Comparison of pressure profiles for plain and square notched 2:1 elliptic slot jets at M_j=1.0. Plain ellipse: X-Y plane,•; X-Z plane, ∘. Square notched ellipse: X-Y plane, ■; X-Z plane, □

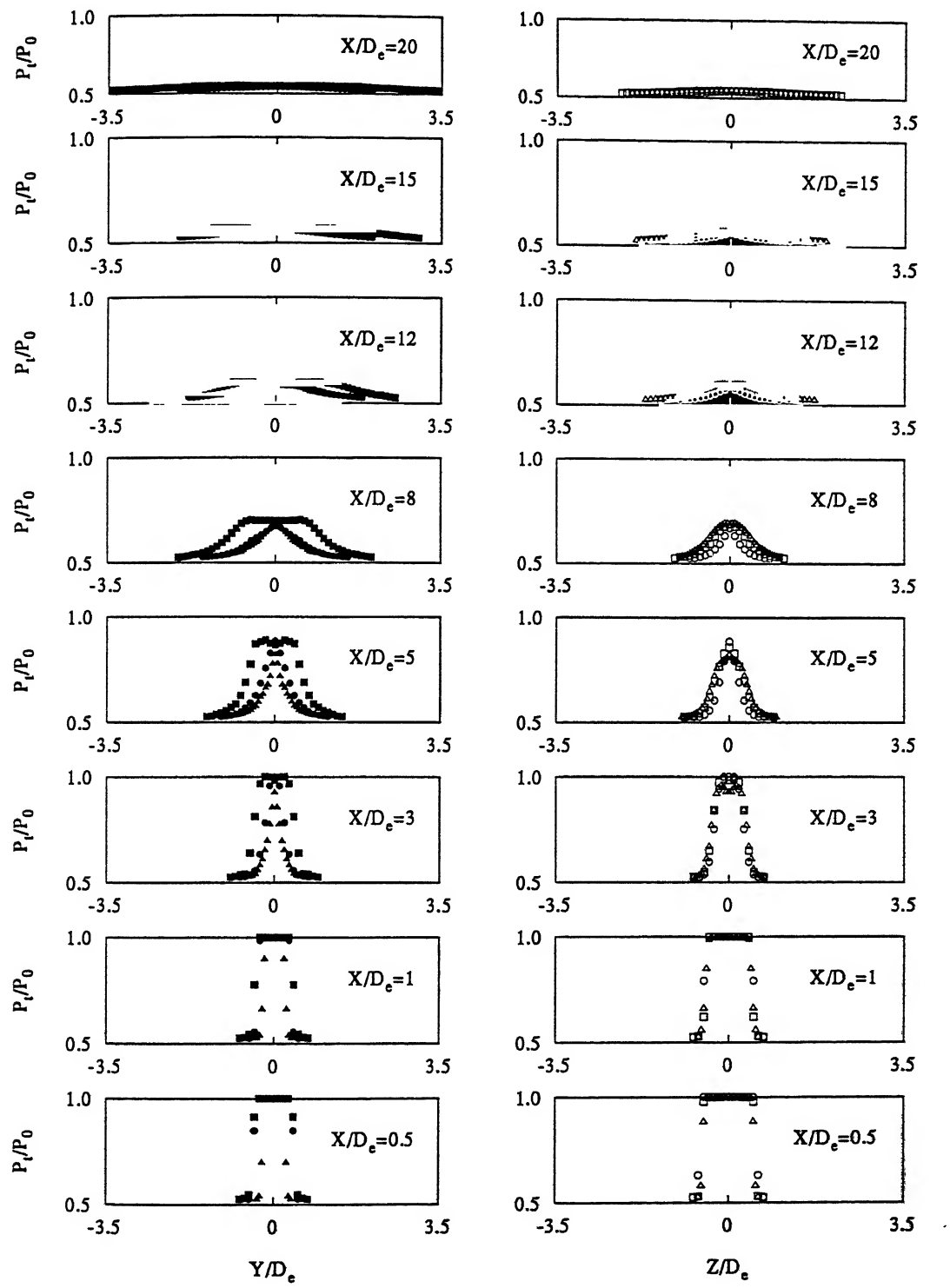

Figure 5.11: Comparison of pressure profiles for plain and square notched 2:1 elliptic slot jets at M_J=1.0. Semi-circular notch: X-Y plane,•; X-Z plane, ∘. Square notched ellipse: X-Y plane, ■; X-Z plane, □. triangular notch: X-Y plane, ▲; X-Z plane, △

the exit, i.e., at X/D_e=0.5, in the notched plane,i.e., X-Y plane, it is clearly seen that the pressure remains constant for a larger extent of the orifice width for square notch with a gradual decrease of pressure thereafter, indicating a lesser extent of restricted growth in that plane due to larger angle of sharp corners in this notch geometry relative to the triangular notch case. This is because the angle of the sharp corner has a strong role to play in the introduction of discontinuities in the shear layer[4] which prevent the roll up of uniform vortices in this region[3]. Further, the restricted growth of the jet in the notched plane increases as the angle of corner decreases. As such the sharp corners in the triangular notch ellipse restricts the growth of the jet in the notched plane, greater relative to square notch, and as such the pressure drops to the ambient earlier and faster as seen by closer pressure profiles to the centreline for this notch. The pressure profiles for the semi-circular notched ellipse lies in between the square and triangular notched cases.

Further downstream of exit location, the notched plane shows progressive spread of shear layer towards the jet centreline for both the cases with the shear layer for triangular notched ellipse spreading faster. This is the cause for a shorter core-length for triangular notch case. Further, the spread of the shear layer towards the surroundings is the fastest for square notch followed by plain ellipse and finally, by triangular notch case. This observation validates our explanation in the preceding section that the square notch shows a favourable effect in the notched plane due to its geometry. Beyond $5.0D_e$, square notch shows considerably higher spread relative to the triangular and semi-circular notched jets and continues to do so up to $20D_e$. However, beyond $8.0D_e$, triangular notched jet catches up with the semi-circular notched jet and the two jets spread equally thereafter.

Let us now observe the effect of notch geometry on the spread of the jet in the unnotched plane, i.e., X-Z plane. In contrast to the notched plane, beyond $3.0D_e$, triangular notched jet begins to show higher spread followed by square and semi-circular notched jets up to $15.0D_e$. This observation supports the argument in the preceding section regarding relatively better growth of triangular notch jet in the major plane than in minor plane as governed by its geometry. The higher restricted growth of the jet in the notched plane(due to sharper vertex angle) results in a more intense growth of jet in the unnotched plane, since the area available for pressure relief is the same for each jet. The trend of higher growth of triangular notched case continues downstream up to $15.0D_e$, after which square and triangular notched jets show

approximately the same spread. The semi-circular notched jet, however, shows lower spread than the other notched jets in the X-Z plane.

Thus, from the viewpoint of spread, square notch seems to be more favourable for spread in notched plane whereas triangular notch for spread in unnotched plane.

5.2.3 Jet Half-Width Growth

The jet half-width growth, $r_{0.5}$, is defined[4, 1] as the radial/lateral distance from the jet axis to the location where the local pressure/velocity drops to half of its centreline value. Figures 5.12(a)-(c) show the jet spread where the jet half-width is shown as a function of downstream distance. Here, $r_{0.5}$ is divided by D_e, the equivalent diameter of non-circular slot.

Figures 5.12(a)-(b) show the effect of underexpansion level on the jet half-width growth for the plain and square notched elliptic cases. The jet-spread for plain ellipse is observed to remain approximately the same along the X-Y plane at the two Mach number tested. However, for the notched case relative to the plain jet, Figs. 5.12(a)-(b), the spread in the notched plane increases considerably after $5.0D_e$ both for M_j=1.0 and 1.52 whereas it remains approximately the same along unnotched plane.

Figure 5.12(c) show the comparison of jet half-width growth for plain and square notched cases at M_j=1.0 in notched(X-Y) and unnotched(X-Z) planes, respectively. It is quite interesting to note that, compared to the plain jet, the square notched jet shows a considerable increase in jet growth in the notched plane after $5.0D_e$ as seen in Fig. 5.12(c). The jet growth along the X-Z plane, however, remains approximately the same for both plain and notched ellipse. Thus, the presence of notch is favourable from spread point of view at both M_j=1.0 and 1.52. This is a favourable characteristic, since generally with increasing level of underexpansion the spread decreases.

5.2.4 Centreline Pressure Decay

In the preceding section, it was observed that each notch geometry introduces different spread rates in the elliptic-slot jet. The difference in spread between these individual jets also results in different centreline pressure decay. Figure 5.13(a) shows the decay of centreline pressure with axial distance for the four cases investigated at M_j=1.0. The Pitot pressure P_t are

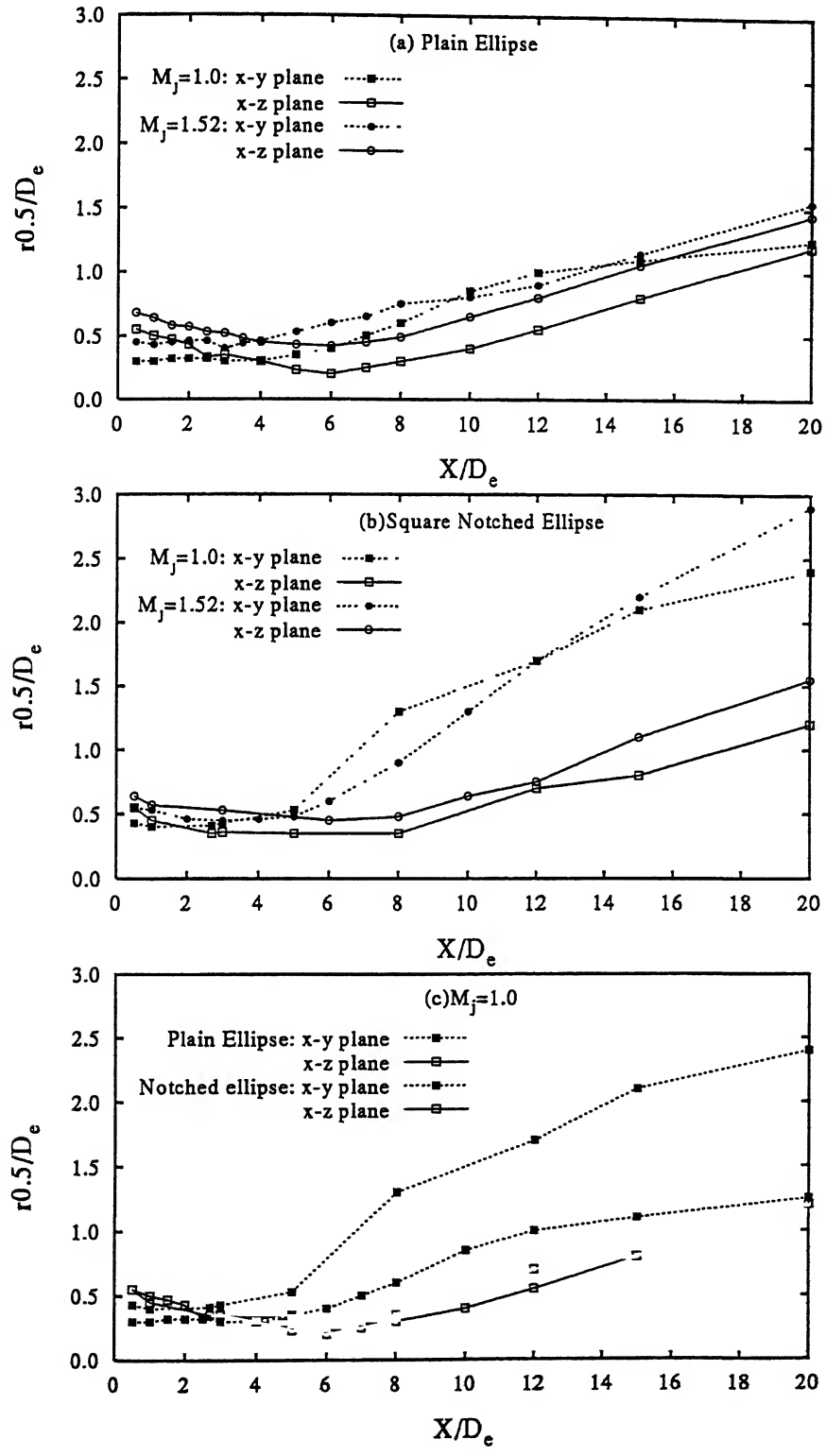

Figure 5.12: (a)-(b) Effect of level of underexpansion on jet half-width growth (c) Effect of notch introduction on the jet growth at full expansion

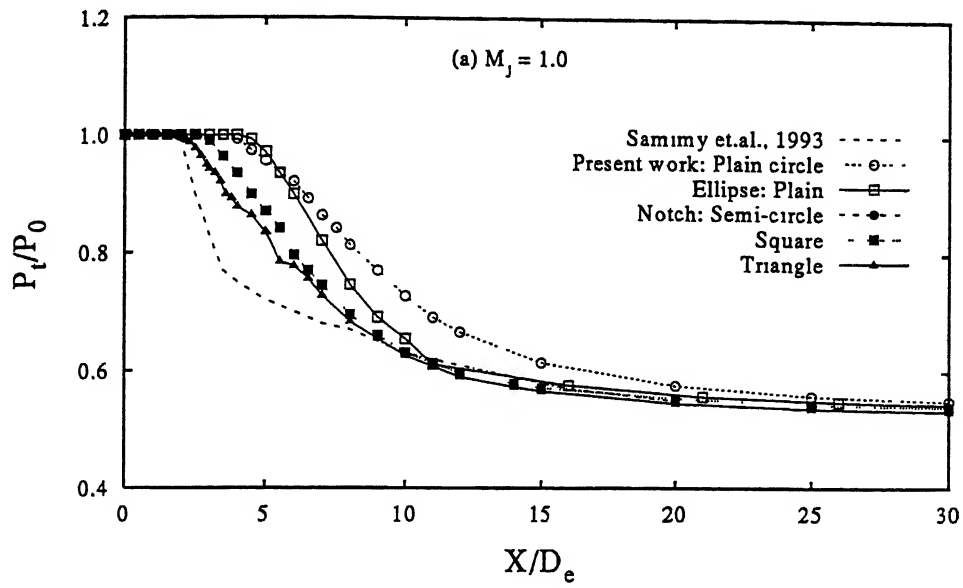

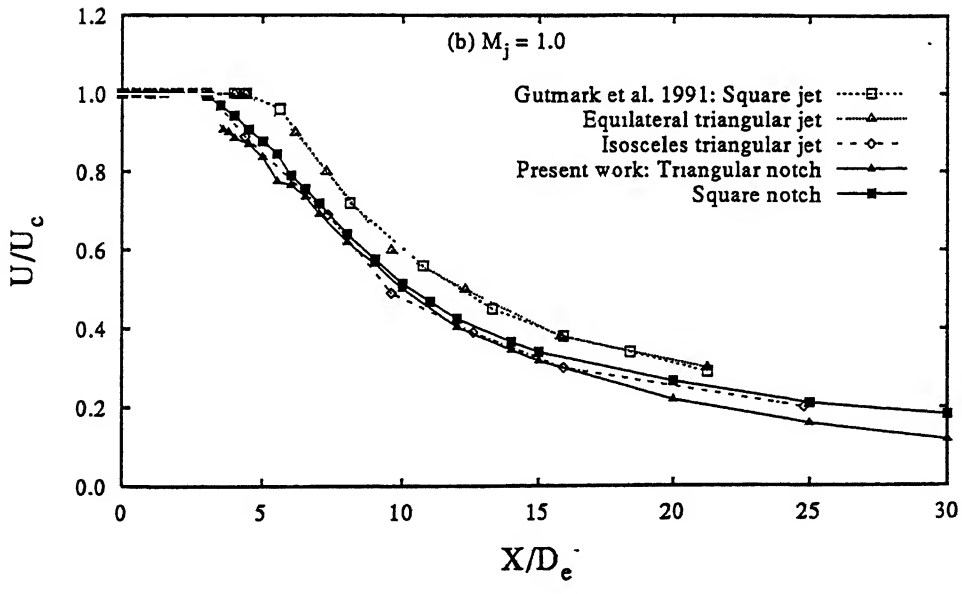

Figure 5.13: (a) Centreline pressure decay comparison for the cases investigated, (b) Comparison of present centreline decay results with Gutmark *et al* [4] triangular and square nozzles

divided by the stagnation pressure P_0 and plotted against the non-dimensionalised downstream distance X/D_e. A faster centreline pressure decay is usually a reasonable measure of faster jet spread[12]. The plot clearly indicates that under the action of the notch, the jet decays faster than the plain cases with the plain ellipse having the least decay followed by semi-circular, square and finally, by the triangular notched ellipse which has the maximum. Also, it is evident that the plain ellipse has the longest core-length followed by the semi-circular, square and finally by the triangular notched ellipse, which has the shortest. This observation at full-expansion confirms the flow enhancement brought about by the use of sharp corners in the notch geometry of an elliptic jet. It is worth emphasizing here that when higher small-scale mixing is desired close to the jet exit, a sharper notch angle is beneficial. This is in confirmation to Gutmark *et al*[4] observation that as the vertex angle is decreased from 90^o, higher fine-scale mixing is introduced in the initial shear layers resulting in the faster spread of shear layers towards the jet centreline. Once the end of the core is encountered, the mixing initiated at the exit of the jet gets amplified as is seen by the lower decay. Beyond $30.0D_e$ all the jets decay at almost the same rate oblivious of the initial geometry. The two tab case in a circular nozzle of Samimy*et al*[12] is included in the plot for the purpose of qualitative comparison with the present work. It is clearly seen that the core-length for the triangular notched ellipse is the same as that of Samimy's work. The decay of the two tab case is the maximum with a slower decay after $9.0D_e$.

Let us now compare our results with that of Gutmark *et al*[4] on equilateral triangle and square nozzle jets. It is, however, to be remembered that slot and nozzle jets have different decay characteristics. Slot jets have the presence of slender vortical structures due to extremely thin initial boundary layer(if not negligible) in them[1]. These slender vortices have thin cores(thus high vorticity) resulting in strong azimuthal variations in induced velocity. These effects combine to result in shorter potential core-length relative to jets exiting from contoured nozzles[1] which have relatively higher boundary layer growth. Figure 5.13(b) shows such a plot at M_j=1.0. Square and equilateral nozzle jets show similar centreline decay. However, isosceles triangle shows a shorter core-length and faster decay thereafter. This difference in decay of these jets is primarily due to higher turbulence level at the centre of the jet[4]. Relative to the equilateral triangular and square nozzle jets, our present work of ellipse with triangular notch shows much shorter core-lengths and faster decay. Triangular notched elliptic-slot jet shows the

shortest core-length of $1.7D_e$ of all the cases. This may be due the higher spread of elliptic jet coupled with sharp cornered notches that initiates higher mixing in these jets, as is apparent from the Figure.

5.2.5 Flow Visualization and Shock-structure

At underexpanded conditions(i.e., when the settling chamber pressure P_0 was further increased) the jet core was observed to be dominated by expansion-compression wave cell structures. In a supersonic underexpanded elliptic jet, the series of bouncing expansion and compression waves generate a non-symmetric structure of shock-cells, as is seen in Figure 5.14(a)-(b) for plain ellipse in major and minor-axis plane(Pics. 47, 49). This is primarily attributed to the angles of oblique shocks and expansion fans being different in the two planes of the jet due to which the flow changes direction in a non-symmetric pattern[21]. From the shadowgraph pictures, it is discernible that the lateral dimension of shock-cells decreases in the downstream direction in the major plane, Fig 5.14(a), whereas it increases slightly in the minor plane, Fig. 5.14(b). This is an indication of axis-switching phenomena in supersonic underexpanded jets[21]. Relative to underexpanded circular jet, the plain elliptic jet shows a faster diffusion of shock-cells. This is due to higher spreading rates of elliptic jets in the minor-axis plane[21](Pics. 47,49).

According to Norum[16] and Wlezien[17], the shape of the nozzle exit geometry greatly influences the nature of downstream development of shocks. Further, introducing sharp corners in the exit geometry causes changes in the jet behaviour at the different regions in its circumference and hence, the shock-cell geometry which eventually affects the jet noise characteristics[122]. Figures 5.15(a)-(b)(Pics. 63, 65), show the shadowgraph pictures of notched elliptic jet in the unnotched and notched planes, respectively. Relative to its plain counterpart, Figs. 5.15(a)-(b), notches are seen to modify the initial shock-cell development. Additional expansion and compression waves are seen to emanate from the notches. The interaction of these additional waves with the evolving shear layers leads to appreciable changes in the shock structure. Also, the thicker shear layers emanating from the corners help diffuse the shock structure faster[4]. The notched jet, as a result of the above combined effects, is seen to result in shorter shock-cells relative to the plain elliptic case.

Further details of the shock strength and jet decay for the underexpanded elliptic-slot jet is illustrated by Pitot tube traverses along the jet centreline. Figure 5.16(a) shows the centreline

Figure 5.14 (a): Shadowgraph picture of plain elliptic slot jet in the major-axis plane, M_j=1.5

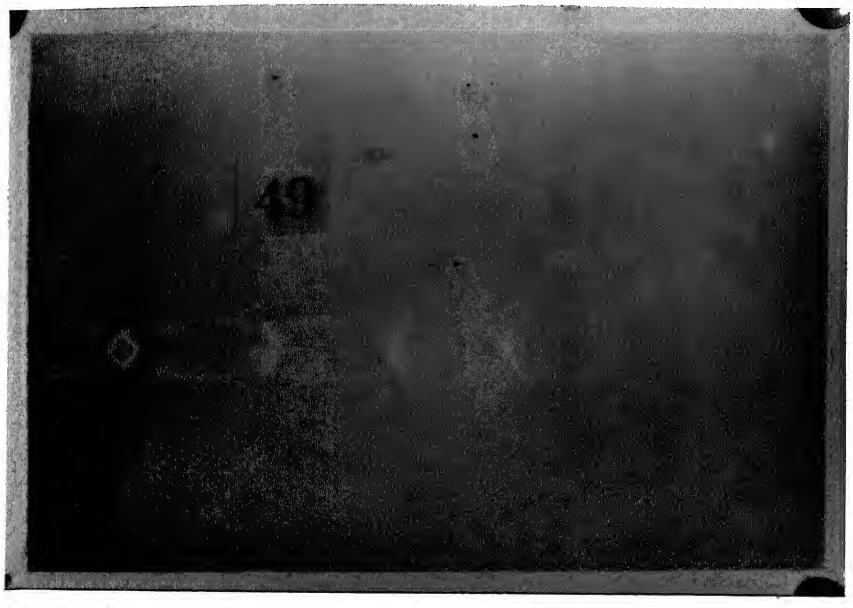

Figure 5.14 (b): Shadowgraph picture of plain elliptic slot jet in the minor-axis plane, M_j=1.5

Figure 5.15 (a): Shadowgraph picture of square notched elliptic slot jet in the unnotched/major-axis plane, M_j=1.5

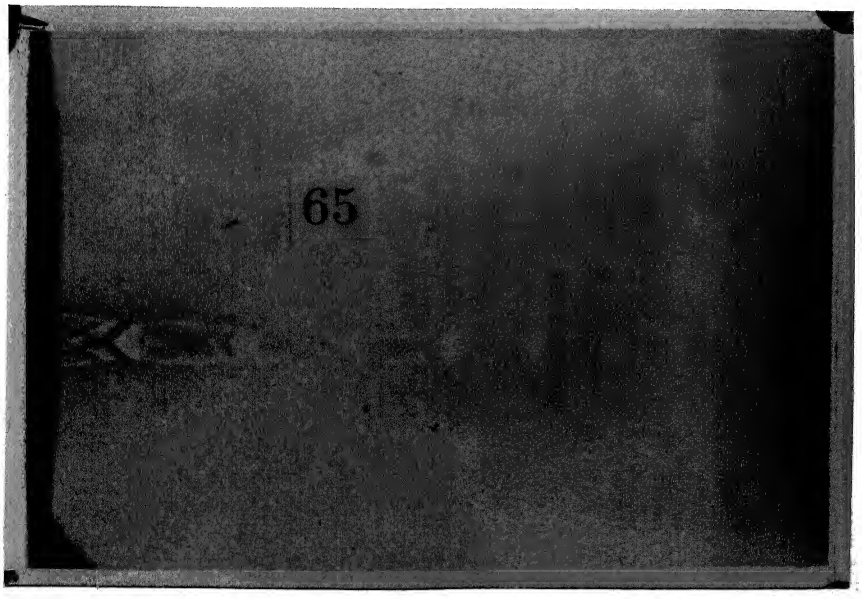

Figure 5.15 (b): Shadowgraph picture of square notched elliptic slot jet in the notched/minor-axis plane, M_j=1.5

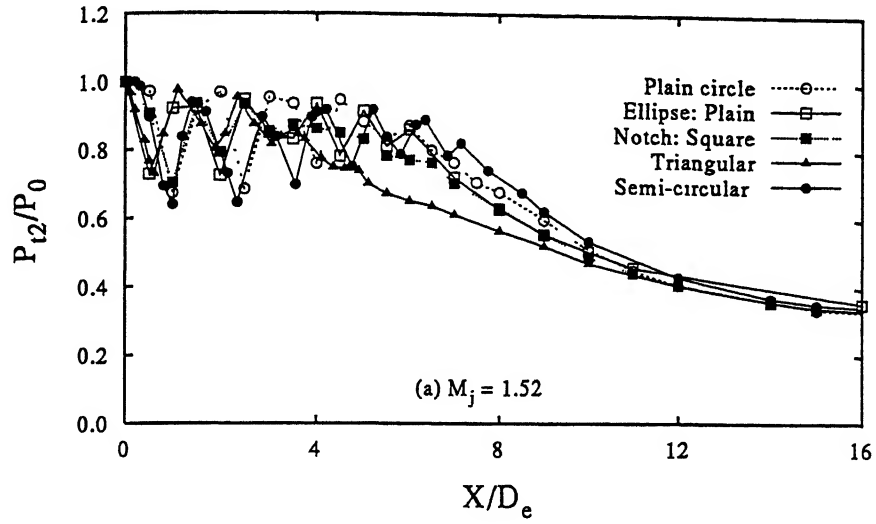

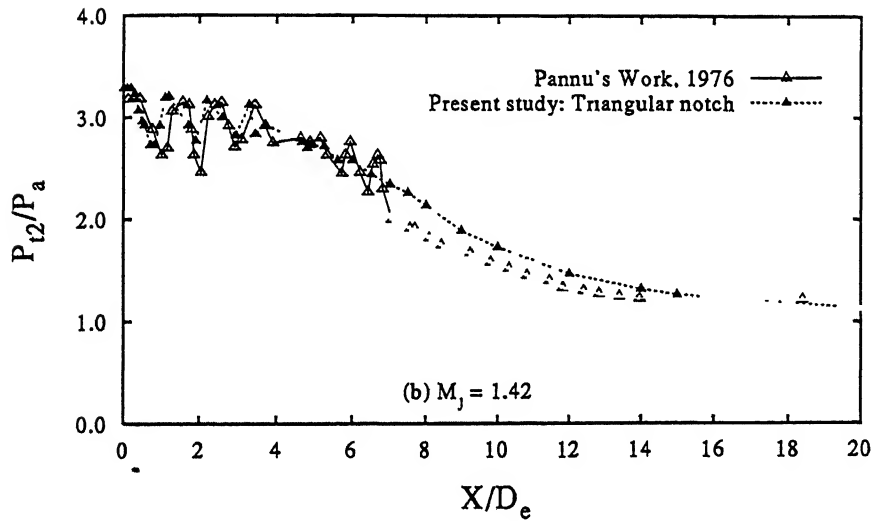

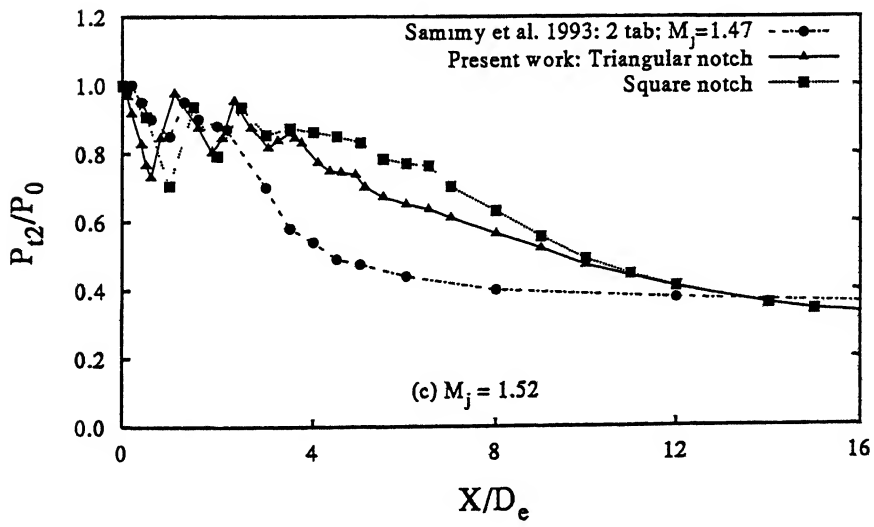

Figure 5.16 Shock-structure/strength comparison for the cases investigated at underexpanded conditions

conical circular nozzle generates small-scale structures that shield the shock-structure of the jet and hence, act as silencers to jet noise. Further, this fine-scale mixing initiated from the sharp corners causes faster spread of shear layers towards the jet centreline[4] and hence, seems to weaken the shocks in underexpanded jets. In the present study, the low velocity regions observed in the notched plane of elliptic slot jets seem to diffuse the shocks faster relative to plain jet. Further, these low velocity regions may also help to shield the shocks and act as silencers to noise radiation in these notched jets.

5.2.6 Shock-cell Length and Screech Tone

The third and fourth shock-cells have long been known to be the main source of shock-associated noise[16, 18]. Also, choked jet-noise and hence, the screech frequency are primarily dependent on the length of these shock-cells and hence, on the strength of these shocks in the shock-cell system[16]. Therefore, the effect of notch on the average length of shock-cells(up to four cells) for the present cases was investigated. Figures 5.17(a) shows the variation of L_{avg}/L_a Vs M_j. Here, L_{avg} is the measured average shock-cell length and L_a the semi-major axis length of the plain case. This value of L_a is also used for non-dimensionalizing the average shock cell length of the notched ellipse and hence, is referred to as the equivalent semi-major axis length. For comparison, Tam's theory[113] for elliptic jets is included. It can be seen clearly that plain ellipse agrees well with Tam's theory though the curve for the present case lies a little below it. For notched cases, a decrease in the average length of shock-cells is seen with the curve following the trend of Tam's theory but lying well below the plain case. This is primarily attributed to the secondary structures shed from the corners[3, 46, 4, 60] of notches which affect the initial evolution of shear layers and hence, result in faster diffusion of shocks(shorter shock-cell lengths). Upto M_j=1.3, there is an erratic behaviour in L_{avg} for notched cases but beyond M_j=1.3, all the cases show a clear trend. Square notch shows a maximum reduction in third shock-cell length at M_j=1.52 followed by triangular notch and finally, by the semi-circular notch case which has no sharp corner in its geometry.

Figure 4.17(b) shows a plot of predicted Strouhal number(fL_a/U_j) of the screech tone versus the fully expanded Mach number M_j. As the Mach number increases, the Strouhal number of screech decreases. This decrease is due to the increase in shock-cell spacing with Mach number, which causes an increase in the screech wavelength and consequently a

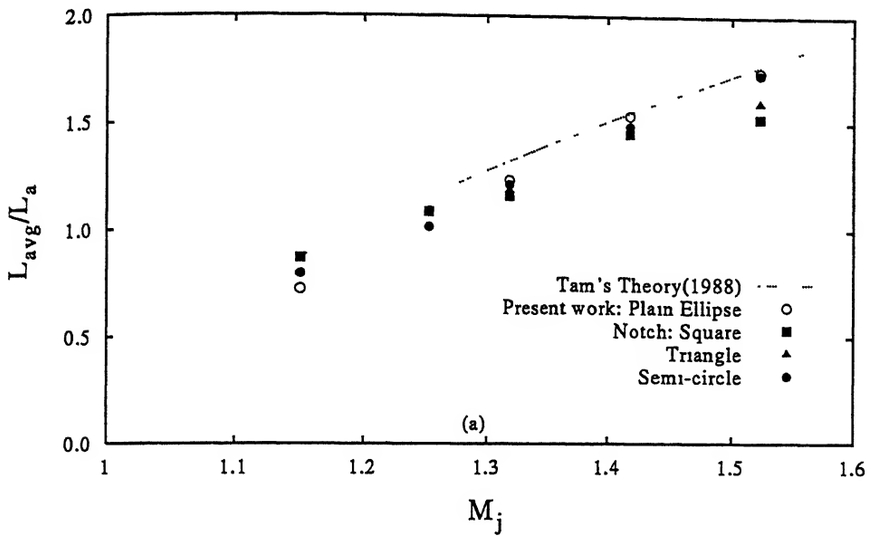

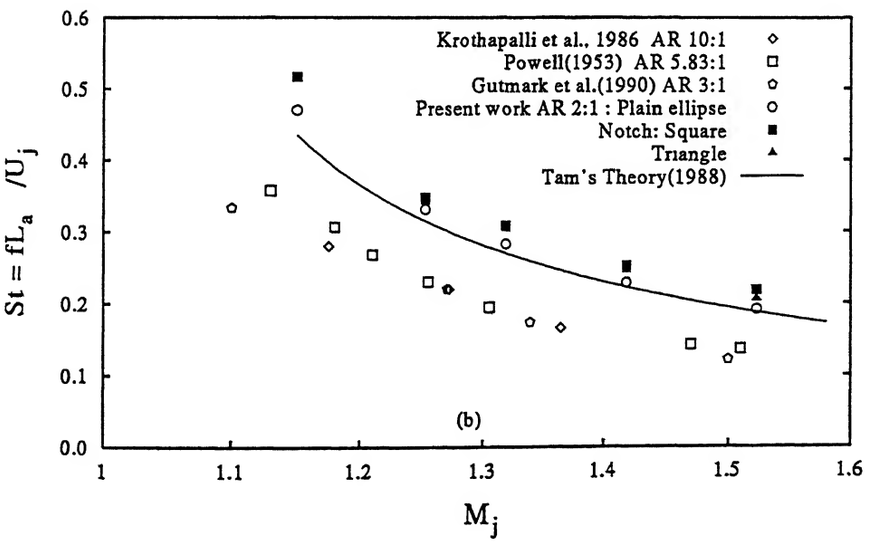

Figure 5.17: (a) Variation of average shock cell length with M_j, (b) Plot of predicted Strouhal number of screech tone with M_j

decrease in screech frequency[110]. This may be due to the emergence of different instability modes or interaction of shear layer structures with the compression or expansion waves[3]. In the calculation of predicted Strouhal number, the average shock-cell length, L_{avg}, was considered up to four shock cells at different underexpanded levels. This value of L_{avg} was used in the screech tone frequency formula obtained by Tam *et al*[95] in conjunction with Tam's formula[113] for shock-cell length of elliptic jets with aspect-ratio less than four. In Fig. 5.17(b), Tam's analytic solution[113] of the screech Strouhal number versus M_j for elliptic jets, is also shown for comparison of our present work with Tam's theory. The present work shows good agreement with Tam's analytic solution with the points following the same trend though they lie a little above it. This is once again due to effects typical to slot jets. Since with increasing M_j, an increase in Strouhal number relative to other cases indicates decrease in shock-cell spacing[110], the plot clearly shows that square notch is expected to have better noise characteristics followed by triangular notch relative to its plain counterpart. This may be due to thicker shear layers emanating from the corners resulting in faster diffusion of shock-cells[4]. Experimental work for rectangular jets is also included to show the Strouhal number trends in literature and for comparison with rectangular and elliptic jets. These points lie well below Tam's theory for 2:1 elliptic jets. However, these are measured Strouhal number values instead of predicted values.

5.2.7 Aeroacoustic Characteristics

From a practical point of view, noise reduction is probably the most important challenge of all. Past experiences indicate that improved mixing in the jet flow has invariably the beneficial side effect of substantial noise reduction[33]. Improved mixing reduces turbulence and hence, noise[30, 33]. Since it is envisaged that future generation of High Speed Civil Transport(HSCT) will have non-circular nozzle geometry[33], most of the current noise reduction effort have been channeled into development of enhanced mixing devices. It has been recognised in literature that noise from shock-containing supersonic jets consist of three principle components, namely, the dominant part of turbulent mixing noise, the broadband shock-associated noise and the screech tone all of which are generated by large-scale structures/instability waves of the jet flow[95, 33, 32]. The last two sources exist, of course, only when a shock-cell structure is present inside the jet flow.

The experimentally observed characteristics of sound radiation from fully expanded(shock-free) and underexpanded(shock-containing) elliptic-slot jets with and without the notches are described in the present section. In particular, the characteristics of *broadband* shock-associated and *turbulent* mixing noise from underexpanded jets are examined over an extensive envelope of supercritical jet operating conditions and observer angle. Further, the spectral and directional characteristics of both types of noises will be identified.

Acoustic Spectrum Analysis

In the far-field, the measured frequency of screech tone is the same regardless of the direction of observation[95]. This is in contrast to the strong directional dependence of the broadband shock-associated noise. However, the spectrum analysis is done at only one polar/observation angle, $\theta = 150^o$ to the upstream jet direction. Further, the earlier studies reveal[95, 33] that the fundamental screech tone frequency is always smaller than the frequency of broadband shock-associated noise.

Figures 5.18(a)-(b) shows the far-field spectral characteristics of a plain elliptic-slot jet for acoustic radiation at $\theta = 150^o$ to the jet upstream direction with the jet operating at full expansion and at underexpanded condition with an equivalent Mach number, M_j=1.5. The acoustic spectra is, however, measured only in the notch/minor-axis plane of ellipse. The power spectrum of the fully expanded jet, Fig. 5.18(a) is broad and smooth and consists of purely turbulent mixing noise. A peak in the jet mixing noise at 8 kHz is observed. On the other hand, when the jet is operated at underexpanded condition, the acoustic spectrum contains an extra noise contribution due to the presence of shock structure in the jet flow, in addition to the turbulent mixing noise, as seen by the higher noise intensity in the spectrum, see Fig. 5.13(b). Three dominant components of noise are clearly identified from the spectra. Very prominent in this acoustic spectrum is the discrete frequency peak at approximately 16 kHz and is referred to as the *screech* component of jet noise. The low frequency broadband peak occurring at approximately 4-13 kHz, Fig. 5.18(b), to the left of the screech tone is associated with *jet mixing* noise, while the high frequency broadband spectrum to the right of the fundamental screech frequency is the *broadband* shock-associated noise of an underexpanded jet as per the findings of Ponton and Seiner[76] and Tam[33]. Here if we compare the spectral characteristics of plain elliptic-slot jet with that of plain circular-slot jet in chapter 4,

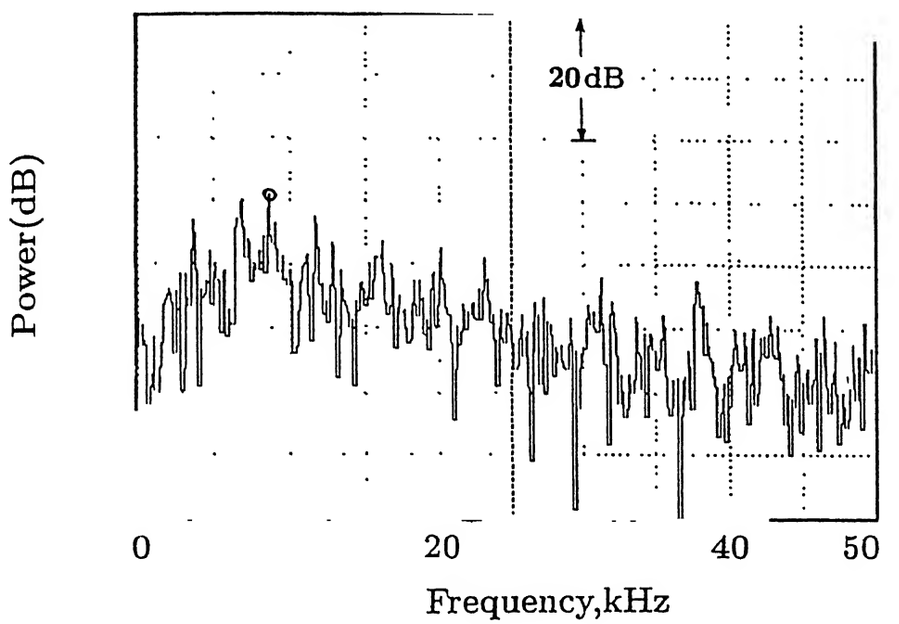

Figure 5.18: (a) Far field spectral characteristics of plain elliptic slot jet at M_j=1.0

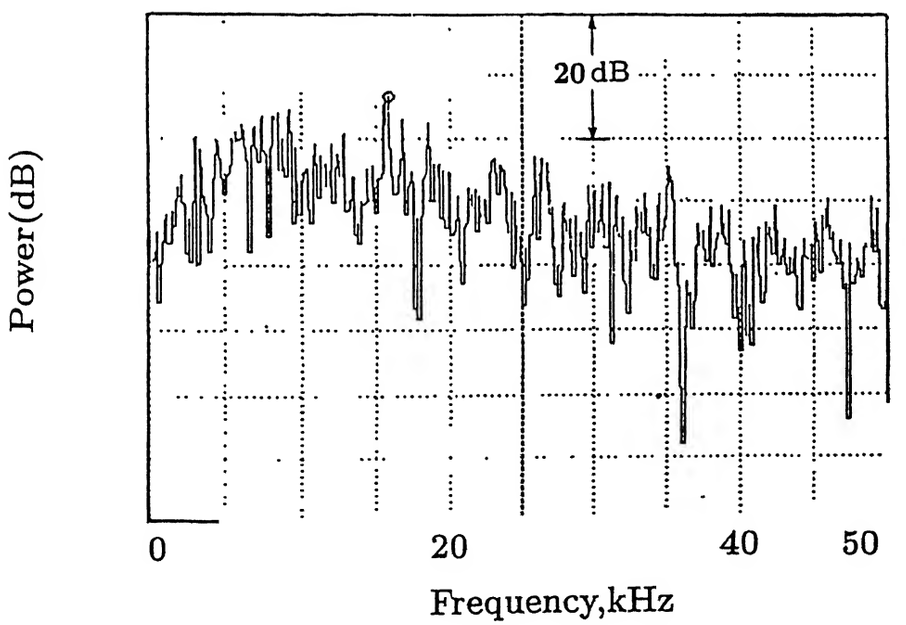

Figure 5.18: (b) Far field spectral sharacteristics of plain elliptic slot jet at M_j=1.5

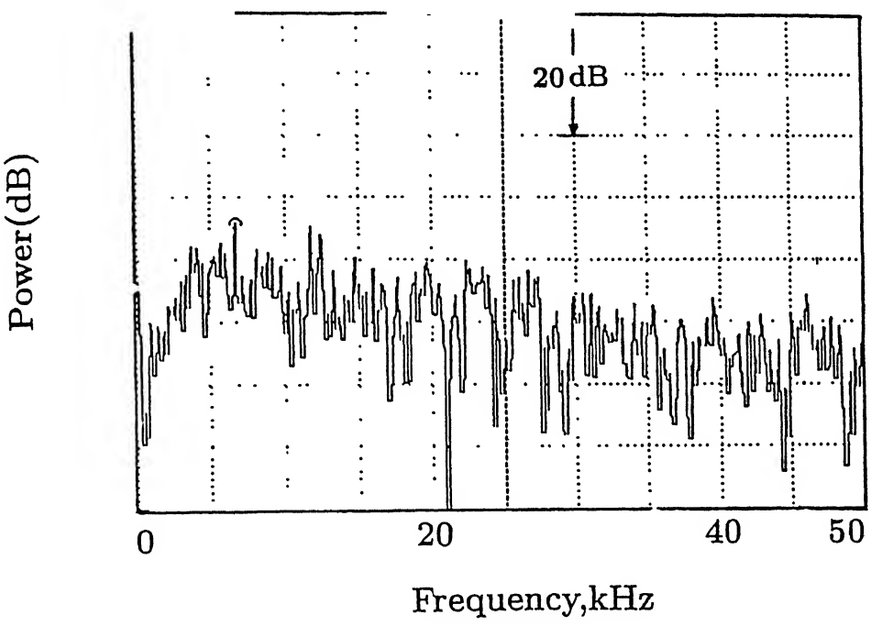

Figure 5.19: (a) Far field spectral characteristics of square notch elliptic slot jet at M_j=1.0

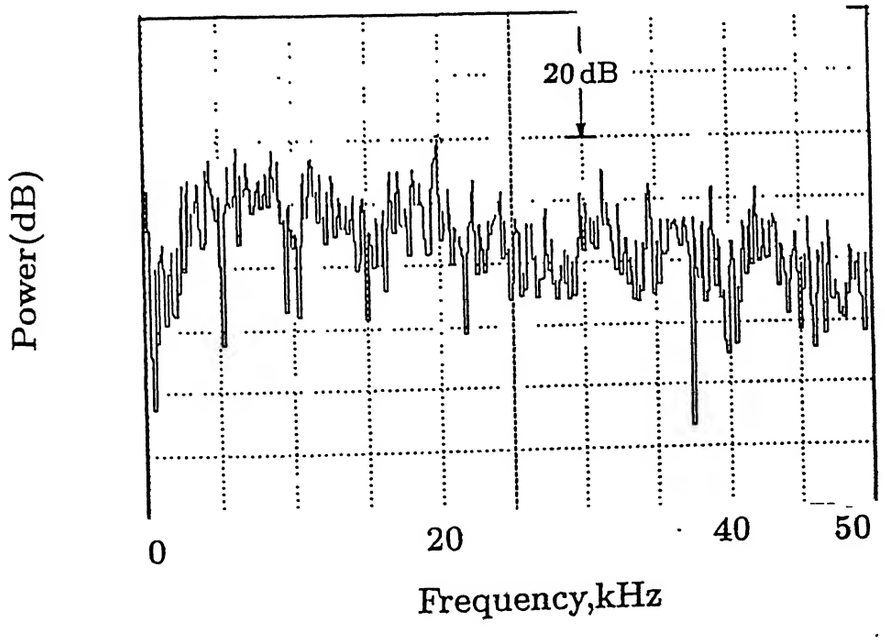

Figure 5.19: (b) Far field spectral characteristics of square notch elliptic slot jet at M_j=1.5

Figs. 5.18(b) and 4.13(b), we find that the peak screech component for ellipse shows a reduction by 4.5 dB. Further, significant reduction in the high frequency broadband shock-noise is observed for ellipse indicating a relatively weaker cell-system relative to plain circular case.

Let us compare the acoustic spectra acquired for elliptic jet with notches with that of plain elliptic jet. Figures 5.19(a)-(b) show such a spectra for a square notch elliptic-slot jet. At full expansion, Fig. 5.19(a) and Fig. 5.18(a), a slight decrease in the low frequency content of jet mixing noise can be seen(5-10 kHz) for notched elliptic jet. Furthermore, the peak noise due to turbulent mixing decreases by 5 dB, relative to the datum jet while the high frequency jet noise remains approximately the same. If a comparison is now made for the underexpanded case, Fig. 5.18(b) and 5.19(b), the square notch jet shows a reduction in the peak component by approximately 7 dB. Furthermore, a shift in the fundamental screech frequency to 20 kHz is evident. The broadband shock-associated noise to the right of this peak shows a slight decrease in the high frequency jet noise, indicating a weaker shock-cell system[76, 26]. On the other hand, the low frequency content, i.e., the jet mixing noise, is observed to decrease significantly. Some similar trends in the acoustic spectrum of triangular and semi-circular notch jets were observed. However, the peak component in triangular case shows a reduction of 5 dB whereas the semi-circular case shows the same magnitude of screech component as the plain elliptic jet. The acoustic spectrum of these notch configurations are not shown since the overall characteristics approximately are the same as that for square notch slot jets shown.

The acoustic spectrum results indicate that the differences in the slot perimeter, provided by variation in notch configuration, may alter the acoustic emission characteristics of these jets not only in the screech component but also in the turbulent mixing and broadband shock noise. These differences point out the corresponding aerodynamic changes[76] brought in by notch introduction and its geometry. The significant differences existing in the jet mixing and broadband shock-noise radiated energy suggests that modification in the jet-noise source mechanisms and hence, the instability characteristics has occured[76].

Overall Sound Pressure Results

The deviation of the jet from symmetry, either by eccentricity, as in the elliptic jet, or by introduction of sharp corners, as in triangular and square jets, causes changes in the jet behaviour at the different regions around its circumference[122]. These changes are related to the local

radius of curvature of the nozzle edge that affects the flow instability characteristics[122, 76], the evolution of large-scale structures, shock-cell development[16, 122, 4, 30], and eventually jet noise characteristics[16, 122, 2].

The far-field noise characteristics of underexpanded elliptic-slot jets with and without notches are presented in Figs. 5.20(a)-(d). The noise intensity is examined at two observer angles, i.e., θ=90°, 150°, R/D$_e$=50, as the level of underexpansion is increased. These values of θ and R/D$_e$ were selected after a detailed survey of literature[66, 118, 26, 76, 119]. The measurements were made from the fully expanded condition to high level of underexpansion with an equivalent Mach number of M$_j$=2.0. It is clearly discernible from the plots, Figs. 5.20(a)-(d), that the noise intensity jumps as soon as shocks begin to appear in the jet flow. Further, worth observing is the difference in OASPL values between major and minor-axis/notch planes.

One of the principal characteristics of the radiation field of a non-circular jet is its dependence on the plane of measurement with respect to the nozzle exit[26]. It has been observed[125], that the noise radiated from an elliptic jet was different in amplitude in the major and minor-axis planes[123]. This difference in noise production according to Crighton[123] was related to the instability characteristics in the two planes which is attributed to different spatial growth rates along the major and minor-axis planes[123, 58] since most of the external fluid is entrained into the jet stream at the minor-axis sides[20]. Further, at underexpansion, the series of bouncing expansion and compression waves generate a non-symmetric structure of cells. The angles of the oblique shocks and expansion fans are different in the two planes of the jet and the flow changes direction in a non-symmetric pattern[21] leading to a variation in the instability characteristics around their circumference. This contribution from shock-shear layer interaction results in a substantial increase in the spreading rate along the minor-axis plane whereas the spread remains approximately the same along major-axis plane[21]. All these factors contribute to a lesser noise intensity along the minor-axis plane[26, 46, 123] relative to major-axis side which behaves more or less like a circular jet.

As the observer moves from θ=90° to 150° the significance of shock-associated noise increases progressively, and at θ=150°, the levels at supercritical pressure ratios are dominated by the contribution from shock noise[66, 76], Figs. 5.20(a)-(d). At θ=90°, in the minor-axis/notched plane, Fig. 5.20(a), the notched jets show approximately same value for all cases up to M$_j$=1.4 with plain ellipse showing slightly lesser noise levels. Plain circular jet shows a

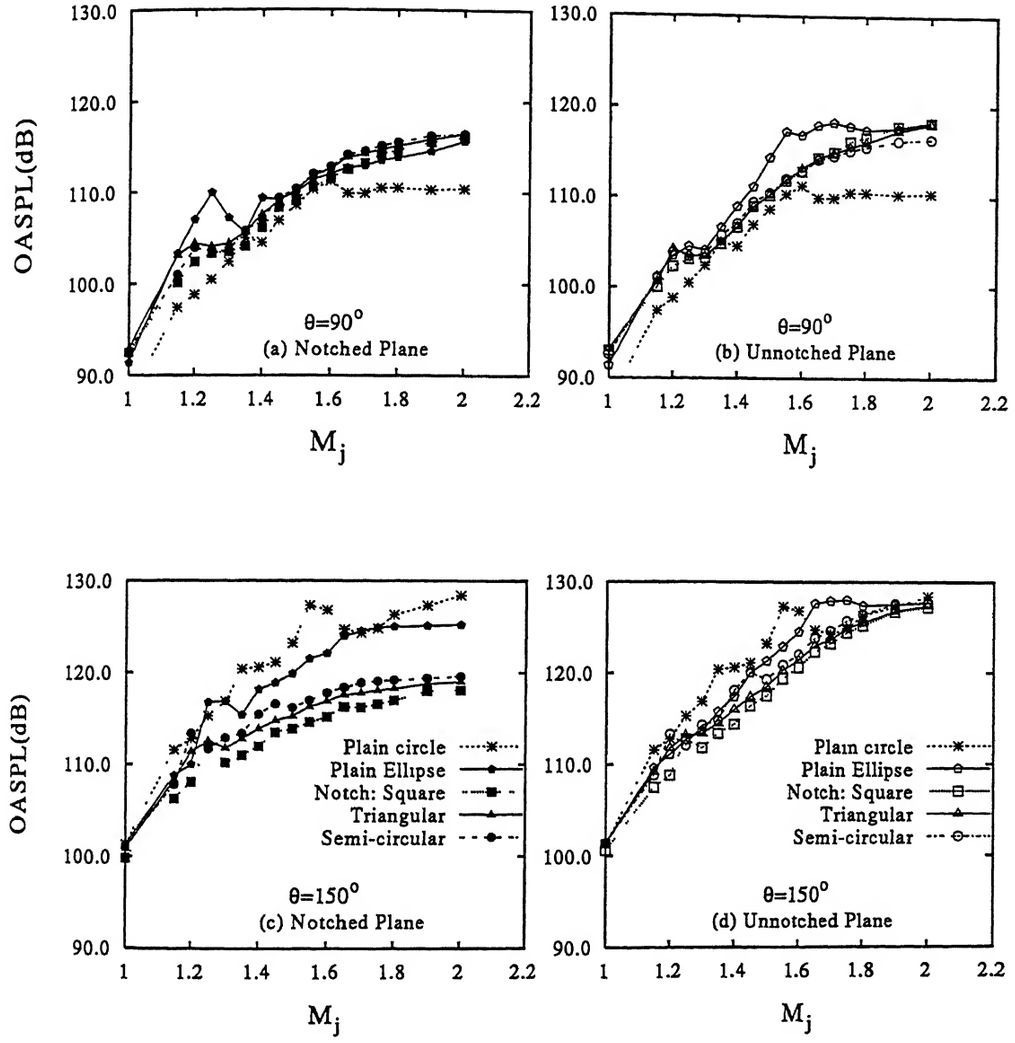

Figure 5.20: Far field overall sound pressure results for plain and notched elliptic slot jets at two polar angles, R/D_e=50.0 from jet exit

minimum sound intensity with higher jet mixing noise from notch jets indicating higher contribution of turbulent mixing noise[66, 33, 118] in elliptic jets. Presence of notch is further seen to slightly increase the mixing noise relative to plain elliptic jet.

In the major-axis/unnotched plane of plain ellipse, the noise contribution is observed to be significantly higher(by 4 dB) relative to that along minor-axis plane, Figs. 5.20(a)-(b), at M_j=2.0. However, the presence of notch in the minor-axis plane brings down the noise levels of these jets along the major-axis plane, relative to plain case(between M_j=1.2 to 1.8), Fig. 5.20(b) thereby slightly reducing the noise gap between the two planes of these jets. This suggests modifications in the shock-shear layer interaction, by notch presence, which affect the jets behaviour and hence, the noise emission characteristics in the two planes.

For observer angle of θ=150°, however, a different trend in OASPL is observed as was also observed by Powell[119]. Since this is the direction in which the shock-associated noise is radiated[66, 76, 33, 118, 32], plain circular-slot jet is seen to radiate significantly higher noise levels relative to that along minor-axis/notched plane of notched jets, Fig. 5.20(c). Slight fluctuation in OASPL values is seen between M_j=1.2 and 1.4 for plain ellipse. This may be due to the jets flapping motion in the minor-axis plane[124, 21] since at certain shock-spacings the jet oscillations are stronger than at others[128, 104]. Since these jet oscillations are directly related to the acoustic emission of broadband shock-associated noise at 30° to the downstream jet direction[32, 33, 76, 66] as such the radiated noise will have a fluctuating value in this range of M_j, as seen in Figs. 5.20(c)-(d). The notched plane shows significant reductions in broadband noise levels for each notch configuration. Plain ellipse is seen to show a 3 dB reduction relative to plain circle at M_j=2.0. Relative to plain ellipse, square notch jet shows a 7.5 dB reduction followed triangular notch with 6.5 dB and semi-circular with 5.5 dB reduction in shock-noise levels. The shock-associated noise levels in the major-axis plane, however, shows approximately same levels for notched jets.

This suggests a weaker shock-cell system in the notched plane of these jets relative to that in the minor-axis plane of plain ellipse. This may be due to the additional expansion and compression waves emanating from the notches as observed from shadowgraph pictures(Pic. 59, 61) which seem the shock-shear layer interaction and hence, the noise source mechanisms significantly in the notch planes of these jets. This difference in acoustic characteristics between major and minor-axis planes is typical of non-circular jets(especially ellipse) where minor-axis sides

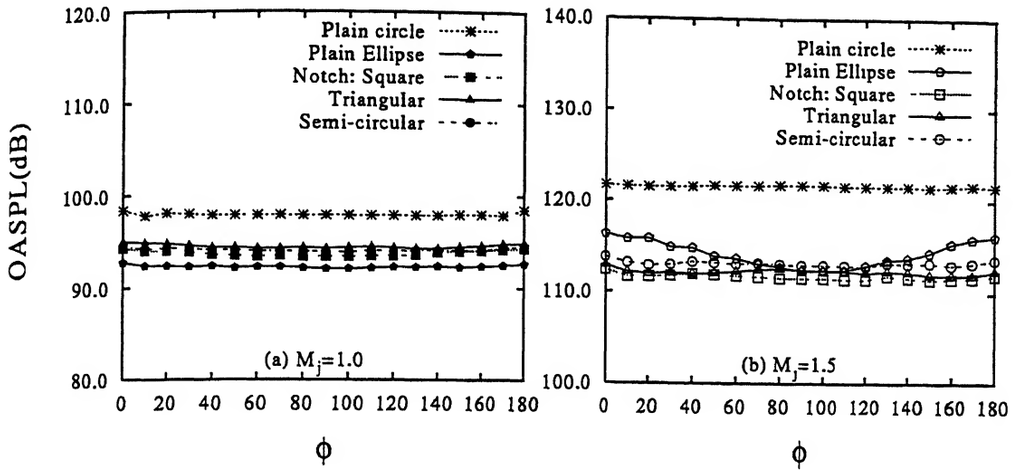

Figure 5.21: Azimuthal directivity of overall sound pressure levels for plain and notched elliptic slot jets at (a) M_j=1.0, (b) M_j=1.5

show lesser noise intensity due to higher spread in this plane relative to major plane[26, 122, 123, 124, 21, 125].

Pannu and Johanneson[8] observed that a triangular notch in a conical nozzle generates small-structures that shielded the shock-structure of the jet and hence, acted as silencers to jet noise. Further, this fine-scale mixing from sharp corners of triangular jets causes a faster spread of shear-layer towards the jet centreline[3] and hence, seems to weaken the shocks in underexpanded jets. It may, therefore, be suggested that the reduction in the magnitude of OASPL is due primarily to the weak shock-cell structure in notch jets and hence, significantly reduced shock-associated noise. Further, the square notch configuration seems to be the best for far-field noise reduction of elliptic-slot jets.

Azimuthal Directivity

It is well known that non-circular jets spread differently in different planes and as such radiate different noise intensities in different planes[26, 21, 125, 124, 123] as has also been seen in the preceding section. The present section discusses the results of azimuthal directivity for jets with and without notches for two values of Mach number, M_j=1.0 and 1.5. The measurements were made starting from major-axis side, passing through the minor-axis side(having the notch) and ending up at the other end of minor-axis side. The microphone was positioned and moved

in a circular arc on a fixed aluminium quadrant, mounted on a tripod stand, at fixed intervals of 10^o, R/D_e=24. Figures 5.21(a)-(b) shows the azimuthal variation of far-field OASPL at $\theta = 90^o$, X/D_e=0.0. At full expansion, plain circle shows the minimum noise intensity without any preferred direction as is expected due to symmetry of slot geometry. Relative to plain circle, plain ellipse shows 1 dB increase in mixing noise. Notched jets, relative to plain ellipse, further show increase in jet mixing noise with triangular notch jet showing maximum value(2 dB increase) followed by semi-circular and square notch jet(3.0 dB). However, a slight decrease(0.5 dB) in noise levels is apparent in the region of the notches(ϕ=80^o to 100^o) /minor-axis plane relative to major-axis plane.

At underexpanded condition, Fig. 5.21(b), the difference in noise radiated from major and minor-axis planes widens and is clearly discernible. This is primarily due to the strong asymmetry of shock angles in the two planes which cause the flow to change direction in a non-symmetric pattern[21]. Further, it has been observed[21] that minor-axis plane is dominated by flapping mode(resulting in larger spread and hence, lesser noise levels) while on the major-axis plane symmetric mode is prevelant. The plain circular jet shows the maximum shock noise with no preferred direction. As much as 8-10 dB reduction is seen in the minor-axis/notched plane relative to plain circular case. The presence of notches further brings down the shock-noise levels significantly in the major-planes of these jets, Fig. 5.21(b). As much as 3 dB to 4.5 dB reduction is observed relative to plain ellipse and this results in the notch jets showing approximately no preferred direction of shock-noise in the two planes. This may be due to the additional expansion and compression waves originating from the notch geometries as seen in the shadowgraph photographs(Pic. 59, 61). These waves seem to circumferentially modify the downstream shock-structure development and hence, alter the acoustic emission of these jets.

As was also seen in the acoustic spectra of plain circular jet, Fig. 4.13(b), the SPL is dominated by a sharp peak characteristic of screech. Spectra of plain and notch ellipse, Fig. 5.18(b) and 5.19(b), show significant reductions in this peak value presumably because the azimuthal curvature variation results in a non-symmetric shock-pattern and effects the feedback system which supports screech mode[16, 17]. Further, the azimuthal dependence may be due to the resulting asymmetric spreading and deflection characteristics of these jets.

Radial Directivity in the Aft-Quadrant

In the preceding sections we have discussed about the spectral, azimuthal dependence and overall sound intensity characteristics with the microphone positioned at two polar angles, θ=90^o, 150^o. In the present and concluding part of our acoustic study on elliptic-slot jets, we will discuss the angular directivity of jet noise in the aft quadrant. Here, the region defined by θ=0-90 degrees is referred to as the forward quadrant and by θ=90-180 degrees as the aft quadrant in accordance with the norms followed by Alvi *et al*[26].

Figures 5.22(a)-(b) show the cases investigated at full expansion in both planes. The jets show a clear and distinct noise intensity pattern. It is discernable that the dominant part of the noise is confined in the aft quadrant at angles greater than 100 degrees in both the planes. Whereas for angles less than 100 degrees, the jet noise is low and relatively independent of direction. It is believed[32, 33. 66, 118] that this low level noise is generated by fine scale turbulence of the jet flow whereas the dominant part is generated directly by large-scale structures in the jet flow. Relative to plain jet, notch jets show higher noise intensity in both planes for all angles in the aft quadrant. This may be due to the dominance of turbulence structures in notch jets in accord with the present understanding of turbulent mixing noise of jets[33]. Further, for notch jets, for $\theta > 140^o$, the jet noise intensity ceases to increase and attains an approximately constant value. Notch geometry, further, has influence on noise intensity. Triangular notch jet shows a dominance, as was also observed in azimuthal directivity plots, of jet noise followed by semi-circular and finally, by square case which shows minimum value.

Figures 5.23(a)-(b) depicts the case of underexpanded(shock-containing) jets at an equivalent Mach number, M_j=1.5. It is discernable from Figs. 5.22 and 5.23, that shock-associated noise dominates over the turbulent mixing noise levels at all angles. The plain circular shows a fluctuating noise intensity pattern between observer angle of 110^o and 130^o. The plain and notch elliptic jets, however, show a distinct variation of OASPL with observer angle.

In the minor-axis/notched plane, Fig. 5.23(b), approximately uniform noise levels are observed up to $\theta = 110^o$ indicating that the noise radiated by shocks in these jets is fairly omnidirectional and is confined for angles greater 110^o. Both plain and notch jets show aprrox-imately same turbulent mixing noise levels up to 110^o. For observer angle greater than 110^o, all the jets show increase in shock-noise levels indicating that the directivity in the forward quadrant is primarily controlled by mixing noise levels[26, 66], whereas in the aft quadrant the

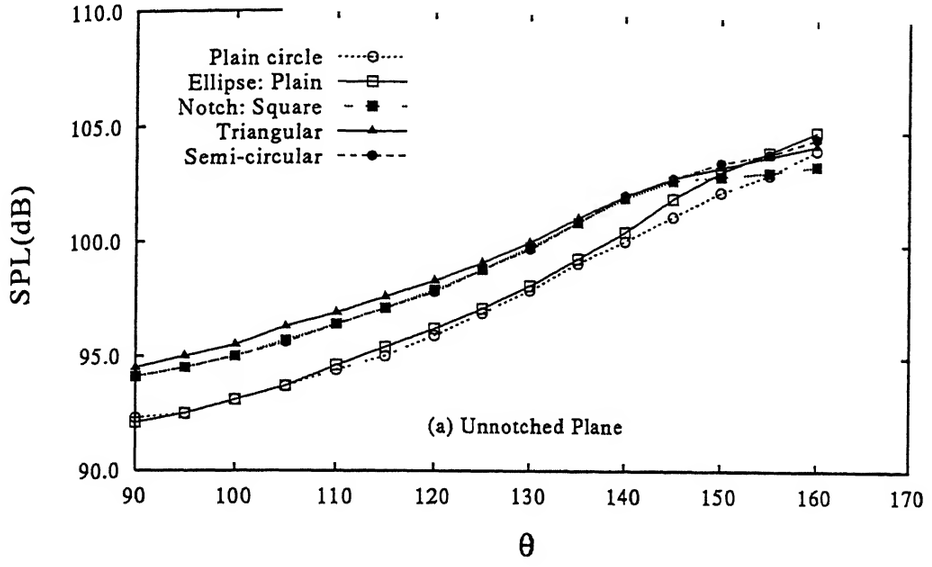

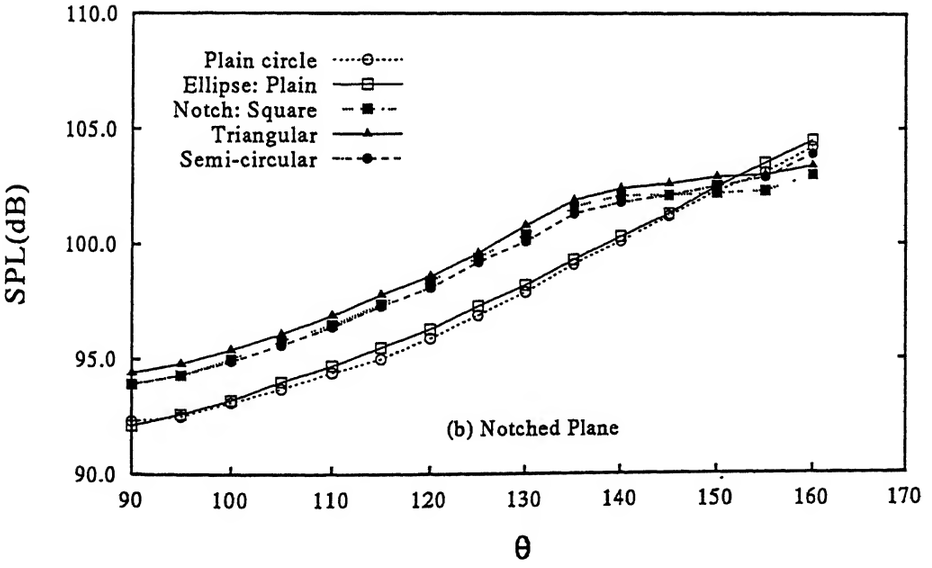

Figure 5.22: Radial directivity for plain and notched elliptic slot jets at M_j=1.0

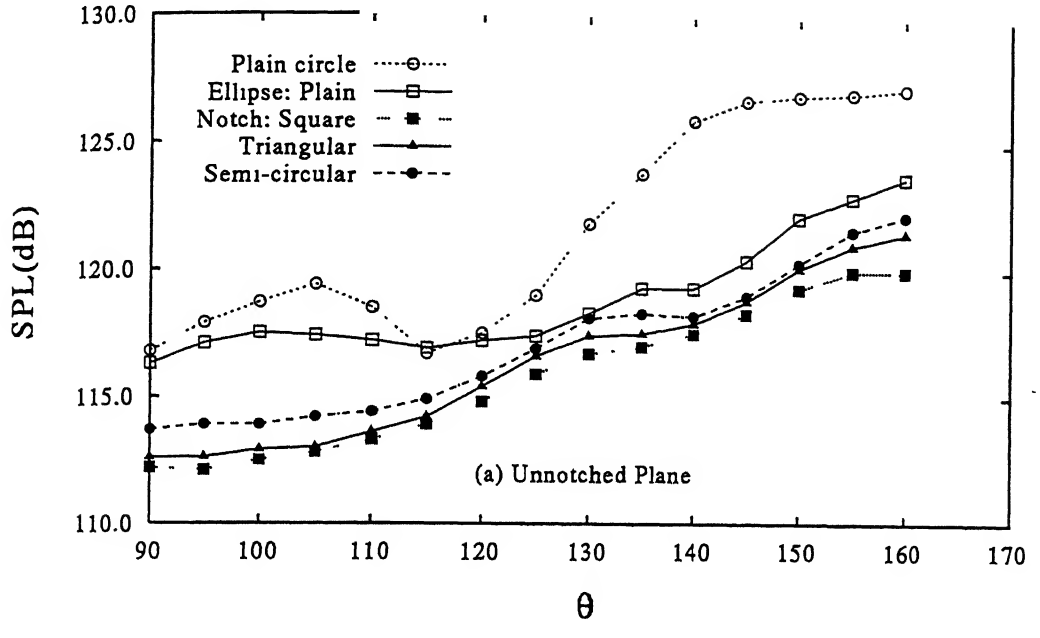

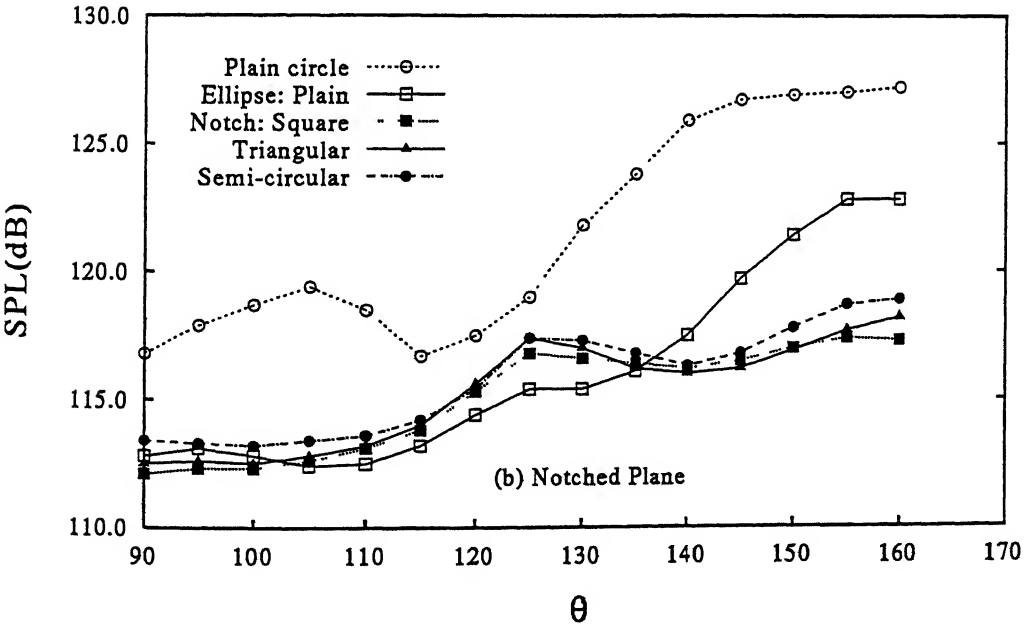

Figure 5.23: Radial directivity for plain and notched elliptic slot jets at M_j=1.5

total noise levels are dominated by shock-associated noise. Plain elliptic case shows a steady increase in shock-noise levels and for $\theta > 135^o$ dominates over the noise from notch jets. However,, for $\theta \geq 155^o$ it attains a uniform value. Notched jets, on the other hand, tend to attain a nearly uniform value for $\theta > 125^o$ and for $\theta = 160^o$ show significantly reduced shock-noise levels. At $\theta = 160^o$, plain ellipse shows a 4.5 dB reduction relative to plain circle while relative to plain ellipse square notch jets shows 5.5 dB reduction followed by triangular case with 4.5 dB and semi-circular case with 3.5 dB reduction.

In the major-axis plane, Fig. 5.23(a), some different trends are observed. Mixing noise levels in the forward quadrant show increased noise relative to minor-axis plane for plain ellipse. notch jets, however, show significant reduction in jet mixing noise(3-5 dB). In the forward quadrant, mixing noise for plain ellipse shows no preferred direction. But in the aft quadrant, relative significance of shock-noise is seen with steady increase in SPL. Cut-out jets show steady increase in shock-noise for $\theta > 105^o$ and reaches a maximum at $\theta = 160^o$. At the maximum observer angle, relative to plain ellipse, square notch jet shows a 4 dB reduction followed by triangular case with 2.5 dB and semi-circular case with 1.5 dB reduction.

In summary, therefore, it appears that the sound intensity of both turbulent mixing and shock-associated noise is relatively dependent upon the notch geometry and hence, the initial jet conditions and shear layer development. Further, major-axis sides radiate higher noise levels relative to minor-axis sides. And, finally the noise intensity is principally a function of jet pressure ratio. In other words, the sound field from jets is characterised by three basic parameters (i) Pressure ratio P_e/P_0 or level of underexpansion P_e/P_a (ii)the observer angle θ, and (iii) the slot perimeter variation(notch geometry) with same area as datum slot.

The total noise from underexpanded jets contains contribution from both mixing and shock-associated noise. Close to the jet exit, the total acoustic field is controlled by turbulent mixing noise and as the observer moves from the forward quadrant into the aft quadrant, the shock-associated noise becomes increasingly important relative to mixing noise levels. From the trends discussed above, it becomes evident that the contribution of shock-associated noise to the total noise is significant at (i) supercritical pressure ratios, (ii) large angles to the downstream jet axis.

5.3 Conclusions

A passive control of achieving near-field mixing enhancement in slot jets is demonstrated. Since mixing is initiated by introducing azimuthal and longitudinal instabilities at the exit plane, azimuthal instability in the form of non-uniform curvature variation, i.e. ellipse, and longitudinal instability in the form of notches is introduced in the exit geometry. These two instabilities result in the faster spread of the shear layer into the jet core. Favourable characteristics are induced by the introduction of sharp corners in the periphery of the slot. The conclusions on the basis of the observations made are the following:

- The plain elliptic-slot jet is observed to grow slowly along the major-axis plane with a simultaneous faster growth along the minor-axis plane. This is in conformation to earlier studies that elliptic jets undergo axis-switching phenomena.

- The sharp corners and flat sides of the notch greatly influence the jet growth in the notched plane[3]. Since same area is available for pressure relief, the higher jet growth in the notched plane intensifies the axis-switching phenomena thereby causing the jet to entrain more of ambient fluid towards the centreline.

- The square notch provides low velocity regions in the notched plane whereas the triangular notch about the notched plane in between the major and minor planes.

- The arrangement plays a vital role in inducing high rates of mixing throughout the jet field as seen from mass-flux ratio plots wherein the sharp cornered notched jet shows significant increase in m/m_e for all test conditions and hence, results in favourable jet characteristics.

- The presence of a sharp corner in the notch geometry induces higher mixing thereby showing drastic reduction in core-lengths. Notched elliptic jets show a drastic reduction of the core length followed by a faster decay for both P_e/P_a=1.0 and P_e/P_a=2.0.

- The angle of the notch corner seems to play a strong role in controlling the mixing characteristics in elliptic jets with the triangular notch showing minimum core-length and maximum decay.

- The square notched elliptic jet shows highest spread in both the minor-axis and major-axis side relative to the triangular and semi-circular notched elliptic jets. This higher spread is observed to be independent of the level of underexpansion. Spread in the major-axis side is not much affected.

- Relative to its plain counterpart, notches are seen to modify the initial shock-cell development. Additional expansion and compression waves are seen to emanate from the notches. The interaction of these additional waves with the evolving shear layers leads to appreciable changes in the shock structure. Also the thicker shear layers emanating from the corners help diffuse the shock structure faster[4]. The notched jet, as a result of the above combined effects, is seen to result in shorter shock-cells relative to the plain elliptic case.

- The variation of the average shock cell-length of both plain and notched jets with fully expanded jet Mach number, M_j, follows the trend predicted by Tam[113]. But the shorter cell lengths for notched cases may be due to the relatively faster diffusion of cells due to thicker shear layers emanating from the corners. Square notch shows the weakest of shocks in the jet core.

- The predicted screech tone frequency of plain and notched elliptic-slot jets closely follow Tam's theory. The deviation observed is due to complicated shock-shear layer interaction and secondary instabilities shed from the corners of the notch.

- The low velocity regions observed in the notched plane of elliptic slot jets seem to diffuse the shocks faster relative to plain jet. Further, these low velocity regions may also help to shield the shocks and act as silencers to noise radiation in these notched jets.

- Significant reduction in the high frequency broadband shock-noise is observed for ellipse indicating a relatively weaker cell-system relative to plain circular case.

- Notches are observed to result in reduction of both jet mixing and broadband shock associated noise relative to plain ellipse. Further, square notch shows maximum reduction in screech tone amplitude followed by triangular notched ellipse.

- The acoustic spectrum results indicates that the differences in the slot perimeter, provided by variation in notch configuration, may alter the acoustic emission characteristics of these

jets not only in the screech component but also in the turbulent jet-mixing and broadband shock noise. These differences point out the corresponding aerodynamic changes[76] brought in by notch introduction and its geometry. The significant differences existing in the jet mixing and broadband shock-noise radiated energy suggests that modification in the jet-noise source mechanisms and hence, the instability characteristics has occurred[76].

- The minor-axis side of plain ellipse radiates significantly lesser noise intensity relative to that along major-axis plane. This difference is primarily due to difference in jet spread and shock angles along the two planes.

- At $\phi = 90^o$, notches bring down the noise levels along the major axis plane thereby reducing the noise gap between the two planes. This suggests modifications in the shock-shear layer interaction, by notch presence, which affect the jets behaviour and hence, the noise emission characteristics in the two planes.

- At $\phi = 150^o$, significant reductions in broadband shock noise levels is observed for each notch geometry in the notched plane relative to plain case while the noise levels are approximately the same along major planes. The notches, therefore, seem to modify the shock-shear layer interaction and hence, the noise source mechanisms significantly in the notch planes of these jets.

- The presence of notches further brings down the shock-noise levels significantly in the major-planes of these jets. As much as 3dB to 4.5dB reduction is observed relative to plain ellipse and this results in the notch jets showing approximately no preferred direction of shock-noise in the two planes. The additional waves from the notches seem to circumferentially modify the downstream shock-structure development and hence, alter the acoustic emission of these jets.

- Spectra of plain and notch ellipse show significant reductions in screech tone amplitude presumably because the azimuthal curvature variation and the notch presence results in a non-symmetric shock-pattern and effects the feedback system which supports screech mode[16, 17].

- For observer angle greater than 110^o, all the jets show increase in shock-noise levels indicating that the directivity in the forward quadrant is primarily controlled by mixing

noise levels[26, 66], whereas in the aft quadrant the total noise levels are dominated by shock-associated noise.

Chapter 6

Effect of Aspect-Ratio

Effect of Aspect-Ratio on the Mixing and Noise Characteristics of Plain and Notched Elliptic Slot Jets

6.1 Introduction

In the preceding chapter we have discussed the results obtained by introducing a notch in a small aspect-ratio(2:1) elliptic-slot jet. Further, the effect of notch geometry on the mixing and noise characteristics of 2:1 elliptic jet was investigated. In the present chapter we are extending the investigation to 3:1 and 4:1, i.e., moderate aspect-ratio, elliptic-slot jets. The prime objective is to study the change in the mixing and noise characteristics as the aspect-ratio is increased from small to moderate values.

In literature, investigations have been independently carried out for 2:1[20], 3:1[21, 58] and 5:1[121] aspect-ratio elliptic jets. Previously Hussain and Husain[1] carried out a comparative study of aspect-ratio effect in the range 2:1 and 8:1. He observed that for a given equivalent diameter, the aspect-ratio is an important parameter controlling the deformation and topological changes, i.e., bifurcation, of large-scale vortical structures in elliptic jets, and that the dynamics of low aspect-ratio elliptic jets are basically different from that of jets of moderate to high aspect-ratios. In low aspect-ratio jets, the deformation as well as the self-induced inward and outward displacements of parts of elliptic structures are small[1] and as such there is a dominance of large-scale activity[5]. In higher aspect-ratio jets, the azimuthal deformations take longer time to evolve in the streamwise direction than in small aspect-ratio jets[5]. When the

distortions become appreciable the vorticity is already very diffused and hence, the entrained fluid induced by these diffused vortices would be much lesser[20]. As such there is a dominance of small-scale activity in higher aspect-ratio jets. And since, entrainment of mass-flow is primarily due to large-scale activity, a low aspect-ratio jet shows higher bulk mixing[20, 58]. In addition, the axis-switching location was found to be a linear function of aspect-ratio in elliptic[1] and rectangular[5] jets for the entire range of aspect-ratios studied. However, the jet aspect-ratio in the study of Krothapalli *et al*[5] were quite high; from 5 to 16. In this range of aspect-ratios, the jet behaves more or less like a two-dimensional jet[106, 5, 20].

When a jet is used for mixing purpose or for thrust augmentation, a large mass entrainment, especially near the nozzle, is desired. It was shown by Winant and Browand[41] that in two-dimensional flows, entrainment is dominated by vortex merging alone. However, in three-dimensional elliptic jets, entrainment is due to vortex merging and azimuthal deformation of vortices at the same time[20]. Also, it was observed by Wlezien and Kibens[17] that nozzles with intermediate origins generated non-circular vortices resulting in large entrainment. Thus, the asymmetry of these vortical structures is a technique or a means, active or passive, to enhance entrainment.

The present investigation is aimed at studying the effect of aspect-ratios, from lower to moderate range, i.e., 2:1, 3:1, 4:1, on the mean flow characteristics of elliptic slot jets. All the previous studies have been carried out for incompressible range[106, 40, 1, 5]. In this chapter we extend the study to fully expanded and underexpanded sonic free jets. Also, it has been reported in literature, that the initial development of the jet is largely dependent on the conditions at the nozzle exit flow[30, 106, 58, 4]. As such instability in the form of notches are introduced along the minor-axis side. This has been done, in particular, to enhanced mixing in that plane as has also been discussed earlier. The effect of aspect-ratio and notch geometry on the far-field noise of elliptic slot jets has also been carried out.

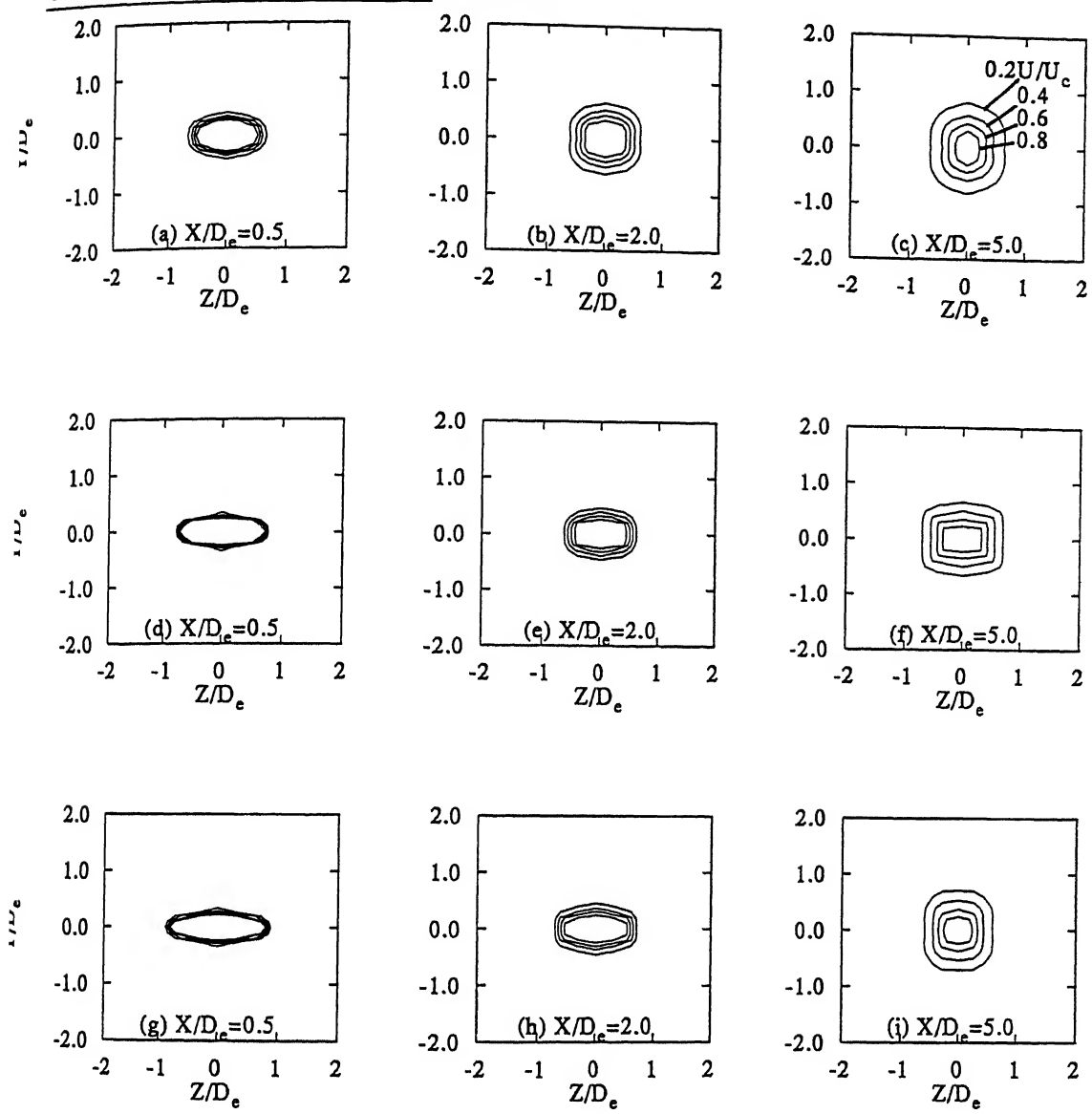

Figure 6.1: Iso-velocity contours for plain elliptic slot jets, M_j=1.0: (a)-(c) 2:1, (d)-(f) 3:1 and (g)-(i) 4:1

6.2 Results and Discussions

6.2.1 Iso-velocity Contours

Figures 6.1(a)-(i) show the iso-velocity contours for plain ellipse with varying aspect-ratio for the fully-expanded case. As observed by Hussain and Husain[1], the plain ellipse grows slowly initially along its major-axis side with simultaneous faster outward movement of the jet along the minor-axis side. Thus, a pumping action[1] starts bringing in ambient fluid towards the

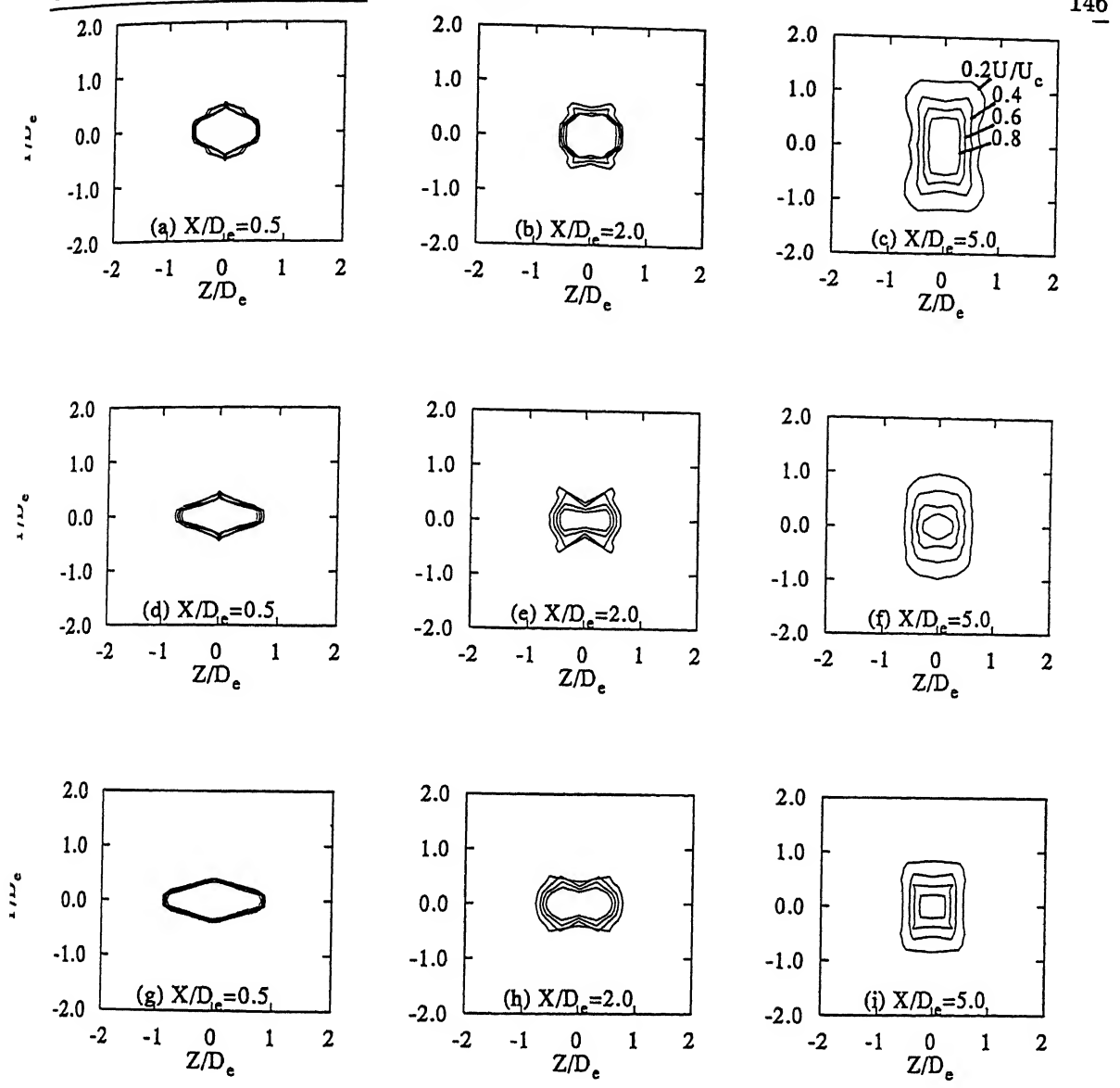

Figure 6.2: Iso-velocity contours for square notched elliptic slot jets, M_j=1.0: (a)-(c) 2:1, (d)-(f) 3:1 and (g)-(i) 4:1

jet-centreline along major-axis side and vice-versa along the minor-axis side, and hence initiating the axis-switching phenomena typical to non-circular jets. This axis-switching phenomena is responsible for higher mixing rates observed in non-circular jets. However, it has been reported[106, 20] that large entrainment is not observed in high aspect-ratio jets and suggested that the optimum value is between 2:1 and 3:1. This fact is evident in the entrainment comparison plots discussed later.

A comparison of the iso-velocity contours at the same axial stations for the plain and square notched jets very clearly indicates the effect introduced in the flowfield by the presence of notches in each aspect-ratio, Figs. 6.1(a)-(i) and 6.2(a)-(i). The physics for this peculiar flowfield in the notched jet lies with the presence of azimuthal instability in the form of sharp corners of the notches and its flat sides as discussed in the preceding chapter on small aspect-ratio jets. It is seen from the contour plots that the 2:1 square notched jet switches axis earlier. Keeping in mind that a smaller spacing between the velocity contours indicates lesser entrainment into the jet and vice-versa, it is observed that as the jets grow in the downstream direction the spacing between the contours for 2:1 case is higher than that for 3:1 and 4:1 jets at X/D_e=5.0. This indicates that the 2:1 square notched elliptic jet entrains more of ambient fluid followed by 3:1 and 4:1 square notched jets.

Let us now try to understand the physics behind this peculiar behaviour of jets as aspect-ratio is increased. It is well known that in low aspect-ratio jets, there is a dominance of large scale activity[5, 20]. And since entrainment of mass-flow is due to large-scale activity, a low aspect-ratio jet shows higher bulk mixing. Now a discontinuity introduced in 2:1 jet in the form of a sharp cornered notch greatly influences the uniform growth of vortices in that plane This effect, however, is reduced as the aspect-ratio is increased to 3:1 jet and finally, to 4:1 jet where it is not seen at all, Figs. 6.1 and 6.2. Since for 3:1 and 4:1 cases, the deformations take relatively longer to evolve the effect of notch does not seem to be as strong as in 2:1 case. Further, the disturbance introduced by the notch in 3:1 jet seems unable to influence the the complete jet growth as the major-axis ends are far off relative to 2:1 case. Also with increasing aspect-ratio, the sharper curvature at the major-axis side seems to contribute to the small-scale activity due to higher azimuthal deformations. These effects delay the azimuthal deformations typical to relatively higher aspect-ratio jets[5]. For 4:1 jet the effect is more pronounced, relatively, so that there is a dominance of small-scale activity from both notch effect(XY-plane) and higher curvature of major-axis side(XZ-plane) as a result of which the jet shows a uniform growth in YZ-plane at X/D_e=2.0, Fig. 6.2(h). Since small-scale activity helps in shielding the shock-associated noise of underexpanded jets and hence, act as silencers[8], 3:1 and 4:1 jets are expected to show considerably lower OASPL than 2:1 jet which, relative to 3:1 and 4:1 jets, have a dominance of large-scale activity as will be seen later.

Figure 6.3(a) shows the effect of aspect-ratio on the entrainment at M_j=1.0 for plain ellipse.

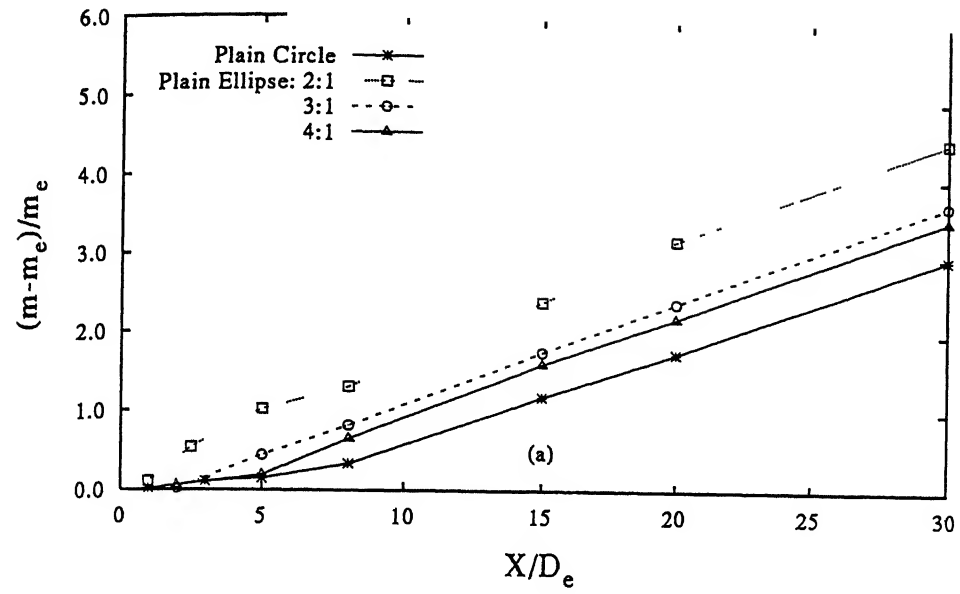

Figure 6.3(a)-(b): Entrainment comparison with aspect-ratio for plain and notched elliptic slot jets at M_j=1.0

In these plots 'm' is the local mass-flux and 'm_e' the mass-flux at the slot exit. For the sake of comparison, entrainment for plain circle is included showing the advantage of using non-circular exit geometries for the purpose of enhanced mixing. The 2:1 elliptic jet shows a significant increase in entrainment relative to plain circular jet. At $1.0D_e$, the increase is 30 percent which goes upto 100 percent at $8.0D_e$(40 percent at $30.0D_e$). Mass-flux ratio of 2:1 jet is followed by 3:1 and 4:1 jet with 3:1 showing slightly higher value than 4:1 jet. All the elliptic cases show

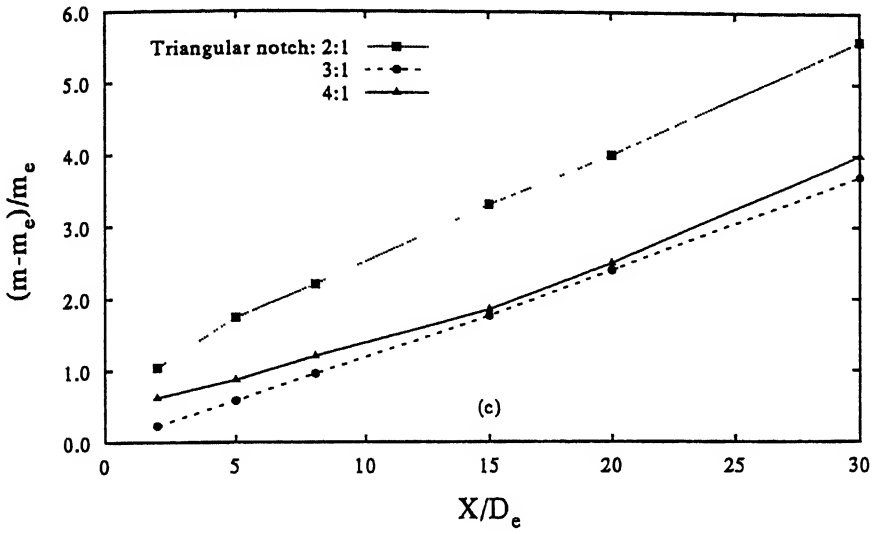

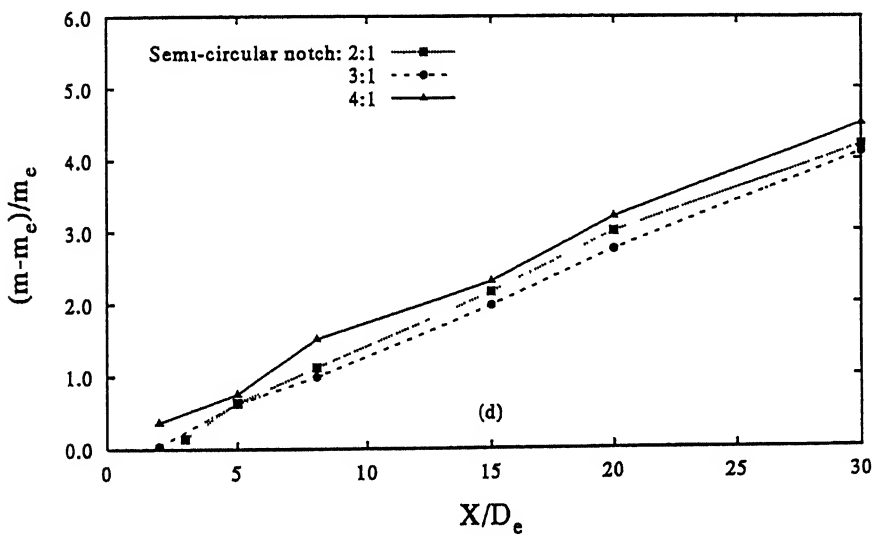

Figure 6.3(c)-(d): Entrainment comparison with aspect-ratio for plain and notched elliptic slot jets at M_j=1.0

higher entrainment than plain circular jet. The decrease in entrainment with increase in aspect-ratio may be attributed to the fact that as the aspect-ratio increases, the azimuthal deformations take longer to evolve in the streamwise direction and by the time they become appreciable, the vorticity has already diffused[106, 5]. The entrained fluid induced by these diffused vortices would be much less and hence, a large mass entrainment was not observed[1] relative to 2:1 elliptic jet.

Let us now study the effect introduced by discontinuities in the form of notches, independ-

ently on aspect-ratio as seen in Figs. 6.3(b)-(d). For square notch, the trend remains the same, with 2:1 showing the maximum value followed by 3:1 and 4:1. For triangular case, the trend is 2:1 jet followed by 4:1 and 3:1, with 4:1 and 3:1 showing approximately the same values. And finally, semi-circular notch, for which it is observed that this notch configuration effects the mass-flow characteristics significantly for elliptic jets. Here, 4:1 jet shows the maximum entrainment followed by 3:1 and 2:1 which do not exhibit any significant difference in values. From the above observations it can be concluded that absence of a sharp corner in a notch seems to be beneficial for mixing characteristics of 4:1 elliptic jet. This notch configuration seems to hasten the azimuthal deformations which are otherwise delayed in high aspect-ratio plain elliptic jets. Similarly an acute angle or a sharp corner in the geometry seems to be advantageous for 2:1 jet and square notch or two sharp corners in 3:1 elliptic jet. Thus, each notch shape seems to initiate the azimuthal deformations in a particular aspect-ratio jet.

Thus, it is clear that the shape of the notch geometry has a strong influence in controlling the mixing characteristics in different aspect-ratio elliptic jets.

6.2.2 Flow Visualization and Shock-Structure

At underexpanded condition, the shock-cells formed by the expansion/compression wave structures inside the jet core were visualized by shadowgraph photography. Pictures 47-49(Fig. 6.4), 51-53(Fig. 6.5), and 55-57(Fig. 6.6) show these shock-structures for underexpanded plain elliptic-slot jets at an equivalent Mach number, M_j=1.5, for aspect-ratios 2:1, 3:1 and 4:1, respectively. For all aspect-ratios, due to azimuthal curvature variation, the angles of oblique shocks and expansion fans are different in the two planes of the jet thereby generating a non-symmetric structure of shock-cells in the two planes. As such the flow changes direction in a non-symmetric pattern along the two planes[21]. The diffusion of shock cells depends upon how fast the mixing region surrounding the cellular pattern grows downstream of nozzle exit plane[4] which in turn depends upon the local radius of curvature of the two planes[122]. For 2:1 ellipse up to 5 shock-cells are discernible in both planes, Fig. 6.4(Pics. 47-49) whereas, four can be seen for 3:1, Fig. 6.5(Pics. 51-53) and only three shock-cells are discernible for 4:1 elliptic slot jet, Fig. 6.5(Pics. 55-57). This itself is an indication that the shock-strength increases with aspect-ratio so that lesser cells are observed for higher aspect-ratio jet relative to lower aspect-ratio jet. However, the shocks beyond the first cell in the minor-axis plane are

Figure 6.4(a): Shadowgraph picture showing the shock development pattern in the major-axis side of 2:1 plain elliptic slot jet; M_j=1.5

Figure 6.4(b): Shadowgraph picture showing the shock development pattern in the minor-axis side of 2:1 plain elliptic slot jet; M_j=1.5

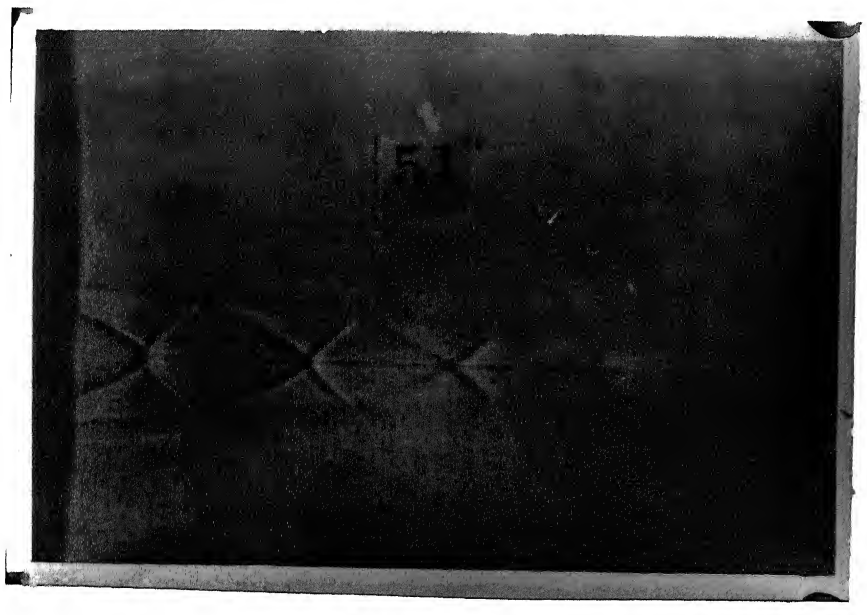

Figure 6.5(a): Shadowgraph picture showing the shock development pattern in the major-axis side of 3:1 plain elliptic slot jet; M_j=1.5

Figure 6.5(b): Shadowgraph picture showing the shock development pattern in the minor-axis side of 3:1 plain elliptic slot jet; M_j=1.5

Figure 6.6(a): Shadowgraph picture showing the shock development pattern in the major-axis side of 4:1 plain elliptic slot jet; M_j=1.5

Figure 6.6(b): Shadowgraph picture showing the shock development pattern in the minor-axis side of 4:1 plain elliptic slot jet; M_j=1.5

obscured by turbulence relative to cells in the major-axis plane. This difference in the diffusion of cells in the two planes is related to the different jet modes predominant in each plane[124]. It has been observed by Gutmark*et al*[124] that flapping motion of jet, which is responsible for higher spread and subsequent faster diffusion of cells, is prevelant along the minor-axis plane for $M_j > 1.15$, while the jet motion along major-axis plane is symmetrical with lower spread. Further, the azimuthal deformations are higher for higher aspect-ratio jets so that the vortical structures diffuse faster as they are closer to the jet centreline along the minor-axis side[1]. As such there is a dominance of small-scale structures, relative to small aspect-ratio jets which results in thicker shear layers and hence, faster diffusion of cells. This fact was also observed in entrainment plots where small aspect-ratio jets show higher entrainment.

Another interesting observation is that the shape of the first shock-cell changes with aspect-ratio. As aspect-ratio increases from 2:1 to 3:1, the angle of the oblique shocks, Fig 6.4(a)(Pic. 47) is gradually seen to increase(with reference to upstream direction) so that for 3:1 case a Mach disk begins to form at the centreline region, Fig 6.5(a)(Pic. 51) which becomes more prominent for 4:1 ellipse, Fig. 6.6(a)(Pic. 55). The flow immediately downstream of the Mach disk is subsonic[129]. Since the surrounding flow in the oblique shock region remains supersonic. A slip line exists at the boundary between the two concentric regions[129] as is observed in the major-planes of 3:1 and 4:1 jets, Fig. 6.5(a)(Pic. 51) and Fig. 6.6(a)(Pic. 55). This change is also observed along the minor-axis plane where the diamond shape at the end of first shock-cell for 2:1 jet is gradually replaced by a single shock in 4:1 jet, Figs. 6.4, 6.5 and 6.6(b)(Pics. 49, 53, 57). In small aspect-ratio jets, the active large-scale activity which helps to have increased mixing makes the entrained mass to penetrate faster towards the jet axis thereby making the shocks to cross-over exhibiting a point junction at the jet axis, Fig. 6.4(a)(Pic. 47). Whereas for large aspect-ratios, the entrained mass through large-scale structures get diffused rather than getting fragmented into small vortices[1]. Therefore, the penetration of the entrained mass towards the jet axis is rather slower compared to small-aspect ratio jets. This process results in large portion of the potential core to propagate downstream unaffected. This results in the emergence of Mach disk structure at the end of the first cell.

Gutmark *et al*[124] in their experiments on 3:1 elliptic jets observed that with Mach disk formation, the noise emission characteristics undergo a reversal with minor-axis plane showing higher noise levels and noise source located near the Mach disk while no source could be located

on the major-axis plane. This suggests that the noise source mechanisms are greatly modified as the aspect-ratio is increased for a particular underexpanded condition and hence, drastically changes the noise characteristics in the two planes, relative to small aspect-ratio elliptic jets.

The presence of notch further modifies the downstream shock-development process. Pics. 63-65(Fig. 6.7), 67-69(Fig. 6.8), 71-73(Fig. 6.9) show the shadowgraph pictures for 2:1, 3:1 and 4:1 jets with square notch placed along the minor-axis sides. Relative to their plain cases, additional expansion and compression waves are seen to emanate from the notches. The interaction of these additional waves with the existing waves leads to appreciable changes in the shock-structure development. In the major-plane for 4:1 notch jet, Fig. 6.9(a)(Pic. 71), the interaction of the additional waves from the notch are observed to alter the angle of the oblique shock at the end of the first cell which slightly reduces the lateral extent of the Mach disk(Pics. 55, 71), Fig. 6.6(a) and Fig. 6.9(a). As such more cells are discernible for notch case indicating reduction in Mach disk strength. Similarly in the minor-axis plane of 4:1 notch jet, some additional waves are discernible in the first and second cell, Fig. 6.9(b)(Pic. 73) while no such thing is observed for 4:1 plain jet(Pic. 57). Further, different notch geometries are observed to cause different modifications in the shock development process in each aspect-ratio jet so that the noise from jets with different notch configuration will result in varying noise characteristics.

Figure 6.10 shows the centerline pressure decay plots for the cases investigated at underexpansion level of 2.0, i.e., M_j=1.52. The oscillations in the data in the upstream regions are due to the stationary shock structure in the jet. In the supersonic regions of the flow, the measured pitot pressure P_{t2} corresponds to the total pressure behind the standing bow shock in front of the pitot probe. In a steady supersonic flow with a single normal shock ahead of the pitot tube, a sharp drop in P_{t2} followed by a rise signifies the presence of a stronger shock wave[18]. The data presented is, therefore, accurate enough to capture the overall features ; e.g, the number of shocks and their spacing etc.[12]. Figure 6.10(a) shows the plot for plain elliptic jets. It is seen from the second, third and fourth shock cells, that the shock strength and spacing for 3:1 and 4:1 ellipse is reduced relative to 2:1 jet. Finally, the jet decay, after the end of the core is maximum for 4:1 jet followed by 2:1 and 3:1 cases, showing better mixing for higher aspect-ratio jets.

Figure 6.10(b) shows the plot when square notch is introduced in the range of aspect-ratios

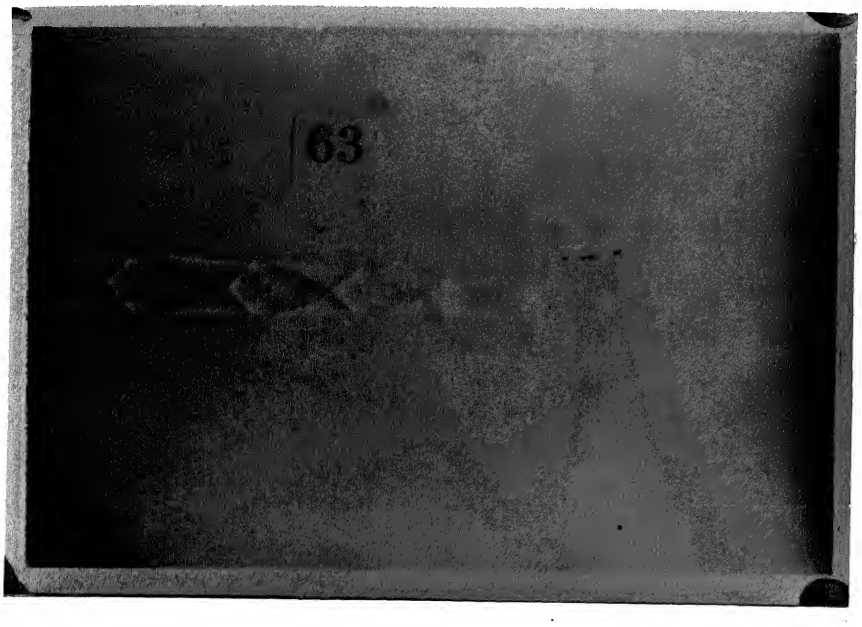

Figure 6.7(a): Shadowgraph picture showing the shock development pattern in the unnotched/major-axis plane of 2:1 square notched elliptic slot jet; M_j=1.5

Figure 6.7(b): Shadowgraph picture showing the shock development pattern in the notched/minor-axis plane of 2:1 square notched elliptic slot jet; M_j=1.5

Figure 6.8(a): Shadowgraph picture showing the shock development pattern in the unnotched/major-axis plane of 3:1 square notched elliptic slot jet; M_j=1.5

Figure 6.8(b): Shadowgraph picture showing the shock development pattern in the notched/minor-axis plane of 3:1 square notched elliptic slot jet; M_j=1.5

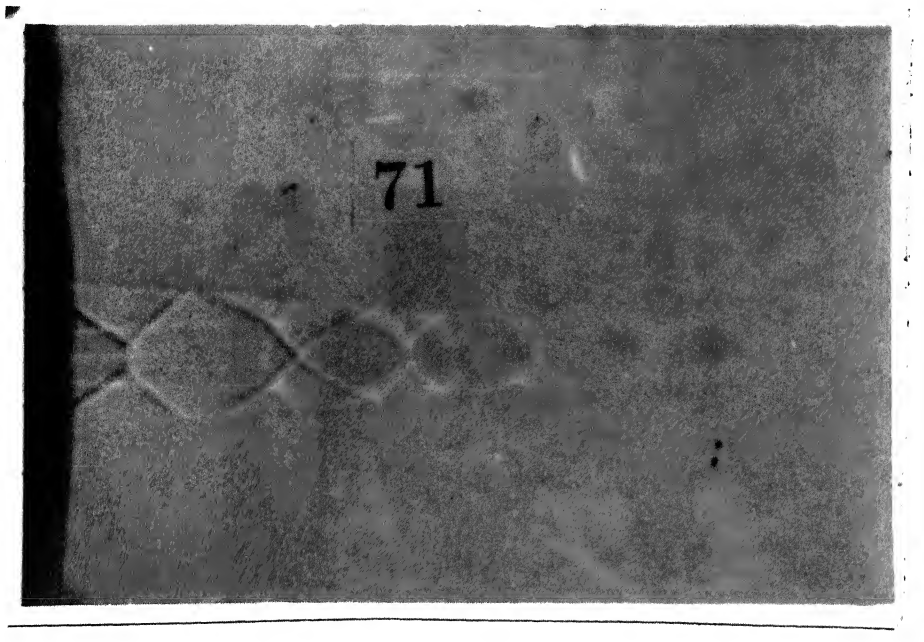

Figure 6.9(a): Shadowgraph picture showing the shock development pattern in the unnotched/major-axis plane of 4:1 square notched elliptic slot jet; M_j=1.5

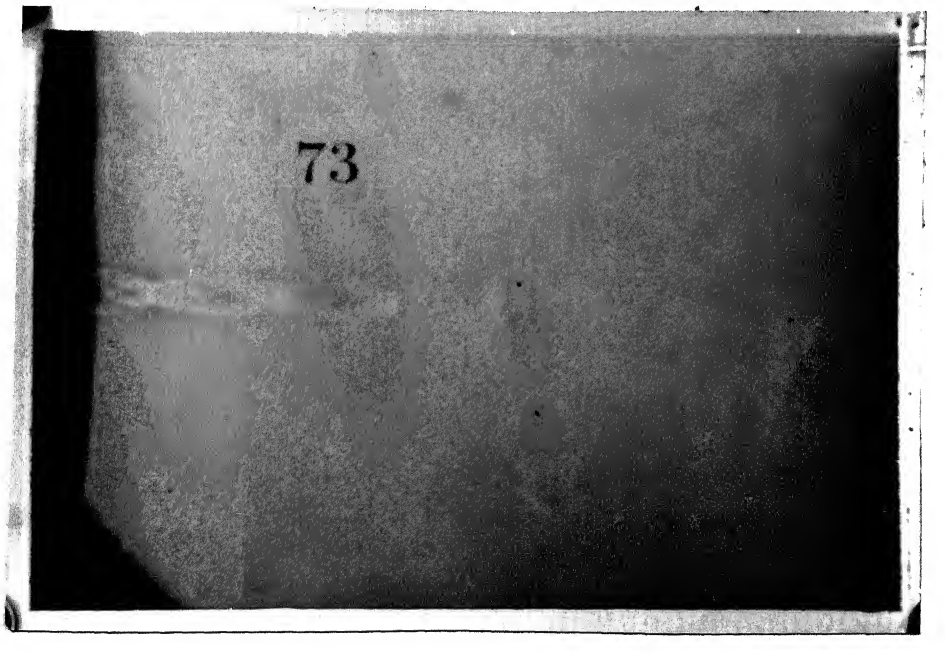

Figure 6.9(b): Shadowgraph picture showing the shock development pattern in the notched/minor-axis plane of 4:1 square notched elliptic slot jet; M_j=1.5

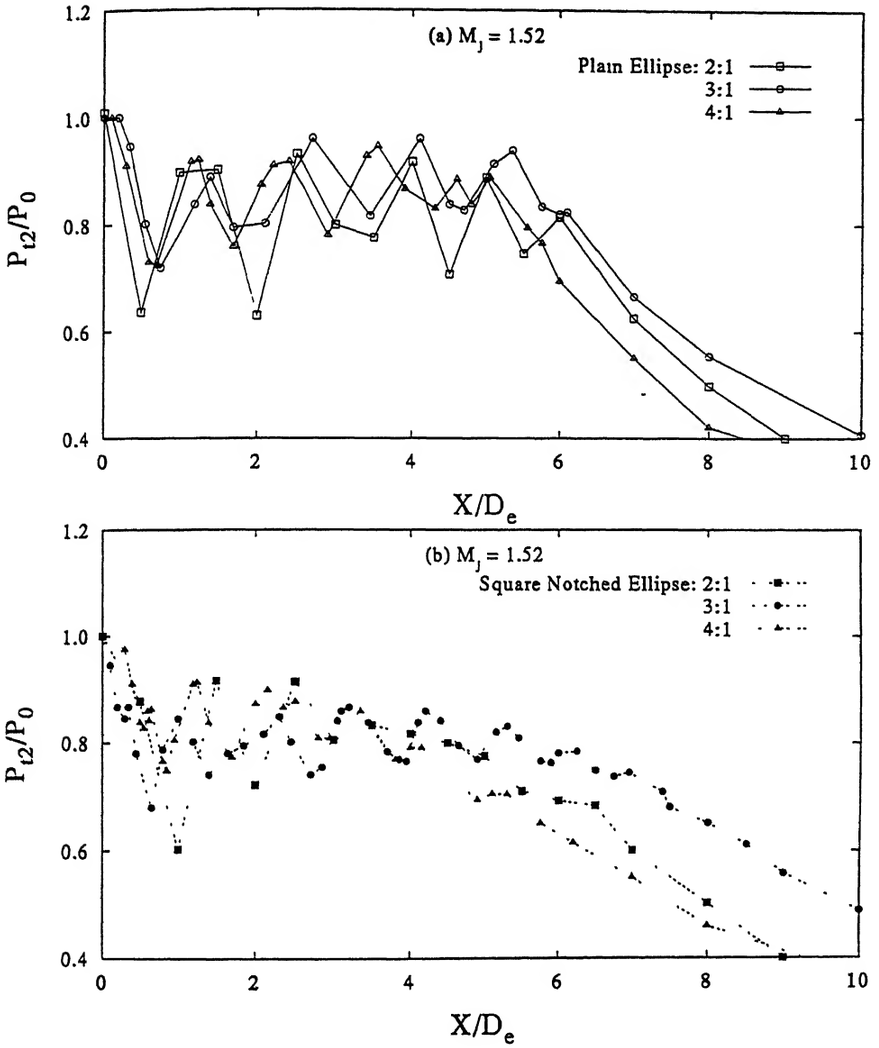

Figure 6.10: Effect of aspect-ratio on the shock strength of underexpanded elliptic slot jets, M_j=1.5

studied. Since all the notched jets showed similar reduction in shock strengths after the first cell, only the case of square notched jets is discussed here. A comparison with plain jets in Fig. 6.10(a) clearly indicates that for first cell, the notched cases show higher shock strength. This is mainly because of the pressure relieving effect of notches as pointed out by Powell[30]. As a result the shock strengths thereafter for all aspect-ratios are reduced relative to plain cases resulting in shorter core-lengths for each aspect-ratio. Relative to its plain case, 4:1 notched jet shows considerable reduction in shock strength for third and fourth cells. Further, a very fast

decay of centreline pressure is observed for triangular notched jets indicating(Fig. not shown here) that the higher intensity of small-scale mixing of the triangular notch persists even at underexpansion. Thus, if high level of fine-scale mixing is desired close to the exit at both full expansion and underexpansion, triangular notch is preferable in elliptic jets. This arrangement is also good for noise reductions. However, better noise reduction is attained by weaker shocks and so square notch should be preferred at the expense of a reduced fine-scale mixing close to the exit relative to the triangular notch case.

6.2.3 Shock-cell Length and Screech Tone

The third and fourth shock-cells have long been known to be the main source of shock-associated noise[50, 104, 18, 67, 33]. Also, choked jet-noise and hence, the screech frequency are primarily dependent on the length of these shock-cells and hence, on the strength of these shocks in the shock-cell system[16, 18]. Therefore, the effect of notch on the length of third and fourth shock-cells for the present cases was investigated. Figure 6.11 shows the variation of L_{avg}/L_a Vs M_j. Here, L_{avg} is the average shock-cell length(up to four cell-spacings) and L_a the semi-major axis length of the plain case for each aspect-ratio. This respective value of L_a is also used for non-dimensionalising the average shock-cell length of the notched ellipse of each aspect-ratio and hence, is referred to as the equivalent semi-major axis length. For comparison, Tam's theory[113] for 2:1, 3:1 and 4:1 elliptic jets is included. It can be seen clearly from Figs. 6.11(a)-(b) that for all the aspect-ratios both plain and notched elliptic jets agree fairly well with Tam's theory[113] though the curves for the present case lie below it. Reduction in average shock-cell length is apparent for notched cases from Figs. 6.11(a)-(b). However, for better comparison Fig. 6.11(c) is plotted which shows the effect of aspect-ratio on shock-cell length reduction. It is seen that for M_j=1.15, plain jet shows a shorter L_{avg}. However, as the Mach number increases, L_{avg} for notched jets show a considerable reduction that reaches a maximum at M_j=1.52. The 3:1 plain jet shows approximately same L_{avg} value as that of the notched case upto M_j=1.32 after which 3:1 notched jet starts to show a reduction. However, 4:1 notched jet shows a considerable reduction in L_{avg} from M_j=1.15 onwards upto the highest value of M_j. Also 4:1 notched jet shows a maximum reduction in L_{avg} at M_j=1.32. For 2:1 and 3:1 notched jets, maximum reduction is observed at M_j=1.52.

Figure 6.12(a)-(c) shows a plots of predicted Strouhal number(fL_a/U_j) of the screech

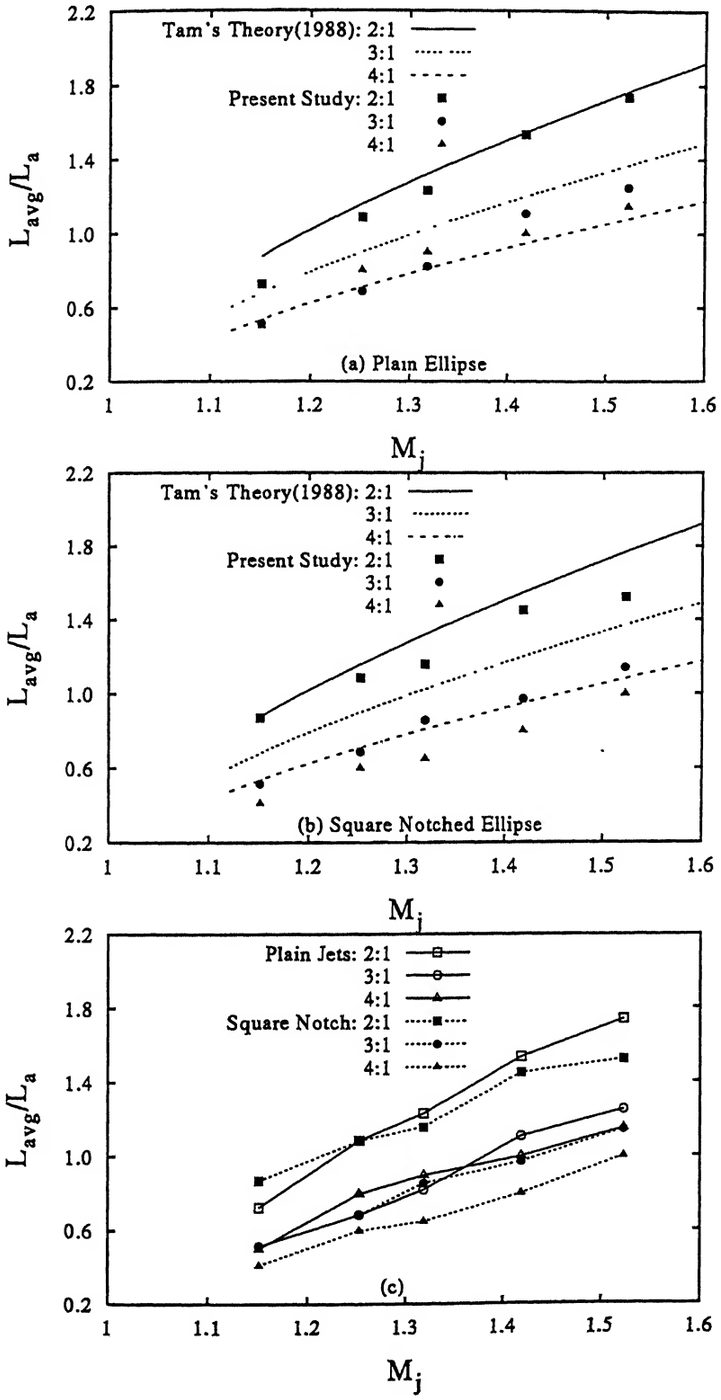

Figure 6.11: Average shock cell variation with M_j showing the effect of aspect-ratio

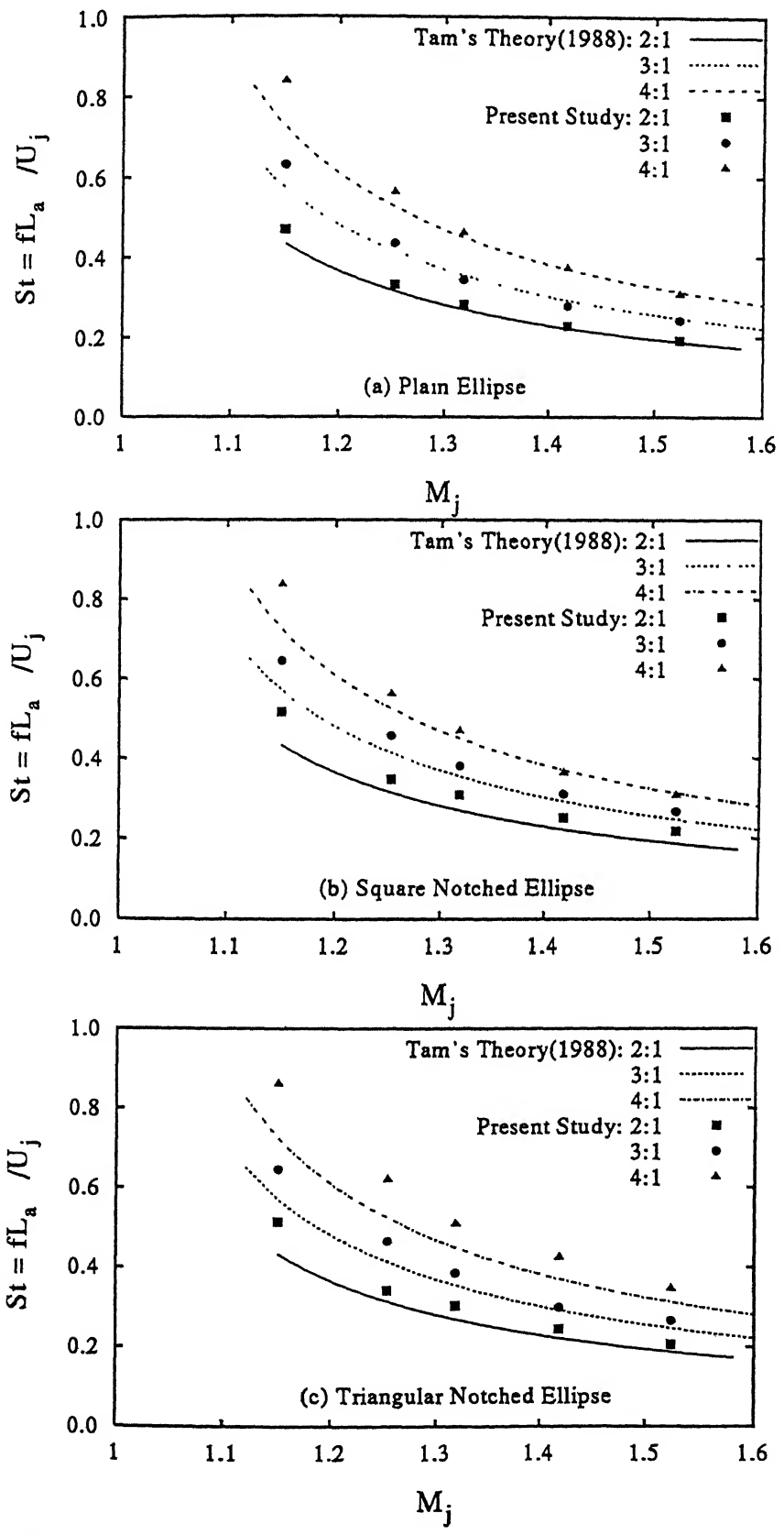

Figure 6.12: Strouhal number variation with M_j showing the effect of aspect-ratio

tone versus the fully expanded Mach number M_j. As the Mach number increases, the Strouhal number of screech decreases. This decrease is due to the increase in shock-cell spacing with Mach number, which causes an increase in the screech wavelength and consequently a decrease in screech frequency[110]. In the calculation of predicted Strouhal number, the average shock-cell length, L_{avg}, was considered up to four shock cells at different underexpanded levels. This value of L_{avg} was used in the screech tone frequency formula obtained by Tam *et al*[95] in conjunction with Tam's formula[113] for shock-cell length of elliptic jets with aspect-ratio less than four. In Figs. 6.12(a)-(c), Tam's analytic solution[95] of the screech Strouhal number versus M_j for elliptic jets of aspect-ratios 2:1, 3:1 and 4:1, is also shown for comparison of our present work with Tam's theory. The present work shows good agreement with Tam's analytic solution for the aspect-ratios investigated with the points following the same trend though they lie a little above it. Since with increasing M_j, an increase in Strouhal number relative to other cases indicates decrease in shock-cell spacing[110], the plots clearly indicates that the shock-cell spacing decreases with increasing aspect-ratio.

6.2.4 Aeroacoustic Characteristics

Acoustic Spectrum Analysis

A survey of the far-field shock-associated noise was conducted to investigate the change in spectral characteristics with variation in aspect-ratio of plain and notched elliptic-slot jets. The measurements were made only in the minor-axis/notched plane of jets. Typical frequency spectrum of the far-field signal at $\theta = 150^o$, for plain elliptic slot jets operating at pressure-ratio of 3.86 corresponding to an equivalent Mach number M_j=1.5 is shown in Fig. 6.13(a)-(c). This pressure-ratio corresponds to the maximum screech sound radiation[67]. The abscissa is the frequency in kHz and the ordinate is the sound power in decibels(dB). Further, the measurements were made only in the notched plane. From the frequency spectrum of each aspect-ratio jet, a principal discrete frequency peak referred to as *screech* is discernible. However, the amplitude of this fundamental screech is observed to vary with aspect-ratio. The spectrum of 2:1 jet shows a peak in the fundamental screech frequency which increases significantly for 3:1 and 4:1 plain elliptic jets. This may be due to the emergence of Mach disk in 3:1 and 4:1 jets as seen in shadowgraph photographs(Pics. 47, 51, 55) which drastically changes the noise field along minor-axis plane[124] relative to small aspect-ratio jet. For 4:1 jet,

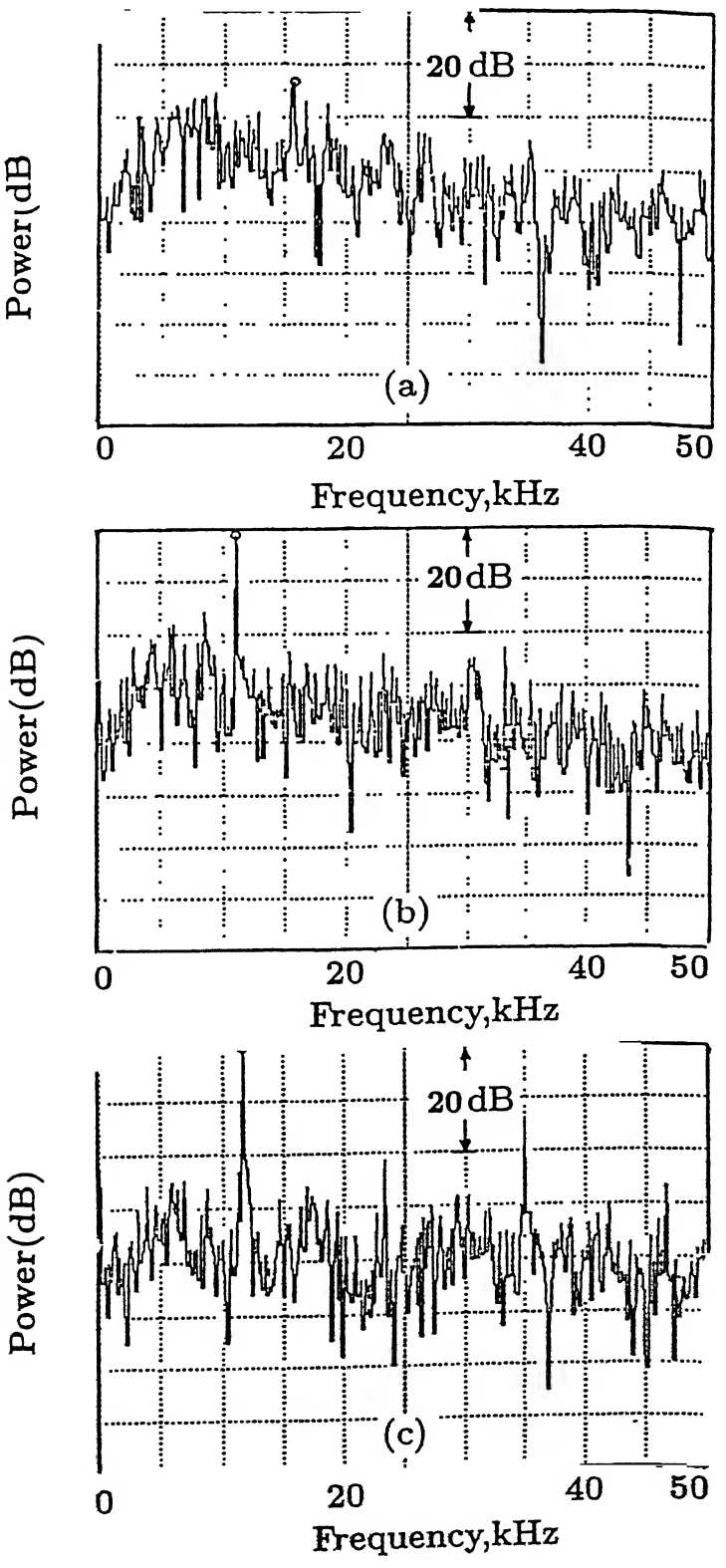

Figure 6.13: Far field spectral characteristics for plain elliptic slot jets at M_j=1.5; (a) 2:1 (b) 3:1 (c) 4:1

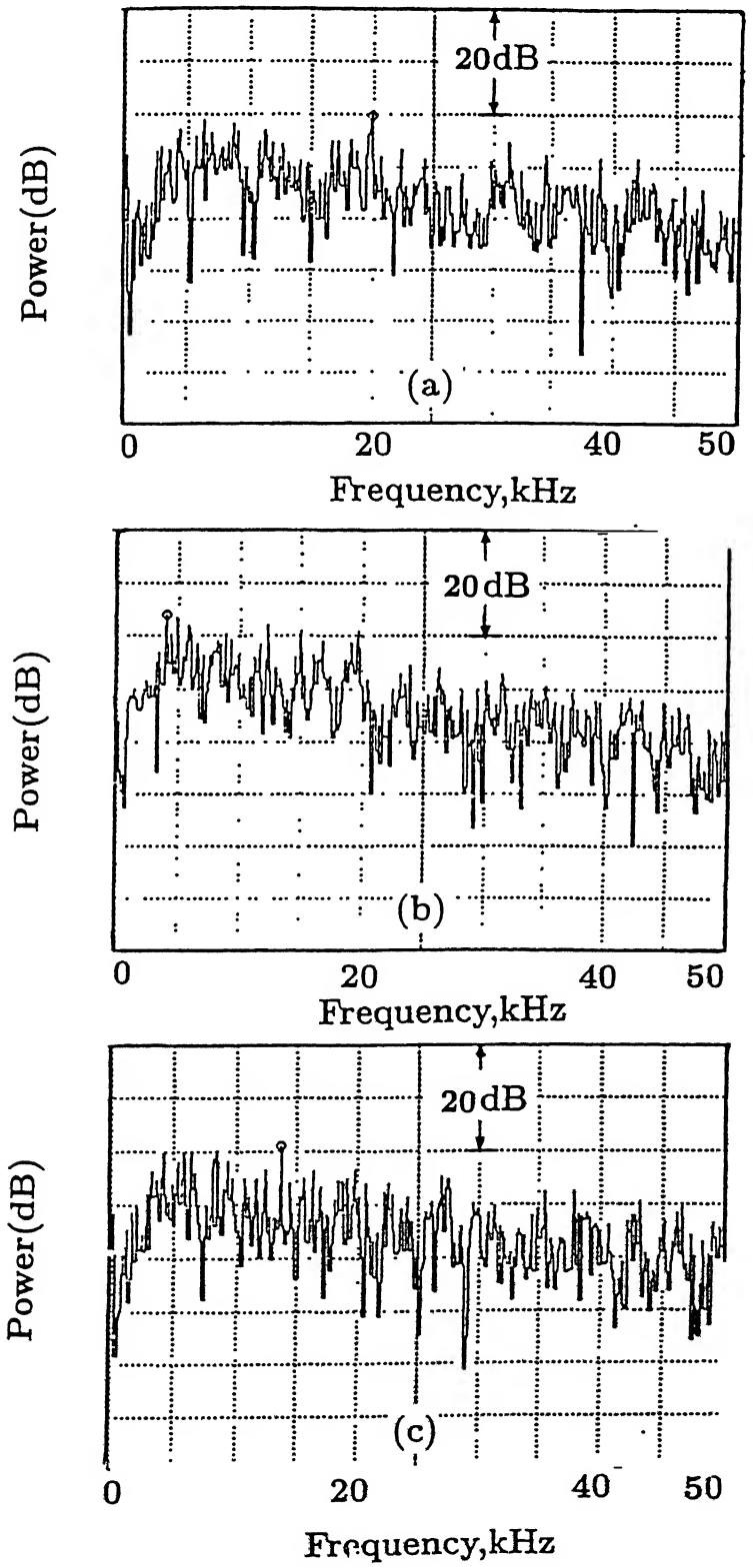

Figure 6.14: Far field spectral characteristics for triangular notched elliptic slot jets at M_j=1.5; (a) 2:1 (b) 3:1 (c) 4:1

second(23.5 kHz) and third(35 kHz) harmonics of the screech frequency are also observed, Fig. 6.13(c).

Further, the jet mixing noise, which dominates the low frequency content of total jet noise, is seen to decrease with increase in aspect-ratio. This may be due to the fact that the mixing noise generation process is closely linked to the characteristics of large-scale instability waves of the jet[118]. The increase in aspect-ratio, therefore, seems to change the instability process that results in reduced far-field noise in the minor-axis sides of these jets. Further, since the broadband shock-associated noise is generated by the interaction of these instability waves in the shear layer of the jet and the shock-cell structure[118, 32, 33, 95], a change in the instability process with aspect-ratio suggests corresponding changes in the far-field radiation of shock-associated noise. A slight decrease in the high-frequency jet noise in the near vicinity of the fundamental screech tone is also observed with increase in aspect-ratio.

The spectral characteristics of each aspect-ratio jet with triangular notch presence are illustrated in Figs. 6.14 (a)-(c). It is observed that the notch presence drastically reduces the amplitude of the fundamental screech frequency for each aspect-ratio, relative to their plain cases, Fig. 6.13. The 2:1 jet shows a 5 dB reduction in amplitude of fundamental component followed by 3:1 case with 15 dB and finally, 4:1 jet with 19 dB reduction. This may be due to modifications in the downstream shock-structure development as observed from the shadowgraph pictures of notched jets(Pics. 63, 67, 71) which weakens the shock-strength.

The differences observed in the spectral characteristics of plain and notched jets with aspect-ratio suggests that the presence of notch alters the acoustic emission characteristics in each of these jets. Since the instability process seems to vary with aspect-ratio, the same notch configuration in different aspect-ratios(which also alters the downstream shock development) seems to weaken the feedback process, thereby drastically reducing the screech amplitudes.

Overall Sound Pressure Results

It has been observed that the variations related to azimuthal curvature of exit geometry changes the jet behaviour at different regions around its circumference and hence, affects the flow instability characteristics[122, 76] along different planes. Further, the variation in shear layer thickness along the circumference effects the downstream shock development[4] and eventually the jet noise characteristics[122, 4, 16, 2]. Since aspect-ratio variation drastically changes the

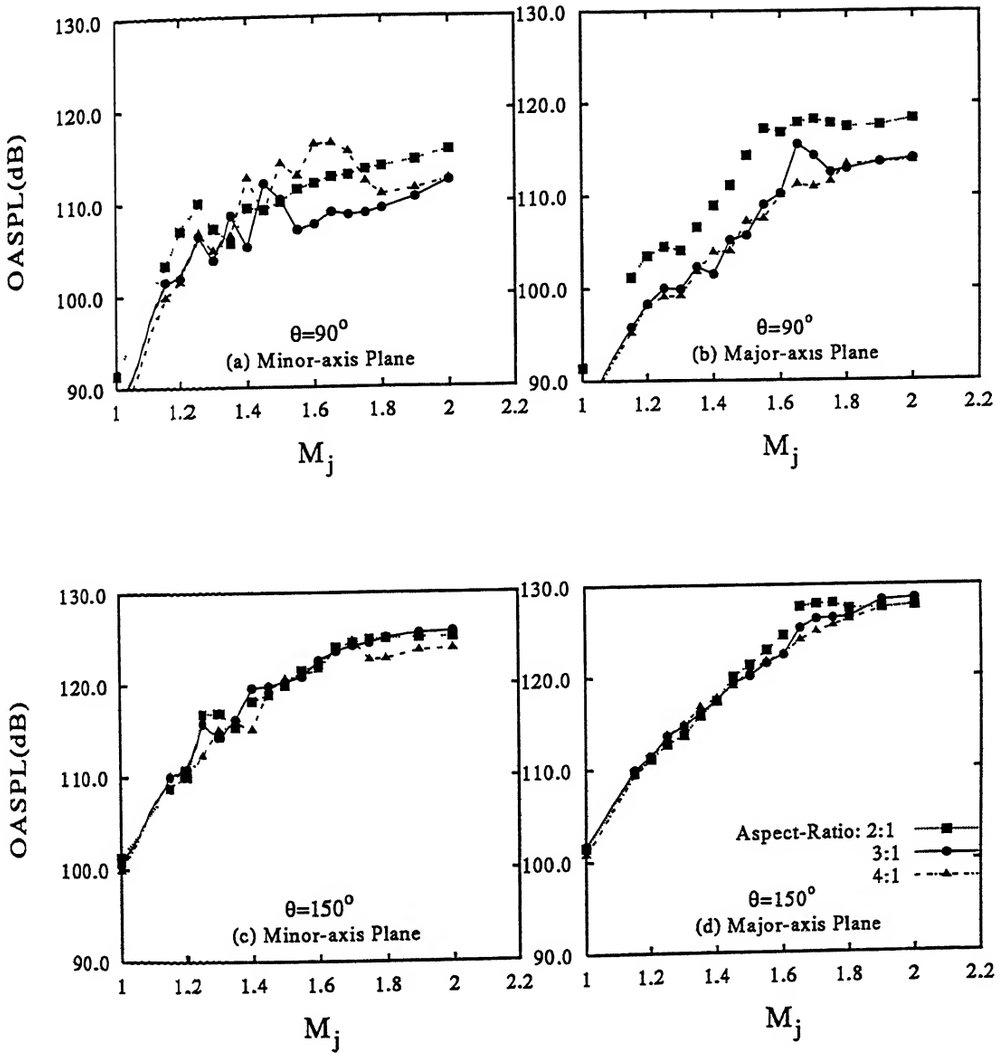

Figure 6.15: Overall sound pressure level variation with M_j showing the effect of aspect-ratio for plain elliptic slot jets

local radius of curvature of elliptic jets along major and minor-axis planes, difference in noise characteristics with aspect-ratio in the two planes are expected.

Figures 6.15(a)-(d) illustrate the far-field noise characteristics of underexpanded plain elliptic-slot jets with variation in aspect-ratio for two observer angles, $\theta = 90^o, 150^o$ to upstream jet axis to study the jet mixing and broadband noise characteristics. At $\theta = 90^o$, in both the planes, 2:1 jet shows higher mixing noise levels relative to 3:1 and 4:1 jets as was also observed in spectral plots. In the minor-axis plane, Fig. 6.15(a), both 3:1 and 4:1 jets show

fluctuating OASPL values up to M_j=1.7 after which they show a clear trend. At M_j=2.0, relative to 2:1 case, 3:1 and 4:1 jets show 3.5 dB to 5 dB reduction in jet mixing noise along minor and major-axis planes, respectively.

The possible cause for this change in mixing noise levels may be that as aspect-ratio is increased, the azimuthal deformations along major-axis increase which cause the vortical structures to diffuse faster as these structures are close to the jet centreline along the minor-axis side[1]. This suggests that in higher aspect-ratio jets, the shear layers are thicker near the nozzle exit, relative to small aspect-ratio jets due to dominance of small-scale activity and hence, such jets show reduced mixing noise levels. This fact was also observed from shadowgraph pictures where lesser number of shocks are discernible as aspect-ratio is increased suggesting thicker shear layers in high aspect-ratio jets.

For observer angle, $\theta = 150^o$, however, some different trends are observed, Figs 6.15(c)-(d). In both the planes, all aspect-ratio jets show approximately same broadband shock-noise levels though the intensity is slightly higher in major-axis plane relative to that along minor-axis plane.

The presence of notch significantly affects the far-field noise characteristics of each aspect-ratio jet. Figures. 6.16(a)-(d) show the case of triangular notch jets. At $\theta = 90^o$, relative to plain jets, Figs. 6.15(a)-(d), notch jets show significant reductions in OASPL for the range of M_j from 1.2 to 1.8 in both planes indicating reduced mixing noise levels relative to plain jets. The mixing noise intensity gap between 2:1 and 4:1 further widens to 5.5 dB in the minor-axis planes. At $\theta = 150^o$, some significant change in the broadband shock-noise intensity of the jets in notch/minor-axis planes are observed relative to plain jets, Figs. 6.12(c)-(d), 6.13(c)-(d), in the entire range of Mach number. At M_j=2.0, as much as 5-7 dB reduction in shock-noise is discernible. However, the presence of notch in the minor-axis plane has only a marginal effect on the noise radiated along the major-axis plane showing only a small reduction of 1 dB, relative to plain cases. Further, the difference in shock-noise intensity in the notch jets between the two planes drifts apart by 9 dB at M_j=2.0 relative to 4 dB change in plain jets. However, the effect of aspect-ratio is observed to be negligible with different aspect-ratio jets showing same noise levels.

The results suggest that changing the aspect-ratio from 2:1 to 4:1 significantly alters the mixing and broadband noise characteristics. The presence of notch in each aspect-ratio,

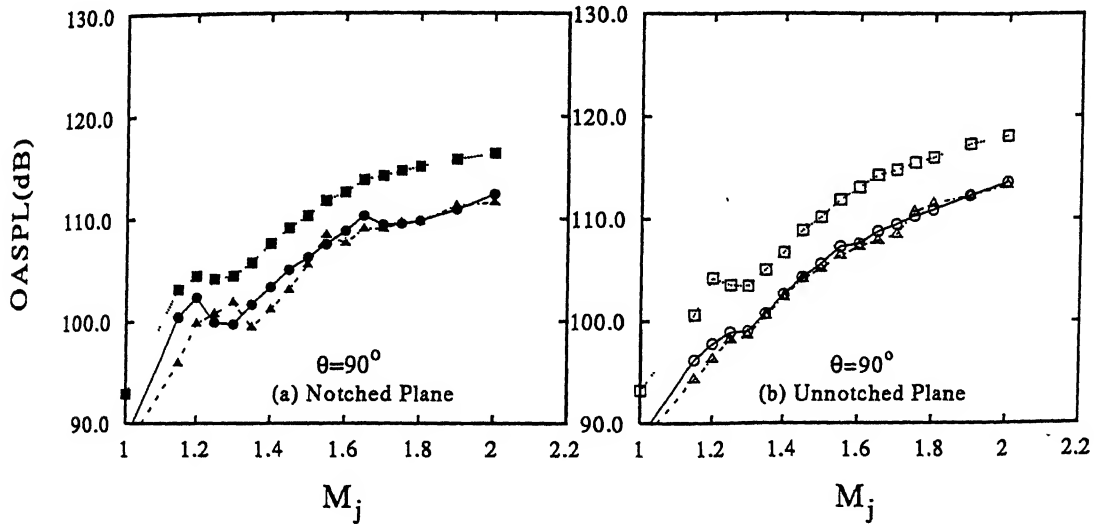

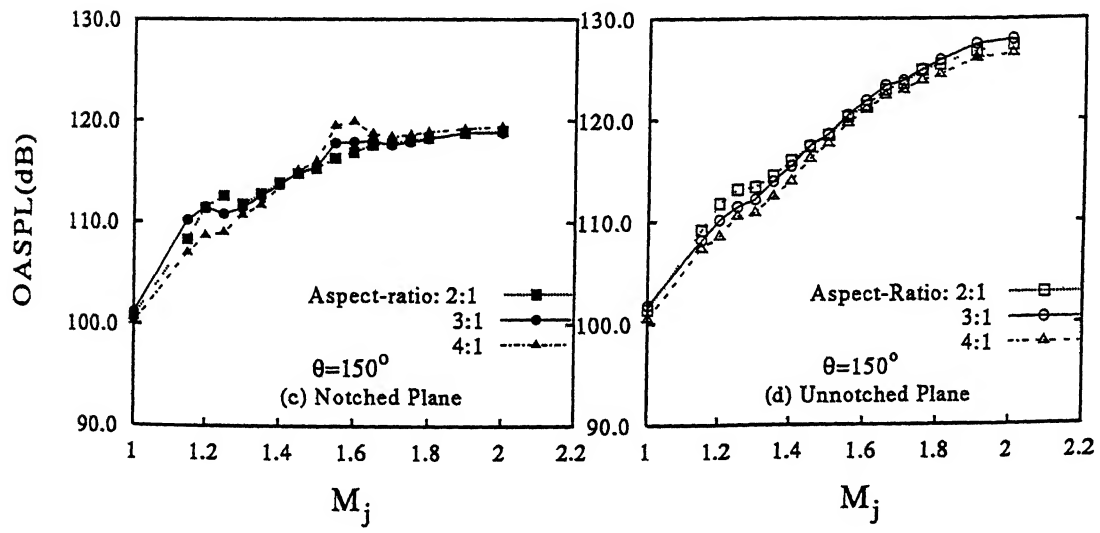

Figure 6.16: Overall sound pressure level variation with M_j showing the effect of aspect-ratio for triangular notched elliptic slot jets

further alters the mixing and shock-associated noise characteristics relative to plain jets. The additional expansion and compression waves emanating from the notches, as observed from shadowgraph pictures in the preceding section, seem to alter and weaken the downstream shock development and hence, the acoustic characteristics significantly.

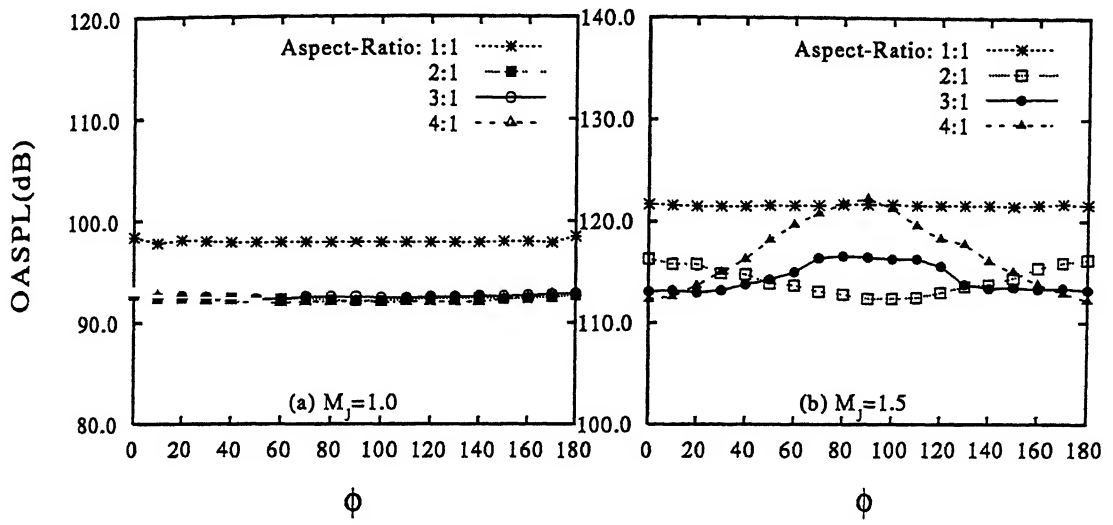

Figure 6.17: Effect of aspect-ratio on the azimuthal directivity for plain elliptic slot jets

Azimuthal Directivity

The azimuthal variation of the far-field OASPL for plain elliptic jets at M_j=1.0 and 1.5 are shown in Figs. 6.17(a)-(b) with the microphone positioned at $\theta = 90^o$, X/D_e=0.0. At full expansion, Fig. 6.17(a), all the aspect-ratios show same noise level with no preferred direction. However, at underexpansion, some peculiar results are obtained, Fig. 6.17(b). Drastic variation in noise radiated from major and minor-axis planes is discernible with aspect-ratio. The 2:1 elliptic jet shows significant reduction in shock-noise levels in the minor-axis plane relative to major-axis plane. However, 3:1 and 4:1 jets show a reversal in noise trend in the two planes. The 3:1 jet shows higher shock-noise level in minor-axis plane relative to its major-axis plane. The noise intensity in the minor-axis plane further increases for 4:1 case while along the major-axis plane the shock-noise levels for 4:1 jet falls below that of 3:1 jet. As much as 4 dB increase in radiated noise for 3:1 jet along the minor-axis plane relative to major plane is observed whereas, this difference in the radiated shock-noise in the two planes goes up to 10 dB for 4:1 jet. This reversal in noise trends in the two planes with increase in aspect-ratio may be due to change in shock-structure development as observed from shadowgraph pictures(Pics. 47, 51, 55). The 2:1 jet showed an oblique shock interaction at the end of the first cell while in 3:1 jet the oblique shock interaction is replaced by the emergence of a Mach disk which becomes more prominent for 4:1 case. The very presence of Mach disk is the main cause of increase in

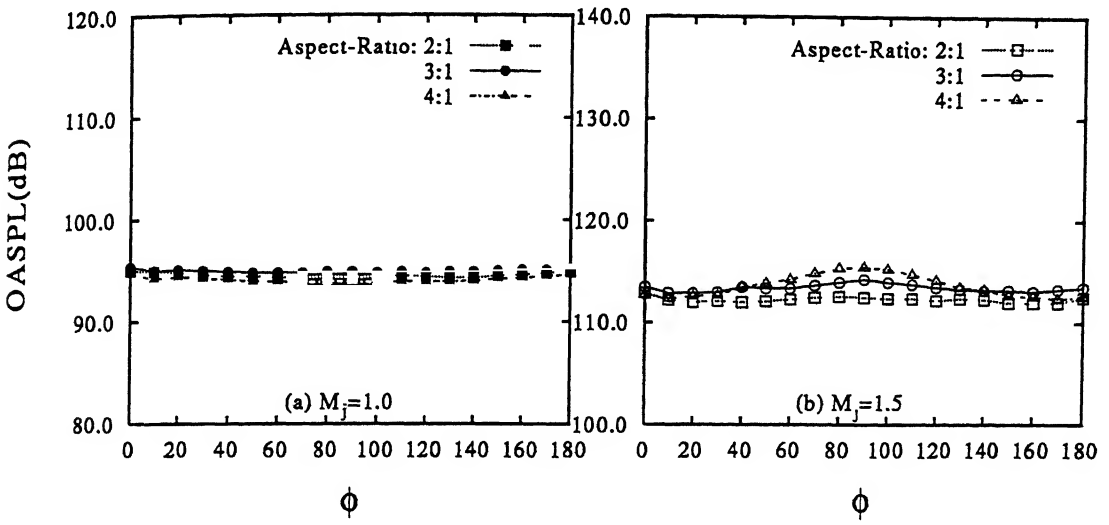

Figure 6.18: Effect of aspect-ratio on the azimuthal directivity for triangular notched elliptic slot jets

shock-noise intensity in the minor-axis plane of 3:1 and 4:1 jets since across the Mach disk higher pressure variations are encountered. However, along the major-axis plane the extent of Mach disk is reduced due to the lesser width of minor-axis side. This fact may be responsible for the significant reduction in noise intensity in the major-axis plane of 3:1(3.5 dB) and 4:1(4 dB) jets relative to 2:1 elliptic jet.

Such a reversal in radiated noise from the two planes of 3:1 elliptic jet has also been observed by Gutmark *et al*[124] with Mach disk formation relative to the case with oblique shock interaction(absence of Mach disk). He further observed that, with the presence Mach disk a strong noise source could be located near the Mach disk along minor-axis plane while no source could be located on the major-axis plane. This suggests that the noise source mechanisms are greatly modified with Mach disk formation and hence, are responsible for the reversal in radiated noise along the two planes as the aspect-ratio is increased from small(2:1) to moderate(3:1 and 4:1) values.

The presence of triangular notch in each of the aspect-ratio does not alter the mixing noise emission at full expansion, Fig. 6.18(a). However, at underexpanded condition the difference in noise level between the two planes decreases. For 2:1 notched jet, the noise levels in the major-axis plane is drastically brought down, by 5 dB, relative to the plain jet. For 4:1 jet, presence of notch does not alter the noise levels in the major-plane, relative to their plain jets

but significantly effects the noise levels along the notch plane. As much as 7 dB noise reduction is observed for 4:1 jet and 3.5 dB for 3:1 jet. Some similar reductions in sound intensity are observed for other notch configurations. For 3:1 jet, square and triangular notches seem to be the best for noise reduction in minor plane(3.5 dB) and semi-circular notch for 4:1 jet with 10 dB reduction.

Thus, it is clear from the azimuthal directivity plots that instability characteristics vary significantly along the two planes with aspect-ratio. In addition, the shock shear layer interaction along the circumference and hence, the noise emission characteristics vary with aspect-ratio. The notch presence, further, alters the acoustic-source mechanism of these jets. However, for small aspect-ratio jets, presence of notch significantly affects the noise intensity in the both minor and major axis planes whereas for moderate aspect-ratio jets, notch presence effects only the acoustic emission characteristics of the plane in which they are made. This may be due to the greater distance between the minor and major axis end which prevents the disturbance introduced in one plane from significantly altering the noise characteristics of other plane.

Radial Directivity in the Aft Quadrant

From the preceding discussion it is clear that the noise radiation mechanisms are greatly altered with aspect-ratio. This change is observed in spectral analysis, azimuthal directivity and OASPL study with microphones positioned at two polar angles, $\theta = 90^o$ and 150^o. The present section discusses the effect of aspect-ratio on angular directivity of radiated noise in the aft quadrant for both plain and notch elliptic-slot jets.

The effect of aspect-ratio on the radial directivity of plain elliptic jets at full expansion in both planes is illustrated in Figs. 6.19(a)-(b). All the aspect-ratio jets show approximately similar mixing noise levels. As these jets are operated at underexpanded condition, M_j=1.5, significant changes in mixing and shock-noise levels become apparent. In minor-axis plane, Fig. 6.20(a), 2:1 elliptic jet shows minimum noise levels which increase significantly with aspect-ratio. This is because of the emergence of Mach disk in higher aspect-ratio jets, the strength of which increases with increase in aspect-ratio. However, in major-axis plane, 2:1 jet shows highest shock-noise with 3:1 and 4:1 showing significantly lower noise levels, Fig. 6.20(b) while

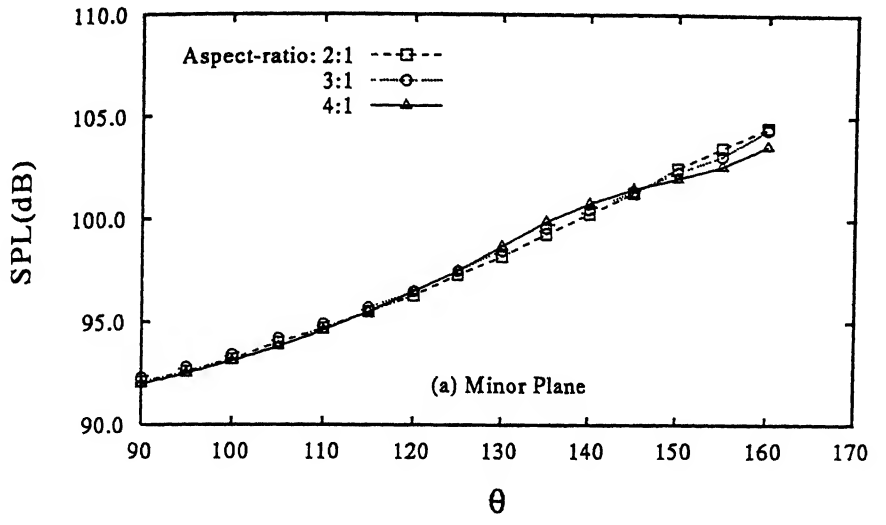

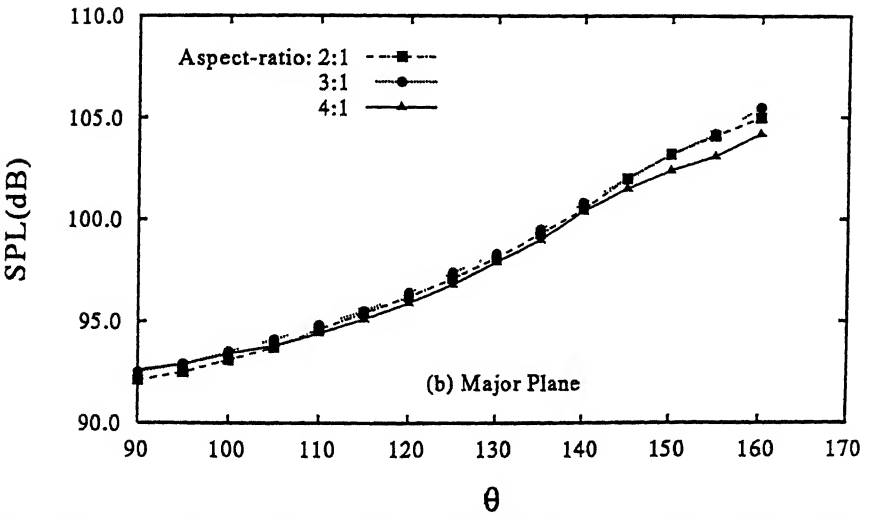

Figure 6.19: Effect of aspect-ratio on the radial directivity of plain elliptic slot jets, M_j=1.0

the shock noise intensity is observed to be the same for each aspect-ratio at $\theta > 130^o$.

Figures 6.21(a)-(b) show the radial directivity plots for different aspect-ratio jets with triangular notch, at full expansion. In both the planes, 2:1 jet shows the highest mixing noise levels followed by 3:1 and 4:1 which has the minimum. At underexpansion, this trend in noise levels gets reversed. In the minor-axis plane, Fig. 6.22(a), 4:1 jet shows the highest shock noise levels followed by 3:1 and 2:1 jets. Relative to their respective plain jets, it is discernible that 4:1 notch jet shows significant noise reduction in the aft quadrant followed by 3:1 case. At $\theta = 90^o$, 4:1 jet shows about 6 dB reduction. At $\theta = 160^o$, 4:1 notch jet shows 6 dB reduction followed by 3:1 with 3.5 dB and 2:1 with 5 dB. However, in the major-axis plane, the

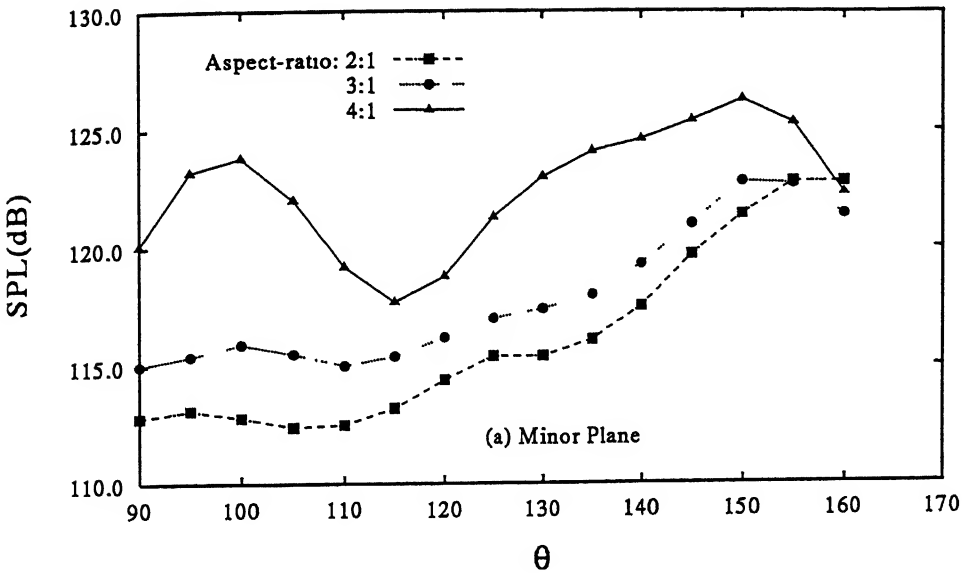
130.0
125.0
120.0
115.0
110.0
SPL(dB)
Aspect-ratio: 2:1
3:1
4:1
(a) Minor Plane
90
100
110
120
130
140
150
160
170
θ

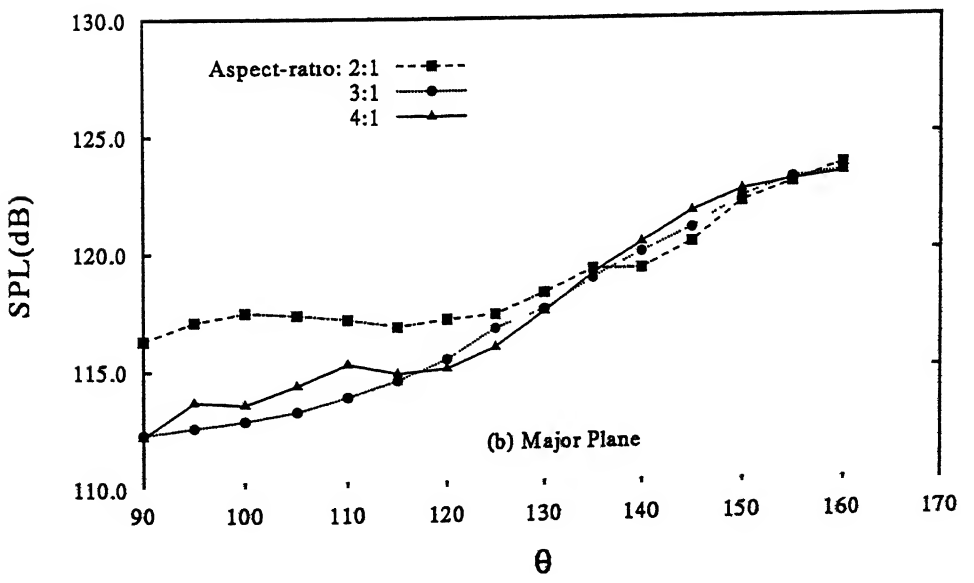
130.0
125.0
120.0
115.0
110.0
SPL(dB)
Aspect-ratio: 2:1
3:1
4:1
(b) Major Plane
90
100
110
120
130
140
150
160
170
θ

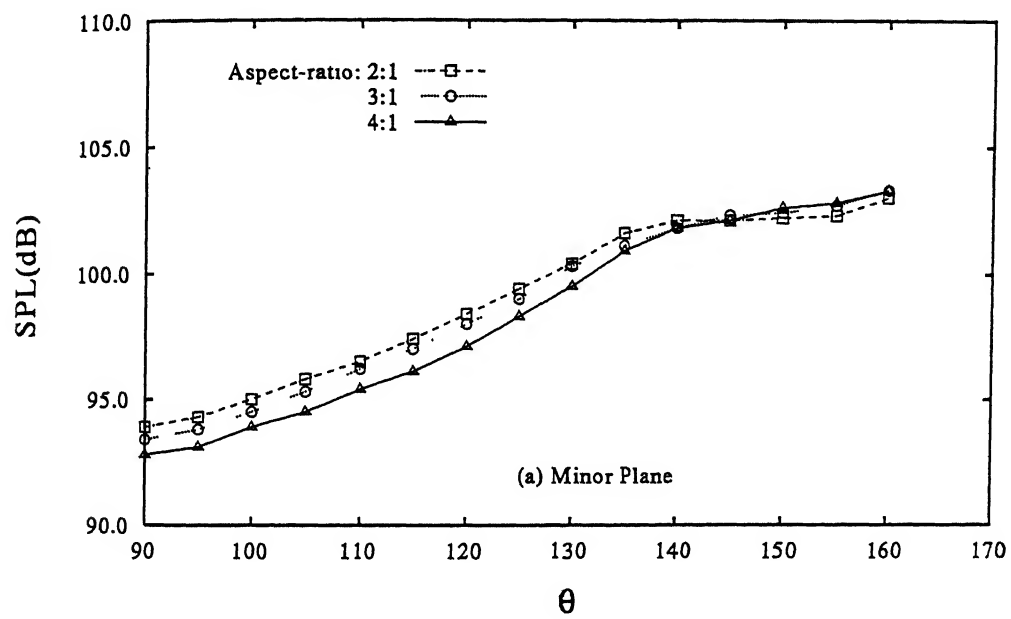

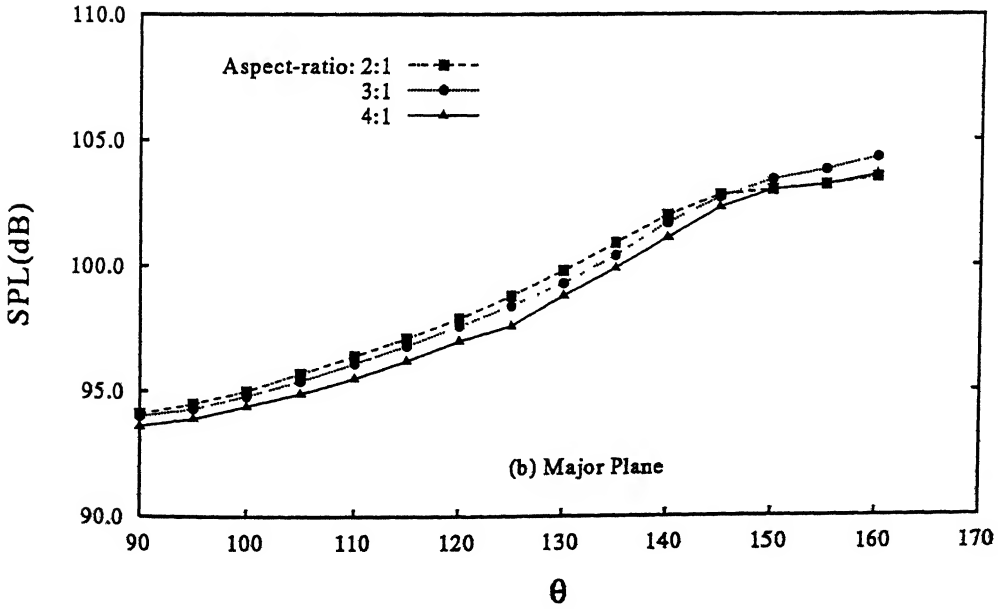

Figure 6.21: Effect of aspect-ratio on the radial directivity of triangular notched elliptic slot jets, M_j=1.0

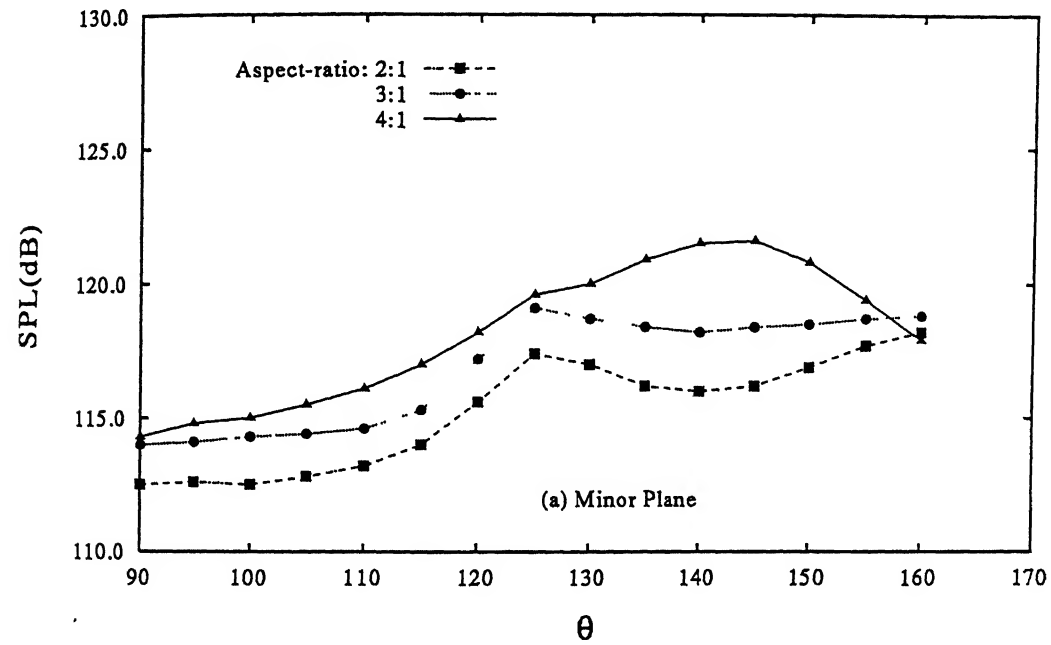

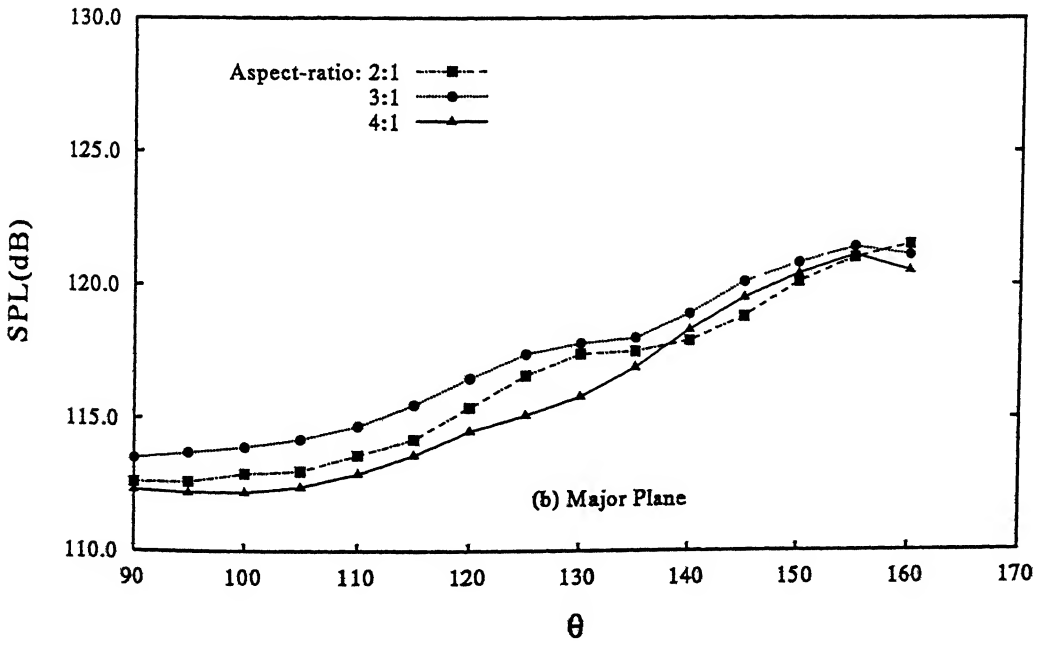

Figure 6.22: Effect of aspect-ratio on the radial directivity of triangular notched elliptic slot jets, M_j=1.5

shock-noise levels do not show significant changes except for 2:1 jet which shows a 4 dB reduction at $\theta = 90^o$. At $\theta = 160^o$, all jets show approximately 2 dB reduction. Further, if the effect of notch configuration is analysed, it is seen that at full expansion, in both planes, triangular notch shows the highest noise followed by square and semi-circular case. Semi-circular notch seems to be the best for 4:1 jet and square and triangular for 3:1 elliptic jet(Figs. not shown).

Thus, with aspect-ratio increase, shock shear-layer interaction process undergoes drastic changes along the minor-axis planes while only slight changes occur along the major-axis plane. Further, notch presence effects shock-noise levels both in major and minor-axis planes significantly. However, drastic reduction in noise are observed for 3:1 and 4:1 jets in minor plane while the notches only slightly effect the noise characteristics along major-axis plane. This clearly indicates that as the distance between the minor and major-axis ends increases with aspect-ratio, any disturbance introduced due to the presence of notch along the minor-axis plane is unable to alter the noise characteristics of major plane while this is not so for small aspect-ratio elliptic jets.

In summary, therefore, it appears that the sound intensity of both turbulent mixing and shock-associated noise is strongly dependent on aspect-ratio. Further, aspect-ratio seems to be a parameter strongly governing the initial conditions, azimuthal deformations, shear-layer development, downstream shock development and hence, alters the noise producing mechanism. In other words, the noise field from elliptic jets is characterised by four parameters, (i) pressure ratio (ii) observer angle, θ (iii) aspect-ratio of slot geometry, and (iv) slot perimeter governed by its configuration.

6.3 Conclusions

The effect of aspect-ratio on the mixing and noise characteristics of elliptic-slot free jets has been investigated. Further, a passive control of achieving near-field mixing enhancement and jet noise reduction in small to moderate aspect-ratio slot jets has been demonstrated.

Following conclusions can be made from the above discussions:

- The entrainment is observed to decrease with increase in aspect-ratio for plain elliptic slot jets. This may be due to the fact that that as the aspect-ratio increases, the azimuthal

deformations take longer to evolve in the streamwise direction and by the time they become appreciable, the vorticity has already diffused[106, 5]. The entrained fluid induced by these diffused vortices would be much less and hence, a large mass entrainment was not observed[1] relative to 2:1 elliptic jet.

- In small-aspect ratio jets, the use of sharp cornered notch geometries seem to be beneficial to the jet mixing characteristics.

- In relatively higher aspect-ratio jets, i.e., 4:1, it is observed that restricting the roll up uniform vortices in the notched plane by use of sharp cornered notch does not help the jet mixing. Rather, a notch with absence of sharp corner, i.e., a semi-circular notch, seems to be favourable for 4:1 jet in engulfing greater ambient mass and hence, better bulk mixing relative to other notched 4:1 jets.

- The shock-strength increases with aspect-ratio so that lesser cells are observed for higher aspect-ratio jet relative to lower aspect-ratio jet. However, the shocks beyond the first cell in the minor-axis plane are obscured by turbulence relative to cells in the major-axis plane. This difference in the diffusion of cells in the two planes is related to the different jet modes predominant in each plane. As aspect-ratio increases from 2:1 to 3:1, the angle of the oblique shocks is seen to increase gradually(with reference to upstream direction) so that for 3:1 case a Mach disk begins to form at the centreline region which becomes more prominent for 4:1 ellipse.

- The interaction of the additional waves, emanating from the notches, with the existing waves leads to appreciable changes in the shock-structure development. In the major-plane for 4:1 notch jet these additional waves are observed to alter the angle of the oblique shock at the end of the first cell which slightly reduces the lateral extent of the Mach disk. As such more cells are discernible for notched case indicating reduction in Mach disk strength. Further, different notch geometries are observed to modify the shock development process in each aspect-ratio jet differently.

- For all the aspect-ratios investigated, both plain and notched elliptic jets agree fairly well with Tam's theory[113] though the curves for the present case lie below it. Reduction in average shock-cell length is apparent for notched cases.

- The present results of predicted Strouhal number show good agreement with Tam's analytic solution for all aspect-ratios with the points following the same trend though they lie a little above it. Since with increasing M_j, an increase in Strouhal number relative to other cases indicates decrease in shock-cell spacing[110], the plots clearly indicate that the shock-cell spacing decreases with increasing aspect-ratio.

- The amplitude of the fundamental screech frequency is observed to increase with increase in aspect-ratio of plain jets. This may be due to the emergence of Mach disk in 3:1 and 4:1 jets, as seen in shadowgraph photographs which drastically changes the noise field along minor-axis plane[124] relative to small aspect-ratio jet. A slight decrease in the high-frequency content of jet noise in the near vicinity of the fundamental screech tone is also observed with increase in aspect-ratio.

- The notch presence drastically reduces the screech amplitude in each aspect-ratio jet. This reduction increases with increase of aspect-ratio. The differences observed in the spectral characteristics of plain and notched jets with aspect-ratio suggests that the presence of notch alters the acoustic emission characteristics in each of these jets. Since the instability process seems to vary with aspect-ratio, the same notch configuration in different aspect-ratios(which also alters the downstream shock development) seems to weaken the feedback process, thereby drastically reducing the screech amplitudes.

- At θ=90^o, 2:1 plain jet shows higher mixing noise levels than 3:1 and 4:1 jets. The notch further brings down the mixing noise levels in each aspect-ratio.

- At $\theta = 150^o$, all aspect-ratio plain jets show approximately same broadband shock noise levels though the intensity is higher along major-axis plane. The notch presence further reduces the shock noise radiated along the minor-axis plane.

- Effect of aspect-ratio has a great dependence on azimuthal directivity of noise. The 2:1 elliptic jet shows significant reduction in shock-noise levels in the minor-axis plane relative to major-axis plane. However, 3:1 and 4:1 jets show a reversal in noise trend in the two planes. The 3:1 jet shows higher shock-noise level in minor-axis plane relative to its major-axis plane. The noise intensity in the minor-axis plane further increases for 4:1 case while along the major-axis plane the shock-noise levels for 4:1 jet falls below

that for 3:1 jet. This reversal in noise radiation with aspect-ratio may be due to the change in shock-structure development. The 2:1 jet showed an oblique shock interaction at the end of the first cell while in the 3:1 jet the oblique shock interaction is replaced by the emergence of a Mach disk which becomes more prominent for 4:1 case. The very presence of Mach disk is the main cause for the increase in shock-noise intensity along the minor-axis plane of 3:1 and 4:1 plain jets.

- Presence of notch alters the azimuthal emission characteristics of these jets. For small aspect-ratio jets, presence of notch significantly affects the noise intensity in the both planes whereas for moderate aspect-ratio jets, presence of notch effects only the acoustic emission characteristics of the plane in which they are made. This may be due to the greater distance between the minor and major end which prevents the disturbance introduced in one plane to significantly alter the noise characteristics of other plane.

- Aspect-ratio shows a radial dependence of noise radiation. The 2:1 plain elliptic jet shows minimum noise level which increases significantly with increase in aspect-ratio.

- Aspect-ratio is a parameter strongly governing the initial conditions, azimuthal deformations, shear-layer development, downstream shock development and hence, alters the noise producing mechanism. In other words, the noise field from elliptic jets is characterised by four parameters, (i) pressure ratio (ii) observer angle, θ (iii) aspect-ratio of slot geometry, and (iv) slot perimeter governed by its configuration.

- Semi-circular notch seems to be the best for 4:1 jet and square and triangular for 3:1 case.

Chapter 7

Summary

High speed jets, both sonic and underexpanded, issuing from circular and elliptic slot geometries with exit modifications exhibit a wide range of flow characteristics in preference to their plain geometries. Mean flow properties such as entrainment, jet spread and jet decay can be controlled to result in enhanced mixing. The near field shock cell structure development in underexpanded jets can be weakened, thereby alleviating the shock associated noise. The characteristics of the observed flows issuing from modified exit geometries can be summarised as follows:

- **Circular Slot Jets:** The circular slot jet development is strongly dependent upon any discontinuity introduced in the form of notches in the slot periphery. These exit geometry modifications in an otherwise circular slot geometry introduce slight aspect-ratio with its major-axis along the notched/modified plane. As such the modified circular slot grows like a jet issuing from non-circular exit geometry with higher spread in the unnotched/unmodified plane and slower spread in the notched/modified plane. This introduces axis-switching thereby resulting in enhanced mixing characteristics. The notch geometry, further has a strong influence on the jet development. Absence of sharp corner in the notch geometry is observed to enhance the mixing in modified circular slots. However, for the far field shock noise reduction, the presence of a corner in the notch is found advantageous. The pressure relieving effect and the enhanced small scale mixing from these notch corners diffuse the shocks faster and, therefore, weaken the shocks in the core relative to an equivalent plain circular jet. This results in significant reduction in screech

tone amplitude and the broadband shock associated noise.

- **Small Aspect-Ratio(2:1) Elliptic Slot Jets:** Jets issuing from elliptic/non-circular exits spread faster along minor-axis plane and grow slowly along the major-axis plane in the immediate vicinity of the exit plane, resulting in axis-switching close to the exit. This phenomena in elliptic jets significantly enhances the mixing process when compared with an equivalent circular jet. Modifying the elliptic slot via notches placed along the minor-axis plane further improves the mean flow characteristics like the entrainment, jet spread and jet decay relative to plain ellipse. However, introduction of notches in ellipse exhibits a trend opposite to that introduced in circular slot jets. The modified elliptic slot spreads more in the notched/modified plane, in contrast to modified circular slot jets. This higher spread along the modified minor-axis plane relative to plain ellipse results in an earlier switch in axis causing the modified elliptic slot jet to bring more of ambient fluid towards the jet centreline. The notch geometry, further influences the jet characteristics. For elliptic jets, sharp corner in the notch significantly improves the mixing process. This is, once again, in contrast to the observed behaviour of the modified circular slots. For underexpanded cases, modified elliptic slots exhibit significantly weakened shocks relative to the plain circle and ellipse. The faster diffusion of shock cells beyond the third cell is suggestive of decreased screech tone amplitudes. The weakened shocks in modified ellipse result in significant reductions in the screech tone amplitudes and broadband shock associated noise. Though the shock noise levels along minor plane are affected only slightly by the notch presence of notch, noise radiated along the major plane of modified ellipse is affected significantly.

- **Effect of Aspect-Ratio for Elliptic Slot Jets:** Aspect-ratio is a strong parameter that governs the deformation of the elliptic vortex and hence, significantly affects the mixing process. The azimuthal deformations are faster in large aspect-ratio jets due to which the vortical structures diffuse faster and hence, there is a dominance of small-scale activity. The small-aspect ratio(2:1) jet has higher large-scale activity and hence, entrains more. Notch introduction enhances the mixing in each aspect-ratio investigated. Notch geometry, further has an influence on the development of the jet from each aspect-ratio. Triangular notch seems to be favourable for 2:1, square notch for 3:1 and semi-circular

notch for 4:1. It appears that as the aspect-ratio is increased, the absence of corner in the notch is favourable in engulfing greater ambient mass resulting in higher bulk mixing. The vortical structures being close to the jet centreline, sharp cornered notches do not help in enhancing the mixing.

Higher aspect-ratio jets radiate dominant screech tone amplitudes relative to small aspect-ratio jets. The noise radiation along the minor-axis plane increases progressively with aspect-ratio while along major-axis plane the noise shows a decreasing trend with aspect-ratio. This is observed due to the emergence of Mach disk in 3:1 and 4:1 jets. Notch introduction, except for 2:1 jet, significantly brings down the noise levels along minor-axis plane but only slightly along major-axis plane. Triangular notch seems to be the best for screech tone reduction while square notch seems favourable for far field broadband shock associated noise reduction. Thus, noise from elliptic slot jets is characterised by four parameters, (i) pressure ratio, (ii) observer angle, (iii) slot perimeter governed by notch configuration, and finally (iv) aspect-ratio of slot geometry.

With increase in aspect-ratio, shock-shear layer interaction process undergoes drastic changes along minor-axis planes.

Scope of Further Research : Though the present investigation has focused attention upon important aspects of the jet flow field from both circular and elliptic slots, there are many other aspects that need to be looked into for a complete understanding of the governing phenomena. The present results clearly point out the various factors that govern the jet flow development process and that relatively small changes in geometry or flow conditions can produce large, seemingly unpredictable variations in mixing and noise characteristics. Further investigations are required to gain insight into the detailed characteristics of these flows. Some of the other aspects which can be explored further are as listed below:

- In case of circular slot jets, effect of other notch configurations such as semi-elliptic and semi-rectangular, both with their minor or major-axis perpendicular to the jet axis need to be investigated.
- The same notch configurations can also be investigated in conical nozzles where they will be introduced in the form of grooves. Further, variation in groove length can yield interesting results. Detailed acoustic study can also be carried out.

- In sharp edged circular conical nozzles, literature indicates study on notches with triangular configuration[8]. Variation in notch geometry can be investigated in these set of nozzles to identify the best configuration for both mixing and noise reduction. Further, aeroacoustic studies on these nozzles will help complete the study.

- The study may also be extended to supersonic jets issuing from convergent-divergent(C-D) nozzles.

- In the case of elliptic slot jets, since triangular notches seem to have a greater influence in improving mixing in modified ellipse, the angle of the vertex in triangular notch can be varied to study the optimum triangular notch shape.

- Also, since entrainment in elliptic jets takes place in between the minor and major-axis planes, notch location and orientation can be varied to alter the mixing and noise characteristics.

- Other notch geometries such as rectangular and elliptic shapes need to be investigated in elliptic slot jets.

- The present investigation on aspect-ratio is carried out only up to moderate values, i.e., 4. Investigations can be extended to higher aspect-ratios. Since the present study reveals that, as aspect-ratio is increased semi-circular notch show favourable characteristics, introduction of semi-elliptic and and semi-rectangular elliptic notches in aspect-ratios > 4 needs further study.

- And finally, to understand the physics governing the mixing process in all the above cases, flow visualization studies using water flow table may be carried out to reveal the dynamics the vortex structures. A detailed study of the turbulence characteristics of the flow field will be helpful for a clear understanding of the mixing process.

Bibliography

[1] Hussain, A.K.M.F. and Hussain, H.S. "Elliptic Jets Part I: Characteristics of Excited and Unexcited jets". *Journal of Fluid Mechanics*, Vol.208:pp. 257–320, 1989.

[2] Gutmark E. Schadow K.C. Koshigoe, S. and A. Tubis. "Wave Structures in Jets of Arbitrary Shape. Part III. Triangular Jets". *Physics of Fluids*, Vol.31(No.6):pp. 1410–1419, 1988.

[3] Gutmark, E. and Schadow, K.C. "Selective Flow Control in Triangular Jets". *Experiments in Fluids*, Vol.6:pp. 129–135, 1988.

[4] Schadow, K.C. Gutmark, E. and K.J. Wilson. "Subsonic and Supersonic Combustion Using Non-Circular Injectors". *Journal of Propulsion and Power*, Vol.7(No.2):pp. 240–249, 1991.

[5] Bagdanoff, D., Krothapalli, A. and K. Karamcheti. "On the Mixing of a Rectangular Jet". *Journal of Fluid Mechanics*, Vol.107:pp. 201–220, 1981.

[6] Raman, G. "Cessation of Screech in Underexpanded Jets". *2nd AIAA/CEAS Aeroacoustics Conference*, May 6-8:pp. 1–27, 1996.

[7] Bradbury, L.J.S. and Khadem, A.H. "The Distortion of a Jet by Tabs". *Journal of Fluid Mechanics*, Vol.70:pp. 801–813, 1975.

[8] Pannu, S.S. and Johanassen. "The Structure of Jets from Notched Nozzles". *Journal of Fluid Mechanics*, Vol.74(Part 3):pp. 515–528, 1976.

[9] Clemens, N.T. and Mungal, M.G.. "Two and Three-Dimensional Effects in the Supersonic Mixing Layer". *AIAA Journal*, Vol.30(No.4):pp. 973–981, 1992a.

[10] Kim J.H., Clancy,P.S. Samimy, M. "Supersonic Jet Noise Reduction and Mixing Enhancement through Nozzle Trailing Edge Modifications". *AIAA paper 97-0146*, 35th Aerospace Sciences Meeting and Exhibit:pp. 1–27, Jan 6-10, 1997.

[11] Roshko, A.. "Structure of Turbulent Shear Flows: A New Look". *AIAA Journal*, Vol.14:pp. 1349–1357, 1976.

[12] Zaman, K.B.M.Q., Samimy, M. and M.F. Reeder. "Effect of Tabs on the Flow and Noise Field of a Axisymmetric jets". *AIAA Journal*, Vol.31(No.4):pp. 609–619, 1993.

[13] Reeder,M.F., Zaman, K.B.M.Q. and Samimy, M. "Control of an Axisymmetric Jet using Vortex Generators". *Physics of Fluids*, Vol.6(No.2):pp. 778–793, 1994.

[14] Buzyna G., Lourence,L., Krothapalli, A. "Streamwise Vortices in an Underexpanded Axisymmetric Jet". *Physics of Fluids(A)*, Vol.3(No.8):pp. 1848–1851, 1991.

[15] Samimy M., Elliott,G.S., Arnette, S.A. "On Streamwise Vortices in High Reynolds Number Supersonic axisymmetric jets". *Physics of Fluids*, Vol.5(No.1):pp. 183–202, 1993.

[16] Norum, T.D. "Screech Suppression in Supersonic Jets". *AIAA Journal*, Vol.21(No.2):pp. 235–240, 1983.

[17] Wlezien, R.W. and Kibens, K. "Influence of Nozzle Asymmetry on Supersonic Jets". *AIAA Journal*, Vol.26(No.1):pp. 27–33, 1988.

[18] McDaniel,J., Krothapalli, A. and Bagdanoff, D. "Effect of Slotting on the Noise of an Axisymmetric Supersonic Jet". *AIAA Journal*, Vol.28(No.12):pp. 2136–2138, 1990.

[19] Eaton J.K., Elkins ,C.J. Longmire, E.K. "Control of Jet Structure by Crown-Shaped Nozzles". *AIAA Journal*, Vol.30(No.2):pp. 505–512, 1992.

[20] Gutmark, E. and Ho, C.M. "Vortex Induction and Mass Entrainment in a Small Aspect-Ratio elliptic jet". *Journal of Fluid Mechanics*, Vol.179:pp. 383–405, 1987.

[21] Gutmark, E. Schadow, K.C., Koshigoe, S. and Wilson, K.J. "Combustion Related Shear Flow Dynamics in Elliptic Supersonic Jets". *AIAA Journal*, Vol.27(No.10):pp. 1347–1353, 1989.

[22] Schadow, K.C. Kraeutle, K.J., Yu, K.H. and Gutmark, E.J. "Supersonic Flow Mixing and Combustion using Ramp Nozzle". *Jounal of Propulsion and Power*, Vol.11(No.6):pp. 1147–1153, 1995.

[23] Papamoschou, D. and Roshko, A.. "The Compressible Turbulent Shear Layer: An Experimental Study". *Journal of Fluid Mechanics*, Vol.197:pp.453–477, 1988.

[24] Samimy, M., Arnette, S.A., Elliott, G.S. "The Characteristics and Evolution of Large-Scale Structures in Compressible Mixing Layers". *Physics of Fluids*, Vol.7(No.4):pp. 864–876, 1995.

[25] Daniel P. Raymer. Aircraft design: A conceptual approach. AIAA Education Series, 1989.

[26] Krothapalli, A., Washington, D., King, C.J., Alvi, F.S. "Aeroacoustic Properties of a Supersonic Diamond-Shaped Jet". *AIAA Journal*, Vol.34(No.8):pp. 1562–1569, 1996.

[27] G.N. Abramovich. The Theory of Turbulent Jets. *MIT Press, MIT, Cambridge, Massachusetts*, 1963.

[28] Otugen, M.V. and Namer, I. "Velocity Measurements in a Plane Turbulent Air Jet at Moderate Reynolds Number". *Experiments in Fluids*, Vol.6:pp. 387–399, 1988.

[29] Steiger, M.H., Sforza, P.M. and Trentacoste, N. "Studies in Three-Dimensional Viscous Jets". *AIAA Journal*, Vol.4(No.5):pp. 800–806, 1966.

[30] Powell, A.. "Survey of Experiments on Jet Noise". *Aircraft Engineering*, (No.1):pp. 2–9, 1954.

[31] Powell, A. "On the Noise Emanating from a Two-dimensional Jet above the Critical Pressure". *The Aeronautical Quarterly*, Vol.4(No.2):pp. 103–121, 1953.

[32] Ahuja, K.K., Tam, C.K.W. and Jones, R.R. III. "Screech Tones from Free and Ducted Supersonic Jets". *AIAA Journal*, Vol.31:pp. 917–922, 1994.

[33] Tam, C.K.W. "Supersonic Jet Noise". *Annual Review of Fluid Mechanics*, Vol.27:pp. 17–43, 1995.

[34] Powell, A. "The Noise of Choked Jets". *Journal of Acoustical Society of America*, Vol.25:pp. 385–389, 1953.

[35] Lau, J.C. "Mach Number and Temperature Effects on Jets". *AIAA Journal*, Vol.18(No.6):pp. 609–610, 1980.

[36] Funabiki, K., Ariga, H., Abe, T. and Hiraoka, K. "Effect of Pressure Gradient on the Supersonic Mixing Layer". *AIAA Journal*, Vol.30(No.10):pp. 2564–2566, 1992.

[37] Bradbury, L.J.S. "The Structure of a Self-Preserving Turbulent Plane Jet". *Journal of Fluid Mechanics*, Vol.23:pp. 31–64, 1965.

[38] Wygnansky, I. Gutmark, E. "The Planer Turbulent Jet". *Journal of Fluid Mechanics*, Vol.73:pp. 465–495, 1976.

[39] Morris,P.J., Fisher, M.J. Lau, J.C. "Measurements in Subsonic and Supersonic Free Jets using Laser Velocimeter". *Journal of Fluid Mechanics*, Vol.93:pp. 1–27, 1979.

[40] Brown, G.L. and Roshko, A. "On Density Effects and Large Structures in Turbulent Mixing Layers". *Journal of Fluid Mechanics*, Vol.64:pp. 775–816, 1974.

[41] Winant, C.D. and Browand, F.K. "Vortex Pairing: The Mechanism of Turbulent Mixing Layer Growth at Moderate Reynolds Numbers". *Journal of Fluid Mechanics*, Vol.63:pp. 237–255, 1974.

[42] Winter Fourguettw, D.C. "Control of Large-Scale Structure Formation and Vortex Pairing using Photoacoustic Forcing". *Experiments in Fluids*, Vol.10:pp. 157–160, 1990.

[43] Dimotakis, P.E. and Brown, G.L. "The Mixing Layer at High Reynolds Number: Large-Structure Dynamics and Entrainment". *Journal of Fluid Mechanics*, Vol.78(No.3):pp. 535–560, 1976.

[44] Hollingsworth, D.K. and Mungal, M.G. "Organised Motion in a very High Reynolds Number Jet". *Physics of Fluids(A)*, Vol.1(No.10):pp. 1615–1623, 1989.

[45] Gutmark, E., Wilson ,K.J., Schadow, K.C. "Compressible Spreading Rates of Supersonic Coaxial Jets". *Physics of Fluids*, Vol.10:pp. 161–167, 1990.

[46] Schadow, K.C., Parr, T.P, Hanson-Parr, D.M., Wilson, K.J. Gutmark, E. "Non-Circular Jets in Combustion Systems". *Experiments in Fluids*, Vol.7:pp. 248–258, 1989.

[47] Samimy, M. and Elliot, G.S. "Effects of Compressibility on the Charcteristics of Free Shear Layers". *AIAA Journal*, Vol.28(No.3):pp. 439–445, 1990.

[48] Bogdanoff, D.W. "Compressibility Effects in Turbulent Shear Layers" *AIAA Journal*, Vol.21(No.6):pp. 926–927, 1983.

[49] Schadow, K.C., Gutmark, E.J and Yu, K.H. "Mixing Enhancement in Supersonic Free Shear Flows". *Annual Review of Fluid Mechanics*, Vol.27:pp. 375–437, 1995.

[50] Glass, D.R. "Effects of Acoustic Feedback in the Spread and Decay of Supersonic Jets". *AIAA Journal*, Vol.6(No.10):pp. 1890–1897, 1968.

[51] Lai, M.C., Faeth, G.M., Chuech, S.G. "Structure of Turbulent Sonic Underexpanded Free Jets". *AIAA Journal*, Vol.27(No.5):pp. 549–554, 1989.

[52] Davis, M.R. "Identification of Vortex Motions in Turbulent Mixing of Choked Jets". *Experiments in Fluids*, Vol.6:pp. 335–343, 1988.

[53] Crow, S.C. and Champagne, F.H. "Orderly Structure in Jet Turbulence". *Journal of Fluid Mechanics*, Vol.48:pp. 547–591, 1971.

[54] Hussain, A.K.M.F., Husain, H.S. "Controlled Excitation of Elliptic Jets". *Physics of Fluids*, Vol.26(No.10):pp. 2763–2766, 1983.

[55] Pimshtein, V.G. "Disturbance Generation in Supersonic Jets Under Acoustic Excitation". *AIAA Journal*, Vol.32(No.7):pp. 1345–1349, 1994.

[56] Tam, C.K.W. "Excitation of Instability Waves in a Two-Dimensional Shear Layer by Sound". *Journal of Fluid Mechanics*, Vol.89(No.2):pp. 357–371, 1978.

[57] Ahuja, K.K., Brown, W.H., Lepicovsky, J. and Morris, P.J. "Acoustic Control of Free Jet Mixing". *Journal of Propulsion and Power*, Vol.2(No.4):pp. 323–330, 1986.

[58] Gutmark, E. and Schadow, K.C. "Flow Chracteristics of Orifice and Tapered Jets". *Physics of Fluids*, Vol.30(No.11):pp. 3448–3454, 1987.

[59] Quinn, W.R. "Development of a Large Aspect-Ratio Rectangular Free Jet". *AIAA Journal*, Vol.32(No.3):pp. 547–554, 1994.

[60] Sfier, A.A. "Investigation of Three-Dimensional Turbulent Rectangular Jets". *AIAA Journal*, Vol.17(No.10):pp. 1055–1060, 1979.

[61] Marster, G.F. and Fotheringham, J. "The Influence of Aspect-Ratio on Incompressible, Turbulent FLows from Rectangular Slots". *The Aeronautical Quarterly*, Vol.31(No.4):pp. 285–305, 1980.

[62] Marster, G.F. "Spanwise Velocity Distributions in Jets from Rectangular Slots". *AIAA Journal*, Vol.19(No.2):pp. 148–152, 1981.

[63] Batchelor. Intoduction to Fluid Mechanics. *Cambridge Universıty Press, London, NY*, 1967.

[64] Morrison, G.L., McLaughlin, D.K. and Troutt, T.R. "Experimental of the Instability Waves in a Supersonic Jet and their Acoustic Radiation". *Journal of Fluid Mechanics*, Vol.69(Part 1):pp. 73–95, 1975.

[65] Husain, H.S. and Hussain, F. "Elliptic Jets Part II. Dynamics of Coherent Structures: Pairing". *Journal of Fluid Mechanics*, Vol.233:pp. 439–482, 1991.

[66] Tanna, H.K. "An Experimental Study of Jet Noise, Part II: Shock-Associated noise". *Journal of Sound and Vibration*, Vol.50:pp. 429–444, 1977.

[67] Hsia, Y., Bagdanoff, D., Krothapalli, A. and Karamcheti, K. "Role of Screeching Tones in the Mixing of an Underexpanded Rectangular Jet". *Journal of Sound and Vibration*, Vol.106(No.11):pp. 119–143, 1986.

[68] Norum, T.D. and Seiner, J.M. "Broadband Shock Noise from Supersonic Jets". *AIAA Journal*, Vol.20(No.1):pp. 68–73, 1982.

[69] Smith, C.R., Gretta, W.J. "The Flow Structure and Statistics of a Passive Mixing Tab". *Journal of Fluids Engineering*, Vol.115(No.6):pp. 255–263, 1993.

[70] Elliot, G.S., Reeder, M.F., Samimy, M. "Investigation of the Effects of Tabs on Supersonic Jets Using Advanced Diagnostics". *Journal of Propulsion and Power*, Vol.12(No.4):pp. 742–751, 1996.

[71] Krothapalli, A., Wishart, D.P. and Mungal, M.G. "Supersonic Jet Control via Point Disturbances inside the Nozzle". *AIAA Journal*, Vol.31(No.7):pp. 1340–1341, 1993.

[72] Kibens, V., Wlezien, R.W. "Passive Control of Jets with Intermediate Origins". *AIAA Journal*, Vol.24(No.8):pp. 1263–1270, 1986.

[73] Wlezien, W.R. "Nozzle Geometry Effects on Supersonic Interaction". *AIAA Journal*. Vol.27(No.10):pp. 1361–1367, 1989.

[74] Maeda, H., Ishji, R., Umeda, Y. "Discrete Tones Generated by the Impingement of a High Speed Jet on a Circular Cylinder". *Physics of Fluids*, Vol.30(No.8):pp. 2380–2388, 1987.

[75] Rice, E.J and Raman, G. "Supersonic Jets from Bevelled Rectangular Nozzles". *ASME Paper*, 33-WA/NCA-26, 1993.

[76] Ponton, M.K. and Seiner, J.M. "The Effects of Nozzle Exit Lip Thickness on Plume Resonance". *Journal of Sound and Vibration*, Vol.154(No.3):pp. 531–549, 1992.

[77] Wlezien, W.R. "Nozzle Geometry Effects on Nozzle Asymmetry of Supersonic Jets". *AIAA Paper 87-2694*, 1987.

[78] Ferris0, D.H., Johnson, R.F., Bradshaw, P. "Turbulence in Noise Producing Region of a Circular Jet". *Journal of Fluid Mechanics*, Vol.19:pp. 591–624, 1964.

[79] Sarohia, V. and Massier, P.F. "Experimental Results of Large-Scale Structures in Jet Flows and their Relation to Jet Noise Production". *AIAA Journal*, Vol.16(No.8):pp. 831–835, 1978.

[80] Hussain, A.K.M.F. and Zaman, K.B.M.Q. *Journal of Fluid Mechanics*, Vol.103:pp. 133, 1981.

[81] Williams, F., Smith, W. Bishop, K.A. "On the Noise Sources of the Unsuppressed High Speed Jet". *Journal of Fluid Mechanics*, Vol.50:pp. 21–31, 1971.

[82] Mull, H.R. "Effect of Jet Structure on Noise Generation by Supersonic Nozzles". *AIAA Journal*, Vol.31(No.2):pp. 147–149, 1959.

[83] Franken, P.A., Westervelt, P.J., Dyer, I. "Jet Noise Reduction by Induced Flow". *Journal of Acoustical Society of America*, Vol.30(No.8):pp. 761–764, 1958.

[84] Powell, A. "On the Mechanism of Choked Jet Noise". *Proceedings of Physical Society of London*, Vol.66:pp. 1039–1056, 1953a.

[85] Morris, P.J. "Flow-Characteristics of the Large-Scale Wave like Structures of a Supersonic Round Jet". *AIAA Journal*, Vol.53:pp. 223–244, 1977.

[86] Tam, C.K.W. "Supersonic Jet Noise Generated by Large-Scale Disturbances". *Journal of Sound and Vibration*, Vol.38:pp. 51–79, 1975.

[87] Morrison, G.L., Troutt, T.R., McLaughlin, D.K. "Reynolds Number Dependence on Supersonic Jet Noise". *AIAA Journal*, Vol.15:pp. 526–532, 1977.

[88] Tam, C.K.W. and Burton, D.E. "Sound Generated by Instability Waves of Supersonic Flows. Part I, Two-Dimensional Mixing Layers. Part II, Axisymmetric Jets". Vol.138:pp. 249–295, 1984.

[89] Lighthill, M.J. "On Sound Generated Aerodynamically, I General Theory". *Proceedings of the Royal Society of London*, Series A(No.211):pp. 564–587, 1952.

[90] Lighthill, M.J. "On Sound Generated Aerodynamically, II Turbulence as a Source of Sound". *Proceedings of the Royal Society of London*, Series A(No.222):pp. 1–32, 1954.

[91] Lighthill, M.J. "Jet Noise". *AIAA Journal*, Vol.1(No.7):pp. 1507–1517, 1963.

[92] Ffowcs, J.E. "The Noise from Turbulence Convected at High Speeds". *Philos. Transaction of Royal Society of London*, Series A(No.255):pp. 469–503, 1963.

[93] Ribner, H.S. "Quadrupole Correlations Governing the Pattern of Jet Noise". *Journal of Fluid Mechanics*, Vol.38:pp. 1–24, 1969.

[94] Tam, C.K.W. and Tanna, H.K. "Shock-Associated Noise of Supersonic Jets from Convergent-Divergent Nozzles". *Journal of Sound and Vibration*, Vol.81:pp. 337–358, 1982.

[95] Seiner, J.M., Tam, C.K.W. and Yu, J.C. "Proposed Relationship Between Broadband Shock-Associated Noise and Screech Tones". *Journal of Sound and Vibration*, Vol.110:pp. 309–321, 1986.

[96] Tam, C.K.W. "Stochastic Model Theory of Broadband Shock Associated Noise from Supersonic Jets". *Journal of Sound and Vibration*, Vol.116:pp. 265–302, 1987.

[97] Tam, C.K.W. "Broadband Shock Associated Noise of Moderately Imperfectly Expanded Supersonic Jets". *Journal of Sound and Vibration*, Vol.140:pp. 55–71, 1990.

[98] Bhat, T.R.S., Chen, G., Morris, P.J. "A Linear Shock-Cell Model for Jets of Arbitrary Exit Geometry". *Journal of Sound and Vibration*, Vol.132(No.2):pp. 199–211, 1989.

[99] Pack, D.C. "A Note of Prandtl's Formula for the Wavelength of a Supersonic Gas Jet". *Quaterly Journal of Mechanics and Applied Mathematics*, Vol.3:pp. 173–181, 1990.

[100] Krejsa, E.A., Khavaran, A., Kim, C.M. "Significance of Shock Structure on Supersonic Jet Noise of Axisymmetric Nozzles". *AIAA Journal*, Vol.32(No.9):pp. 1920–1923, 1994.

[101] Hubbard, H.H. and Lassiter, L.W. "Experimental Studies of Jet Noise". *Journal of Acoustical Society of America*, Vol.25(No.3):pp. 381–384, 1953.

[102] Hay, J.A. and Rose, E.G. "In-Flight Shock-Cell Noise". *Journal of Sound and Vibration*, Vol.11(No.4):pp. 411–420, 1970.

[103] Yu, J.C., Seiner, J.M. "Acoustic Near-Field Properties Associated with Broadband Shock Noise". *AIAA Journal*, Vol.22(No.9):pp. 1207–1215, 1984.

[104] Hammitt, A.G. "The Oscillations and Noise of an Overpressure Sonic Jet". *Journal of Aerospace Sciences*, Vol.28(No.9):pp. 673–680, 1961.

[105] Abdel-Fattah, A.M. "Discrete Tone Emission from High-Pressure Ratio Supersonic Jets from C-D Nozzles". *AIAA Journal*, Vol.26(No.3):pp. 283–291, 1988.

[106] Trentacoste, N. and Sforza, M.P. "Further Experimental Results for Three-Dimensional Jets". *AIAA Journal*, Vol.5(No.5):pp. 885–891, 1967.

[107] Hussain, A.K.M.F. and Ramjee, V. "Effects of Axisymmetric Contraction Shape on Incompressible Turbulent Flows". *Trans. ASME, Journal of Fluids Engineering*, Vol.98:pp. 58–59, 1976.

[108] Quinn, W.R. "Experimental and Numerical Study of a Turbulent Free Square Jet". *Physics of Fluids*, Vol.31(No.5):pp. 1017–1025, 1988.

[109] Taghavi, R. and Raman, G. "Enhanced Mixing of Multiple Supersonic Rectangular Jets by Synchronized Screech". *AIAA Journal*, Vol.32(No.12):pp. 2477–2480, 1994.

[110] Raman, G. and Rice, E.J. "Mixing and Noise Benefit Versus Thrust Penalty in Supersonic Jets using Impingement Tones". *Proceedings of 30th AIAA/ASME/SAE/ASEE Joint Propulsion Conference*, (No.6):pp. 27–29, 1994.

[111] J.P. Holman. Experimental methods for engineers. *5th Edition, McGraw Hill International Editions*, 1996.

[112] Srinivasan, K. Flow and Noise Characteristics of Non-Circular Jets. Ph.D Thesis, Department of Aerospace Engineering, Indian Institute of Technology, Kanpur, 1998.

[113] Tam, C.K.W. "The Shock-Cell Structures and Screech Frequency of Rectangular and Nonaxisymmetric Supersonic Jets". *Journal of Sound and Vibration*, Vol.121(No.1):pp. 135–147, 1988.

[114] Fuchs, H.V., Michel, U. "Far-Field Condition in Jet Noise Experiments". Vol.19(No.2):pp. 141–147, 1981.

[115] Lush, P.A. "Measurements of Subsonic Jet Noise and Comparison with Theory". *Journal of Fluid Mechanics*, Vol.46:pp. 477–500, 1971.

[116] Ahuja, K.K. "An Experimental Study of Subsonic Jet Noise and Comparison with Theory". *Journal of Sound and Vibration*, Vol.30:pp. 317–341, 1973.

[117] Bridges, J. and Hussain, F. "Direct Evaluation of Aeroacoustic Theory in a Jet". *Journal of Fluid Mechanics*, Vol.240:pp. 469–501, 1992.

[118] Soderman, P.T., Allen, C.S., Hayer-J.A., Jaeger, S.M., Krothapalli, A. "Flight Effects on the Far-Field Noise of a Heated Supersonic Jet". *AIAA Journal*, Vol.35(No.6):pp., 1997.

[119] Powell, A. "Experimental Comparison between Noise from Unheated Subsonic Air Jets having 4:1 Elliptic and Circular Orifices". *Letter to the Editor*, Vol.30(No.7):pp. 642–653, 1958.

[120] Rathakrishnan, E. Instrumentation, measurements and experiments in fluids. Book to be published.

[121] Quinn, W.R. "On Mixing in an Elliptic Turbulent Free Jet". *Physics of Fluids(A)*, Vol.1(No.10):pp. 1716–1721, 1989.

[122] Schadow, K.C., Bicker, C.J., Gutmark, E. "Near Acoustic Field and Shock Structure of Rectangular Supersonic Jets". *Experiments in Fluids*, Vol.28(No.7):pp. 1163–1170, AIAA Journal.

[123] Crighton, D.G. "Instability of an Elliptic Jet". *Journal of Fluid Mechanics*, Vol.59:pp. 665–667, 1973.

[124] Schadow, K.C., Wilson, K.J., Gutmark, E., and Bicker, C.J. "Near-Field Pressure Radiation and Flow Characteristics in Low Supersonic Circular and Elliptic Jets". *Physics of Fluids*, Vol.31(No.9):pp. 2524–2532, 1988.

[125] Ho, C.M. and Gutmark, E. "Near-Field Pressure Fluctuations of an Elliptic Jet". *AIAA Journal*, Vol.23(No.3):pp. 354–358, 1985.

[126] Chen, P., Seiner, J.M., Tam, C.K.W. "Relationship between Instability Waves and Noise of High Speed Jets". *AIAA Journal*, Vol.30(No.7):pp. 1747–1752, 1992.

[127] Dhanak, M.R. and Debernardinis, B. "The Evolution of an Elliptic Vortex Ring". *Journal of Fluid Mechanics*, Vol.109:pp. 189–216, 1981.

[128] Rice, E.J., Raman, G. "Instability Modes Excited by Natural Screech Tones in a Supersonic Rectangular Jet". *Physics of Fluids*, Vol.6(No.12):pp. 3999–4008, 1994.

[129] Donaldson, C.D. and Snedeker, R.S. "A Study of Free Jet Impingement. Part I. Mean Properties of Free and Impingement Jets". *Journal of Fluid Mechanics*, Vol.45(No.2) pp. 281–319, 1971.

Appendix

Uncertainty Analysis

Introduction

The general procedure for estimating the uncertainties in the calculated quantities using measured data is described below. The derived general expression has been employed to demonstrate the estimation of uncertainties associated with flow Mach number calculated using the measured values of total pressure and the ambient pressure.

General procedure

Let x_1, x_2, x_3, ...x_i,.. be the independent parameters(variables) in the experimental measurement, and u_1, u_2, u_3, ...u_i,.. be the relative uncertainties of x_1, x_2, x_3, ..x_i,... Let R be the experimental result calculated from the measured data.

The first step in the procedure is to analyze how errors in the x_i propagate into the calculation of R from the measured values. The quantity R can be expressed as

$$R = R(x_1, x_2, x_3, ..., x_i, ...x_n)$$

The effect of error in measuring individual x_i on R may be estimated by analogy to derivative of a function.

A variation δx_i in x_i would cause R to vary according to

$$\delta R_i = \frac{\partial R}{\partial x_i}\delta x_i$$

For applications, it is convenient to normalize the above equation by dividing throughout by R to obtain

$$\frac{\delta R_i}{R} = \frac{1}{R}\frac{\partial R}{\partial x_i}\delta x_i = \frac{x_i}{R}\frac{\partial R}{\partial x_i}\frac{\delta x_i}{x_i}$$

Equation(1) might be used to estimate the uncertainty interval in the result R, due to variation in x_i. To do this, substitute the uncertainty interval for x_i, namely

$$u_{R_i} = \frac{x_i}{R}\frac{\partial R}{\partial x_i}u_{x_i}$$

Uncertainty in R due to the combined effect of uncertainty intervals in x_i may be obtained by considering

- the random error in each variable as a range of values within the uncertainty interval
- the fact that it is unlikely that all errors will add to the uncertainty at the same time.
- It can be shown that the best representation for the uncertainty interval of the result is

$$u_R = \pm\left[\left(\frac{x_1}{R}\frac{\partial R}{\partial x_1}u_1\right)^2 + \left(\frac{x_2}{R}\frac{\partial R}{\partial x_2}u_2\right)^2 + ... + \left(\frac{x_n}{R}\frac{\partial R}{\partial x_n}u_n\right)^2\right]^{1/2}$$

This equation is the general expression for estimating the uncertainties in any calculated value from measured data. However, this expression has to be cast in the appropriate form before using it to estimate the uncertainty.

Uncertainty in Flow Mach Number

In this section, a procedure to estimate the uncertainty in flow Mach number M which is calculated from the measured total pressure and ambient pressure is given. The steps involved are as follows:

Obtain an expression for the uncertainty in determining the Mach number of a flow from measurements of total pressure P_t and the ambient pressure P_a. The Mach number in terms of P_t and P_a is

$$M = \left\{\left[\left(\frac{P_t}{P_a}\right)^{\frac{\gamma-1}{\gamma}} - 1\right]\frac{2}{\gamma-1}\right\}^{1/2} = \chi^{1/2}\ (say)$$

Differentiating, we get

$$\begin{aligned} dM &= \frac{\partial M}{\partial P_t}dP_t + \frac{\partial M}{\partial P_a}dP_a \\ &= \frac{1}{\chi}\left[\frac{1}{\gamma P_a}\left(\frac{P_t}{P_a}\right)^{-2/\gamma}dP_t + \frac{1}{\gamma P_a}\left(\frac{P_t}{P_a}\right)^{\frac{\gamma-1}{\gamma}}dP_a\right] \\ \frac{\partial M}{\partial P_t} &= \frac{1}{\chi}\left[\frac{1}{\gamma P_a}\left(\frac{P_t}{P_a}\right)^{-2/\gamma}\right] \end{aligned}$$

$$\frac{\partial M}{\partial P_a} = \frac{1}{\chi}\left[\frac{1}{\gamma P_a}\left(\frac{P_t}{P_a}\right)^{\frac{\gamma-1}{\gamma}}\right]$$

The uncertainty in M can be obtained from

$$u_M = \pm\left[\left(\frac{P_t}{M}\frac{\partial M}{\partial P_t}u_1\right)^2 + \left(\frac{P_a}{M}\frac{\partial M}{\partial P_a}u_2\right)^2\right]^{1/2}$$

where u_1 and u_2 are the relative uncertainties of P_t and P_a.

High fluctuations in Pitot(total) pressure were observed during measurements in the underexpanded flow field. By repeated observations, it was estimated that the maximum possible error in the measurement of total pressures(corresponding to the maximum stagnation pressure of 2050mm(gauge) i.e $M_j = 1.52$) would be around 60 mm.

Hence, the relative uncer+ainty in total pressure P_t is

$$\begin{aligned} u_{P_t} &= = u_1 = \pm\frac{\text{expected error in measured } P_t}{P_t \text{ measured}} \\ &= \pm\frac{60 \text{ mm}}{2050 \text{ mm}} \quad \text{(for example)} \\ &= \pm 0.03 = 3\% \end{aligned}$$

The relative uncertainty in barometric height (ambient pressure) is

$$u_{P_a} = u_2 = \pm\frac{0.5 \text{ mm}}{730 \text{ mm}} = 0.000685$$

$$\begin{aligned} \frac{P_t}{M}\frac{\partial M}{\partial P_t} &= \frac{P_t}{\chi}\frac{1}{\chi}\left[\frac{1}{\gamma P_a}\left(\frac{P_t}{P_a}\right)^{-2/\gamma}\right] \\ &= \frac{1}{\gamma\chi^2}\left(\frac{P_t}{P_a}\right)^{(\gamma-2)/\gamma} = 0.4587 \end{aligned}$$

Similarly, we get

$$\frac{P_a}{M}\frac{\partial M}{\partial P_a} = \frac{1}{\gamma\chi^2}\left(\frac{P_t}{P_a}\right)^{(\gamma-1)/\gamma} = 0.7674$$

$$\begin{aligned} \chi &= \left\{\left[\left(\frac{1500}{730}\right)^{0.286} - 1\right]\frac{2}{0.4}\right\} = 1.069 \\ \chi^2 &= 1.1436 \end{aligned}$$

$$\begin{aligned} u_M &= \pm\left[(0.4587 \times 0.03)^2 + (0.7674 \times 0.000685)^2\right]^{1/2} \\ &= \pm 0.0138 \\ &= \boxed{\pm 1.38\%} \end{aligned}$$

List of Publications

International Conferences

1. S.B.Verma and E.Rathakrishnan,"Studies on Elliptic Jets with Passive Controls", *Proceedings of Fluids Engineering Division Conference*, FED-Vol. 237, Vol. 2, ASME, 1996, pp. 555-560.

2. S.B.Verma and E.Rathakrishnan, "Mixing Benefit and Noise Characteristics of Notched Elliptic-Slot Jets", Sent for the forthcoming AIAA conference, 1998.

Journal Articles

1. S.B.Verma and E.Rathakrishnan,"Studies on Underexpanded sonic Free Jets from Elliptic and Circular Slots", Communicated to *AIAA Journal*(**accepted partially and is under final revision**).

2. S.B.Verma and E.Rathakrishnan,"Effect of Notch Geometry on the growth and Noise Characteristics of Elliptic Free Slot Jets", Communicated to *Journal of Fluids Engineering.*

3. S.B.Verma and E.Rathakrishnan,"Affect of Aspect-ratio on the growth and Noise characteristics of Plain and Notched Elliptic Free Slot Jets", Communicated to *The Aeronautical Journal.*

4. S.B.Verma and E.Rathakrishnan,"Effect of Notch Geometry on the growth and Noise Characteristics of Circular Free Slot Jets", Communicated to *Proceedings of Institution of Mechanical Engineers: Journal of Aerospace Engineering*(**under second revision**).

5. S.B.Verma and E.Rathakrishnan, "Noise Attenuation and Enhanced Mixing in Notched Elliptic-Slot Jets", Communicated to *The International Journal of Turbo and Jet Engines.*